AD-A174 510 DESIGN OF A MULTIPLE INPUT-MULTIPLE OUTPUT FLIGHT CONTROL SYSTEM CONTAINI..(U) AIR FORCE WRIGHT AERONAUTICAL LABS WRIGHT-PATTERSON AFB OH D L SEGNER 1/3

UNCLASSIFIED NOV 84 AFWAL-TR-84-3093 F/G 1/3 NL

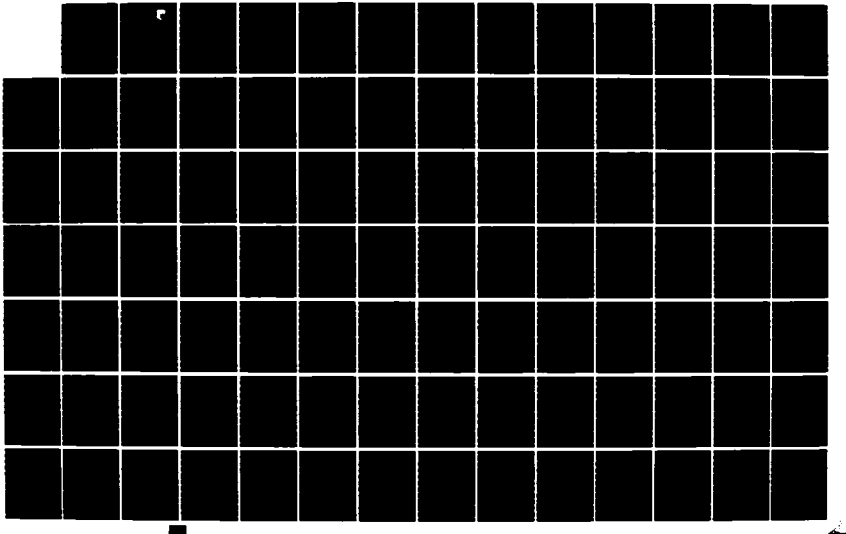

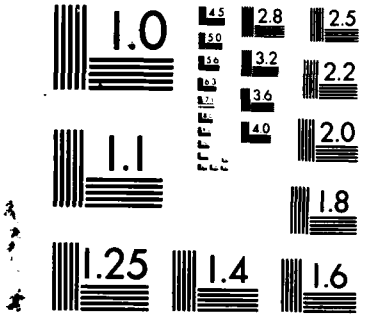

(2)

AFWAL-TR-84-3093

DESIGN OF A MULTIPLE INPUT-MULTIPLE OUTPUT FLIGHT CONTROL SYSTEM CONTAINING UNCERTAIN PARAMETERS

David L. Segner

Control Systems Development Branch
Flight Control Division

November 1984

Final Report for Period September 1981 - July 1984

Approved for public release; distribution unlimited

FLIGHT DYNAMICS LABORATORY
AIR FORCE WRIGHT AERONAUTICAL LABORATORIES
AIR FORCE SYSTEMS COMMAND
WRIGHT-PATTERSON AIR FORCE BASE, OHIO 45433-6553

NOTICE

When Government drawings, specifications, or other data are used for any purpose other than in connection with a definitely related Government procurement operation, the United States Government thereby incurs no responsibility nor any obligation whatsoever; and the fact that the Government may have formulated, furnished, or in any way supplied the said drawings, specifications, or other data, is not to be regarded by implication or otherwise in any manner licensing the holder or any other person or corporation, or conveying any rights or permission to manufacture, use, or sell any patented invention that may in any way be related thereto.

This technical report has been reviewed and is approved for publication.

Report was cleared in accordance with Air Force Institute of Technology policy.

David L Segner

DAVID L. SEGNER, Project Engineer
AFWAL/FIGL

Harry M. Snowball

HARRY M. SNOWBALL, Chief
Control Data Group
Control Systems Development Branch

FOR THE COMMANDER:

Evard H. Flinn

EVARD H. FLINN, Chief
Control Systems Development Branch
Flight Control Division

Frank A. Scarpino

FRANK A. SCARPINO, USAF
Chief, Flight Control Division

"If your address has changed, if you wish to be removed from our mailing list, or if the addressee is no longer employed by your organization please notify AFWAL/FIGL, W-PAFB, OH 45433-6553 to help maintain a current mailing list."

Copies of this report should not be returned unless return is required by security considerations, contractual obligations, or notice on a specific document.

UNCLASSIFIED

SECURITY CLASSIFICATION OF THIS PAGE

REPORT DOCUMENTATION PAGE

1a. REPORT SECURITY CLASSIFICATION: Unclassified	1b. RESTRICTIVE MARKINGS
2a. SECURITY CLASSIFICATION AUTHORITY	3. DISTRIBUTION/AVAILABILITY OF REPORT: Approved for public release; distribution unlimited.
2b. DECLASSIFICATION/DOWNGRADING SCHEDULE	
4. PERFORMING ORGANIZATION REPORT NUMBER(S): AFWAL-TR-84-3093	5. MONITORING ORGANIZATION REPORT NUMBER(S)
6a. NAME OF PERFORMING ORGANIZATION: Flight Dynamics Laboratory; 6b. OFFICE SYMBOL (If applicable): AFWAL/FIGL	7a. NAME OF MONITORING ORGANIZATION
6c. ADDRESS (City, State and ZIP Code): Wright-Patterson AFB, OH 45433	7b. ADDRESS (City, State and ZIP Code)
8a. NAME OF FUNDING/SPONSORING ORGANIZATION; 8b. OFFICE SYMBOL (If applicable)	9. PROCUREMENT INSTRUMENT IDENTIFICATION NUMBER
8c. ADDRESS (City, State and ZIP Code)	10. SOURCE OF FUNDING NOS.

PROGRAM ELEMENT NO.	PROJECT NO.	TASK NO.	WORK UNIT NO.
62201F	2403	07	03

11. TITLE (Include Security Classification): Design of a Multiple Input-Multiple (cont'd)

12. PERSONAL AUTHOR(S): David L. Segner

13a. TYPE OF REPORT	13b. TIME COVERED	14. DATE OF REPORT (Yr., Mo., Day)	15. PAGE COUNT
Final	FROM Sep 1981 TO Jul 1984	1984 November	234

16. SUPPLEMENTARY NOTATION: This research was written as a Masters Thesis for the Air Force Institute of Technology

17. COSATI CODES			18. SUBJECT TERMS (Continue on reverse if necessary and identify by block number)
FIELD	GROUP	SUB. GR.	
09	04		Multivariable control; multiple input-multiple output; control theory; flight control; uncertain plants; robustness; quantitative feedback
01	03		

19. ABSTRACT (Continue on reverse if necessary and identify by block number)

A quantitative feedback synthesis technique is used to design a lateral flight controller for a horizontal translation maneuver. Professor Isaac Horowitz, Weitzmann Institute of Science, Rehovot, Israel developed this technique. The technique, which is performed in the frequency domain, uses feedback to achieve the desired system response despite parameter variation.

A computer program generates an aircraft model for several flight conditions. The aircraft model includes canards (vertical and horizontal), ailerons, rudders, maneuvering flaps and jet flaps. These models are simplified to three input-three output systems. A single controller is designed for all of the flight conditions. Robustness is accomplished by considering parameter variation throughout the design method. The design is simulated and the results presented.

(Continued)

20. DISTRIBUTION/AVAILABILITY OF ABSTRACT	21. ABSTRACT SECURITY CLASSIFICATION
UNCLASSIFIED/UNLIMITED ☒ SAME AS RPT ☐ DTIC USERS ☐	Unclassified

22a. NAME OF RESPONSIBLE INDIVIDUAL	22b. TELEPHONE NUMBER (Include Area Code)	22c. OFFICE SYMBOL
Snowball, Harry	513-255-7229	AFWAL/FIGL

DD FORM 1473, 83 APR EDITION OF 1 JAN 73 IS OBSOLETE

SECURITY CLASSIFICATION OF THIS PAGE

Block 11 (Cont'd)

Output Flight Control Systems Containing Uncertain Parameters

Block 19 (Cont'd)

The method used is presented. A discussion of the results is presented, including suggestions on improvements to the design. Recommendations for further investigations are provided.

Block 3 (Cont'd)

must be referred to AFWAL/FIGL, WPAFB, OH 45433 and must include the statement of terms and conditions contained in Atach 21 to AFR 300-6.

FOREWORD

This report is the result of research performed in the Flight Dynamics Laboratory from September 1981 through July 1984. This research was written as a masters thesis for the Air Force Institute of Technology.

This research is relevant to current projects in integrated controls, multivariable controls and reconfiguration. The Quantitative Feedback Theory (QFT) synthesis technique used in this report is applicable to linear and non-linear minimum phase systems.

This research is one of a series of work efforts directed towards the application of new design methods by Dr. Isaac Horowitz of the Weitzmann Institute of Science, Rehevot, Israel.

Table of Contents

		Page
Foreword		iii
List of Figures		viii
List of Tables		viii
List of Symbols		ix
I.	INTRODUCTION	1
	1. Background	1
	2. Problem	4
	3. Assumptions	4
	4. Scope	5
	5. Thesis Outline	5
II.	QUANTITATIVE FEEDBACK TECHNIQUE THEORY: SINGLE INPUT-SINGLE OUTPUT (SISO) SYSTEM	7
	1. Introduction	7
	2. General Procedure	7
	3. Problem Definition	8
	4. System Specifications	10
	5. Plant Templates	14
	6. Nichols Chart	16
	7. Nominal Plant	17
	8. Derivation of Bounds for the Loop Transmission, L	18
	9. L(jω) Bounds on the Nichols Chart	19
	10. Universal High Frequency (UHF) Bound	25
	11. Shaping of the Nominal Loop Transmission, L_0	26
	12. Solving for the Compensator, G	27
	13. Design of the Prefilter, F	27
	14. Summary	29
III.	QUANTITATIVE FEEDBACK TECHNIQUE THEORY: MULTIPLE INPUT-MULTIPLE OUTPUT (MIMO) SYSTEM	31
	1. Introduction	31
	2. The MIMO Plant	31
	3. MIMO Compensation	35
	4. Constraints on the Plant Matrix	38
	5. Effective SISO Loops	38
	6. Basically Non-Interactive (BNIC) Loops	43
	7. Summary	43

Page

IV. AIRCRAFT MODEL 44

1. Introduction 44
2. Aircraft Description 44
3. Lateral Equation Model 50
4. Flight Conditions 51

V. DESIGN OF THE FIRST TWO LOOPS 53

1. Introduction 53
2. The Problem 53
3. The Plant Matrices 53
4. System Specifications 55
5. Choosing Which Loops to Design First 60
6. Plant Template 62
7. Bounds for the First Two Loops 64
8. Shaping the Open Loop Transfer Function 69
9. The Compensator G 74
10. Summary 74

VI. DESIGN OF THE FINAL LOOP 77

1. Introduction 77
2. Design of the Loop Transmission, L_2 77
3. Design of the Prefilter, F_{22} 85
4. Summary 88

VII. SIMULATION RESULTS 89

1. Introduction 89
2. Compensator Characteristics 89
3. Loop Responses 90
4. Comparison of Loop Responses and Bounds 98
5. Different Command Inputs 99
6. Summary 110

VIII. DISCUSSION AND CONCLUSIONS 111

1. Summary of Thesis 111
2. Discussion of the Results 111
3. Possible Improvements for this Design 112
4. Comments on the QFT Technique 114
5. Recommendations and Conclusions 115

Bibliography 117

Appendix A: Loop Transmission Shaping Example A-1

Appendix B: The Transfer Function Matrices of the Plant . . . B-1

Page

Appendix C: Loop 1 and Loop 3 Designs C-1

Appendix D: Loop 2 Design D-1

Appendix E: Designed Controller Responses E-1

List of Figures

Figure		Page
2-1	Single Input-Single Output (SISO) Control Loop with Two Degrees of Freedom	9
2-2	Design Limits for a Step Input (Time Domain)	11
2-3	Pole-Zero Pattern for a Third Order Control Ratio . . .	12
2-4	Design Limits for a Step Input (Frequency Domain) . . .	13
2-5	Plant Templates on the Nichols Chart (3:II-9)	15
2-6	Generating Bounds on the Nichols Chart (3:II-13) . . .	21
2-7	Composite Bound for $\omega = 1$ rad/sec (3:II-16)	23
2-8	Nominal Transmission Loop, L_o Shaped (3:II-16)	24
2-9	Requirements of F (3:II-19)	28
2-10	Bounds on the Prefilter, F	30
3-1	A MIMO Plant	32
3-2	State Space Block Diagram for Eq. 3-2	33
3-3	MIMO Control Structure (Two-By-Two System)	36
3-4	Two-By-Two MIMO System Schematic	36
3-5	MIMO Control Structure (Three-By-Three System)	37
3-6	Three-By-Three MIMO System Schematic	37
3-7	Effective SISO Loops (in general)	40
3-8	Effective SISO Loops Two-By-Two (Boxed in Loops) Three-By-Three (All 9 Loops)	41
4-1	FPCC Aircraft (7:43)	45
4-2	Flight Control Layout and Function (7:35)	46
5-1	Time Domain Response Functions used to Generate System Specifications (2:52)	56

Figure		Page
5-2	Time Domain Response Functions used to Generate System Specifications (2:57)	56
5-3	Frequency Domain System Specifications (Bode Plant on the Equivalent Transfer Functions)	61
5-4	Equivalent SISO Systems for a 3 x 3 MIMO System	63
5-5	Loop 1 (L_1) Design Bounds	66
5-6	Nominal Loop 1 (L_{10}) Design	72
6-1	Q_{22e} Plant Templates	80
6-2	L_{20} Design Bounds	82
6-3	L_{20} Design	84
6-4	Prefilter F_{22} Envelope	87
7-1	Compensator Responses (Step input of 1 ft/sec)	91
7-2	b_{12} Design Bound (r(t) = 1 ft/sec)	93
7-3	b_{22} Upper Design Bound (r(t) = 1 ft/sec)	94
7-4	b_{32} Design Bound (r(t) = 1 ft/sec)	95
7-5	a_{22} Lower Design Bound (r(t) = 1 ft/sec)	96
7-6	Case 2 r(t) = 1 ft/sec	97
7-7	t_{12} Responses to Different Inputs (FC #2)	100
7-8	t_{22} Responses to Different Inputs (FC #2)	101
7-9	t_{32} Responses to Different Inputs (FC #2)	102
7-10	Flight Condition #1 Step Input = 48 ft/sec (2:47) . .	107
7-11	Flight Condition #2 Step Input = 32 ft/sec (2:52) . .	108
7-12	Flight Condition #3 Step Input = 22.4 ft/sec (2:57) .	109

List of Tables

Table		Page
5-1	Time Domain System Specifications (approximated from previous thesis (2))	55
5-2	Equivalent Transfer Function Specifications	55
5-3	L_1 Loop Bounds	67
5-4	L_{10} Values	73
5-5	G_1 Values	75
5-6	$(L_1)_1$ Values	75
5-7	$(L_1)_2$ Values	76
6-1	Q_{22e} Values	79
6-2	(ΔValues, $\Delta = \lvert b_{22}\rvert - \lvert a_{22}\rvert$)	81
6-3	L_{20} Values	83
6-4	Closed Loop System Values $(\frac{L_2}{1 + L_2})$	85
7-1	Loop Responses (Step input of 1 ft/sec)	98
7-2	Loop 1 Responses to Different Inputs	103
7-3	Loop 2 Responses to Different Inputs	104
7-4	Loop 3 Responses to Different Inputs	105
7-5	Comparison of Responses Previous Thesis and This Thesis (2:62-63)	106

List of Symbols

β	sideslip angle
δ_a	aileron deflection
δ_j	jet flap deflection
δ_m	maneuver flap deflection
δ_r	rudder deflection
δ_{vc}	vertical canard deflection
Δ	difference between two bounds
Δ_v	change in magnitude at high frequency
γ	ratio of effective plant transfer functions
θ	pitch angle
ϕ	roll angle (bank angle)
ψ	yaw angle
ω	unit of frequency (rad/sec or deg/sec)
AFIT	Air Force Institute of Technology
a_{ij}	modeled response bound (lower limit)
b_{ij}	modeled response bound (upper limit)
$B(j\omega)$	design bound
$B_D(j\omega)$	disturbance nominal design bound
$B_o(j\omega)$	composite nominal design bound
$B_R(j\omega)$	command input design bound
BNIC	basically non-interactive case
C.E.	characteristic equation
det $\underline{P}$	determinant of $\underline{P}$
d_{ij}	effective disturbance

F	prefilter in single loop design
$\underline{F}$	prefilter matrix
FC	flight condition
FDL	Flight Dynamics Laboratory
FPCC	Flight Propulsion Control Coupled
FPCCSIM	digital computer simulation of the FPCC aircraft
F_v	final value
f_{ij}	element of $\underline{F}$
G	primary compensator element in single loop design
$\underline{G}$	diagonal compensator matrix
g_i	element of $\underline{G}$ (matrix is diagonal)
K_m	maximum gain allowed
L	control loop transmission
L_a	point in space used to find design bounds analytically
$(L_i)_j$	loop transmission i at flight condition j
L_o	nominal loop transmission
MIMO	multiple input-multiple output
M_p'	maximum peak value
P	plant transfer function
P_o	nominal plant transfer function
$\underline{P}$	plant matrix of system transfer functions
p_{ij}	element of $\underline{P}$
$(P_i)_j$	loop i plant, flight condition j
$\underline{P}_o$	nominal plant matrix
p	angular velocity around X-axis (roll)
$\underline{Q}$	inverse elements of $\underline{Q}$ $(q_{ij} = 1/q_{ij}')$

$\underline{Q}'$	inverse of plant matrix (P^{-1})
QFT	Quantitative Feedback Theory
Q_{22e}	effective plant for loop 2
q_{ij}'	element of $\underline{Q}'$
q_{ij}	element of $\underline{Q}$ ($q_{ij} = 1/q_{ij}'$)
rhp	right half plane
s	Laplace operator ($s = j\omega$)
SISO	single input-single output
$\underline{T}$	system outputs
T	compensated system transfer function
T_{max}	maximum value of closed loop system (no prefilter, F)
T_{min}	minimum value of closed loop system (no prefilter, F)
T_D	disturbance response transfer function (1/[1 + L])
t_{ij}	element in $\underline{T}$
T_L	lower bound for system response
t_p	time to peak value
t_r	rise time (time to 94% of final value)
T_R	command response transfer function (FL/[1 + L])
t_s	settling time
T_u	upper bound for system response
UHF	universal high frequency
v	velocity perturbation in the Y-direction (sideslip velocity)

DESIGN OF A MULTIPLE INPUT-MULTIPLE OUTPUT FLIGHT CONTROL SYSTEM CONTAINING UNCERTAIN PARAMETERS

I. INTRODUCTION

The approach used to design the flight controller in this research project is the Quantitative Feedback Theory (QFT) technique developed by Dr. Isaac Horowitz of the Weizmann Institute of Science, Rehovot, Isreal. He used this technique on several projects for the U. S. Air Force (14). This frequency response technique was used to successfully design controllers for several difficult systems; for example, the FY-16 CCV aircraft (12).

The U. S. Air Force is interested in this technique as a method to synthesize multiple input-multiple output (MIMO) controllers. In this thesis, a lateral flight controller is designed for the Flight Propulsion Control Coupled (FPCC) aircraft.

1. Background

An aircraft sitting on the ground is, in general, a stable, decoupled system. In the air, an aircraft becomes a nonlinear and highly coupled MIMO system whose model contains parameter uncertainty. The aircraft system includes many inputs, some from flight control surfaces, e.g. rudder, ailerons, spoilers, flaps, elevator and canards. Also, inputs come from propulsion units or engines (e.g. thrust), and from other sources such as gusts. Some of the system outputs controlled are velocity, angular displacements and angular rates of the aircraft body relative to some reference axis system.

Ideally, each input affects only the one or two outputs it is designed to affect. In practice, one input affects many outputs because the inputs and outputs of an aircraft system are strongly interrelated, or coupled. The input to output relationships usually are not linear nor are they known with much certainty. For example, the ailerons control the roll rate, which controls the bank angle. But, an aileron deflection also causes a yaw rate and a pitch angle change. The deflected surfaces cause asymmetric drag on the wing, thus a yaw, and the changing lift vector resulting from the change in bank angle causes a pitch change.

The classical mathematical model considers the MIMO relationships invariant and linear in a small region around an equilibrium point (6:152-155). Next, the MIMO system is decoupled into several independent single input-single output (SISO) problems (5:162). The designer learns the art of decoupling mostly through experience. Only experience helps decide which simplifications are appropriate. The resulting designs are often successful, but only after much trial and error (14:1).

Currently many controller designs use modern or optimal control techniques. These control design techniques use the state space representation of the system model (5:523-601). These techniques normally require many complex matrix operations. Robustness using these design techniques is not guaranteed and is difficult to obtain when unavailable state information must be estimated. (See Reference 11 for more critique). Robustness is defined in this paper as a single controller which maintains the desired aircraft performance throughout the flight envelope. Another method studied at the Air Force Institute of

Technology (AFIT) and in the Flight Dynamics Laboratory (FDL) at Wright-Patterson Air Force Base, is the output feedback, high gain, asymptotic method of Professor Brian Porter of the University of Salford, U.K. This method guarantees robustness in the design, but the amount of robustness, or range of uncertainty over which the design performs satisfactory, is not predictable.

Another method developed by Dr. Horowitz (10-17) and used in this thesis, guarantees to satisfy the system performance specifications. System responses to inputs or plants which are within the expected input or plant ranges are guaranteed acceptable. Thus, the design satisfies the system specifications of many plant and input combinations by designing for only a finite number of combinations. Therefore the QFT technique is robust. Dr. Horowitz's technique begins the design assuming uncertainty in the plant, the disturbances and the performance specifications. The differential equations or the state space model for the system represents the MIMO plant. Several equivalent SISO systems, which contain disturbance and parameter uncertainty, are synthesized through elementary matrix operations. This reduction from a MIMO system to several SISO systems is mathematically rigorous. A design is performed for each SISO system using the system performance specifications and information derived from the MIMO system. If the designed controller synthesized for each SISO system meets all of its specifications, then the final controller is guaranteed to meet the MIMO specifications (14).

The flight controller designed in this thesis is for a "paper" aircraft. This hypothetical aircraft was developed under a FDL contract by Lockheed-California, Honeywell and Pratt-Whitney (7,8). This

hypothetical aircraft is statically unstable and incorporates canards and jet flaps for maneuverability (7,8). The contractors provided FDL with a computer simulation of this aircraft, FPCCSIM (9). This program simulates the FPCC aircraft at different flight conditions. Additional computer programs used during this thesis are TOTAL (an interactive design program), a program to invert three-by-three transfer function matrices (Appendix F) and programs generated by the author of this thesis specifically for the QFT technique (Appendix F).

2. Problem

This thesis presents a design of a MIMO feedback lateral flight controller for an aircraft using the Quantitative Feedback Theory (QFT) technique developed by Professor Horowitz. The controller is designed for the Flight Propulsion Control Coupled (FPCC) "paper" aircraft, using results from FPCCSIM (a computer simulation) for the aircraft model. The resulting design is compared qualitatively to a design previously accomplished for this aircraft, using Professor Porter's state variable MIMO feedback technique (2). Also, the cost for achieving desired performance despite uncertainties is discussed. The design method is outlined such that it can be applied to similar problems by anyone with a background in control theory and frequency response methods.

3. Assumptions

The basic modeling assumptions are a flat non-rotating earth reference frame, a quasi-static airflow, a rigid aircraft and a constant aircraft mass (4:21-23). These assumptions limit the problem to one achievable in one thesis and not by the capability of the QFT technique.

The assumptions for the model, in both this author's design and the previous design (2) are the same.

Another assumption is the computer simulation, FPCCSIM, is a good representation of an actual aircraft system. Also, the results of the previous design, using the Porter method (2) are assumed correct.

4. Scope

This thesis demonstrates the designed analog controller operates satisfactorily, meeting all specifications at the three flight conditions used. The three flight conditions are 2.3 mach at 40,000 feet, 0.9 mach at 30,000 feet and 0.6 mach at sea level. Computer simulation demonstrates the performance of the designed controller. Robustness is demonstrated by using inputs in the simulation, other than the design input and comparing these results with the specifications.

5. Thesis Outline

First the design technique is described. Chapter II describes the QFT design technique for a SISO system, followed by a presentation of the MIMO design approach in Chapter III. Next, in Chapter IV, the FPCC aircraft and FPCCSIM computer simulation are described. The computer program FPCCSIM generates the aircraft model. After completion of this basic background information, the design performed for this thesis is explained in detail.

Chapter V contains the system specifications used for the design of the lateral flight controller, which are derived from the time response curves of the previously designed controller (2).

The design is in Chapters V and VI. The design is originally performed manually, then verified by computer software generated for

this method by the author of this paper (Appendix F) and the computer aided design program TOTAL. Evaluation of the design is continuous. During the design phase, changes or compromises are made in the design as appropriate. This demonstrates the method's "transparency" or ability to evaluate difficulties in the system during the design phase. The designer knows when a problem exists and what needs modification to alleviate the problem. The cost in bandwidth of any change is evaluated quickly. These changes do not affect the original assumptions (see Section I-3) nor the system performance specifications of the final controller.

Chapter VII contains the computer simulation and compares the results to the system performance specifications. Then the design is compared qualitatively to the previously designed controller using Professor Porter's method. A discussion and conclusions follow in Chapter VIII. Recommendations for further studies using the QFT technique are also included.

II. QUANTITATIVE FEEDBACK THEORY:

SINGLE INPUT-SINGLE OUTPUT (SISO) SYSTEM

1. Introduction

This section presents an overview of the QFT technique, as used in this thesis. The technique description is adapted from Chapters II and III of Robert Betzold's thesis (3). The explanations and examples are essentially the same, with some modification.

2. General Procedure

This section presents the general procedure for this technique. A more detailed explanation of the technique follows in this and the next chapter. Chapters V and VI contain the design performed using this technique in detail.

With a single input-single output (SISO) system defined, begin the Quantitative Feedback Theory (QFT) technique with the specifications for the system. The QFT technique requires the system specifications in the frequency domain (Section II-4). Next, the plant transfer function matrix model, $\underline{P} = [p_{ij}]$, is generated because the QFT technique requires the frequency responses of the plant (Section II-5).

The system specifications and the plant models help define the limitations or bounds for the system at every frequency of interest, ω, (Section II-8). Due to uncertainties in $\underline{P}$, $\underline{P}$ has different values at each ω. This resulting set of $\underline{P}(j\omega)$, forms a template of p_{ij}. Plant templates are made for a number of frequencies in the region of interest. The plant templates and the system limitations generate design bounds on the Nichols Chart (Section II-9). Another design bound, the Universal

High Frequency (UHF) Bound maintains a safety margin for stability (Section II-10). The Nichols Chart [log (L) with loci of constant magnitude and phase of $L/(1 + L)$] is convenient for finding the bounds on a nominal loop transmission, L_o. The loop transmissions, or open loop transfer functions, around the MIMO plant are the basic means of achieving the desired response specifications despite uncertainties. L_o is designed from the design bounds using the plant templates (Section II-11). From L_o, the compensator is synthesized using $L_o = P_o G$ where G is the compensator, P_o is the nominal plant and L_o is the nominal loop transmission (Section II-12). With the loop characteristics known the prefilter, F, is designed (Section II-13). This completes the design technique for a SISO system.

3. Problem Definition

Consider a single input-single output (SISO) system for simplicity. The plant transfer function, P, contains uncertainties in its parameters (gains, zeros and poles). The system specifications define the desired response of the system, to command inputs and/or disturbances. Therefore, the problem is to achieve the desired response despite the uncertainties in the plant.

In the SISO system in Fig. 2-1, r(t) is the command input and d(t) is the disturbance input, both of which contain uncertainties. P is the plant, which contains uncertainties. G, the compensator, and F, the prefilter are designed to force the system to have acceptable responses. The system output, y(t), is a member of the set of acceptable responses Y(t). The plant input is x(t).

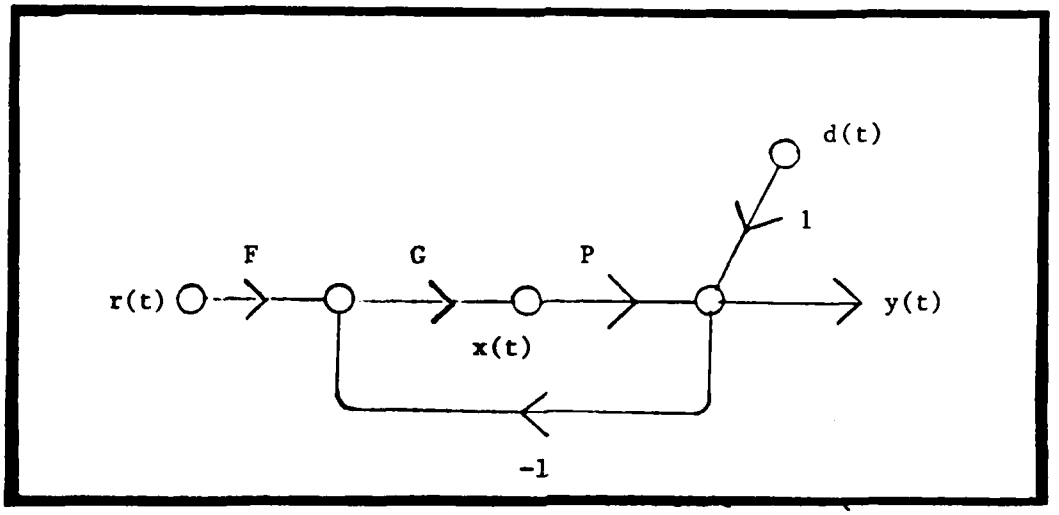

Fig. 2-1 Single Input-Single Output (SISO) Control Loop with Two Degrees of Freedom

The quantities r(t) and y(t) are assumed measurable and y(t) is assumed available for feedback. Since both signals, r(t) and y(t) are accessible, a two degree-of-freedom structure is used (see Fig. 2-1). Thus, the designer has two compensator elements, F and G (14:13). Also assume r(t), y(t) and p(t), where $y(t) = p(t) * x(t)$, are all Laplace Transformable functions (14:8).

Figure 2-1 has four transfer functions of interest. The loop transmission, L, is defined as $L = GP$. The system control ratio due to the command and disturbance inputs are respectively;

$$T_R = Y(s)/R(s) = \frac{FG\ P}{(1 + GP)} = \frac{FL}{(1 + L)} \qquad (2\text{-}1)$$

$$T_D = Y(s)/D(s) = \frac{1}{(1 + GP)} = \frac{1}{(1 + L)} \qquad (2\text{-}2)$$

and the transfer functions relating the plant input to the command and disturbance inputs are respectively;

$$I_R = X(s)/R(s) = \frac{FG}{(1 + GP)} = \frac{FG}{(1 + L)} \qquad (2\text{-}3)$$

$$I_D = X(s)/D(s) = \frac{-G}{(1 + GP)} = \frac{-L/P}{(1 + L)} \qquad (2\text{-}4)$$

The design specifications can impose constraints on any combination of these transfer functions, but for this example and for simplicity, only the first two functions are constrained.

4. System Specifications

The system specifications, or closed-loop response tolerances, define the acceptable frequency domain output response to inputs; disturbance(s) in terms of an upper limit and/or command(s), in terms of an upper and lower limit. Any response within these bounds is assumed acceptable.

The response specifications are required in the frequency domain for this technique. Often, the system specifications are defined in the time domain, using characteristics such as maximum peak value (M_p), settling time (t_s), time to peak value (t_p), final value (F_v) and maximum gain allowed (K_m). These characteristics are based upon a specific forcing function, such as a step input. The specifications might be defined as a bounded region in the time domain, where the desired system response to an input is in the region enclosed by the upper (T_U) and lower (T_L) limits, as in Fig. 2-2. The system response to a disturbance input, T_D, is normally defined as $|y(t)| \leq |T_D|$.

(Fig. 2-2). Thus, only a disturbance specification upper limit is necessary for the disturbance response.

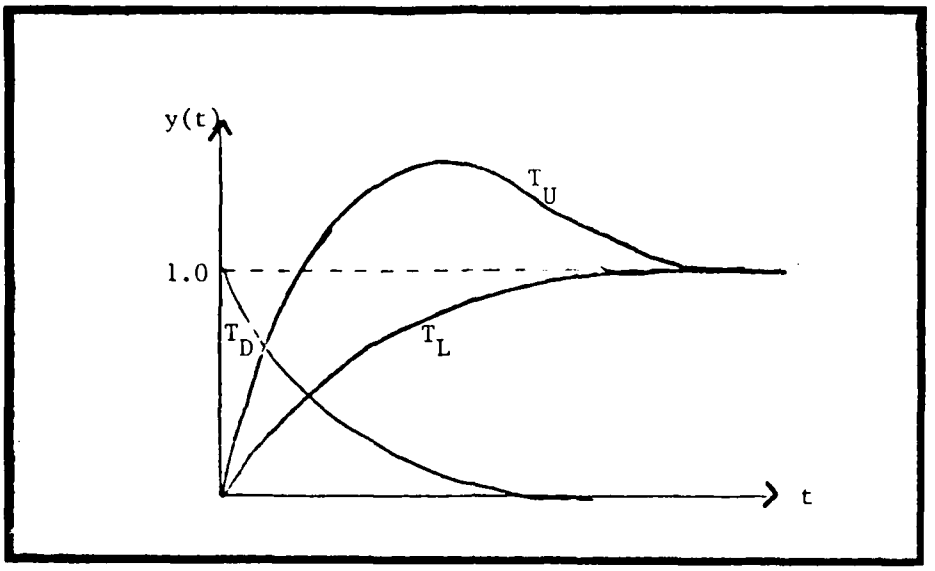

Fig. 2-2 Design Limits for a Step Input (Time Domain)

To use the QFT technique, translate the time domain specifications into the frequency domain. Do this by generating a transfer function which yields the same response characteristics as the time domain system performance specifications given. One method is to use pole-zero placement as described in Section 12-2 of Reference 5. A third order control ratio model with one zero is suggested for the response to a step input:

$$M = \frac{A(s + z_1)}{(s^2 + 2\zeta_n s + \omega_n^2)(s + p_3)} \qquad (2\text{-}5)$$

The pole-zero pattern of the above transfer function is in Fig. 2-3. Adjust the locations of the roots until the response of the modeled control ratio matches the desired upper and lower bound.

During the modeling of the equivalent frequency domain specifications, consider the frequency domain characteristics. At all frequencies the magnitude difference should be as large as possible between the upper and lower limits. If the lower limit has a greater pole to zero ratio than the upper limit, the magnitude difference approaches infinity as the frequency, ω, approaches infinity.

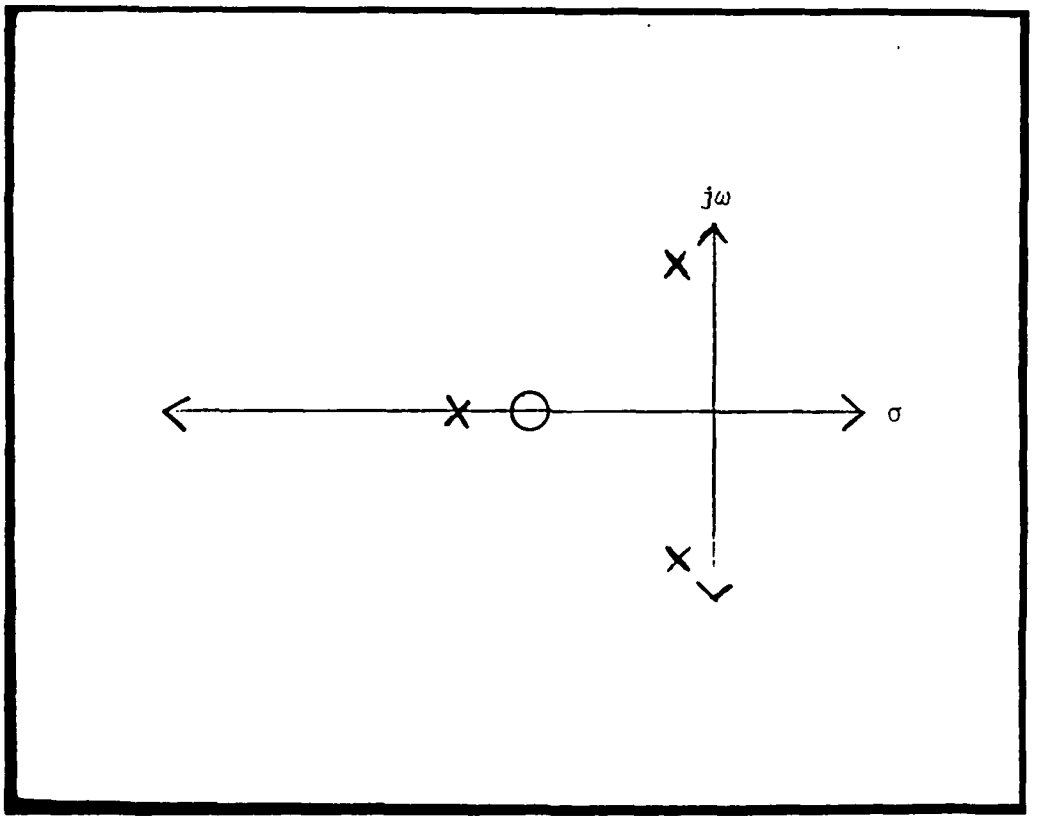

Fig. 2-3 Pole-Zero Pattern for a Third Order Control Ratio

A Bode Plot (magnitude plot of the frequency response) for each control ratio representing a time response bound is drawn. These plots represent the system specifications in the frequency domain (Fig. 2-4).

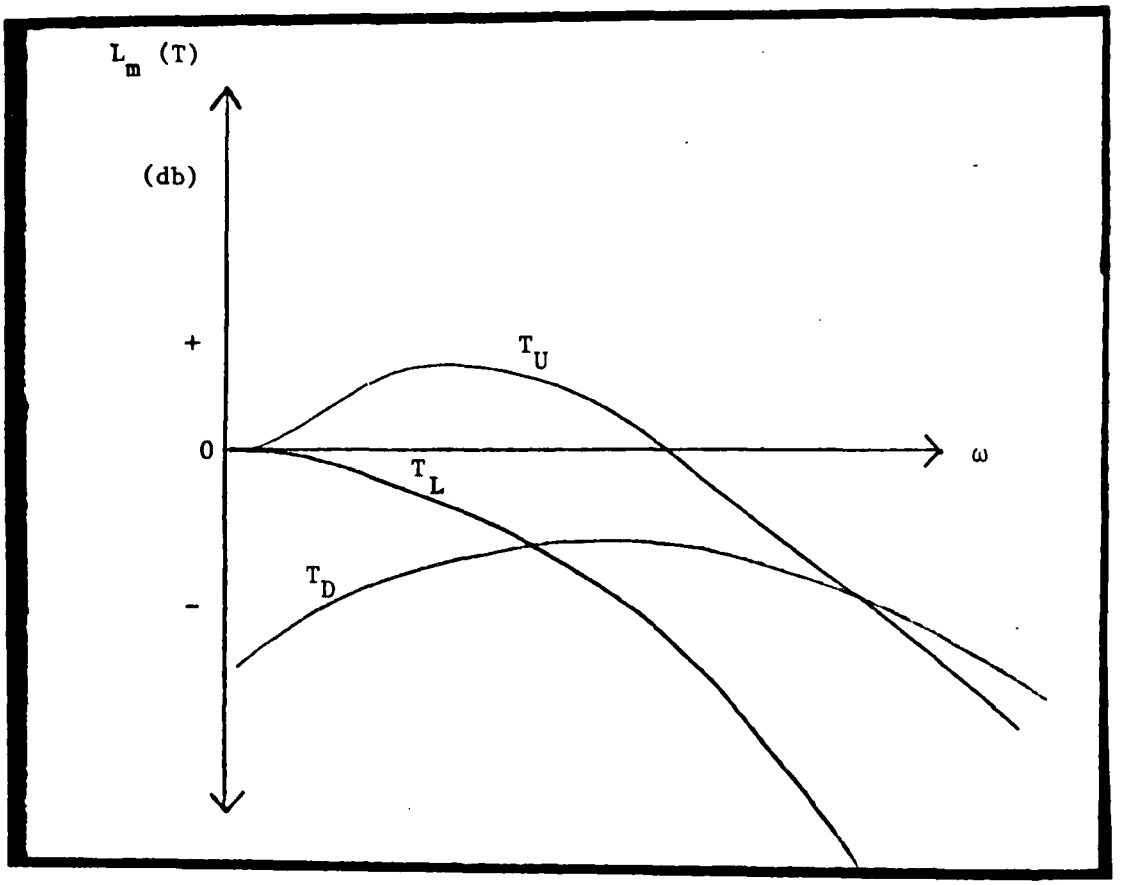

Fig. 2-4 Design Limits for a Step Input (Frequency Domain)

These equivalent frequency domain specifications generate the bounds on the loop transmission, $\underline{L}(j\omega)$.

The system specification models affect the final design in several ways. If the entire set of acceptable responses is not considered, the system may be overdesigned, thus the bandwidth of the system is larger than necessary. If the frequencies of interest change, then the models need changing, else the design may be overdesigned or not acceptable.

5. Plant Templates

A plant template is a plot representing the range of uncertainty in the plant, P, at a given frequency (16:290). For example, let $P(s) = K/s(s + a)$ where K and a are uncertain. Given $2.0 < K < 8.0$ db and $0.5 < a < 2.0$ db , an infinite number of possible P's exist due to the uncertainties in K and a. Generate the plant template by plotting $\text{Lm}[\underline{P}(j\omega)]$ vs $\text{Ang}[\underline{P}(j\omega)]$ for all possible values of K and a at a sufficient number of frequencies in the range of interest. This generates a set of complex numbers with finite boundaries for any frequency. The templates are drawn on the Nichols Chart because the chart is calibrated in db vs phase angles and this method uses the Nichols Chart. Only the boundary of the template need calculating. Find the boundary of the template by holding all but one variable constant, i.e., in the example above set $K = 2$ and vary a incrementally from 0.5 thru 2.0. The size of the increments are determined by the designer. If the shape is simple, use fewer points (larger increments) or if the shape is irregular use more points (smaller increments). The frequency response at $\omega = 1$ rad/sec for the P's obtained above provides a set of points from A ($K = 2$, $a = 0.5$) to D ($K = 2$, $a = 2$) on the Nichols Chart (Fig. 2-5). The process continues, holding all but one variable constant, and varying that one variable over its entire range of

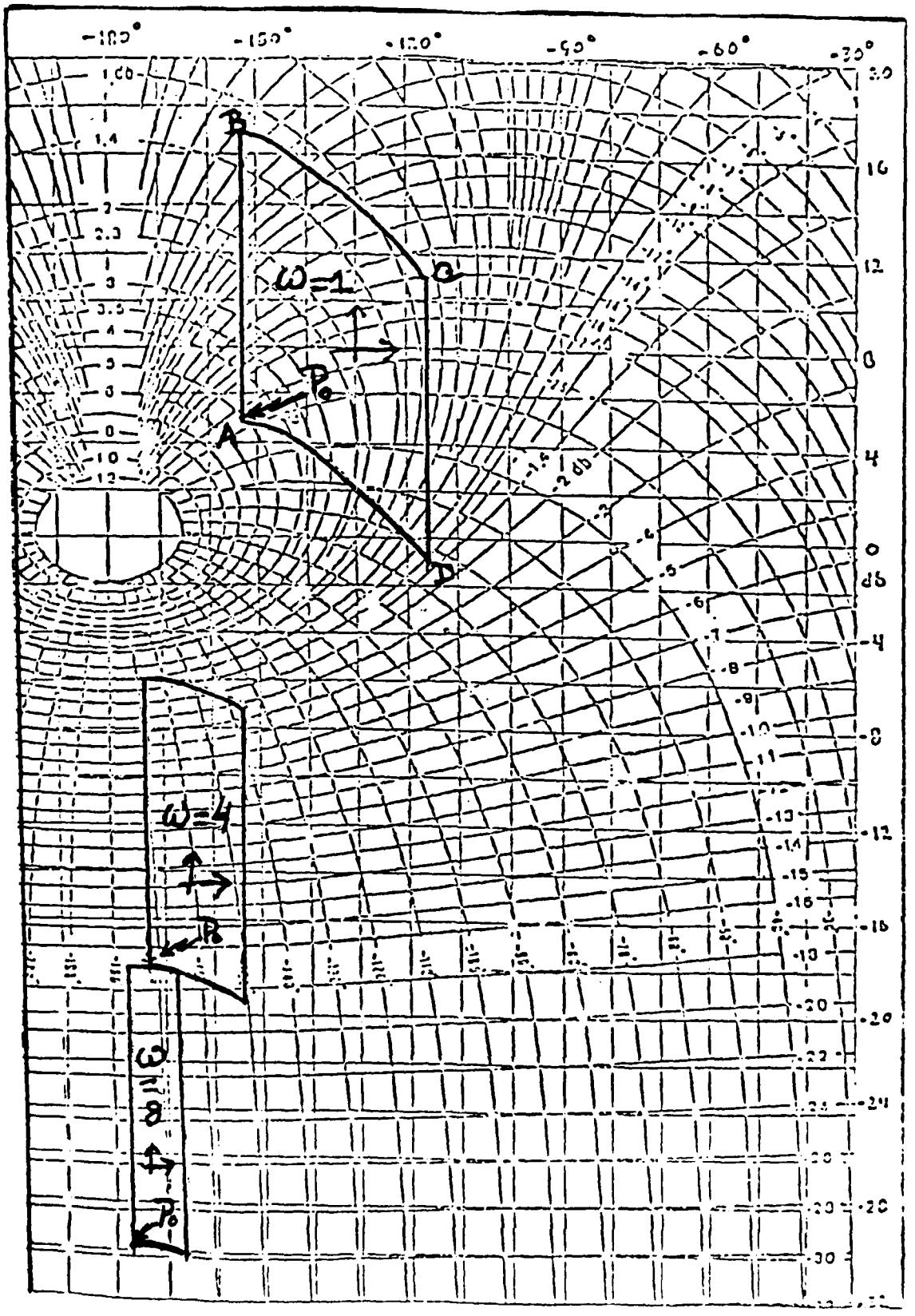

Fig. 2-5 Plant Templates on the Nichols Chart (3:II-9)

uncertainty. Increment the constants while the changing variable is exercised over its entire range of uncertainty for each set of constants. The sets of points at each frequency define the plant template for that frequency. Do this at every frequency for which a plant template is desired. For example, given $a = 0.5$, vary K from 2 thru 8 to obtain Line A ($a = 0.5$, $K = 2$) to B ($a = 0.5$, $K = 8$). Now set $a = 2.0$, and vary K from 2 thru 8. Complete the template by connecting the four corners with appropriately curved lines. Make a plant template for many frequencies, the designer decides on the intervals between and the number of frequencies. One procedure is to make templates at regular intervals, such as every octave. A set of templates for the example is in Fig. 2-5. Note the size changes of the plant templates (the plant template for $\omega = 8.0$ rad/sec is smaller than the plant template $\omega = 1.0$ rad/sec) in Fig. 2-5 at the different frequencies, this is caused by the range of uncertainty in P.

6. Nichols Chart

The design of the loop transmission, L, and the prefilter, F, is performed on the Nichols Chart. Let F be equal to one and then the open loop transmission of a unity feedback system, $L = GP$, plots onto the horizontal (magnitude in decibels) and vertical (phase angle in degrees) scales of the Nichols Chart. At any given frequency, read the magnitude (in decibels) and phase angle (in degrees) of $T_R = L/(1 + L)$ directly from the superimposed curved loci $[L/(1 + L)]$. Also any point on the loci corresponding to the magnitude and phase angle of T_R corresponds to the magnitude and phase angle of L on the horizontal and vertical scales (5:332-334). The correspondence between L and T_R is important because the design is performed using this relationship.

The Nichols Chart is also used for disturbance rejection. Given that $T_D = 1/(1 + L)$ (Eq. 2-2) and using the transformation, $L = 1/m$ (1:152-155), the system control ratio becomes $T_D = m/(1 + m)$ and this is of the same form as $T_R = L/(1 + L)$. This enables the design of the loop transmission inverse, m, directly on the Nichols Chart. Turn the Nichols Chart upside down, reflect the phase angle of the L lines about the -180 degree line (i.e., -190 becomes -170, -200 becomes -160, etc.), and reverse the signs on the magnitude lines and this enables the design of L directly on the Nichols Chart. The horizontal and vertical scales still correspond to the magnitude and phase angle of L, but the superimposed curved loci now correspond to the magnitude and phase of $1/(1 + L)$ (1:155). For the disturbance rejection design, only the magnitude is necessary. This assumes the disturbance has its maximum affect possible on the system at every frequency. Thus ignore the curved lines representing the phase angles. In practice for a disturbance rejection design, turn the Nichols Chart upside down and modify the scales as described above. Thus design L directly without using the dummy variable, m.

7. Nominal Plant

Choose an arbitrary specific plant parameter set to generate $P_o(j\omega_i)$, a reference or nominal plant used in the design method. P_o generates the bounds on the Nichols Chart for the nominal loop transmission, L_o, where $L_o = P_o G$. P_o is only a reference and therefore is anywhere, even outside the set of P's. It is usually convenient to choose a P_o that lies within the set of possible P's, thus being a point on the templates. A corner of the template is convenient, since this

transfer function is already known and calculated for each template. In the above example, the lower left hand corner, point A, is chosen as the nominal $[P_o = 2/s(s + 0.5)]$ (Fig. 2-5). It helps to mark the reference point, P_o, on every template because the P_o chosen may not remain in the same relative location on each template.

8. Derivation of Bounds for the Loop Transmission, L

The system specifications generate the bounds for each loop transmission, L, in the form of regions permitted. If T(s) uniquely defines the response, y(t), to a step input, then T(s) is completely specified for a stable, minimum phase (no right half plane poles or zeros) system, by the magnitude of the frequency response, $|\underline{T}(j\omega)|$ (14,16). The frequency response of $|\underline{Y}(j\omega)|$ varies between the upper (T_U) and the lower (T_L) bounds. For the example, at $\omega = 1$ rad/sec , assume $|\underline{Y}(j1)|$ varies from 0.7 to -0.8 db. The relative variation is therefore $|(0.7) - (-0.8)| = 1.5$ db . The allowable relative change in $\underline{Y}(j\omega)$ at any frequency is given by

$$\Delta Lm\ [\underline{Y}(j\omega_i)] = \Delta Lm\ [\underline{T}_U(j\omega_i)] - \Delta Lm\ [\underline{T}_L(j\omega_i)] \qquad (2\text{-}6)$$

where $\underline{T}_U(j\omega)$ and $\underline{T}_L(j\omega)$ are the frequency domain bounds on $\underline{Y}(j\omega)$.

The relationship between the relative change and the control ratio is as follows. From Fig. 2-1 and Eq. 2-1, $\Delta Lm\ (Y) = \Delta Lm\ (T) = \Delta Lm\ [FL/(1 + L)]$ where $L = G\,P$ and G and F are known, i.e. contain no uncertainty. Then;

$$\Delta Lm\ [\underline{Y}(j\omega_i)] = \Delta Lm\ [\underline{T}(j\omega_i)] = \Delta Lm\ [\underline{L}(j\omega_i)/[1 + \underline{L}(j\omega_i)]] \qquad (2\text{-}7)$$

Assuming G and F are known with certainty or the uncertainty is negligible (else include it in P), the relative change in $\underline{L}(j\omega_i)$ is equal to the relative change in the plant, $\underline{P}(j\omega_i)$.

$$\Delta Lm\ [\underline{L}(j\omega_i)] = \Delta Lm\ [\underline{P}(j\omega_i)] \qquad (2\text{-}8)$$

Parameter uncertainty in P is the cause of the variation. The problem is to find L_o such that $\underline{T}(j\omega)$ is within the acceptable range. Thereby the relative change requirements on the closed-loop response are satisfied over the entire range of P's uncertainty. The system specifications are the requirements on the closed-loop response, $\underline{Y}(j\omega)$, and therefore also $\underline{T}(j\omega)$ (Eq. 2-7). Next transfer the constraints for the loop transmission, $\underline{L}(j\omega)$, to the Nichols Chart (14:18,16:291).

9. L(jω) Bounds on the Nichols Chart

The relative uncertainty in L is equivalent to the range of uncertainty in P above (Eq. 2-8). Remember, the plant template is a plot of the range of uncertainty in P at a given frequency. Since Lm (L) = Lm (P) + Lm (G) and Ang (L) = Ang (P) + Ang (G) , a template can be translated (but not rotated) horizontally or vertically on the Nichols Chart. The horizontal and vertical translations correspond to the angle and magnitude requirements on $G(j\omega)$ at a given frequency (16:290). Drawing lines on the template to reference the horizontal and vertical helps maintain the correct orientation on the Nichols Chart (see Fig. 2-5).

Using the templates generated for the example in the previous sections, place the template for $\omega = 1$ rad/sec at position A in Fig. 2-6. The area covered by the template corresponds to the variation in L due to the uncertainty in P. Recall the correspondence of L and T explained in Section II-6. Read the maximum and minimum values of T covered by the template from the superimposed curved magnitude contours of the Nichols Chart (the contours of constant Lm $[\underline{T}(j\omega)]$). If this difference (approximately 10 db) between the maximum and minimum values is greater than the allowable difference (1.5 db) in T at $\omega = 1$, $\Delta Lm\ [\underline{T}(j\omega_i)]$ (Eq. 2-7 and Fig. 2-6), shift the template vertically upwards, as in Fig. 2-6, until the variation covered by the template is equal to $\Delta Lm\ [\underline{T}(j\omega_i)]$ (position B in Fig. 2-6). If the difference is less than allowed, then translate the template downward until the variation covered by the template is equal to the difference allowed. When the position where the allowable variation and that covered by the template are equal, transfer the point for the nominal plant from the template onto the Nichols Chart. This point, read from the horizontal and vertical scales of the Nichols Chart, corresponds to a bound, $\underline{B}(j\omega)$, for the magnitude and phase angle values of the L_o. The nominal loop transmission, $L_o(j\omega_i)$, is given by

$$L_o(j\omega_i) = G(j\omega_i)\ P_o(j\omega_i) \qquad (2\text{-}9)$$

Repeat this process horizontally across the chart for different values of $Ang(L_o)$. The points form a curve, $B_R(j\omega_i)$, representing the boundary of $L_o(j\omega_i)$ at $\omega = \omega_i$ on the Nichols Chart. As long as the $L_o(j\omega_i)$

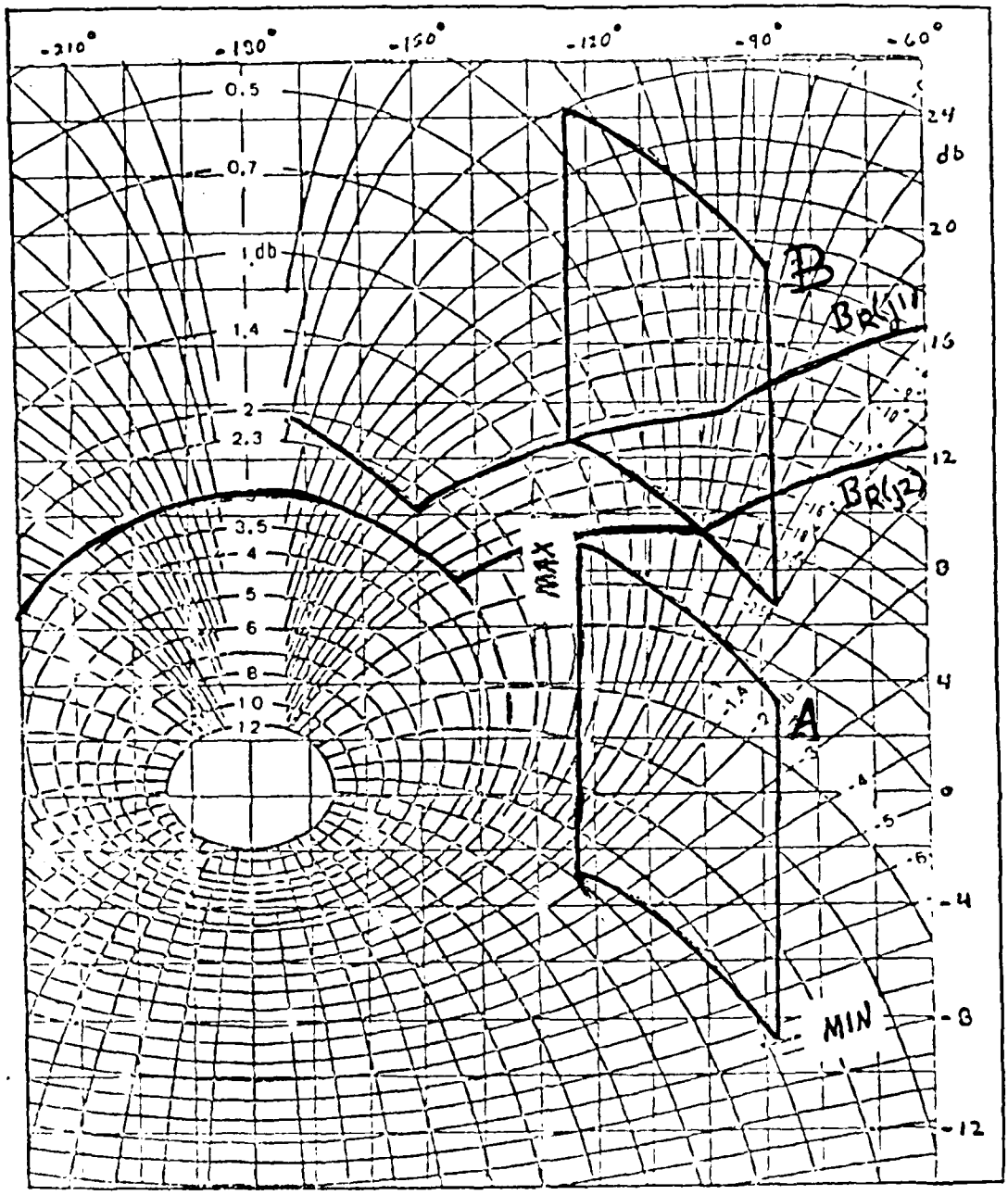

Fig. 2-6 Generating Bounds on the Nichols Chart (3:II-13)

lies above or to the right of the curve, $B_R(j\omega_i)$, the variation in T is less than or equal to the relative change allowed by the system specifications at ω_i. Repeat this process at every frequency of interest, thereby generating a set of design bounds, $\underline{B}_R(j\omega)$, for $L_o(j\omega)$ (16:291-292).

In order to effectively reject the disturbance, the following inequality must be satisfied:

$$1/|1 + \underline{L}(j\omega)| \leq |\underline{C}(j\omega)| \tag{2-10}$$

where $|\underline{C}(j\omega)|$ is the magnitude of the boundary, T_D, in Fig. 2-4. Convert the magnitudes to decibels, rearrange the terms and the inequality becomes:

$$Lm\ [1 + \underline{L}(j\omega)] \geq -Lm\ [\underline{C}(j\omega)] \tag{2-11}$$

Place a template on the modified Nichols Chart (remember the Nichols Chart is modified for the disturbance rejection case, Section II-6) such that its lowest point rests on the contour of constant $Lm\ [1 + L(j\omega_i)]$ equal to $-Lm\ [\underline{C}(j\omega_i)]$, the disturbance bound ($B_D(j\omega_i)$), at the frequency, ω_i. Transfer the nominal point to the Nichols Chart as before and slide the template along the bound, $B_D(j\omega_i)$ for $L_o(j\omega_i)$. Repeat this process, forming a set of bounds, $B_D(j\omega)$, for each frequency of interest.

Turn the Nichols Chart upright again. Currently two bounds exist for every frequency of interest. The command response bounds, B_R, and

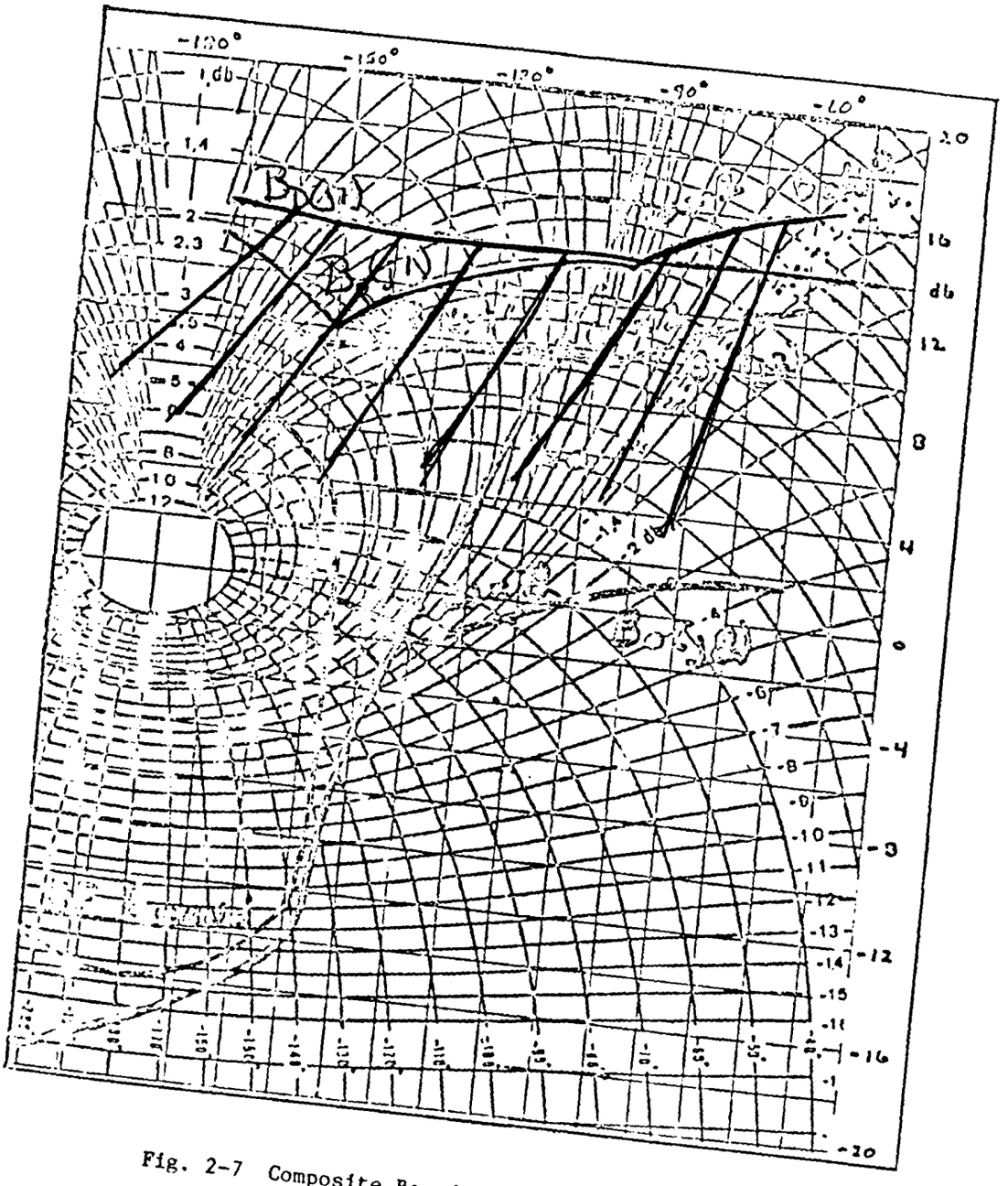

Fig. 2-7 Composite Bound for ω = 1 rad/sec (3:II-16)

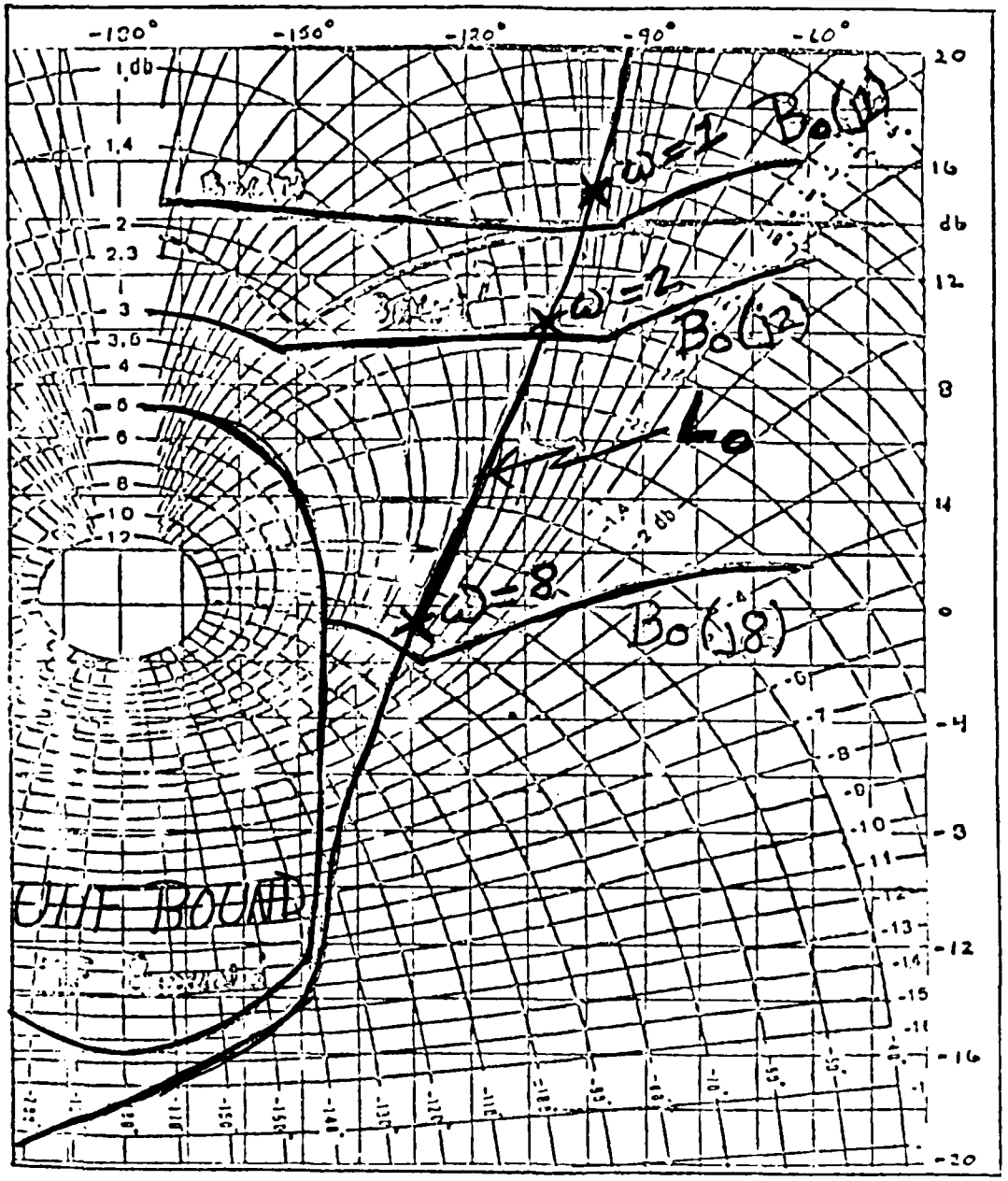

Fig. 2-8 Nominal Transmission Loop, L_o Shaped (3:II-16)

the disturbance rejection response bounds, B_D (see Fig. 2-7). Form the composite bound, B_o, by eliminating the lower of the two bound lines at each phase. Thus, the composite bound consists of the worse of the two bounds for every ω_i. Repeat this process for every frequency, thus forming a set of nominal bounds, $B_o(j\omega)$ (see Fig. 2-8). Use these worst bounds to shape the L_o.

10. Universal High Frequency (UHF) Bound

The Universal High Frequency (UHF) Bound ensures a positive gain and phase margin for the loop transmission, L. As the frequency approaches infinity, the plant templates become narrower, until they are considered a vertical line. The allowable variation in T also increases as frequency increases. The result is the bound of $L_o(j\omega)$ tends at high frequency to a very narrow region around 0 db and -180 degree point (the origin) on the Nichols Chart. The UHF Bound is used to avoid placing a closed-loop pole near the $j\omega$ axis, which results in a oscillatory disturbance response. As the frequency increases, the L_o bounds tend to follow the ovals encircling the origin. Choose one of the ovals near the origin as the bound. For this example choose the contour of constant magnitude corresponding to 5 db (Fig. 2-8). Find the template with the greatest vertical displacement, Δv db, from the templates of highest frequencies, Δv is also determined accurately by finding the maximum change in the limit of Lm $[\underline{P}(j\omega)]$ as ω approaches infinity. Translate the 5 db oval down the length of the template, Δv db, as in Fig. 2-8. This defines the UHF bound (14:20-22).

11. Shaping of the Nominal Loop Transmission, L_o

The shaping of the nominal loop transmission to satisfy the boundaries of L_o is an important step in the design. Design the nominal L, L_o, to satisfy the bounds by synthesizing a transfer function such that the magnitude and phase does not violate any of the boundaries. Do this by trial and error. One way to start the L_o design, is to use P_o. This avoids any implicit cancellation of roots in determining G. This also simplifies some of the work later, since $L_o = G P_o$, where P_o and L_o are known.

The optimal design of L_o has the lowest achievable bandwidth to solve the bounds. The optimal L_o has the value of the bound at every frequency. In practical designs, the goal is to have the value of L_o be higher than, but as close as possible to, its corresponding bound. Thus, L_o has greater bandwidth than the optimal L_o. Therefore, the design is a tradeoff between getting the optimum path for L_o (minimum bandwidth) which requires many poles and zeros and using a simpler L_o (larger bandwidth) with fewer poles and zeros.

At high frequency, relative to the frequencies of interest, add poles (normally complex pairs) to lessen the bandwidth of the design as rapidly as possible.

Figure 2-8 shows a practical design for the above example. Any right half plane (rhp) poles and/or zeros of P_o are included in the L_o to avoid any attempt to cancel the rhp poles or zeros with poles or zeros in G. For another example and a discussion of loop transmission shaping see Appendix A.

12. Solving for the Compensator, G

Find the compensator G from L_o.

$$L_o = G P_o$$

$$G = L_o/P_o \qquad (2\text{-}12)$$

If the L_o does not contain the roots of P_o, then the compensator G must cancel them. This cancellation occurs only for the purpose of design. In actual implementation, cancellation does not result (nor is it necessary) since P varies over the entire range of uncertainty. With G known, the loop transmission, L, can be determined for any particular plant $P(j\omega)$.

The L_o is properly shaped when it meets all of the design requirements, either on or above the bound, $B_o(j\omega_i)$, at each frequency. With a properly shaped nominal loop transmission, the variation in T (resulting from the uncertainty in P) is less than or equal to the allowable relative change in T, defined by the system specifications (16:291). The final step is to design the prefilter, F.

13. Design of the Prefilter, F

A properly designed L_o only guarantees that the variation in $|T(j\omega)|$ is less than or equal to the allowed variation. The prefilter positions the Lm $[T(j\omega)]$ within the frequency domain system specifications envelope. For the example the magnitude of the frequency response must remain within the bounds T_U and T_L (see Fig. 2-4). The bounds are redrawn in Fig. 2-9. One method to find the prefilter is as follows. Place the nominal point of the $\omega = 1$ rad/sec plant template on the Nichols Chart where the $L_o(j1)$ point occurs. Record the maximum and

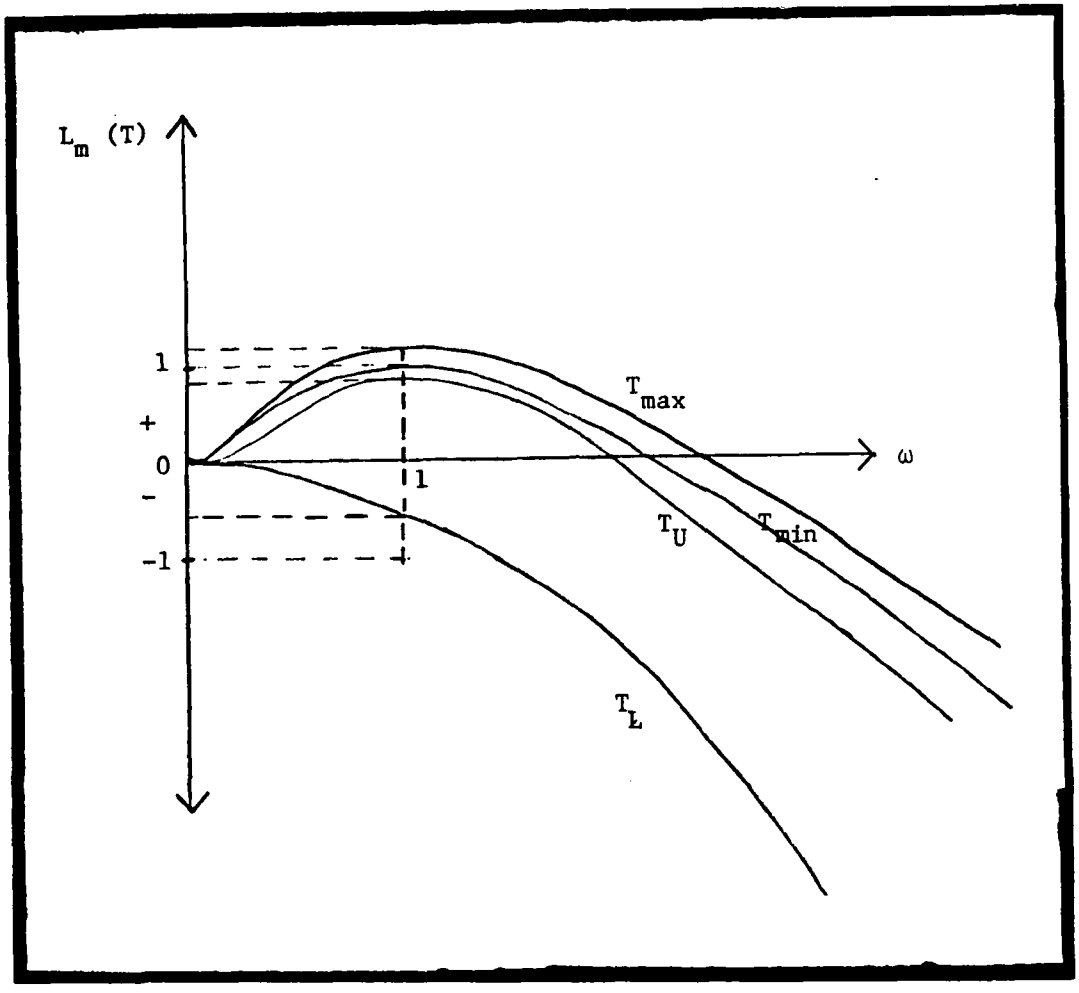

Fig. 2-9 Requirements of F (3:II-19)

minimum values of Lm (T). For the example, the values are 1.2 and 1.0 db. Compare these values found to the maximum and minimum values allowed by the frequency domain system specifications of Fig. 2-9 at $\omega = 1$ rad/sec. For the example the values are 0.7 and -0.8 db. Determine the range, in decibels, Lm (T) must raise or lower the response

to fit within the bounds T_U and T_L. For example, at ω = 1 rad/sec, the actual Lm (T) must be $0.7 < Lm\,[T(j1)] < -0.8$ db. From the plot of L_o, the range of Lm (T) is $1.2 < Lm\,[T(j1)] < 1.0$ db. To lower Lm [T(j1)] into the desired range, the prefilter, Lm (F) required is

$$(0.7 - 1.2) > Lm\,[F(j1)] > (-0.8 - 1.0)$$

$$\text{or } -0.5 > Lm\,[F(j1)] > -1.8 \quad \text{(see Fig. 2-9)} \quad (2\text{-}13)$$

Repeat the process for each frequency corresponding to the plant templates used. Thus the difference between the T_U and T_{max} curves and the difference between the T_L and T_{min} curves indicate the requirements for F as a function of frequency (Fig. 2-9).

The bounds on F, $[Lm\,(T_U) - Lm\,(T_{max})] > Lm\,(F) > [Lm\,(T_L) - (T_{min})]$, are plotted as a function of frequency (Fig. 2-10). Using the straight line approximation, determine the transfer function, F, whose magnitude lies within these bounds. This transfer function is the prefilter (16:301).

The single loop design is now complete. The system response is guaranteed to remain within the bounds of the system performance specifications, provided the uncertainty in P stays within the range predicted by the model (16:288).

14. Summary

This chapter presented an overview of the Quantitative Feedback Theory (QFT) technique of Dr. Horowitz for a SISO system. The technique is performed completely in the frequency domain, requiring only simple

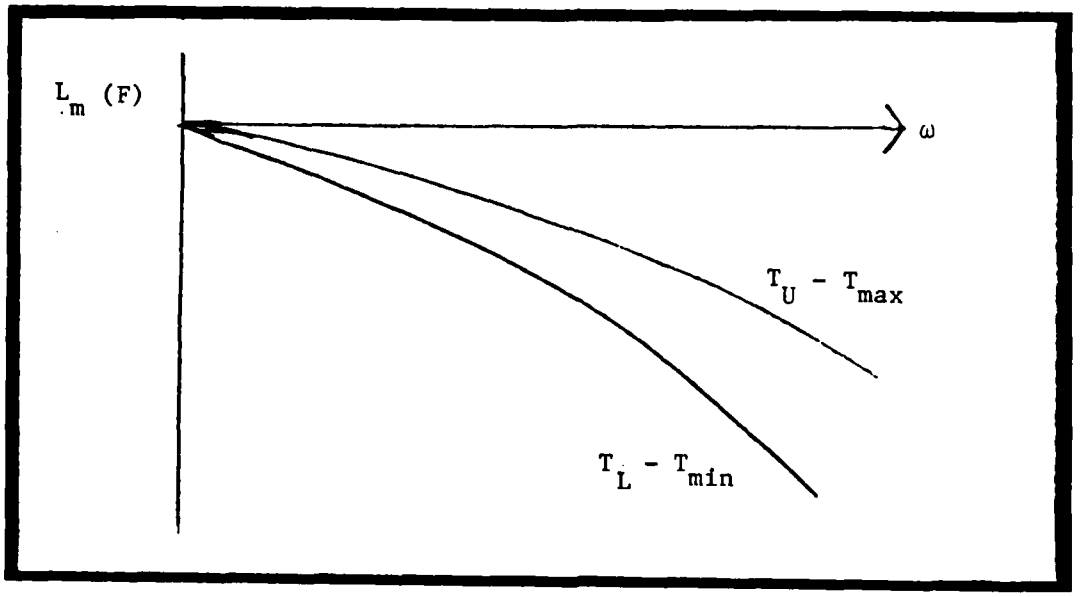

Fig. 2-10 Bounds on the Prefilter, F

algebraic calculations. Nichols Charts and Bode Plots are used extensively and much of the technique is performed graphically.

The problem is defined, then the system specifications are translated into the frequency domain. These specifications generate limits or boundaries of the frequency response for the system control ratio and the loop transmission. Two compensator elements, G and F, control the system response to inputs and disturbances such that the system response meets the system performance specifications.

III. QUANTITATIVE FEEDBACK THEORY:

MULTIPLE INPUT-MULTIPLE OUTPUT (MIMO) SYSTEM

1. Introduction

The design for a MIMO system involves the design of equivalent SISO system loops. The design process for these individual loops are the same as the design of a SISO system described in Chapter II.

In general, an n x n MIMO system can be represented in matrix notation as

$$\underline{y} = \underline{P}\underline{u} \tag{3-1}$$

where $\underline{y}$ = vector of plant outputs

$\underline{u}$ = vector of plant inputs

$\underline{P}$ = plant matrix of transfer functions relating $\underline{u}$ to $\underline{y}$

The P matrix is formed from either the system state space matrix representation or from the system linear differential equations.

Professor Horowitz has shown, by using fixed point theory (15), that the inverse of the P matrix, referred to as $\underline{Q}'$, contains elements which are the inverse of n^2 single loop transfer functions equivalent to the original MIMO plant. Thus, the MIMO problem is separated into n equivalent SISO systems and n^2 prefilter/disturbance problems, which are each designed as outlined in Chapter II (13:677).

2. The MIMO Plant

Consider the multiple input-multiple output plant of Fig. 3-1. The n x 1 input vector, $\underline{u}$, produces an n x 1 output vector, $\underline{y}$. $\underline{P}$, the n x n plant matrix, describes the relationship between $\underline{y}$ and $\underline{u}$. $\underline{P}$ is only an

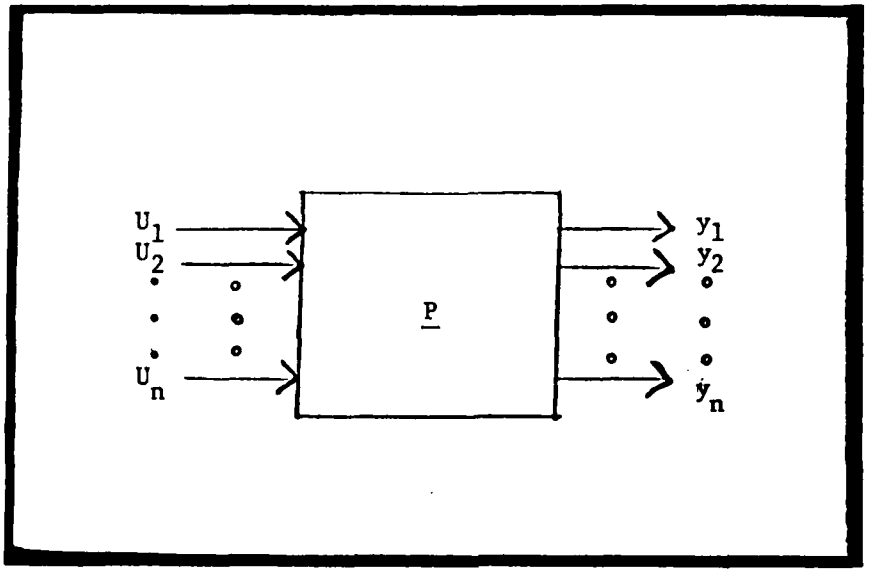

Fig. 3-1 A MIMO Plant

element in $\underline{P}$, the set of all possible plant matrices. Assume the uncertainty in $\underline{P}$ can be determined, or at least bounded. Also assume the input and output vectors are of the same dimension. This appears restrictive, but with n inputs, at most only n outputs are independently controlled (17:530-536). If the model defines an unequal number of inputs and outputs, the first task is to modify the model such that the dimensions of the input and output are the same.

The state space representation for a MIMO system is:

$$\dot{\underline{x}} = \underline{A}\underline{x} + \underline{B}\underline{u}$$

$$\underline{y} = \underline{C}\underline{x} \qquad (5:93) \qquad (3\text{-}2)$$

The block diagram representing these equations is in Fig. 3-2.

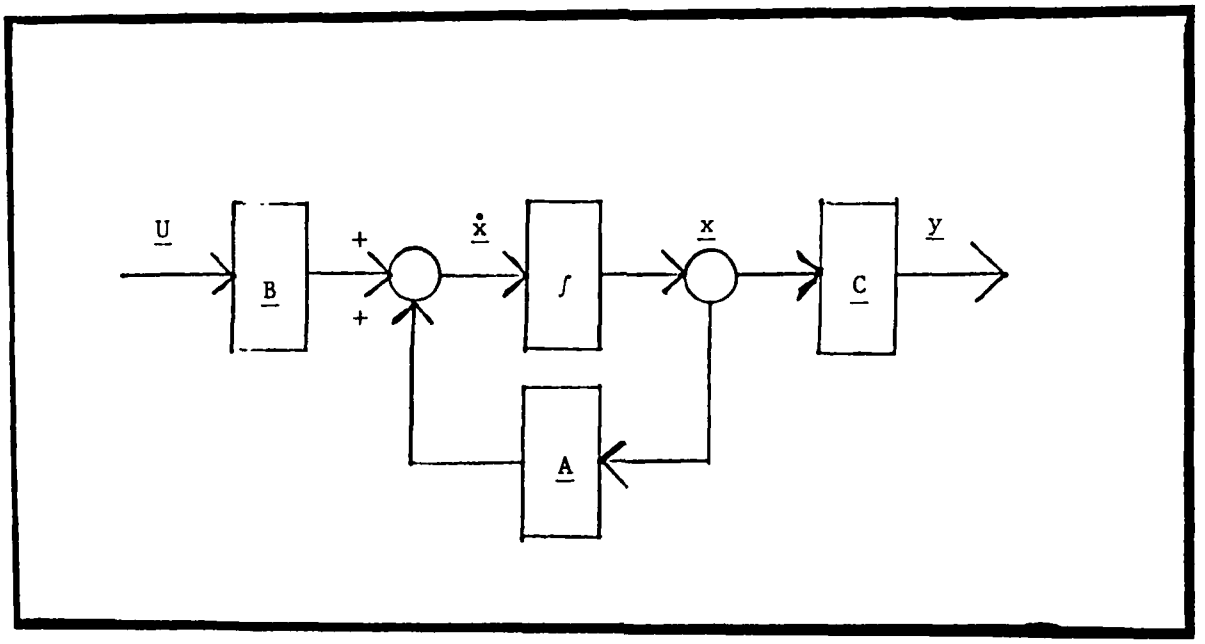

Fig. 3-2 State Space Block Diagram for Eq. 3-2

If the plant model is in terms of n coupled, linear, time invariant differential equations, the general plant model for a second order system is:

$$(a)y_1 + (bs^2 + cs)y_2 = (f)u_1 + (g)u_2$$

$$(ds)y_1 + (e)y_2 = (h)u_1 + (i)u_2 \qquad (3\text{-}3)$$

where a thru i are constant coefficients, the y's are the outputs and the u's are the inputs. In matrix notation the system looks like:

$$\begin{bmatrix} a & bs^2 + cs \\ ds & e \end{bmatrix} \underline{y} = \begin{bmatrix} f & g \\ h & i \end{bmatrix} \underline{u} \qquad (3\text{-}4)$$

Let the matrix premultiplying the output vector, $\underline{y}$, be $\underline{M}$ and the matrix premultiplying the input vector, $\underline{u}$, be $\underline{N}$. The system now looks like:

$$\underline{My} = \underline{Nu} \qquad (3\text{-}5)$$

The plant matrix needed is defined by:

$$\underline{y} = \underline{Pu} \qquad (3\text{-}6)$$

Thus, the plant matrix, $\underline{P}$, is

$$\underline{P} = \underline{M}^{-1}\underline{N} \qquad (3\text{-}7)$$

Another method used to generate $\underline{P}$, is to use the state space matrices directly. Although any number of states are represented, assume that the input and output vectors, $\underline{u}$ and $\underline{y}$, are of the same dimensions. Assuming the system is linearized and the $\underline{A}$, $\underline{B}$ and $\underline{C}$ matrices are time invariant, the plant matrix is:

$$\underline{P} = \underline{C}[s\underline{1} - \underline{A}]^{-1}\underline{B} \qquad (3\text{-}8)$$

This plant matrix is actually a member of a set of possible plant matrices, whose set is caused by the uncertainty in the plant parameters.

In practice, only a finite set of $\underline{P}$ matrices are formed representing the plant under varying conditions.

3. MIMO Compensation

The basic MIMO compensation structure for a two-by-two MIMO system is in Fig. 3-3. The structure for a three-by-three MIMO system is in Fig. 3-5. These systems are similar to the SISO system of Chapter II. They consist of the uncertain plant matrix, $\underline{P}$, the diagonal compensation matrix, $\underline{G}$, and the prefilter matrix, $\underline{F}$. This thesis only considers a diagonal $\underline{G}$ matrix, though a non-diagonal G matrix gives the designer much more flexibility in his design (12:14-15). A more detailed schematic of the two-by-two MIMO system is given in Fig. 3-4 and the three-by-three MIMO schematic is in Fig. 3-6. The $\underline{G}$ and $\underline{F}$ functions are the same as the G and F of the SISO system.

In general $\underline{G} = \text{diag}\,[g_i]$, $\underline{F} = [f_{ij}]$ and $\underline{P} = [p_{ij}]$:

$$\underline{G} = \begin{bmatrix} g_1 & 0 & \cdots & 0 \\ 0 & g_2 & \cdots & 0 \\ \vdots & \vdots & & \vdots \\ 0 & 0 & \cdots & g_n \end{bmatrix} \quad \underline{F} = \begin{bmatrix} f_{11} & f_{12} & \cdots & f_{1n} \\ f_{21} & f_{22} & \cdots & f_{2n} \\ \vdots & \vdots & & \vdots \\ f_{n1} & f_{n2} & & f_{nn} \end{bmatrix} \quad \underline{P} = \begin{bmatrix} p_{11} & p_{12} & \cdots & p_{1n} \\ p_{21} & p_{22} & \cdots & p_{2n} \\ \vdots & \vdots & & \vdots \\ p_{n1} & p_{n2} & & p_{nn} \end{bmatrix} \tag{3-9}$$

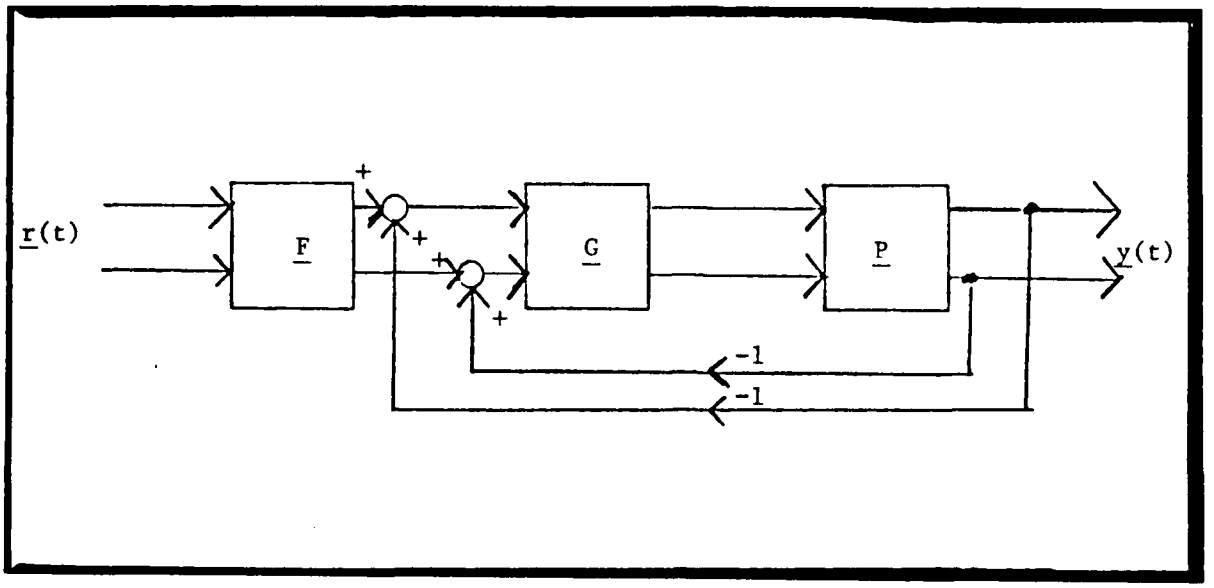

Fig. 3-3 MIMO Control Structure (Two-By-Two System)

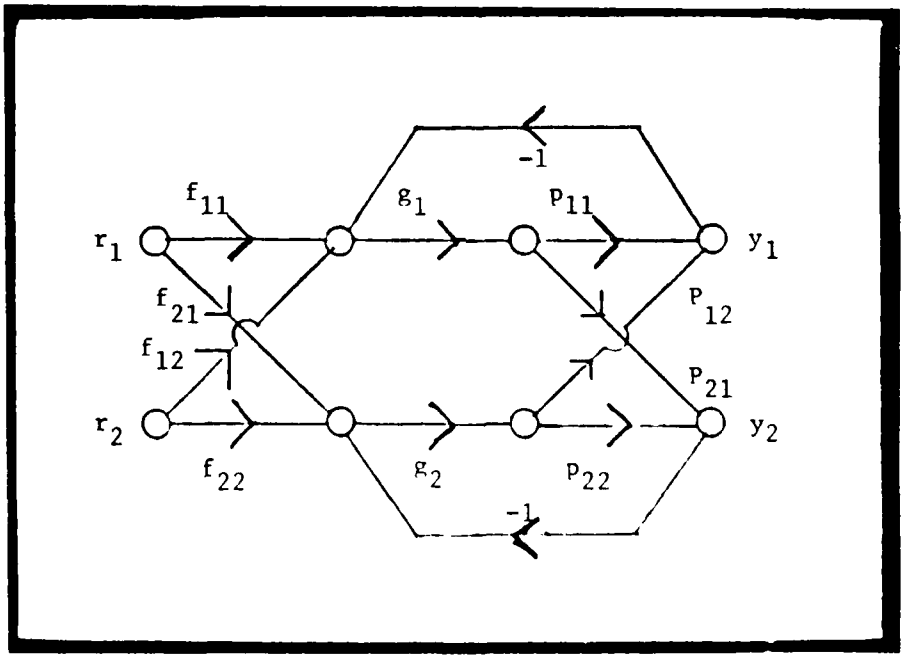

Fig. 3-4 Two-By-Two MIMO System Schematic

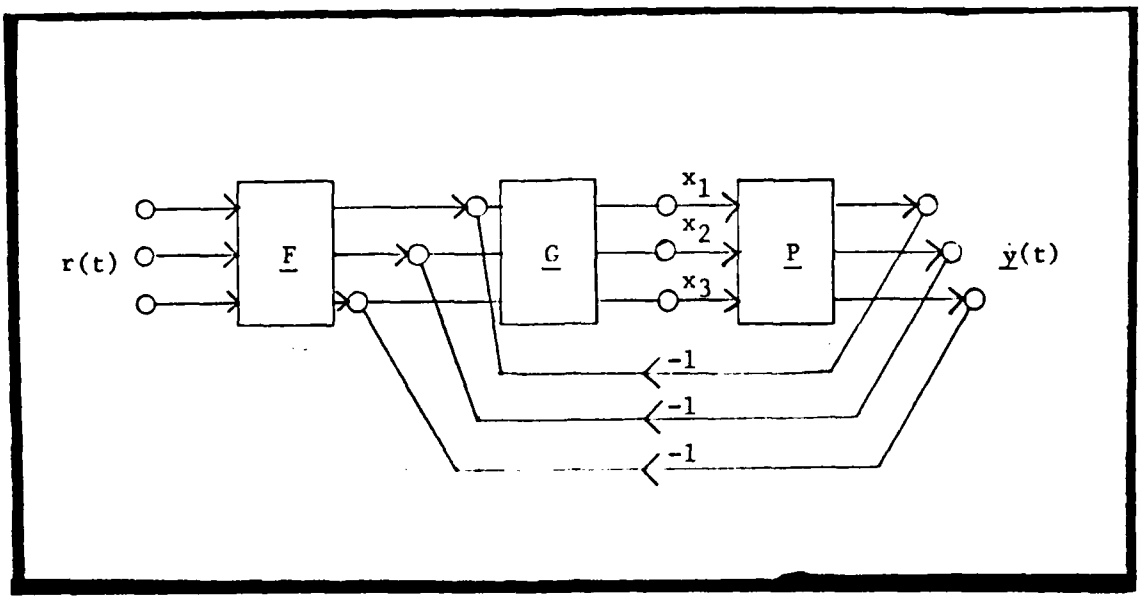

Fig. 3-5 MIMO Control Structure
(Three-By-Three System)

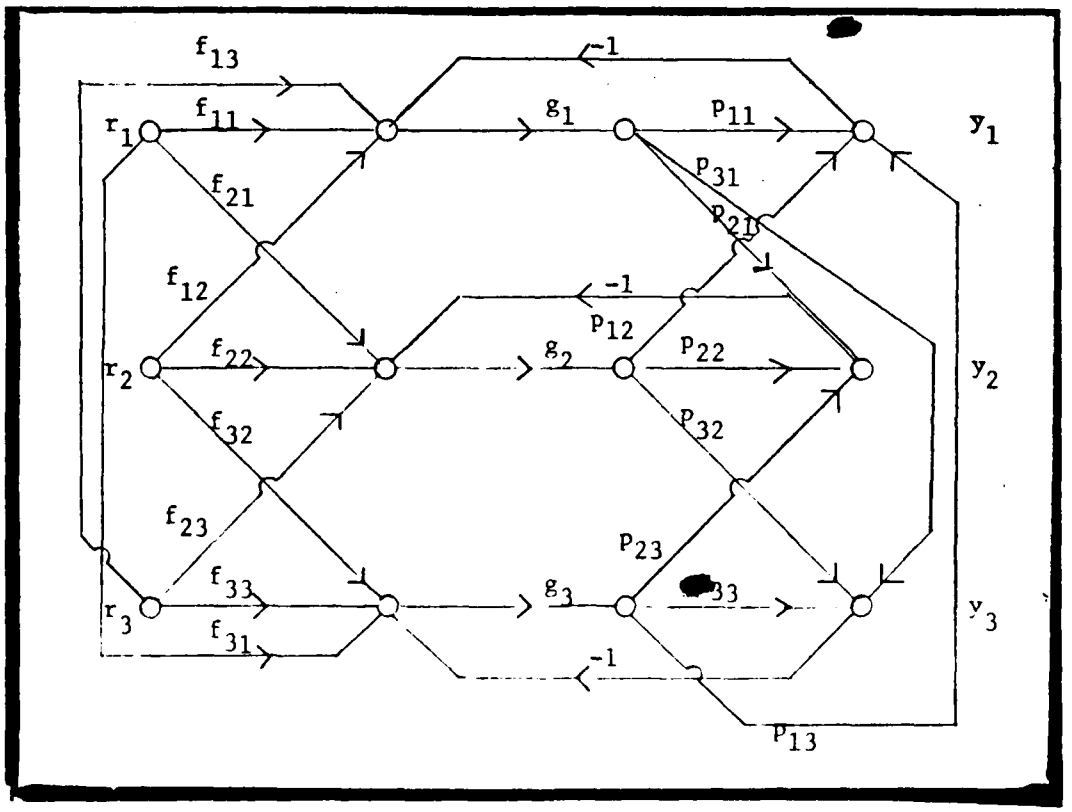

Fig. 3-6 Three-By-Three MIMO System Schematic

Using Eq. 3-9, the matrices for a two-by-two system are:

$$\underline{G} = \begin{bmatrix} g_1 & 0 \\ 0 & g_2 \end{bmatrix} \quad \underline{F} = \begin{bmatrix} f_{11} & f_{12} \\ f_{21} & f_{22} \end{bmatrix} \quad \underline{P} = \begin{bmatrix} p_{11} & p_{12} \\ p_{21} & p_{22} \end{bmatrix} \tag{3-10}$$

4. Constraints on the Plant Matrix

The set of $\underline{P}$ must be tested to ensure that two critical conditions are met (15:86-90):

1. $\underline{P}$ must not be singular for any combination of possible plant parameters. Thus P^{-1} exists.
2. As $s \to \infty$, $|p_{11}p_{22}| > |p_{12}p_{21}|$ for all possible plants for the two-by-two case. As $s \to \infty$, $|p_{11}p_{22}p_{33}| > |p_{11}p_{23}p_{32}| + |p_{12}p_{21}p_{33}| + |p_{12}p_{23}p_{31}| + |p_{13}p_{22}p_{31}| + |p_{13}p_{21}p_{32}|$ for all possible plants for the three-by-three case. See Reference 15 for higher order plants. This condition is necessary only if Eq. 3-7 and the original method (see p. 42-48) are used to generate the plant.

The first condition ensures controllability of the plant. The inverse of $\underline{P}$ produces the effective transfer functions used in the design. If the $\underline{P}$ matrix, in its original ordering of the input and output matrices, does not satisfy the second condition, then a reordering of the input and output matrices might satisfy the condition.

5. Effective SISO Loops

Define the matrix $\underline{Q}' = \underline{P}^{-1}$ whose elements are q'_{ij}:

$$\underline{P}^{-1} = \underline{Q}' = \begin{bmatrix} q'_{11} & q'_{12} & \cdots & q'_{1n} \\ q'_{21} & q'_{22} & \cdots & q'_{2n} \\ \cdot & \cdot & & \cdot \\ \cdot & \cdot & & \cdot \\ \cdot & \cdot & & \cdot \\ q'_{n1} & q'_{n2} & & q'_{nn} \end{bmatrix} \qquad (3\text{-}11)$$

Then the n^2 effective transfer functions are $q_{ij} = 1/q'_{ij}$, symbolically represented by $\underline{Q} = 1/\underline{Q}'$:

$$\underline{Q} = \begin{bmatrix} q_{11} & q_{12} & \cdots & q_{1n} \\ q_{21} & q_{22} & \cdots & q_{2n} \\ \cdot & \cdot & & \cdot \\ \cdot & \cdot & & \cdot \\ \cdot & \cdot & & \cdot \\ q_{n1} & q_{n2} & & q_{nn} \end{bmatrix} \qquad 1/\underline{Q}' = \begin{bmatrix} 1/q'_{11} & 1/q'_{12} & \cdots & 1/q'_{1n} \\ 1/q'_{21} & 1/q'_{22} & \cdots & 1/q'_{2n} \\ \cdot & \cdot & & \cdot \\ \cdot & \cdot & & \cdot \\ \cdot & \cdot & & \cdot \\ 1/q'_{n1} & 1/q'_{n2} & & 1/q'_{nn} \end{bmatrix}$$

$$\underline{P} = [p_{ij}] \qquad \underline{P}^{-1} = [q'_{ij}] = Q' \qquad (3\text{-}13)$$

$$\underline{Q} = [q_{ij}] = 1/\underline{Q}' = [1/q'_{ij}] \qquad \underline{P}^{-1} = [1/q_{ij}] \qquad (3\text{-}14)$$

Reference 15 contains the derivations and proof of this equivalence. The n x n MIMO system is transformed into n^2 SISO problems. The general transformation result of n^2 SISO system loops is in Fig. 3-7. Figure 3-8 shows the four effective SISO loops (in the boxed area) resulting from a two-by-two system and the nine effective SISO loops (13:682) resulting from a three-by-three system.

Each SISO loop in Figs. 3-7 and 3-8 is considered as an individual SISO design problem, which is solved using the procedures explained in

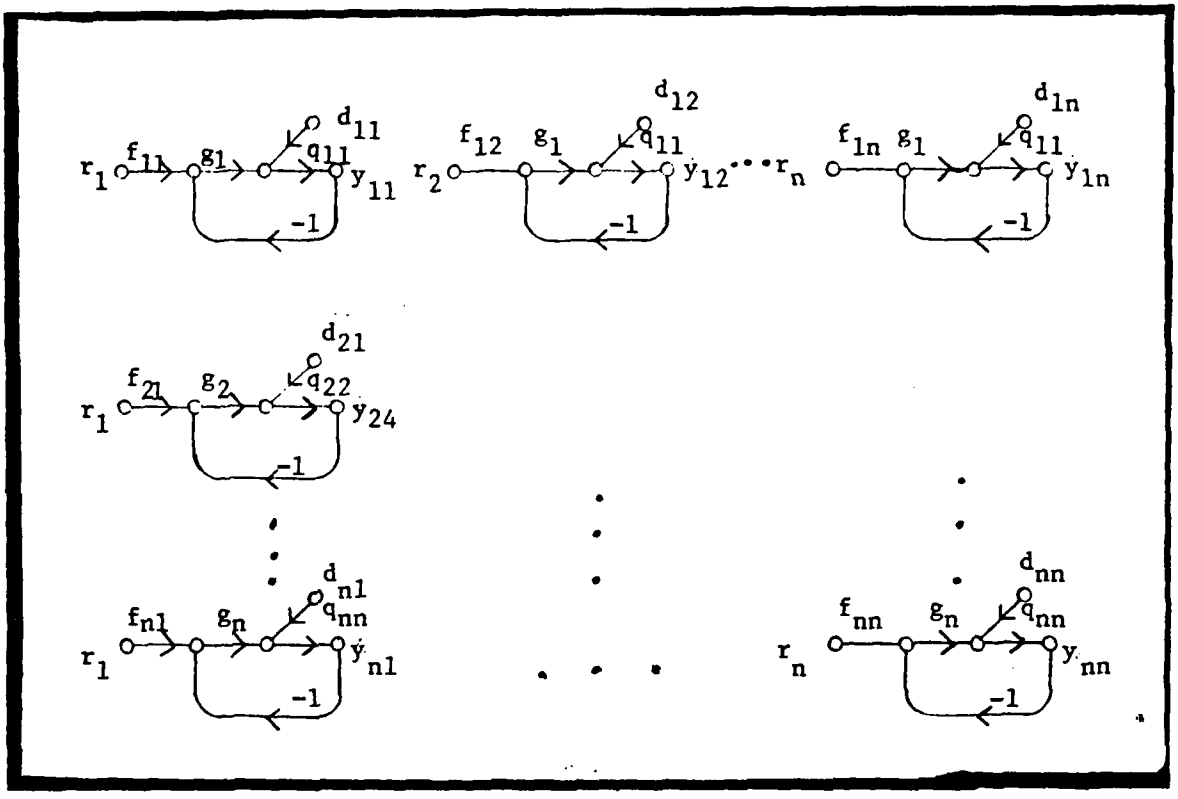

Fig. 3-7 Effective SISO Loops (in general)

Chapter II. The f's and g's are the compensator elements of the $\underline{F}$ and $\underline{G}$ matrices described previously.

The disturbances, d_{ij}, represent the interaction between the loops:

$$-d_{ij} = \sum_{k} \frac{b_{kj}}{q_{ik}}, \quad k \neq i \tag{3-15}$$

where the numerator, b_{kj}, is the upper response bound, (T_U or T_D in Fig. 2-4), for the respective input/output relationship. These are obtained from the design specifications (13:681-687). The first subscript, k, refers to the output variable, and the second subscript, j, refers to

the input variable. Therefore, b_{kj} is a function of the response requirements on the output, y_k, due to the input, r_j. The lower bound, a_{kj}, needs defining only when there is a command input.

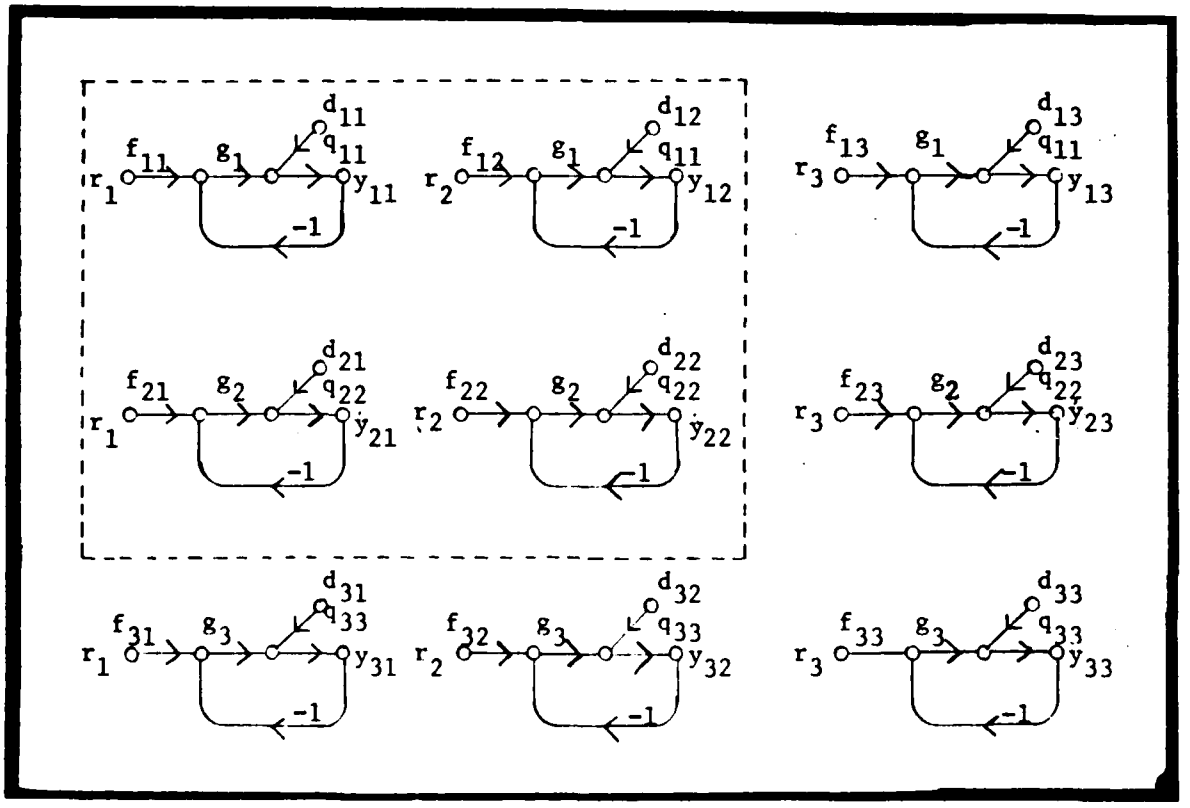

Fig. 3-8 Effective SISO Loops
Two-By-Two (Boxed in Loops)
Three-By-Three (All 9 Loops)

For the disturbance rejection problem, the responses must be less than some bound (i.e. $y_{ij} \leq b_{ij}$). Thus the loop equations become:

$$b_{ij} \geq y_{ij} = \frac{d_{ij} \, |q_{ii}|}{|1 + G_i \, q_{ii}|} \tag{3-16}$$

where $G_i \, q_{ii} = L_i$. Reorganizing:

$$|1 + L_i| \geq \frac{-d_{ij} |q_{ii}|}{b_{ij}} \tag{3-17}$$

using Eq. 3-15, and rewriting Eq. 3-17:

$$|1 + L_i| \geq \frac{\left[\frac{b_{kj}}{q_{jk}} + \frac{b_{ki}}{q_{ik}}\right] |q_{ii}|}{b_{ij}} \tag{3-18}$$

For example, in a three-by-three system for the first loop, L_1, $i = 1$, $j = 2$, and in the first term $k = 2$ and in the second term $k = 3$, Eq. 3-18 becomes:

$$|1 + L_1| \geq \frac{\left[\frac{b_{22}}{|q_{12}|} + \frac{b_{32}}{|q_{13}|}\right] |q_{11}|}{b_{12}} \tag{3-19}$$

Remember only use the magnitude in the disturbance calculations. This assumes the worst case.

Recently, this technique was improved. This improvement involves modifying the q's, using the information from the previously designed

loops, the g's. This reduces the overdesign inherent in the early part of the design process. The final loop, is designed using the exact equation (10:977). The exact equation represents the loop and the interactions caused by the other loops. This thesis uses the original method for the first two loops and the improved method for the last loop.

The order in which the loops are designed may be significant. Any order can be used, but some orders produce less overdesign (less bandwidth) than others. The last loop designed has the least amount of overdesign, therefore do the most constrained loop first, and so on through all of the loops.

6. Basically Non-Interacting (BNIC) Loops

A basically non-interacting (BNIC) loop (13:679) is one in which the output, y_k, due to the input, r_k, is ideally zero. Plant uncertainty and loop interaction makes the ideal response unachievable. Thus, the system performance specifications describe a range of acceptable responses for the commanded output and a maximum tolerable response for the uncommanded outputs. The uncommanded outputs are treated as disturbances.

7. Summary

This chapter describes the multiple input-multiple output system and the plant matrix. Guidelines for finding the $\underline{P}$ matrix, which relates the input vector to the output vector are given.

The separation of the MIMO system into several SISO systems is presented using the $\underline{P}^{-1}$. The equivalent SISO loops are designed according to the SISO design method in Chapter II.

IV. AIRCRAFT MODEL

1. Introduction

The aircraft model in this thesis is a hypothetical aircraft designed by Lockheed, Pratt and Whitney and Honeywell. The aircraft was designed as part of the study, the Flight Propulsion Control Coupling (FPCC) and Dynamic Interaction Investigation (7,8). This hypothetical, or "paper" aircraft is referred to as the FPCC aircraft (Fig. 4-1).

The aircraft's basic design criterion is for a future multimission fighter whose primary function is supersonic/transonic air superiority. Its secondary function is transonic close air support. The aircraft's dash, or top speed is Mach 2.2 to 3. The aircraft's takeoff weight is 34,000 pounds and the maneuvering weight is 29,000 pounds. The maneuvering wing loading is 44.3 pounds per square foot. It is capable of conventional or short takeoffs and landings and has relaxed static stability and direct side force control.

The aircraft uses many flight control surfaces to meet the requirements. The primary flight control surfaces are maneuvering flaps, leading edge flaps, jet flaps, canards, canard flaps, chin canards, upper rudder, lower rudder, and ailerons (Fig. 4-2). The vertical (chin) canards, rudder and ailerons generate the forces for lateral control.

2. Aircraft Description

This thesis involves designing a lateral flight controller. The equations of motion are not explicitly used by the author because the computer simulation program, FPCCSIM, is available. Appendix A of

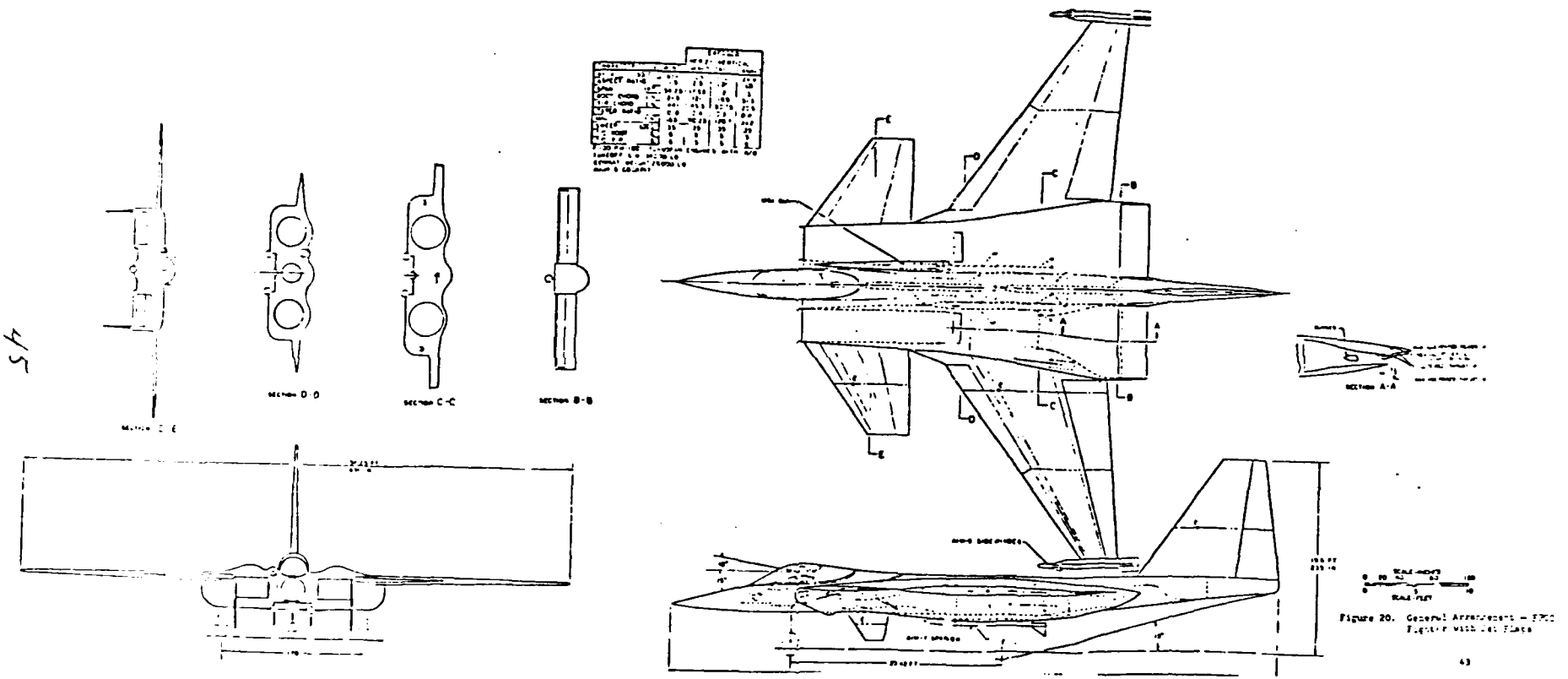

Fig. 4-1 FPCC Aircraft (7:43)

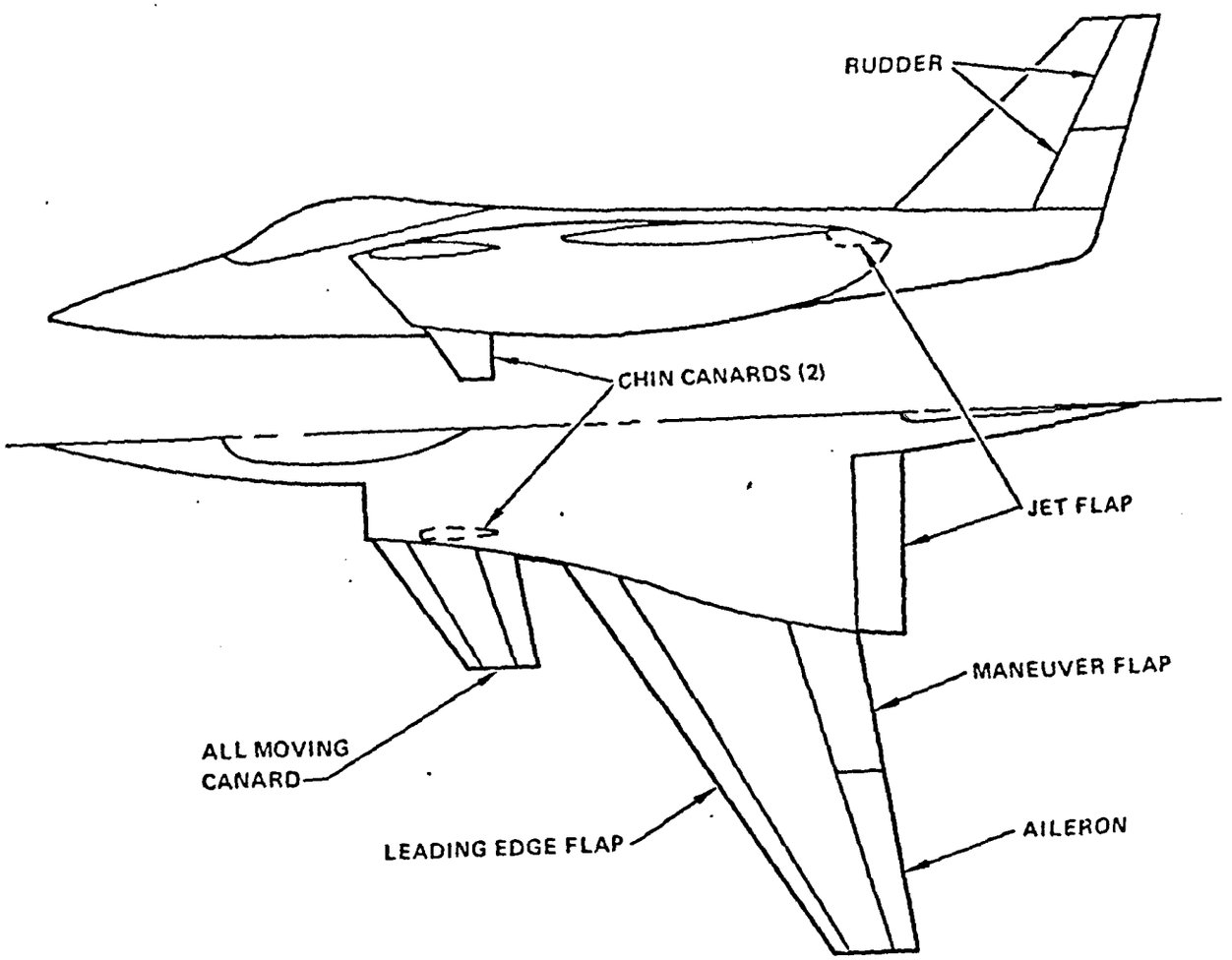

CONTROL FUNCTION	CONTROL SURFACE
LIFT	MANEUVER FLAP L.E. FLAP JET FLAP CANARD
SIDE FORCE	CHIN CANARDS LOWER RUDDER
PITCH	CANARD CANARD FLAP
YAW	UPPER RUDDER LOWER RUDDER
ROLL	AILERON (PER SIDE)

Fig. 4-2 Flight Controls Layout and Function (7:35)

Reference 8, pages 157-163, contains the equations of motion. FPCCSIM generates the state space model of the aircraft at the flight conditions of interest. Note the aircraft is not designed for decoupled maneuvers, though it does have the capability. Also the aircraft is statically unstable at mach 0.9.

The FPCSSIM computer program was written as part of the FPCC study. The FPCCSIM simulation uses a non-linear 6 degree-of-freedom perturbation model. This is the same program used by previous AFIT thesis students in their work using other design techniques.

The command inputs available are roll angle (ϕ), side velocity (v) and yaw rate (r). The commanded inputs are limited in this thesis to deflections of the ailerons, the rudder and the vertical canard. The outputs measured are roll angle, roll rate (p), side velocity and yaw rate.

As stated above, the aircraft model is in the state space form:

$$\dot{\underline{x}} = \underline{A}\underline{x} + \underline{B}\underline{u} \tag{4-1}$$

$$\underline{y} = \underline{C}\underline{x} \tag{4-2}$$

For example, the Eq. 4-3 and 4-4 are outputs from FPCCSIM for the slow speed condition (mach 0.6 at sea level).

The state vector and the control vector are:

$$\underline{A} = \begin{bmatrix}
-2.350 & 1.470 & -0.0106 & 0.0 & 0.0 & 0.0 & 0.0 & 0.0 & 0.0 & 0.0 & 0.0 & 0.0 \\
0.256 & -0.989 & 0.019 & 0.0 & 0.0 & 0.0 & 0.0 & 0.0 & 0.0 & 0.0 & 0.0 & 0.0 \\
13.200 & -666.0 & -0.687 & 32.100 & 0.0 & 0.0 & 0.0 & 0.0 & 0.0 & 0.0 & 0.0 & 0.0 \\
1.000 & 0.018 & 0.0 & 0.0 & 0.0 & 0.0 & 0.0 & 0.0 & 0.0 & 0.0 & 0.0 & 0.0 \\
0.0 & 1.000 & 0.0 & 0.0 & 0.0 & 0.0 & 0.0 & 0.0 & 0.0 & 0.0 & 0.0 & 0.0 \\
0.0 & 0.0 & 1.000 & -12.000 & 669.0 & 0.0 & 0.0 & 0.0 & 0.0 & 0.0 & 0.0 & 0.0 \\
0.0 & 0.0 & 0.0 & 0.0 & 0.0 & 0.0 & -0.463 & 0.0639 & -0.0011 & 0.0 & 0.0 & 0.0 \\
0.0 & 0.0 & 0.0 & 0.0 & 0.0 & 0.0 & 674.0 & -2.820 & -0.0568 & -0.577 & -0.00049 & -0.000461 \\
0.0 & 0.0 & 0.0 & 0.0 & 0.0 & 0.0 & -12.100 & 0.105 & -0.0297 & -32.100 & 0.00067 & -0.000073 \\
0.0 & 0.0 & 0.0 & 0.0 & 0.0 & 0.0 & 1.000 & 0.0 & 0.0 & 0.0 & 0.0 & 0.0 \\
0.0 & 0.0 & 0.0 & 0.0 & 0.0 & 0.0 & 0.0 & -1.000 & 0.018 & 669.0 & 0.0 & 0.0 \\
0.0 & 0.0 & 0.0 & 0.0 & 0.0 & 0.0 & 0.0 & 0.018 & 1.000 & 0.0 & 0.0 & 0.0
\end{bmatrix} \quad (4\text{-}3)$$

$$\underline{B} = \begin{bmatrix}
0.198 & 0.0 & 0.0 & 0.166 & -0.0275 & 0.0487 & 0.0 & 0.0 & -0.968 & 0.968 \\
0.00727 & 0.0 & 0.0 & -0.188 & 0.0368 & 0.00153 & 0.000029 & -0.000029 & -10.300 & 10.300 \\
0.0 & 0.0 & 0.0 & 1.780 & 0.581 & 0.0 & 0.0 & 0.0 & 0.0 & 0.0 \\
0.0 & 0.0 & 0.0 & 0.0 & 0.0 & 0.0 & 0.0 & 0.0 & 0.0 & 0.0 \\
0.0 & 0.0 & 0.0 & 0.0 & 0.0 & 0.0 & 0.0 & 0.0 & 0.0 & 0.0 \\
0.0 & 0.0 & 0.0 & 0.0 & 0.0 & 0.0 & 0.0 & 0.0 & 0.0 & 0.0 \\
0.0 & 0.640 & -0.0966 & 0.0 & 0.0 & -0.043 & 0.0 & 0.0 & 0.0 & 0.0 \\
0.0 & -1.430 & -4.730 & 0.0 & 0.0 & -0.616 & -0.000035 & -0.000035 & 0.0 & 0.0 \\
0.0 & 0.518 & 0.0198 & 0.0 & 0.0 & 0.00092 & 0.00109 & 0.00109 & 0.0 & 0.0 \\
0.0 & 0.0 & 0.0 & 0.0 & 0.0 & 0.0 & 0.0 & 0.0 & -387.0 & -387.0 \\
0.0 & 0.0 & 0.0 & 0.0 & 0.0 & 0.0 & 0.0 & 0.0 & 0.0 & 0.0 \\
0.0 & 0.0 & 0.0 & 0.0 & 0.0 & 0.0 & 0.0 & 0.0 & 0.0 & 0.0
\end{bmatrix} \quad (4\text{-}4)$$

$$\underline{x} = \begin{bmatrix} p \\ r \\ v \\ \phi \\ \psi \\ y \\ q \\ w \\ u \\ \theta \\ h \\ x \end{bmatrix} \qquad \underline{u} = \begin{bmatrix} \delta_a \\ \delta_c \\ \delta_{mf} \\ \delta_r \\ \delta_{vc} \\ \delta_j \\ F_1 \\ F_2 \\ CDI_1 \\ CDI_2 \end{bmatrix} \tag{4-5}$$

where the plant state space elements ($\underline{x}$) are:

- p body axis roll rate (rad/sec)
- r body axis yaw rate (rad/sec)
- v body axis side velocity (ft/sec)
- ϕ roll angle (rad)
- ψ yaw angle (rad)
- y cross range position reference to initial body axis (ft)
- q body axis pitch rate (rad/sec)
- g body axis pitch rate (rad/sec)
- w body axis vertical velocity (ft/sec)
- u body axis forward velocity (ft/sec)
- θ pitch angle (rad)
- h altitude (ft)
- x down range position reference to initial body axis (ft)

and the control input elements ($\underline{u}$) are:

δ_a	sum of both aileron deflections (deg)
δ_c	horizontal canard deflection (deg)
δ_{mf}	maneuver flap deflection (deg)
δ_r	rudder deflection (deg)
δ_{vc}	vertical canard deflection (deg)
δ_j	jet flap deflection with respect to fuselage line (deg)
F_1	net thrust engine 1 (lbs)
F_2	net thrust engine 2 (lbs)
CDI_1	inlet drag coefficient 1
CDI_2	inlet drag coefficient 2

Appendix B contains the FPCCSIM generated matrices. FPCCSIM also gives the trim condition of the aircraft for the flight condition. For this flight condition, 0.6 mach at sea level, the angle of attack is 1.03 degrees at 0.6 mach with a dynamic pressure of 533.04 lbs/sq in and a forward velocity of 670.5 ft/sec.

3. Lateral Equation Model

The above matrices are simplified by noting they contain both the lateral and longitudinal terms. The lateral terms in the plant state space matrix, $\underline{A}$, are p, r, v, ϕ, y, and ψ. Both y and ψ are eliminated with little degradation of the model. The lateral terms in the control input matrix, $\underline{B}$, are δ_a, δ_r, δ_{vc}, F_1, F_2, CDI_1 and CDI_2. The first three terms are the significant contributors in the lateral mode. Thus, the model is simplified to a 4 x 4 plant state space matrix and a 4 x 3 control input matrix. Simplifying and rewriting:

$$\begin{bmatrix} \dot{\phi} \\ \dot{v} \\ \dot{r} \\ \dot{p} \end{bmatrix} = \begin{bmatrix} 0.0 & 0.0 & 0.0180 & 1.0000 \\ 32.100 & -0.687 & -666.0 & 13.2 \\ 0.0 & 0.0190 & -0.989 & 0.256 \\ 0.0 & -0.0103 & 1.47 & -2.35 \end{bmatrix} \begin{bmatrix} \phi \\ v \\ r \\ p \end{bmatrix}$$

$$+ \begin{bmatrix} 0.0 & 0.0 & 0.0 \\ 0.0 & 1.78 & 0.581 \\ 0.00727 & -0.188 & 0.0368 \\ 0.198 & 0.166 & -0.0275 \end{bmatrix} \begin{bmatrix} \delta_a \\ \delta_r \\ \delta_{vc} \end{bmatrix} \qquad (4\text{-}6)$$

$$\begin{bmatrix} \phi \\ v \\ r \end{bmatrix} = \begin{bmatrix} 1.000 & 0.0 & 0.0 & 0.0 \\ 0.0 & 1.000 & 0.0 & 0.0 \\ 0.0 & 0.0 & 1.000 & 0.0 \end{bmatrix} \begin{bmatrix} \phi \\ v \\ r \\ p \end{bmatrix} \qquad (4\text{-}7)$$

The other lateral models are in Appendix B.

4. Flight Conditions

The three flight conditions used represent the aircraft's operational envelope. There is a slow speed condition, Flight Condition #1 (FC #1), which is at maximum weight (34,000 pounds) at sea level with full dry thrust (no afterburner) and a speed of 0.6 mach. The cruise condition, Flight Condition #2 (FC #2), is at maneuvering weight (29,000 pounds) at 30,000 feet and a speed of 0.9 mach. The third case, Flight Condition #3 (FC #3), is at maneuvering weight at 40,000 feet and a speed of 2.3 mach.

The maneuver performed is a horizontal translation. This maneuver requires displacing the aircraft laterally without a yaw rate or bank angle. The maneuver is performed by commanding a side velocity. The roll angle and yaw rate, generated by coupling with the side velocity, are commanded to zero. Any roll angle or yaw rate resulting from the coupling effects is treated as a disturbance, since it is desired that both remain zero.

The three flight conditions and the maneuver are the same that a previous thesis (2) used with a different design technique. Part of this thesis compares the results from that thesis to this one (Chapter VIII). Therefore, the same state space plant matrices must be used. Thus, the flight conditions are matched such that the three plant state space matrices are the same.

V. DESIGN OF THE FIRST TWO LOOPS

1. Introduction

This section presents in detail the first two loops designed for the flight controller. First the plant matrices are generated and then the system specifications are chosen. Next the order in which to design the loops is selected and the plant templates generated. The design phase begins by generating bounds for the first two loops and then designing the open loop transfer functions.

2. The Problem

Design a lateral flight controller for the horizontal translation maneuver using the QFT technique. The plant, the Flight Propulsion Control Coupled (FPCC) aircraft, is modeled as a three input-three output system in the lateral axis (Section IV-3). From Section IV-4, the only input is side velocity, v. Optimally, the other two control variables whose inputs are zero (roll angle, ϕ and yaw rate, r) remain zero. The system specifications are derived from the responses of a previous thesis (2).

3. The Plant Matrices

The QFT technique requires the plant description in the transfer function form. The FPCCSIM computer program generates state space models for each of the flight conditions (FC). Another computer program generates the transfer function plant matrix from the state space matrices for each FC.

Appendix B contains the full aircraft state space matrices. Since this design includes only the lateral axis, the full state space matrices are unnecessary. Simplify the full state space matrices as explained in Section IV-3, to a three-by-three system. These sets of matrices are the plant models. Appendix B lists the simplified lateral mode state space matrices. A computer program generates the plant transfer function matrices, $\underline{P}$ (in Appendix B), using the lateral mode state space matrices as input. With the plant in the form of transfer function matrices (one for each flight condition considered), calculate the $\underline{Q}$'s using:

$$\underline{P}^{-1} = \underline{Q}' \tag{3-13}$$

$$\underline{Q} = [q_{ij}] = 1/\underline{Q}' \qquad \underline{P}^{-1} = [1/q_{ij}] \tag{3-14}$$

For example, the $\underline{Q}$ transfer function matrix for the takeoff condition (FC #1) is:

$$\underline{Q}_1 = 0.03565 \begin{bmatrix} \frac{1}{0.1747\ (s+0.08111)\ (s+2.1268)} & \frac{1}{-0.00094\ (s+1.7126)} & \frac{1}{0.1423\ (s-5.2379)} \\ \frac{1}{0.004224\ (s+3.2787)\ (s-17.352)} & \frac{1}{0.00749\ (s+0.9848)} & \frac{1}{-0.1151\ (s-42.2796)} \\ \frac{1}{-0.01294\ (s+2.0513)\ (s+46.472)} & \frac{1}{0.03843\ (s+0.5093)} & \frac{1}{0.3526\ (s+73.6488)} \end{bmatrix}$$

Appendix B contains the $\underline{Q}$'s for all of the flight conditions.

4. System Specifications

The system specifications on t_{ij} where $\underline{T} = [t_{ij}]$, are formulated in the frequency domain. This thesis uses the system specifications from the response functions of a previous thesis (2). These responses are used because a military specification for the horizontal translation maneuver did not exist. Based on the response curves of the previous thesis (Figs. 5-1 and 5-2), synthesize the frequency domain system specifications from the time domain responses (see Section II-4). Table 5-1 contains the specifications in the time domain. The b's are defined the same as in Section III-5 (i.e. b_{32} defined as the maximum acceptable response of the third loop due to an input at the second loop).

Table 5-1 Time Domain System Specifications
(approximated from previous thesis (2))

	t_r	t_p	t_s	M_p	F_v
b_{22}	1.3	3.7	6.0	1.33	1.0
b_{32}	1.0	1.0	5.6	0.03	0.0
b_{12}	1.2	1.2	9.8	0.05	0.0
a_{22}	2.2		3.8	1.0	1.0

Table 5-2 Equivalent Transfer Function Specifications

	t_r	t_p	t_s	M_p	F_v
b_{22}	0.75	1.86	5.58	1.31	1.0
b_{32}		0.24	9.5	0.03	0.0
b_{12}		1.6	10.5	0.05	0.0
a_{22}	2.12		3.76	1.0	1.0

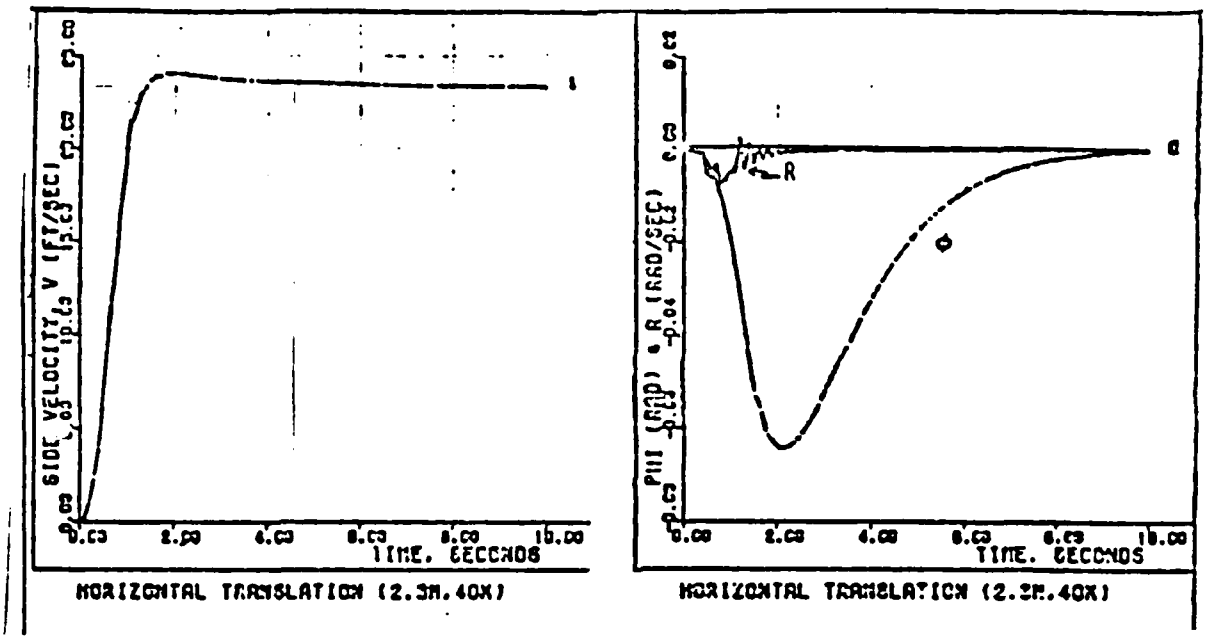

Fig. 5-1 Time Domain Response Functions used to Generate System Specifications (2:52)

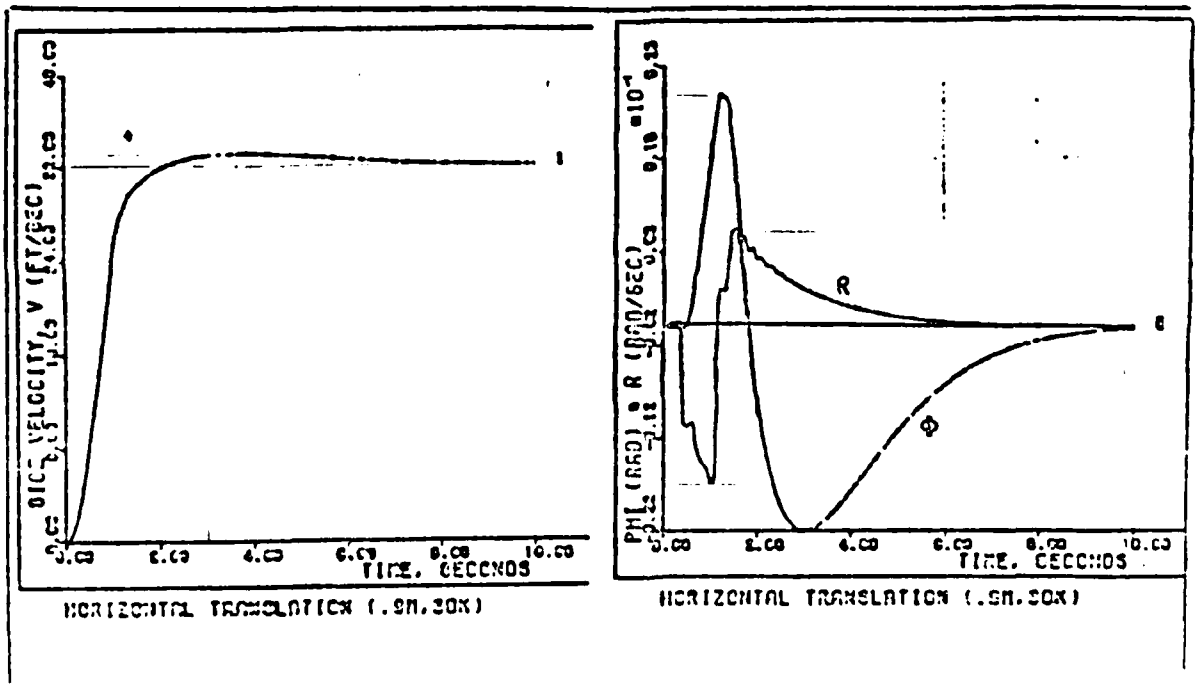

Fig. 5-2 Time Domain Response Functions used to Generate System Specifications (2:57)

Using these time domain system response curves of the previous thesis, generate the equivalent frequency domain system specifications (using the method in Section II-4). Some leeway in defining the system specifications exists. The synthesis of the equivalent transfer functions includes compromises. A transfer function which satisfies all of the time domain specifications requires many iterations to synthesize. Thus choose a few of the specification criteria as important ones and compare these important criteria of the equivalent transfer functions to the desired time domain specifications. The important specifications chosen are the peak value (M_p), the final value (F_v) and the rise time (t_r). Using these three specification criteria, the equivalent transfer functions are synthesized faster and are of a simpler order than if all of the time domain specifications are matched. This is a compromise between the work and time necessary to generate the transfer functions and how close the transfer function specifications are to the time domain specifications.

An iterative process is used to generate the equivalent transfer functions. As an example, the synthesis of the loop 2 lower bound, a_{22}, follows. Since only specific responses are given, a range of acceptable responses is generated based on the responses and experience. Using the criteria from the previous thesis (Fig. 5-1 and 5-2), a_{22}, the lower bound, is overdamped with no overshoot. The response starts at zero and settles to a final value of one. The rise time is approximately 2 sec and the settling time is about 4 sec (Table 5-1).

Using the known information as a starting point, synthesize a_{22}. Since it is overdamped, try a damping ratio greater than one. Since the final value is one, the steady state response must be one. The

frequency response characteristics of the final transfer function is also important. Remember the response should decrease as fast as possible in the frequency domain (it is a lower bound) thereby giving the largest possible region between the upper bound, b_{22}, and a_{22}. Thus, desire a transfer function with three more poles than zeros, or at least two more poles than zeros.

Start the iterations by assuming a set of poles with a natural frequency, such as five, and a damping ratio greater than one. Keep the natural frequency constant and vary the damping ratio. Start with a damping ratio of one. Call this a_{x1}, $a_{x1} = 25/(s^2 + 10s + 25)$. The time response criteria of a_{x1} are $M_p = 1$, $F_v = 1$, $t_r = 0.672$ and $t_s = 1.167$. The responses, t_r and t_s are too fast. Try a damping ratio of two, $a_{x2} = 25/(s^2 + 20s + 25)$. This yields $M_p = 1$, $F_v = 1$, $t_r = 1.646$ and $t_s = 2.9756$, where t_r and t_s are still too fast, but they are closer to the desired response than a_{x1}. Thus increase the damping ratio again. Try a damping ratio of three, $a_{x3} = 25/(s^2 + 30s + 25)$. This yields $M_p = 1$, $F_v = 1$, $t_r = 2.562$ and $t_s = 4.595$, where t_r and t_s are now too slow. Of the three functions, a_{x2} is the best.

The designer decides this is not close enough, therefore the iteration process continues. Try adding another pole to a_{x2}, $a_{x2} = 25/(s^2 + 20s + 25)(s + 1)$. This yields $M_p = 1$, $F_v = 1$, $t_r = 2.9499$ and $t_s = 5.1998$. Now t_r and t_s are too slow. Try a pole at two, $a_{x2} = 50/(s^2 + 20s + 25)(s + 2)$. This yields $M_p = 1$, $F_v = 1$, $t_r = 2.116$ and $t_s = 3.76$, which are close to the desired specifications. Try a pole at three, $a_{x2} = 75/(s^2 + 20s + 25)(s + 3)$. This yields $M_p = 1$, $F_v = 1$, $t_r = 1.8866$ and $t_s = 3.416$, where t_r and t_s are too fast. The a_{x2}

function with the pole at -2 gives the best results. The designer considers the time response from this function, $a_{x2} = 50/(s^2 + 20s + 25)(s + 2)$ close enough. Thus the iterative process ends and a_{22} is synthesized.

The transfer function chosen is not the only possible solution. The designer decides when the equivalent transfer function specifications match the desired specifications well enough. The harder the bounds are to satisfy, the more careful the synthesis of these equivalent transfer functions must be. The QFT technique uses the values of the equivalent transfer functions in the frequency domain, and these values are sometimes referred to as the equivalent frequency domain system specifications.

Use the same procedure to synthesize equivalent transfer functions for the three other bounds. The upper bound for L_2, b_{22}, also settles to a final value of one, thus it too has a steady state value of one. The other two bounds, b_{32} and b_{12}, settle at zero. They need a zero (a numerator root) at the origin.

Some of the lesser important specification criteria are violated. These violations are minor, less than 5% (Table 5-2) and believed to only slightly degrade the model. This approximation does not affect the comparison between the two theses. Three decibels (3 db gain margin) is selected as the Universal-High Frequency (UHF) Bound.

The equivalent transfer functions obtained are:

$$\frac{1.506\ (s + 2)(s + 5)}{(s + 8)(s + 0.5811 + j1.243)(s + 0.5811 - j1.243)}$$

$$b_{32} = \frac{-0.33\ s\ (s - 1)(s + 1.4)}{(s + 0.3)(s + 1.5)(s + 2)(s + 4)}$$

$$b_{12} = \frac{0.36\ s(s - 2)(s + 0.25)}{(s + 0.15)(s + 0.5)(s + 2)(s + 5)}$$

$$a_{22} = \frac{50}{(s + 18.66)(s + 2)(s + 1.34)}$$

This iterative process is also explained in Section II-4. Fig. 5-3 shows the Bode Plot of the equivalent frequency domain system specifications. Note the upper level and lower bound, b_{22} and a_{22}, define an envelope which the system response is between. Notice both of the other bounds (which are effectively upper bounds) are below the upper bound of the desired system response, b_{22}. Also the two bounds, b_{12} and b_{32}, are below 0 db, which means these responses are attenuated. The larger the difference between the envelope of acceptable responses (the region between b_{22} and a_{22}) and the bounds (b_{32} and b_{12}) of the undesired responses, the easier to perform the design. Since the QFT technique uses the system specifications explicitly, the designer knows during the design phase, when a specification is violated and can take appropriate action. Thus using these system specifications this design should have at least similar system responses as the previous thesis (2).

5. Choosing Which Loops to Design First

With the system specifications and the plant matrices in the required form, the design phase begins. Design the loop with the highest bandwidth requirements last, since the last loop designed contains the least amount of overdesign compared to the other loops

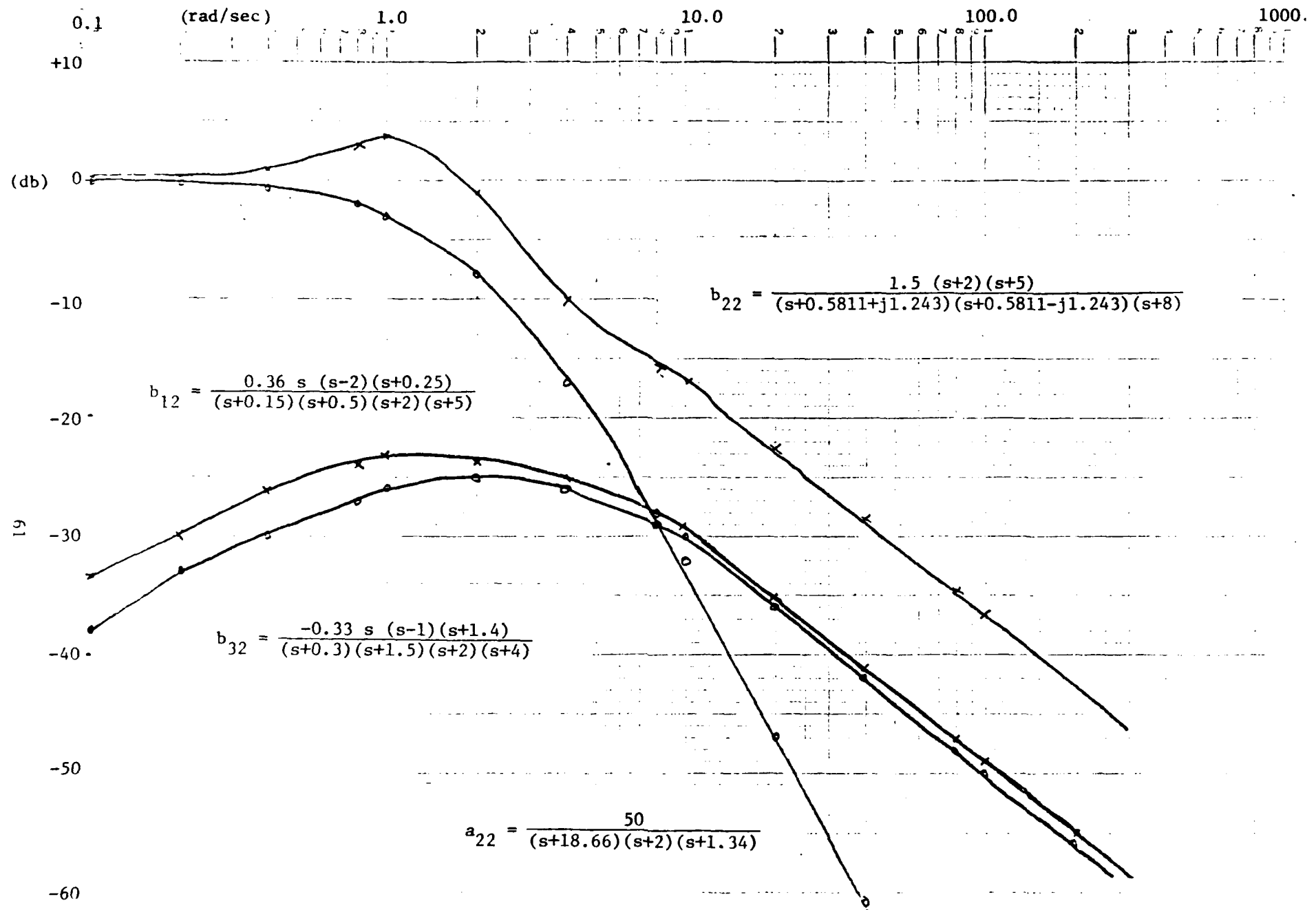

Fig. 5-3 Frequency Domain System Specifications (Bode Plot of the Equivalent Transfer Functions)

(Section III-5). Remember the maneuver performed, a horizontal translation has only one non-zero commanded input, the side velocity, v. Loop 2 (L_2) includes the input command and the coupling effects from the other two loops, and the other two loops, L_1 and L_3, contain only the interaction (or coupling) effects as input (Section III-5). Thus, of the nine possible loops in a three-by-three system (see Fig. 3-8), this system requires only three loops designed (Fig. 5-4). Design L_2 last, since this loop is expected to require more bandwidth than the other two loops. Also, L_2 requires more calculations because it involves both command input and "disturbance" input terms, whereas the other two loops only contain "disturbance" terms. Design either of the other two loops, L_1 (roll angle, ϕ) and L_3 (yaw rate, r), first since this thesis uses the non-interacting (the original, not the improved; see Section III-5 and III-6) method for the first two loops. Therefore the design of these two loops do not explicitly affect one another.

Since both loops, L_1 and L_3 use the same design method, this chapter presents only one loop, L_1. Appendix C contains the L_3 loop design.

6. Plant Templates

Generate the plant templates for each frequency of interest. Choose the frequencies of interest as follows. Flight control systems usually operate between one and four hertz, which is 6.28 to 25.08 rad/sec. Therefore use a decade on either side. This choice is at the designer's discretion based upon the amount of uncertainty at the frequencies of interest (Section III-5). Use as the intervals, octaves between the decades (also decided by the designer). The frequencies of interest

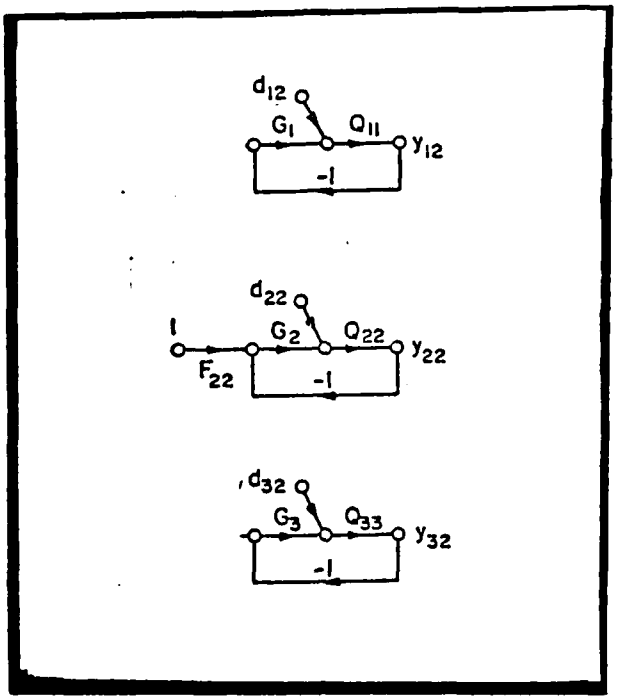

Fig. 5-4 Equivalent SISO Systems for a 3 x 3 MIMO System

chosen are; 0.1, 0.2, 0.4, 0.8, 1.0, 2.0, 4.0, 8.0, 10.0, 20.0, 40.0, 80.0 and 100.0 rad/sec. Table C-1 lists the values of q_{11} (Table C-2 contains q_{33}). L_1 uses the q_{11} term as the plant (L_3 uses q_{33}). Fig. C-1 shows a Bode Plot of the q_{11} and q_{33} terms. These magnitudes generate the plant templates as explained in Section II-5. Fig. C-2 shows the plant templates ($[q_{ij}]$ sets) for L_1 and Fig. C-3 for L_3.

With the plant templates generated and the system bounds defined, calculate the bounds for each loop.

7. Bounds for the First Two Loops

L_1 and L_3 are effectively disturbance rejection loops (no command input). The system equations for L_1 and L_3 (Fig. 5-4 and Eq. 3-20) are:

$$|1 + L_1|^{-1} \leq \frac{b_{22}\left|\frac{q_{11}}{q_{12}}\right| + b_{32}\left|\frac{q_{11}}{q_{13}}\right|}{b_{12}} \qquad (5\text{-}1)$$

$$|1 + L_3|^{-1} \leq \frac{b_{22}\left|\frac{q_{33}}{q_{32}}\right| + b_{12}\left|\frac{q_{33}}{q_{31}}\right|}{b_{32}} \qquad (5\text{-}2)$$

These expressions require four ratios, $|q_{11}/q_{12}|$, $|q_{11}/q_{13}|$, $|q_{33}/q_{32}|$ and $|q_{33}/q_{31}|$ (Tables C-1 thru C-6). Remember from Section II-8, $|q_{ii}/q_{ij}|$ is a ratio of magnitudes, not an equation. Only use the magnitude of the q terms. For example, for FC #3, at a frequency of 10 rad/sec; q_{11} = -51.3 db, q_{12} = 7.6 db and q_{13} = -38.3 db. Thus:

$$\left|\frac{q_{11}}{q_{12}}\right| = -58.9 \text{ db}$$

$$\left|\frac{q_{11}}{q_{13}}\right| = -13.0 \text{ db}$$

This in effect considers the worst case; the q terms have their maximum affect on the nominal bounds. The system expressions also require the magnitudes of the bounds b_{22}, b_{32} and b_{12}. Table C-7 lists the magnitudes of these terms. Substituting these values into Eqs. 5-1 and 5-2 yields the bounds (in decibels) for the appropriate loop. For example, for FC #3, at ω = 10 rad/sec, b_{22} = -17.4 db, b_{32} = -30.4 db, b_{12} = -29.9 db, $|q_{11}/q_{12}|$ = -58.9 db and $|q_{11}/q_{13}|$ = -13.0 db. Substituting these values into Eq. 5-1:

$$|1 + L_1|^{-1} \leq \frac{-17.4\ (-58.9) + -30.4\ (-13.0)}{-29.9}$$

and simplifying:

$$|1 + L_1|^{-1} \leq \frac{-76.3 + -43.4}{-29.9} = \frac{-43.2}{-29.9} = -13.3 \text{ db}$$

Table 5-3 lists the boundary values for the L_1 loop (Table C-8 lists the L_3 loop). Generate the bounds for the first loops designed. As explained in Section II-8 use the highest bound of the three flight conditions at each frequency as the nominal bound. Now transfer the nominal bounds for L_1 to the Nichols Chart, as explained in Section II-8 (Fig. 5-5).

Remember the design performed is actually for a nominal (reference) loop transmission, L_{10}, where $L_{10} = G_1 P_{10}$ (Section II-11). This design method uses a nominal plant, P_o (Section II-7) which can be anywhere. For this example, P_{10} is chosen as flight condition (FC) #3 (Fig. C-2).

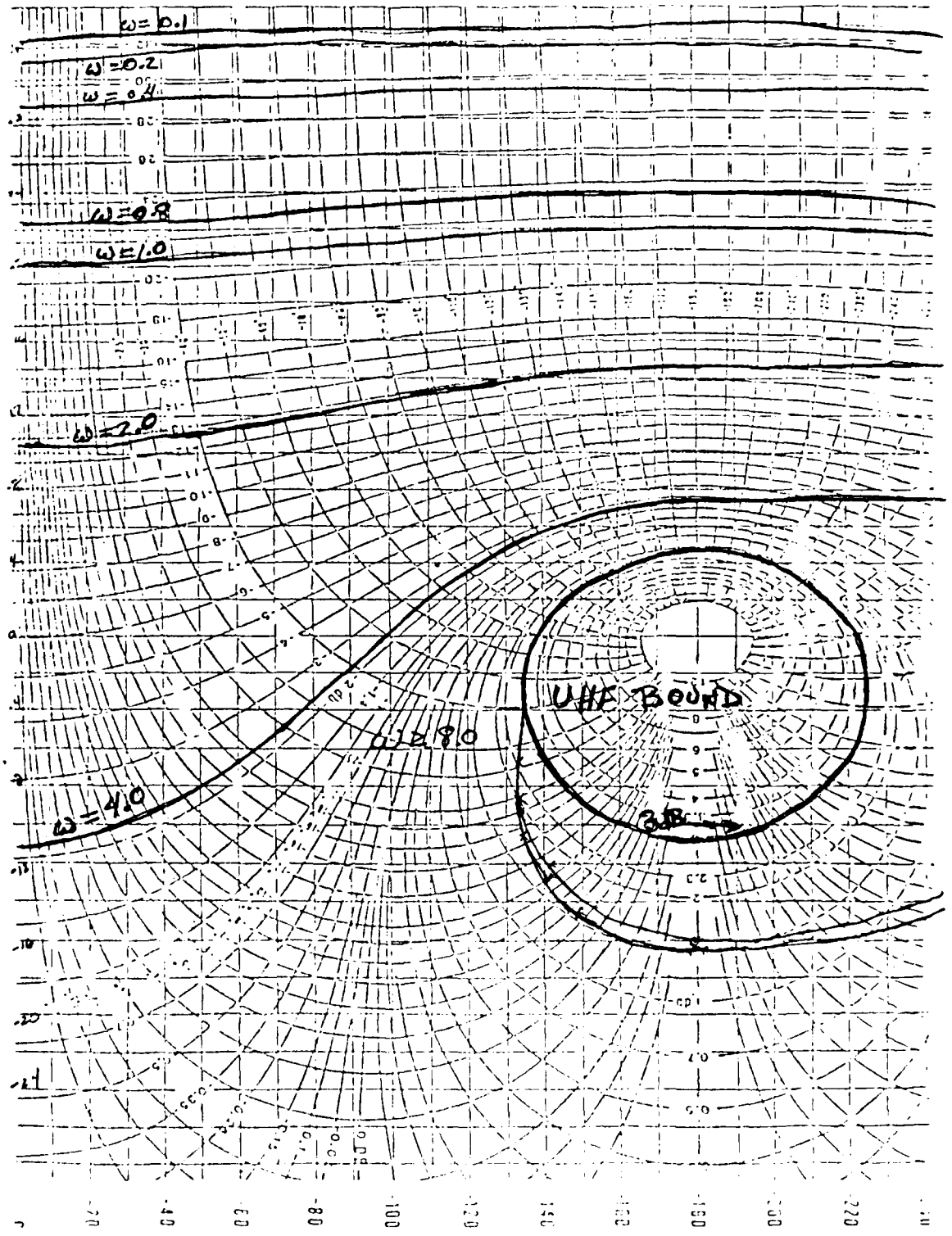

Fig. 5-5 Loop 1 (L_1) Design Bounds

Table 5-3 L_1 Loop Bounds

Freq. (rad/sec)	FC #1 (db)	FC #2 (db)	FC #3 (db)	Nominal Bound (db)
0.1	20.52	23.52	32.62	32.62
0.2	16.21	23.04	31.70	31.70
0.4	10.66	20.41	28.76	28.76
0.8	4.82	15.30	23.22	28.22
1.0	3.08	13.36	21.07	21.07
2.0	-2.99	5.78	12.74	12.74
4.0	-10.76	-4.32	2.20	2.20
8.0	-18.88	-15.56	-9.57	-9.57
10.0	-21.27	-19.09	-13.39	-13.39
20.0	-28.02	-28.93	-24.72	-24.72
40.0	-34.25	-36.84	-34.64	-34.25
80.0	-35.23	-43.50	-42.66	-35.23
100.0	-42.28	-45.53	-44.92	-42.28

Thus, in this example L_{10} is the same as L_1 for FC #3 $[(L_1)_3]$. This reference loop transmission is a means for finding the loop compensator, G_1 (Section II-12). With G_1 known from L_{10}, $L_{10} = G_1 P_{10}$, the loop transmissions for any plant can be derived, $(L_1)_i = G_1 (P_1)_i$. Thus in synthesizing a nominal loop transmission it is the compensator which is being designed.

Use the nominal bounds for designing the L_{10}. The nominal bounds are the worst bounds from the set of bounds generated for the L_1 loop. From Table 5-3, the bounds for L_1, at each of the three flight conditions of interest are listed. If the worst bounds are not used, the designed G would not guarantee the loop transmissions to satisfy their system specifications at each flight condition, because one flight condition might violate the system specifications. Thus use the nominal bounds to synthesize a L_{10}, and thereby design G_1 such that the system specifications are met at all of the flight conditions of interest.

For example, transfer the $\omega = 2$ rad/sec bound onto the Nichols Chart. Take the template corresponding to $\omega = 2$ rad/sec for L_1 (Fig. C-2). Since this is a disturbance rejection problem, invert the Nichols Chart (Section II-9) and the template. The reference point, or nominal plant used (Section II-7), is FC #3. With the template inverted, the reference point is at the bottom of the template. The nominal bound calculated for $L_1(j2.0)$ is 12.7 db (Table 5-3). Put the lowest point of the template (in this example, the reference point) on the Nichols Chart at the bound (12.7 db curve). Remember the horizontal and vertical reference on the template must stay parallel to the horizontal and vertical lines of the Nichols Chart. Slide the template along the bound, 12.7 db, transferring the reference mark from the template to the Nichols Chart at enough intervals to enable drawing a representative curve through these marks. Since the lowest point of the template is the reference point, the curve drawn is the 12.7 db curved line (Fig. 5-5), this is the design bound. When the UHF Bound (the 3 decibel curve chosen in Section V-4), becomes the limiting bound (for L_1, when $\omega > 8$ rad/sec) notice the template causes an offset from the UHF Bound (Fig. 5-5). If any other nominal plant was chosen this offsetting effect would occur at the other frequencies as well. Note from Fig. 5-5 at low frequency the bounds tend towards a straight line across the Nichols Chart, but tend to encircle the UHF Bound as the frequency increases. The UHF Bound keeps the open loop transfer function design from going to the origin, -180 degrees and 0 db, which causes an instability. The L_3 design bounds are in Fig. C-5.

Do this at all frequencies of interest. Every frequency of interest has a bound. In the example, as the frequency increases, the nominal bounds are encompassed by the UHF Bound. Therefore use the UHF Bound for the design bound at these frequencies because the UHF Bound is more restrictive.

8. Shaping the Open Loop Transfer Function

With the bounds drawn, shape the nominal open loop transfer function, L_{10}, as explained in Section II-11 and Appendix A. Iterations used to shape L_{10}, are in Table C-9 and Fig. C-4. This table demonstrates the shaping is not difficult once the pattern develops and experience is gained.

For example, starting with the nominal plant (poles at -0.3343 and -1.0054) the slope of the magnitude line after the second pole, on the Bode Plot, is -12 db/octave. At this slope the value of L_{10} is 11.0 db at $\omega = 2$ rad/sec and -1.0 db at $\omega = 4$ rad/sec. This is slightly low for the 2 rad/sec design bound (approximately 13 db) and is also low for the 4 rad/sec design bound (approximately 2 db). Thus the slope is increased by adding a zero which increases the slope of the line to -6 db/octave after the zero is added. The problem is where to add the zero. Using a straight edge at a slope of -6 db/octave, line up the 13 db point at 2 rad/sec and the current magnitude line on the Bode Plot whose slope is -12 db/octave. The point where the straight edge and the -12 db/octave line cross, is the value of the zero which satisfies the $\omega = 2$ rad/sec design bound of 13 db. Remember this is a straight line approximation and the corner points change depending on other roots near them.

Looking ahead, the slope of the line needs decreasing to achieve a magnitude close to the 4 rad/sec design bound of 2.2 db. Thus, need to add another pole and this lowers the curve at the 2 rad/sec point. Therefore instead of using the point that the straight edge and the -12 db line crossed (1.7), move the zero to 1.3. After passing the 2 rad/sec point the curve needs to decrease quickly to achieve the 4 rad/sec bound, 2 db. Before making more changes based on the magnitude of L_{10}, check the phase of the current design to the design bound on the Nichols Chart (Fig. 5-5). The phase of the current design at $\omega = 4$ rad/sec is -150 degrees. On the Nichols Chart find the point on the 4 rad/sec design bound at -150 degrees. The magnitude is 7 db. Thus the bound used on the Bode Plot approximation is 7 db for $\omega = 4$ rad/sec (not 2 db). Using the same technique as above, add a pole to decrease the slope, slide the straight edge at a slope of -12 db/octave along the 7 db at 4 rad/sec point until it crosses the previous -6 db/octave slope. The crossing point is about 3.2, thus add a pole at 3.2.

The curve now looks good until 20 rad/sec where the slope needs decreasing again. Using the same technique as above, add a zero at about 12.5. Now check the current results on the Nichols Chart for the phase angle and magnitudes. From Fig. 5-5 the value for the current L_{10} design at 2 rad/sec is 13 db and -139 degrees. From the Nichols Chart the design bound magnitude for 2 rad/sec at -139 degrees is 14 db. Thus the current design is about 1 db too low and requires raising. Notice that as the phase angle becomes more positive (L_{10} curve moves left on the Nichols Chart) the magnitude of the design bound decreases, for example the magnitude for the $\omega = 2$ rad/sec design bound at -130 degrees

is 13 db. The value of the current design for ω = 4 rad/sec is 7 db and -142 degrees. From the Nichols Chart notice the design bound is 6 db at -142 degrees. Thus the current design is barely satisfactory, but it violates the 2 rad/sec design bound.

Try replacing the last pole-zero combination. Remember it is helpful to add phase as well as increase the magnitude. This is accomplished by adding the pole later (use 3.5 instead of 3.2) which increases the magnitude and adding the zero earlier (use 6.5 instead of 12.5) which adds phase angle. From the Nichols Chart (Fig. 5-5 and 5-6), these points satisfy the bounds. The next frequency of interest is 8 rad/sec. Notice on the Nichols Chart that the balance of frequencies share the same design bound. Now desire the L_{10} design to follow the 8 rad/sec bound. Try adding a complex pole pair to bend the L_{10} curve around the design bound as close as possible, this keeps the bandwidth of the design as small as possible. Using a phase response chart (Fig. C-7), approximate the complex pair.

From the Nichols Chart at 10 rad/sec, the current L_{10} design has 12 degrees of phase difference between its value and the design bound. Using the phase response chart, use a 12 degree angle change and choose a damping ratio of 0.7 at 10 rad/sec, yields a ratio of frequency to natural frequency of 0.18. Thus the natural frequency is 56. This yields complex poles at -39 + j40 and -39 - j40. Calculate the L_{10} values with these poles added and compare it with the design bounds. This now satisfies the bound (Fig. 5-6). This finishes the shaping of L_{10}. Putting together the winning poles and zeros yields the synthesized L_{10}:

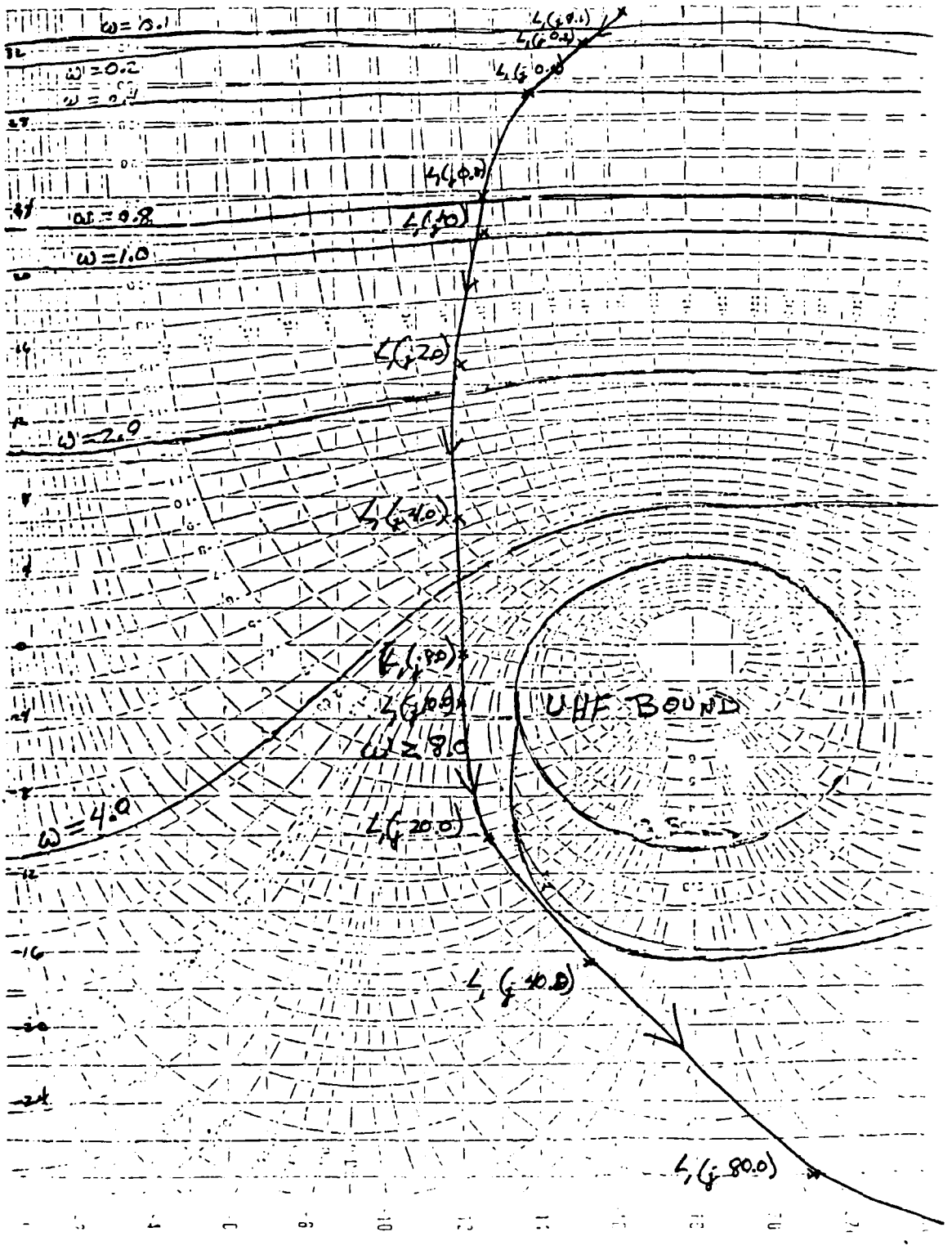

Fig. 5-6 Nominal Loop 1 (L_{10}) Design

$$L_{10} = \frac{20000\ (s + 1.3)(s + 6.5)}{(s - 0.3343)(s + 1.0054)(s + 39 - j40)(s + 39 + j40)(s + 3.5)}$$

Fig. 5-6 presents the open loop transfer function shaped for L_{10}.

Table 5-4 contains the L_{10} values at the frequencies of interest. Compare these values with the Nichols Chart (both phase and magnitude) as a check on the L_{10} designed. L_{30} is in Fig. C-6 and Table C-10. The L_{30} does not meet the bounds for L_{30} at $\omega > 40$ rad/sec (see Fig. C-6). This is not significant because the lower frequencies are more important (designer's discretion). Note that at this time in the design phase, without any simulation, the technique reveals that unless a change is made in the L_{30} design, the L_3 system responses may not be acceptable at the higher frequencies ($\omega > 40$).

Table 5-4 L_{10} Values

$$L_{10} = (L_1)_3 = \frac{20000\ (s + 1.3)(s + 6.5)}{(s-0.3343)(s+1.0054)(s+3.5)(s+39-j40)(s+39+j40)}$$

Freq. (rad/sec)	Magnitude (db)	Phase (degrees)
0.1000	32.8692	-165.5262
0.2000	31.8553	-153.4085
0.4000	29.1167	-138.0508
0.8000	24.0916	-126.5848
1.0000	22.0762	-124.3932
2.0000	15.0893	-121.3318
4.0000	7.3771	-121.6171
8.0000	-0.4459	-121.4610
10.0000	-2.8098	-121.7914
20.0000	-9.6176	-129.7032
40.0000	-16.7481	-159.1405
80.0000	-28.9832	-210.3114
100.0000	-34.3069	-223.4646

9. The Compensator G

With L_{10} formed, it is easy to calculate the compensator, since $L_{10} = G_1 P_{10}$. The open loop transfer functions for all three flight conditions are now calculated. The open loop transfer function for the three flight conditions of the first loop is defined $(L_1)_i = G_1(P_1)_i$, where i = 1, 2 or 3. This generates the open loop transfer function for each flight condition, from which the closed loop system is found. Tables 5-4 thru 5-7 show the compensator and open loop transfer functions.

The method to perform the L_3 design is similar to the L_1 loop. The results are in Appendix C.

10. Summary

This completes the first part of the design which presents the two loops, loop 1 (L_1) and loop 3 (L_3). The next chapter presents the design of the last loop, L_2. The last two chapters present and discuss the simulations of the system. Also, the design is compared with that of the previous thesis (2) which uses a different technique.

Table 5-5 G_1 Values

$$G_1 = \frac{72968.9364(s + 1.3)(s + 6.5)}{(s+3.5)(s+39+j40)(s+39-j40)}$$

Freq. (rad/sec)	Magnitude (db)	Phase (degrees)
0.1000	35.0559	3.5003
0.2000	35.1243	6.9517
0.4000	35.3857	13.5316
0.8000	36.2716	24.6034
1.0000	36.8123	28.9373
2.0000	39.4710	41.4688
4.0000	42.9981	49.0513
8.0000	46.9956	53.7688
10.0000	48.4810	54.3821
20.0000	53.6781	48.3766
40.0000	58.5797	19.8985
80.0000	58.3835	-30.7920
100.0000	56.9359	-43.8691

Table 5-6 $(L_1)_1$ Values

$$(L_1)_1 = \frac{14887.6143\ (s + 1.3)(s + 6.5)}{(s+0.0811)(s+2.1268)(s+3.5)(s+39+j40)(s+39-j40)}$$

Freq. (rad/sec)	Magnitude (db)	Phase (degrees)
0.1000	32.4903	-50.1496
0.2000	28.0434	-66.3479
0.4000	22.6577	-75.6586
0.8000	17.2298	-80.2219
1.0000	15.5555	-81.6086
2.0000	10.3308	-89.4492
4.0000	4.0262	-101.7876
8.0000	-3.2314	-110.7626
10.0000	-5.5178	-113.1465
20.0000	-12.2184	-125.3210
40.0000	-19.3214	-156.9418
80.0000	-31.5496	-209.2111
100.0000	-36.8724	-222.6042

Table 5-7 $(L_1)_2$ Values

$$(L_1)_2 = \frac{10499.2715\ (s + 1.3)(s + 6.5)}{(s-0.3328)(s+1.2021)(s+3.5)(s+39+j40)(s+39-j40)}$$

Freq. (rad/sec)	Magnitude (db)	Phase (degrees)
0.1000	25.7683	-164.5305
0.2000	24.7845	-151.4902
0.4000	22.1654	-134.6338
0.8000	17.4858	-121.6278
1.0000	15.6336	-119.2265
2.0000	9.1321	-116.9707
4.0000	1.6705	-118.9780
8.0000	-6.0722	-120.0678
10.0000	-8.4258	-120.6694
20.0000	-15.2197	-129.1371
40.0000	-22.3467	-158.8568
80.0000	-34.5809	-210.1695
100.0000	-39.9045	-223.3710

VI. DESIGN OF THE FINAL LOOP

1. Introduction

This chapter contains the last part of the design which synthesizes the final loop, L_2 and the prefilter, F_{22}. The exact equation for L_2 is used. The method is explained in Section II-9.

2. Design of the Loop Transmission, L_2

With L_1 and L_3 known (Chapter V), now design the final loop, L_2. For this loop use the exact equation for a command input, using the designed L_1 and L_3 from Chapter V. The exact equation is:

$$T_{22} = \frac{L_2 F_{22}[(1+L_1)(1+L_3)-\gamma_{13}]}{(1+L_1)(1+L_2)(1+L_3)-[\gamma_{12}(1+L_3)+\gamma_{13}(1+L_2)+\gamma_{23}(1+L_1)]+\Gamma} \quad (6\text{-}1)$$

where

$$\gamma_{13} = \frac{q_{11}\, q_{33}}{q_{13}\, q_{31}}$$

$$\gamma_{12} = \frac{q_{11}\, q_{22}}{q_{12}\, q_{21}}$$

$$\gamma_{23} = \frac{q_{22}\, q_{33}}{q_{23}\, q_{32}}$$

$$\Gamma = q_{11}\, q_{22}\, q_{33}\, \frac{1}{q_{12}\, q_{23}\, q_{31}} + \frac{1}{q_{13}\, q_{32}\, q_{21}}$$

This loop contains less overdesign than the first two designs because all terms, except the L_2 terms, are known exactly. Now define an effective plant (the plant the system sees) Q_{22e} as:

$$Q_{22e} = \frac{q_{22}}{1 - \dfrac{\gamma_{12}\,(1 + L_3) + \gamma_{23}\,(1 + L_1) - \Gamma}{(1 + L_1)(1 + L_3) - \gamma_{13}}} \qquad (6\text{-}2)$$

or rewriting in an equivalent form:

$$Q_{22e} = \frac{q_{22}[(1 + L_1)(1 + L_3) - \gamma_{13}]}{[(1 + L_1)(1 + L_3) - \gamma_{13}] - [\gamma_{12}\,(1 + L_3) + \gamma_{23}\,(1 + L_1) - \Gamma]} \qquad (6\text{-}3)$$

Substitute Q_{22e} into Eq. 6-1 and rewrite as:

$$T_{22} = \frac{F_{22}\, L_{20}}{(1 + L_{20})} \qquad (6\text{-}4)$$

where $L_{20} = G_{2e}\, Q_{22e} = G_2\, Q_{22}$. Use Q_{22e} to design L_{20} and then derive the compensator, G_2, from L_{20}.

This has the same form as the SISO systems of Chapter II. Generate the plant templates using Q_{22e} as the plant (as

done for L_1 and L_3 in Section V-6). Table 6-1 contains the Q_{22e} values and the templates are in Fig. 6-1. Appendix D contains the Q_{22e} calculations.

Table 6-1 Q_{22e} Values

Freq.	FC #1		FC #2		FC #3	
(rad/sec)	(db)	(degrees)	(db)	(degrees)	(db)	(degrees)
0.1	14.65	11.98	12.72	21.36	24.48	87.27
0.2	15.90	17.09	14.62	19.95	26.77	118.18
0.4	17.73	18.48	16.02	17.45	27.32	-220.24
0.8	20.49	12.92	18.58	15.97	25.96	-203.39
1.0	21.37	5.94	19.99	11.33	25.51	-196.86
2.0	22.93	-17.96	25.61	-23.91	24.33	-183.65
4.0	24.93	-110.00	15.63	-157.93	19.94	-180.43
8.0	7.72	-158.38	0.076	-168.43	11.39	-178.00
10.0	3.27	-160.53	-4.13	-168.80	8.08	-177.15
20.0	-9.27	-159.08	-16.48	-165.83	-3.05	-174.62
40.0	-20.64	-148.40	-28.13	-156.39	-14.75	-170.14
80.0	-30.42	-130.91	-38.63	-139.97	-26.38	-161.38
100.0	-33.14	-124.94	-41.62	-133.75	-30.02	-157.26

This loop requires an upper and lower bound, generated by using b_{22} and a_{22} (Table 5-2 and Fig. 5-3). Calculate the difference between the two bounds at the frequencies of interest, call this difference Δ (Table 6-2). The design proceeds as explained in Section II-9 with Δ defined as the maximum change allowed at each frequency. Slide the templates along the Nichols Chart to achieve these maximum changes. Transfer the reference point from the template to the Nichols Chart at each point where the template exactly satisfies Δ for that phase angle (as done in Section II-9). Do this at enough phase angles to enable drawing a representative curve at each frequency. Remember the UHF bound may not

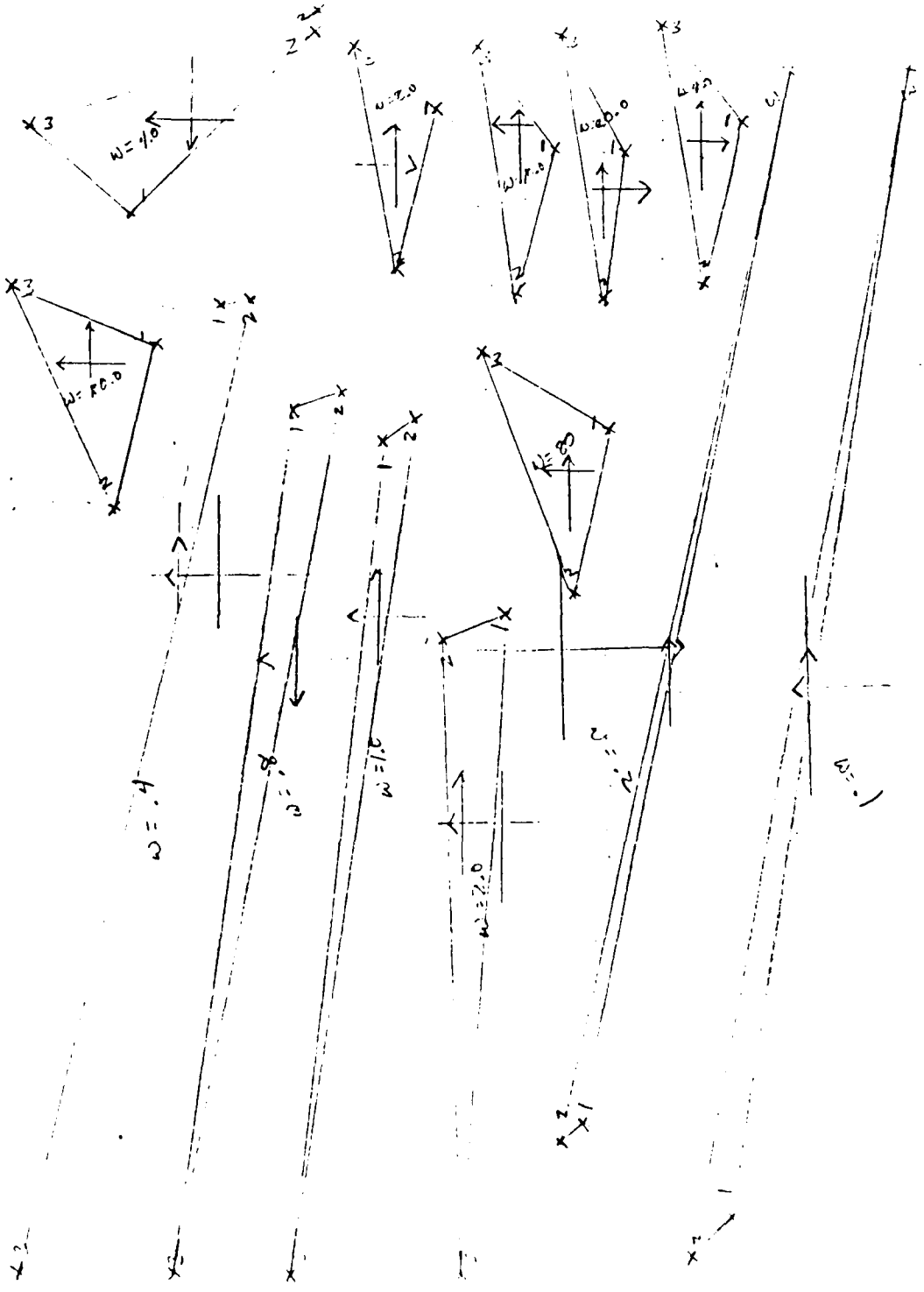

Fig. 6-1 O_{22e} Plant Template

Table 6-2 (Δ Values, $\Delta = |b_{22}| - |a_{22}|$)

Freq. (rad/sec)	b_{22} (db)	a_{22} (db)	Δ (db)
0.1	0.0063	-0.036	0.043
0.2	0.13	-0.14	0.27
0.4	0.62	-0.54	1.16
0.8	2.35	-1.98	4.33
1.0	3.25	-2.91	6.16
2.0	-1.10	-8.15	7.05
4.0	-9.81	-17.15	7.34
8.0	-15.69	-28.68	12.99
10.0	-17.38	-32.78	15.40
20.0	-22.81	-46.86	24.05
40.0	-28.61	-63.02	34.41
80.0	-34.56	-80.44	45.88
100.0	-36.49	-86.18	49.69

be violated. For several of the templates ($\omega \geq 8$ rad/sec) the UHF Bound is the nominal bound. Other templates ($\omega < 8$ rad/sec) use the Δ limit as the nominal bound except at the phase angles where the UHF Bound is more restrictive. After using all of the templates, the L_{20} design bounds are complete (see Fig. 6-2).

The method used to obtain the bounds for $\omega \leq 0.4$ rad/sec is an analytical method. The templates are very large and the differences allowed very small. The template graphically finds a point, call this L_a, such that the difference between L_a and a point on the template, and L_a and any other point on the template is less than or equal to Δ. Thus take two points on the template and find a point at each frequency of interest such that the difference between the distance from L_a to one

AD-A174 510 DESIGN OF A MULTIPLE INPUT-MULTIPLE OUTPUT FLIGHT CONTROL SYSTEM CONTAINI..(U) AIR FORCE WRIGHT AERONAUTICAL LABS WRIGHT-PATTERSON AFB OH D L SEGNER

2/3

UNCLASSIFIED NOV 84 AFWAL-TR-84-3093 F/G 1/3 NL

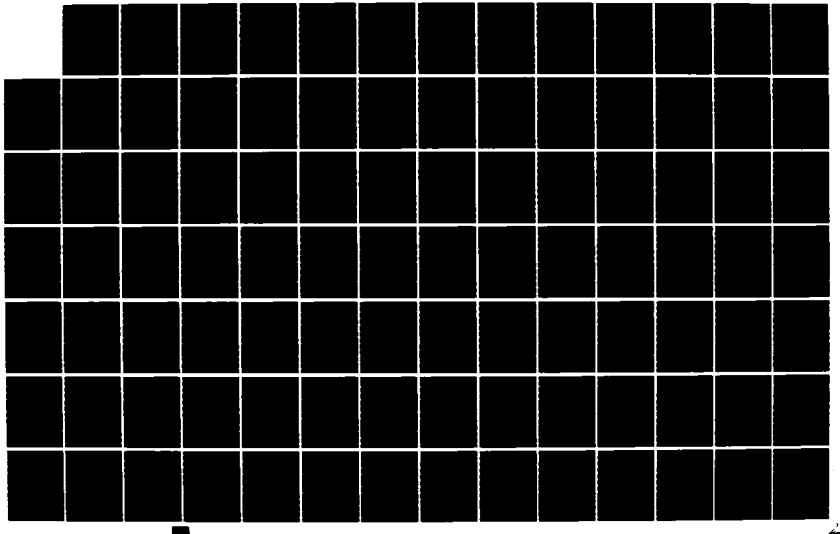

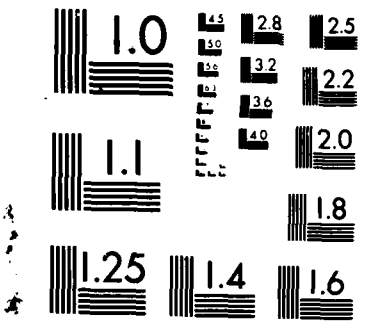

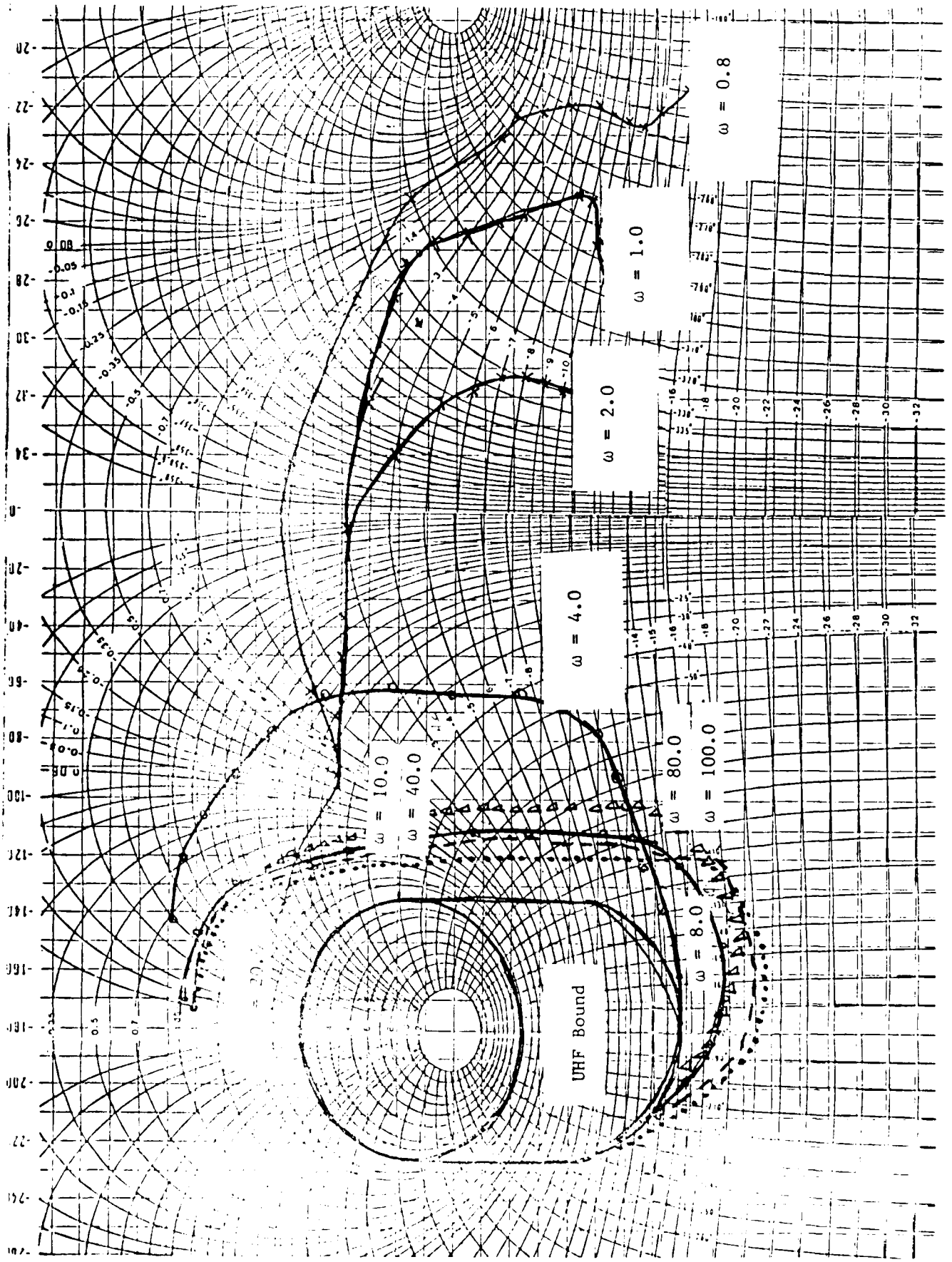

Fig. 6-2 L_{20} Design Bounds

point of the template and the distance from L_a and the other point is less than or equal to Δ. In this thesis this is relatively simple (see Appendix D). Observe the results from the other loops, the pattern indicates the bounds for $\omega \leq 0.8$ rad/sec is greater than 30 db (Fig. 6-2). The bounds are: 48 db at $\omega = 0.1$ rad/sec, 32 db at $\omega = 0.2$ rad/sec and 33 db at $\omega = 0.4$ rad/sec (see Appendix D for the calculations).

A design bound now exists at all the frequencies of interest. Shape L_{20}. The procedure is the same as the shaping performed for the other two loops in Chapter V (see also Section II-11). The results are in Fig. 6-3 and Table 6-3.

Table 6-3 L_{20} Values

$$L_{20} = \frac{12000000.0\ (s+0.18)(s+1)(s+1)(s+1.5)(s+1.2)(s+30)}{(s+0.9848)(s+0.1)(s+0.1)(s+0.4)(s+0.8)(s+8)(s+10)}$$

$$(s+636-j848)(s+636-j848)$$

Freq. (rad/sec)	L_{20} (db)	L_{20} (degrees)
0.1	47.20	-69.01
0.2	40.93	-93.47
0.4	32.81	-107.27
0.8	23.92	-105.68
1.0	21.27	-101.26
2.0	15.11	-82.72
4.0	11.52	-75.22
8.0	7.45	-86.91
10.0	5.58	-92.75
20.0	-1.90	-106.38
40.0	-9.95	-107.69
80.0	-17.01	-104.71
100.0	-19.10	-104.36

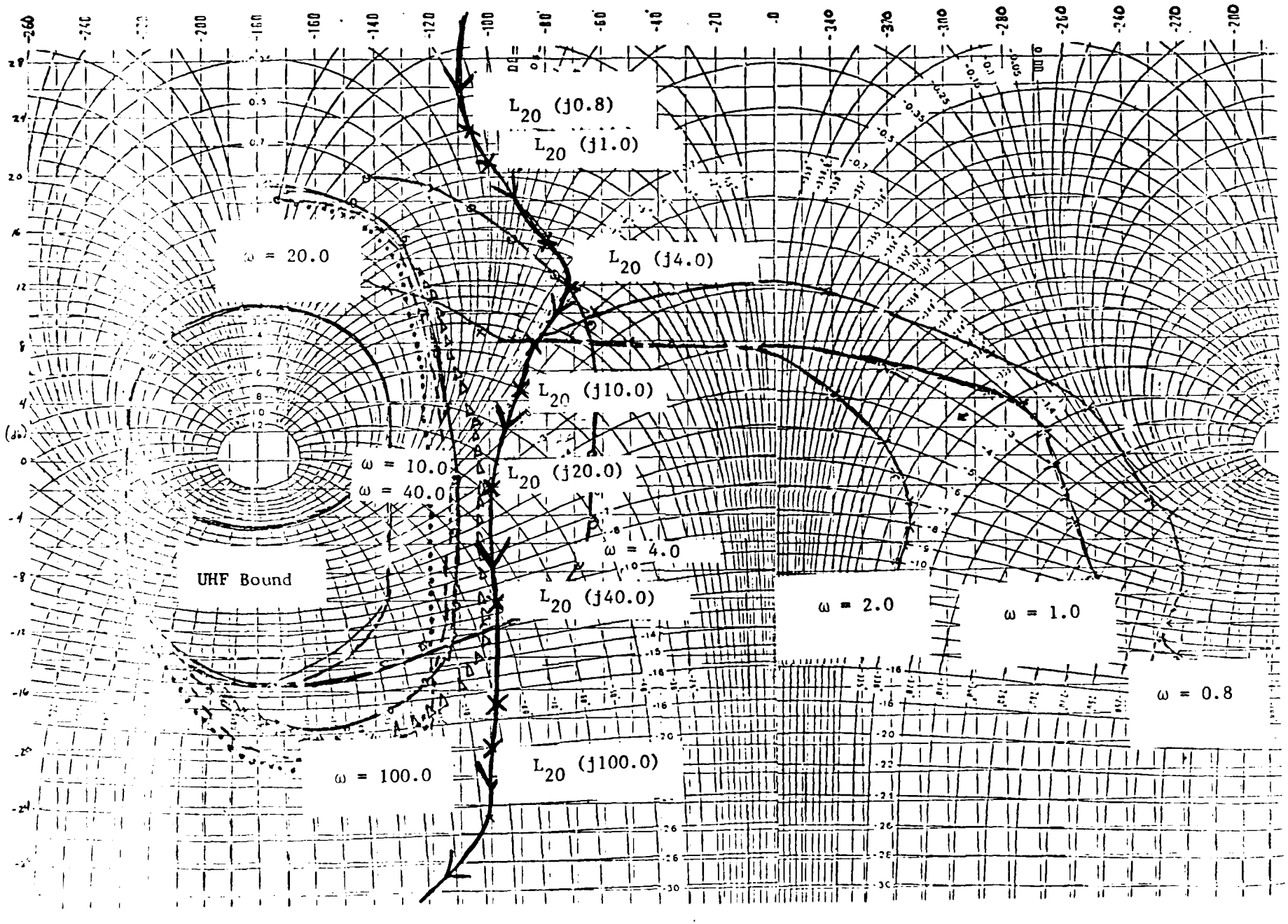

Fig. 6-3 L_{20} Design

3. Designing of the Prefilter, F_{22}

With L_{20} designed, find $(L_2)_i$ using $L_2 = G_2\ (q_{22})_i$ (see Fig. 5-4). The prefilter simply moves the open loop transfer function, L_2, into the acceptable region defined by the upper and lower bounds (Fig. 5-3). The L_{20} design only guaranteed the system responses do not exceed the maximum change, Δ. Compare the results in Table 6-4, the closed loop system $[L_2/(1 + L_2)]$, with the values of b_{22} and a_{22}. The values of the closed loop system is within the acceptable region for $\omega \leq 1.0$ rad/sec. For the frequencies above 1.0 rad/sec the values need decreasing.

Table 6-4 Closed Loop System Values $\left(\frac{L_2}{1 + L_2}\right)$

Freq. (rad/sec)	$\left(\frac{L_2}{1+L_2}\right)_1$ (db)	$\left(\frac{L_2}{1+L_2}\right)_2$ (db)	$\left(\frac{L_2}{1+L_2}\right)_3$ (db)	Maximum Difference (db)
0.1	-0.014	-0.015	-0.00018	-0.015
0.2	0.004	0.030	0.020	0.026
0.4	0.06	0.20	0.11	0.14
0.8	0.13	0.68	0.43	0.55
1.0	0.12	0.79	0.57	0.67
2.0	-0.32	-0.59	0.23	0.82
4.0	-0.81	-2.62	-0.80	1.82
8.0	-0.88	-4.16	-1.28	3.28
10.0	-0.89	-5.06	-1.51	4.17
20.0	-2.67	-11.10	-5.14	8.43
40.0	-9.53	-19.33	-13.02	9.80
80.0	-16.88	-26.64	-20.32	9.76
100.0	-18.91	-28.65	-22.45	9.74

Design the prefilter F_{22}, to shift the response magnitude into the acceptable region. Use only the magnitude values because the L_2 design assured the appropriate phase angle. First draw the envelope into which

the prefilter needs to exist (Fig. 6-4). Do this by comparing the largest value of the closed loop system, T_{max}, to the upper bound, T_U, and the lowest value of the closed loop system, T_{min}, to the lower bound, T_L, at all frequencies of interest (Fig. 2-9). These differences, which must be greater than or equal to zero, define a range on the Bode Plot in which the prefilter exists such that b_{22} and a_{22} envelope the system response curves (Fig. 6-4). For example, at $\omega = 2$ rad/sec, the largest value from the closed loop system responses is 0.23 db (FC #3) and the lowest value is -0.32 db (FC #1) (Table 6-4). The upper bound, b_{22} is -1.10 db and the lower bound, a_{22} is -8.15 db (Fig. 5-3 and Table 6-2). Therefore the upper limit of F_{22} is -1.10 - 0.23 = -1.33 db and the lower limit is -8.15 - -0.32 = -7.83 db. Notice a line sloped at approximately 6 db/octave satisfies the bounds between 1 and 100 rad/sec. Therefore try a simple prefilter with one pole. Remember, the prefilter values are very small for $\omega \leq 1$ rad/sec because the Δ at those frequencies are very small. The prefilter chosen (see Table 6-5) is:

$$F_{22} = \frac{1.404}{(s + 1.4)}$$

This concludes the design. The four parts of the system, the three compensators (one for each loop) and the prefilter for loop 2, designed are:

$$G_1 = \frac{72968.936\ (s + 1.3)(s + 6.5)}{(s + 3.5)(s + 39 + j40)(s + 39 - j40)}$$

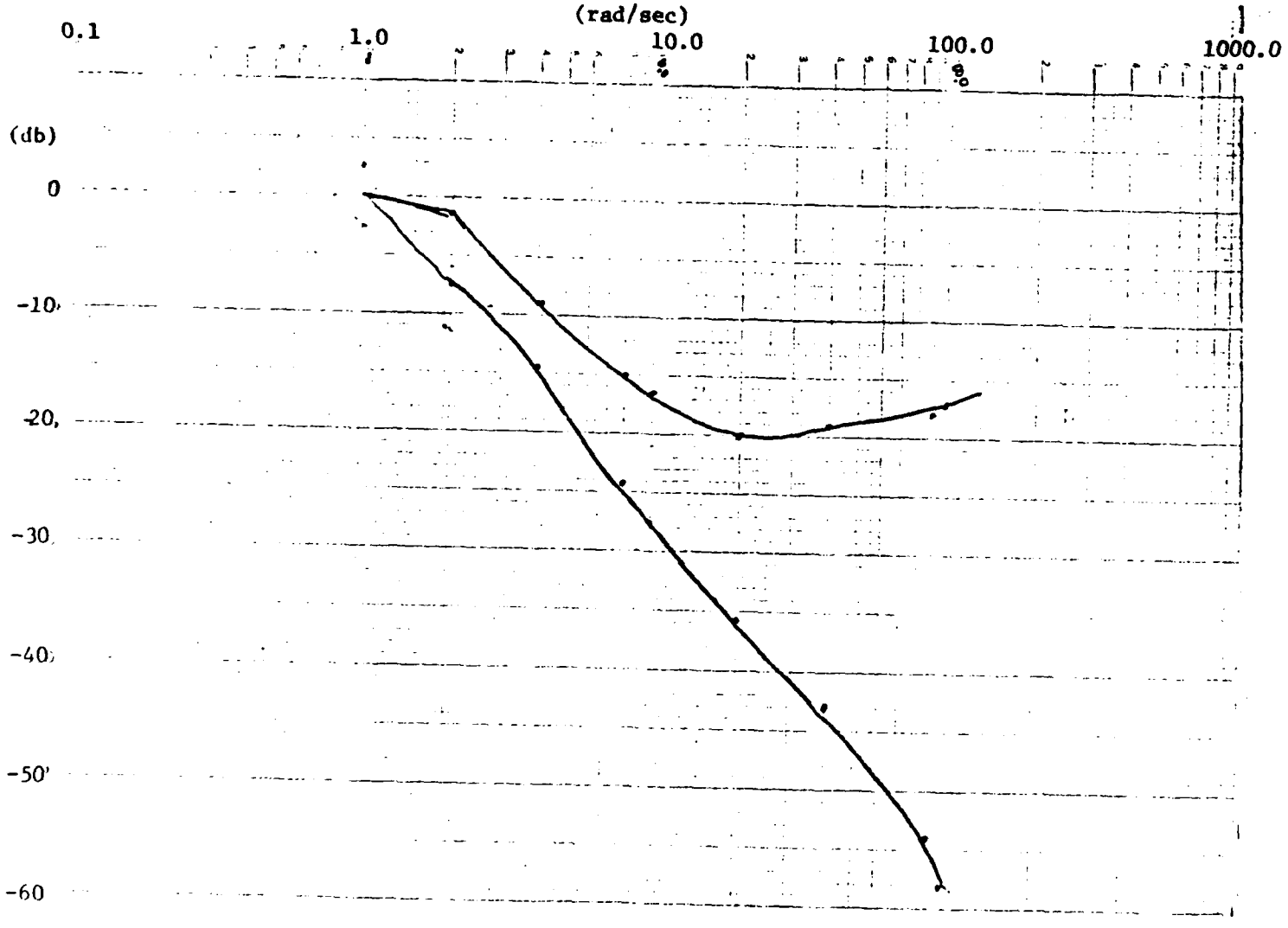

Fig. 6-4 Prefilter F_{22} Envelope

$$G_2 = \frac{2521167.3\ (s + 0.18)(s + 1)(s + 1)(s + 1.5)(s + 1.2)(s + 30)}{(s+0.1)(s+0.1)(s+0.4)(s+0.8)(s+8)(s+10)(s+636+j848)(s+636-j848)}$$

$$G_3 = \frac{98.917}{s(s + 0.7 + j\ 0.714)(s + 0.7 - j\ 0.714)}$$

$$F_{22} = \frac{1.404}{(s + 1.4)}$$

Table 6-5 F_{22} Values

$$F_{22} = \frac{1.404}{(s + 1.4)}$$

Freq. (rad/sec)	F_{22} (db)	F_{22} (degrees)
0.1	0.00	-4.09
0.2	-0.07	-8.13
0.4	-0.32	-15.95
0.8	-1.20	-29.74
1.0	-1.77	-35.54
2.0	-4.81	-55.01
4.0	-9.60	-70.71
8.0	-15.25	-80.07
10.0	-17.14	-82.03
20.0	-23.10	-86.00
40.0	-29.10	-88.00
80.0	-35.12	-89.00
100.0	-37.06	-89.20

4. Summary

This completes the lateral controller designed for this thesis. The last two chapters walked through the design technique used in this thesis. The next few chapters present and discuss the simulations of the design.

VII. SIMULATION RESULTS

1. Introduction

This chapter presents the responses of the lateral controller designed in Chapters V and VI. First the three compensator designs, G_1, G_2, and G_3 are presented. Then the three responses, t_{12}, t_{22}, and t_{32} at all three flight conditions are presented, followed by the three responses at different magnitude step inputs.

2. Compensator Characteristics

From the original specifications in Chapter V both loop 1 and loop 3 response steady state values are zero. Thus the denominator of the compensators must contain a root (pole) at zero. The loop 3 transfer function contains a pole at zero, but the loop 1 transfer function does not. Therefore a pole at zero is added to the loop 1 transfer function. Also a root is added to the numerator (called a zero) such that the response characteristics remain relatively unchanged at the frequencies of interest. The modified G_1 is called G_{1mod}:

$$G_{1mod} = \frac{72968.9364\ (s + 0.25)(s + 1.3)(s + 6.5)}{s(s + 3.5)(s + 39 + j40)(s + 39 - j40)}$$

The two responses are presented in Fig. 7-1.

Basically, bandwidth indicates to which frequency the transfer function amplifies its input signals. The bandwidth of the system is the range of frequencies at which the magnitude of the function is greater than 0 db. Input signal attenuation is desired as soon as possible.

The bandwidth of the compensators are important because it tells for which frequencies the compensator inputs are amplified (in real systems this input signal might be corrupted by noise and other unwanted signals). The responses of the four compensators G_1, G_{1mod}, G_2 and G_3 are in Figs. 7-1. Remember these values are in radians and rad/sec. Using the units of degrees and hertz, the bandwidths of G_2 and G_3 are reasonable, though the bandwidth of G_1 and G_{1mod} are large. The bandwidth of G_{1mod} is 72000 rad/sec (1250 hz). G_1's bandwidth is between 0.1 and 1250 hz. The bandwidth or G_2 is 1610 rad/sec (0.08 hz). The bandwidth of G_3 is 4.6 rad/sec (1.1 hz).

Notice the bandwidth of the compensator with the commanded input, G_2, is much lower than even G_1, though G_2 is designed last.

3. Loop Responses

To simulate the loop responses, use the system equations. Reviewing the original 3 x 3 MIMO system, the matrix equation is;

$$\underline{T} = [1 + \underline{GP}]^{-1} \underline{PFGR} \qquad (7\text{-}1)$$

There are nine terms in $\underline{T}$. Only three of the terms are nonzero because only loop 2 has an input command. Thus the six terms which have an input command to loop 1 or 3 (t_{21}, t_{31}, t_{13}, t_{23}) are zero. Solve the matrix equation for the three scalar equations of interest. The equations are;

Time Response

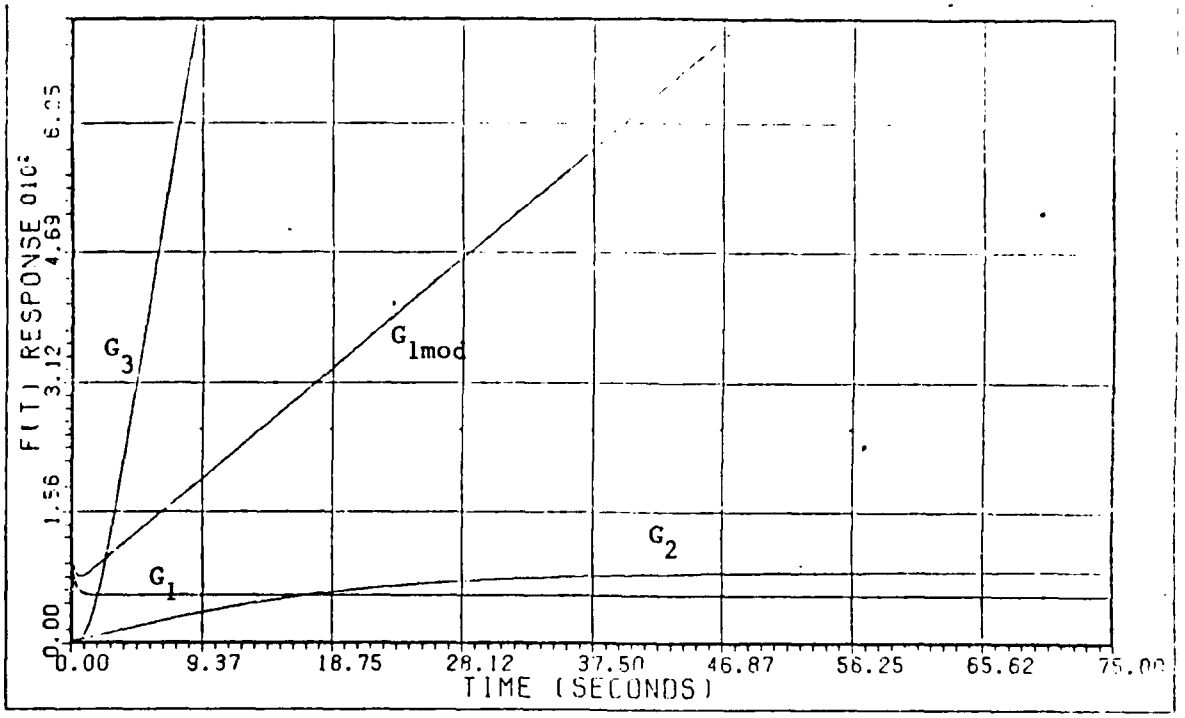

Bode Plot

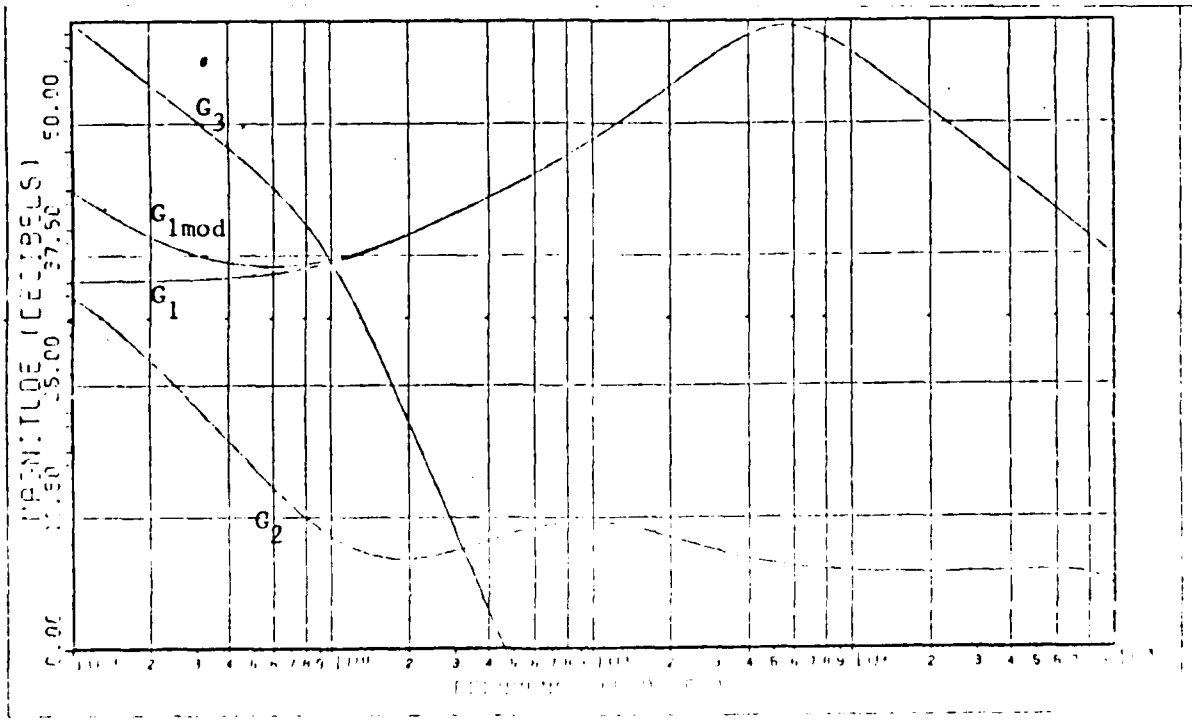

Fig. 7-1 Compensator Responses (step input of 1 ft/sec)

$$t_{12} = \frac{-\left(\frac{t_{22}}{q_{12}} + \frac{t_{32}}{q_{13}}\right) q_{11}}{1 + L_1} \qquad (7\text{-}2a)$$

$$t_{22} = \frac{\left[g_2 f_{22} - \left(\frac{t_{12}}{q_{21}} + \frac{t_{32}}{q_{23}}\right)\right] q_{22}}{1 + L_2} \qquad (7\text{-}2b)$$

$$t_{32} = \frac{-\left(\frac{t_{12}}{q_{31}} + \frac{t_{22}}{q_{32}}\right) q_{33}}{1 + L_3} \qquad (7\text{-}2c)$$

Solve Eq. 7-2b in terms of L_3 and L_1 (see Eq. 6-1). Then solve Eqs. 7-2a and c in terms of t_{22} (see Appendix E).

Generate the loop response using the loop equations derived. Fig. 7-2 through 7-5 contain the design response bounds. Figs. 7-6 contains the FC #2 responses to an input of 1 ft/sec. The time specifications for all of the flight conditions and the design bounds are in Table 7-1.

Comparing the response specifications (Table 7-1), all of the responses satisfy the design bounds. Note that t_{12} response magnitudes are about an order of magnitude less than the design bounds. Thus, the t_p being larger than the design bounds t_p (remember in Section V-4, t_p is not one of the important specification criteria) is not a problem. Note also the shapes of the curves for the bounds and responses are similar (notice the magnitude of the Fig. 7-7(a) curve is 10^{-14}.

Time Response

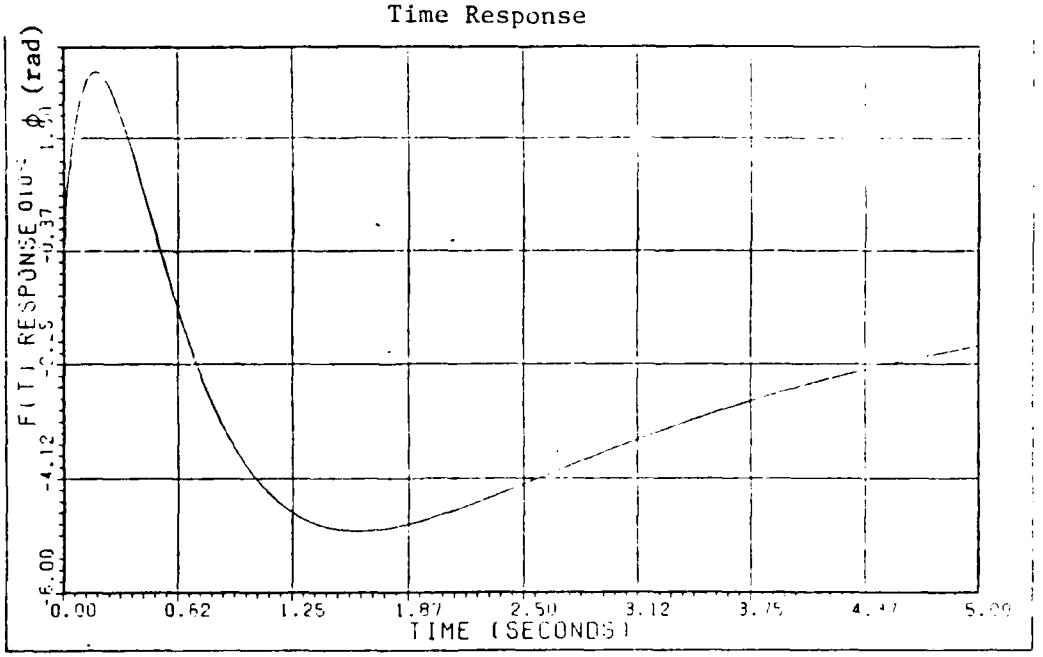

Bode Plot

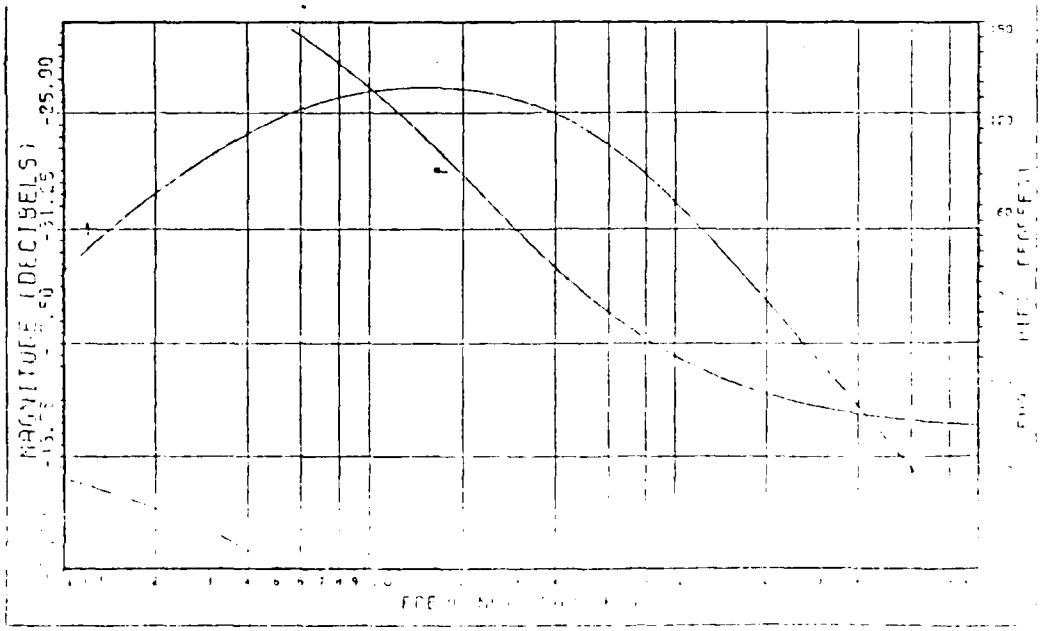

Fig. 7-2 b_{12} Design Bound (r(t) = 1 ft/sec)

Time Response

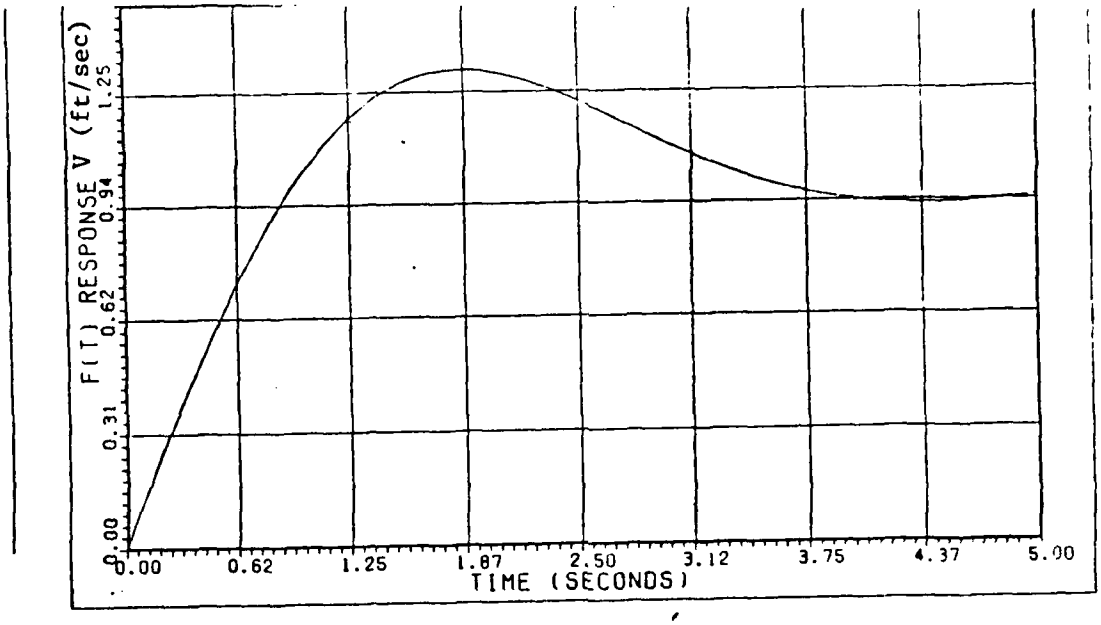

Bode Plot

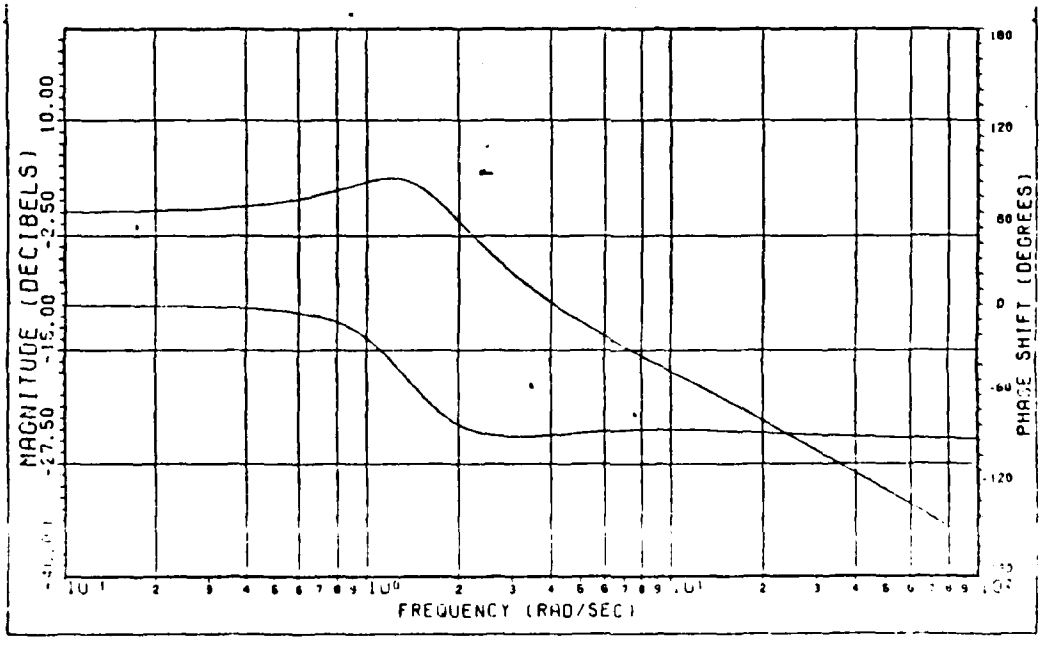

Fig. 7-3 b_{22} Upper Design Bound (r(t) = 1 ft/sec)

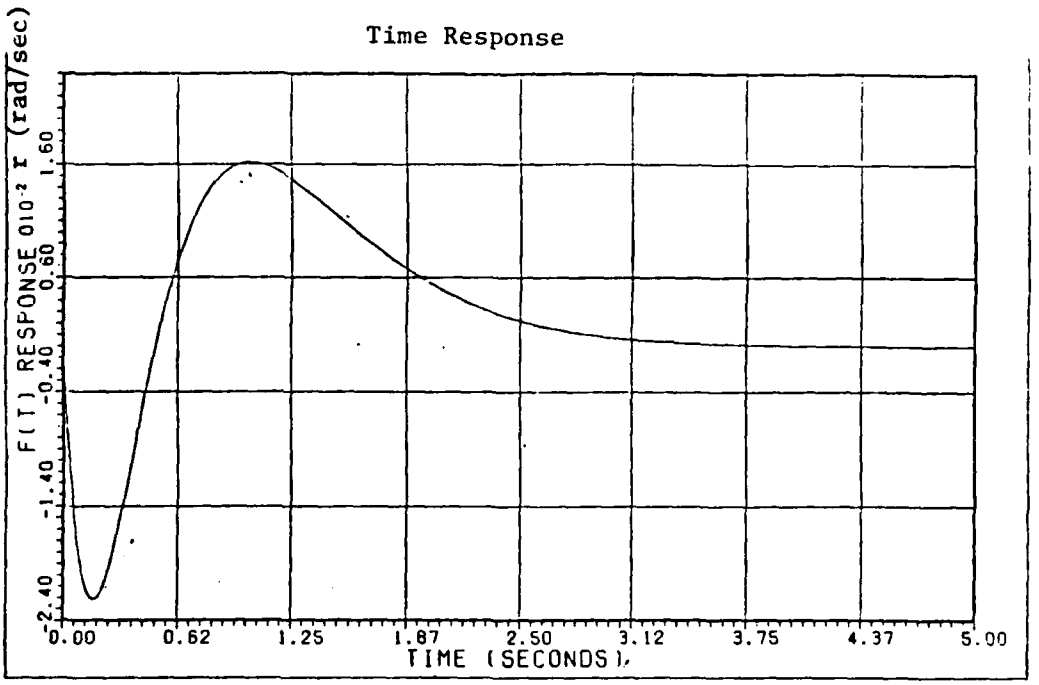

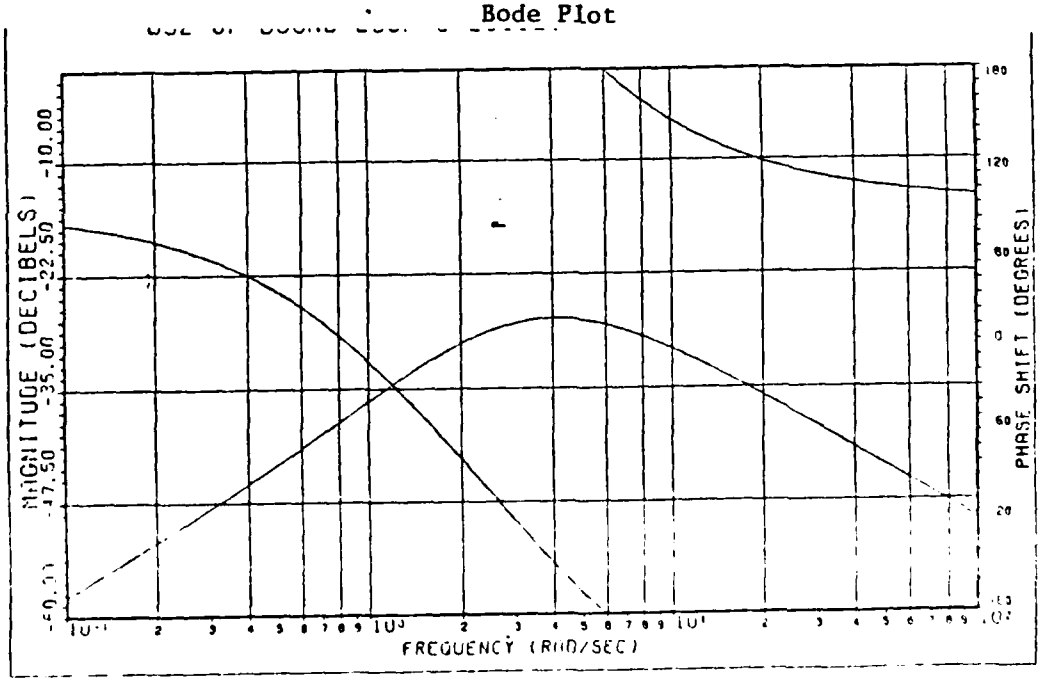

Fig. 7-4 b_{32} Design Bound (r(t) = 1 ft/sec)

Time Response

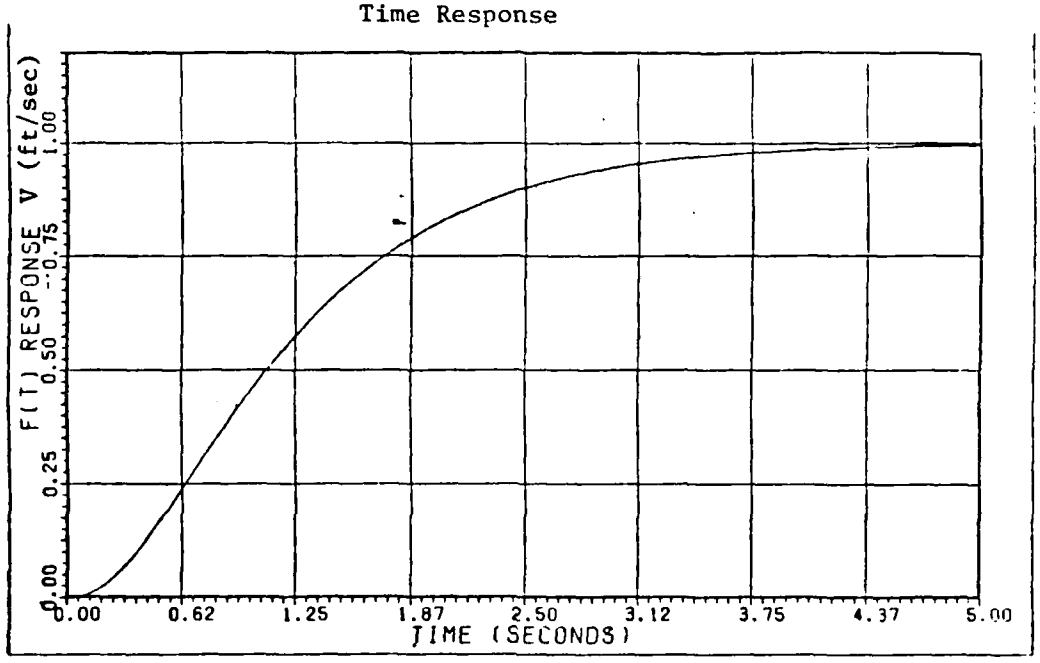

Bode Plot

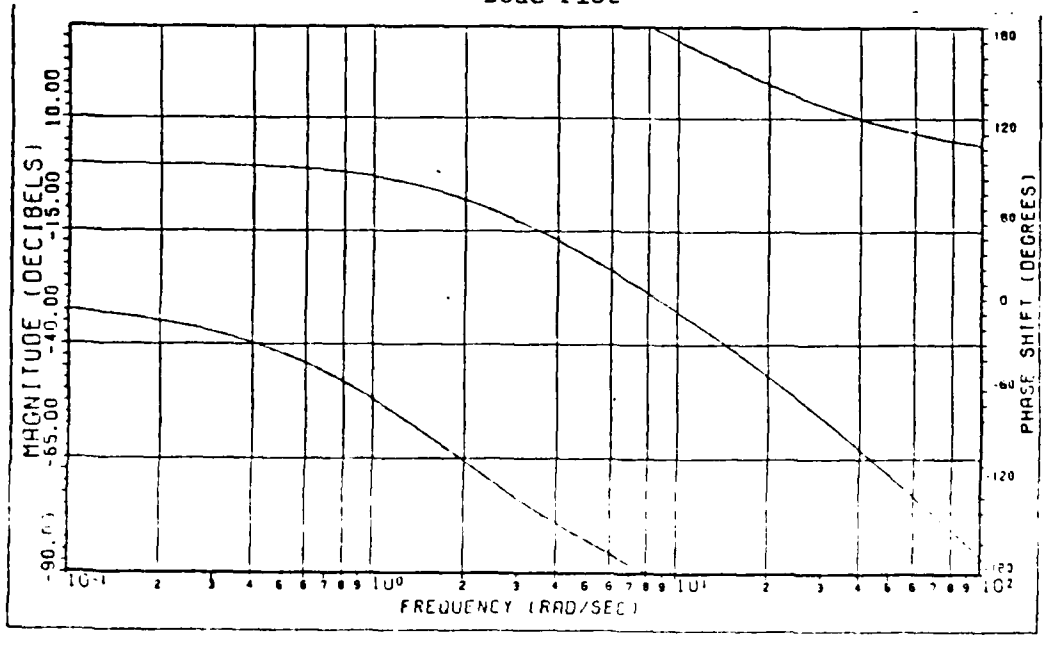

Fig. 7-5 a_{22} Lower Design Bound (r(t) = 1 ft/sec)

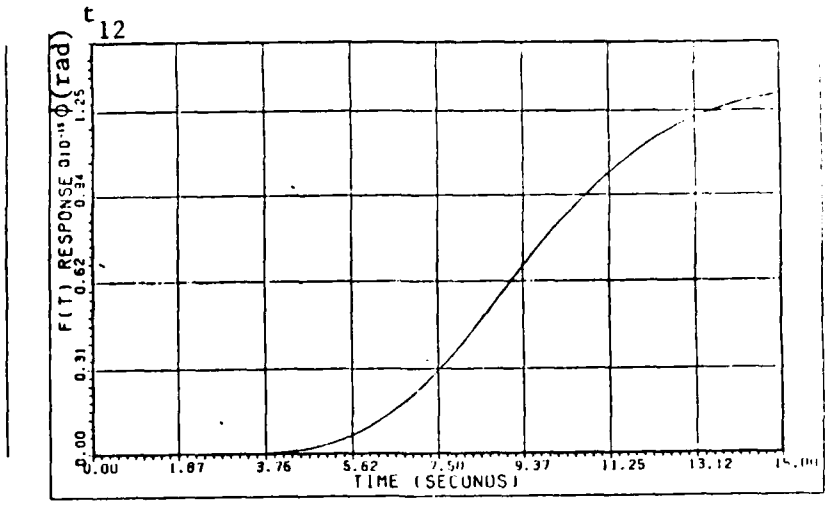

(a)

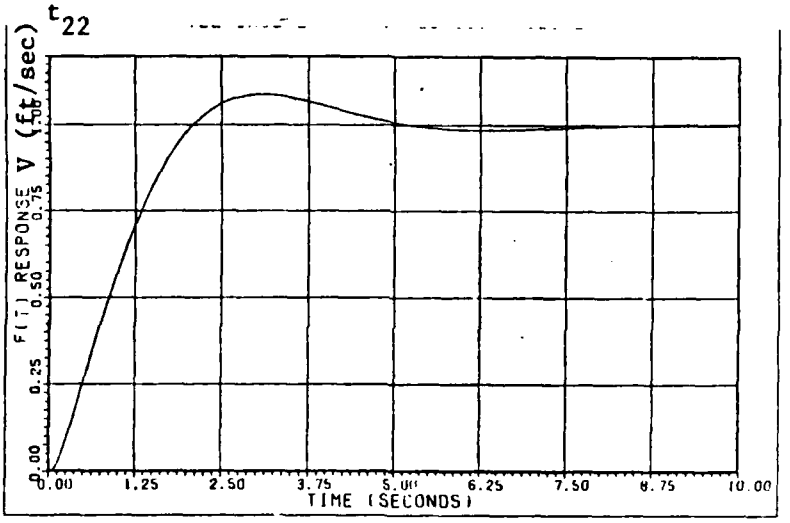

(b)

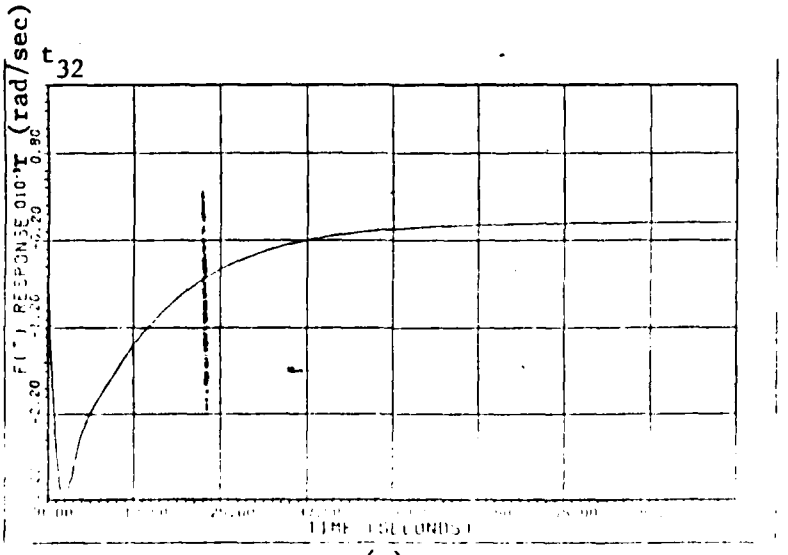

(c)

Fig. 7-6 Case 2 r(t) = 1 ft/sec

Table 7-1 Loop Responses

(Step input of 1 ft/sec)

	t_r	t_d	t_p	t_s	M_p	F_v
b_{12}			1.60		0.0499	0.00
$(t_{12})_1$			6.22		0.0034	0.00
$(t_{12})_2$			15.97		0.000	0.00
$(t_{12})_3$			2.930	14.87	0.033	0.00
b_{22}	0.751	0.950	1.86	5.58	1.31	1.00
$(t_{22})_1$	0.89	11.55	16.17	1.56	1.01	1.00
$(t_{22})_2$	1.46	2.11	3.08	4.61	1.09	1.00
$(t_{22})_3$	0.98	1.37	2.51		1.22	1.00
a_{22}	2.12			3.76	1.00	1.00
b_{32}			0.237		0.309	0.00
$(t_{32})_1$			0.30		0.0034	0.00
$(t_{32})_2$			2.40		0.0032	0.00
$(t_{32})_3$			0.810		0.000935	0.00

4. Comparison of Loop Responses and Bounds

The comparison of specifications is done in the time domain since the specifications are defined in the time domain. Table 7-1 lists the time response specifications for the t_{12}, t_{22} and t_{32} responses and their respective bounds (b_{12}, b_{22}, and b_{32}). Remember the bounds are derived using only a few of the criteria as important (t_r), M_p and F_v, Section V-4).

All of the t_{12} magnitude responses are below the design bound, b_{12}. M_p for b_{12} is 0.05 (step input = 1 ft/sec) and all three of the flight conditions are below this. The t_{22} responses are within their defined envelope (all three flight conditions have a t_r value between the b_{22} and a_{22} values of 0.751 and 2.12, as well as a M_p between 1.0 and 1.3; Table 7-1). The t_{32} responses satisfy the b_{32} bound (b_{32} bound M_p = 0.3 and the three flight conditions are almost two magnitudes smaller).

All three loop transfer functions designed satisfy the design specifications for all of the flight conditions. Thus the design is acceptable.

5. Different Command Inputs

Now try several different magnitude inputs. The inputs used, or the side velocity commanded, are 22.4 ft/sec, 32 ft/sec and 48 ft/sec. Only a representative response (FC #2) for each input is shown here. The results are in Figs. 7-7 through 7-9 and Appendix E.

All of the responses retain their original t_p, t_s, t_d and t_r. The F_v changes appropriately for loop 2, to match the commanded input, i.e. for a step input of 32 ft/sec the F_v is 32 ft/sec (Table 7-3 and Fig. 7-6b and Appendix E). The F_v of the other two loops are zero. The M_p, basically a measurement of the amount of overshoot, remained linear. M_p remained at a constant percentage overshoot in loop 2. For example, for an input of 1 ft/sec, M_p = 1.09 ft/sec and for an input of 32 ft/sec, M_p = 34.86 ft/sec (FC #2). Both responses have an overshoot of 9%. An input of 1 ft/sec to loop 1 results in M_p = 0.0034 rad (FC #1) and an input of 32 ft/sec results in M_p = 0.108 rad (32 x 0.0034). An input of

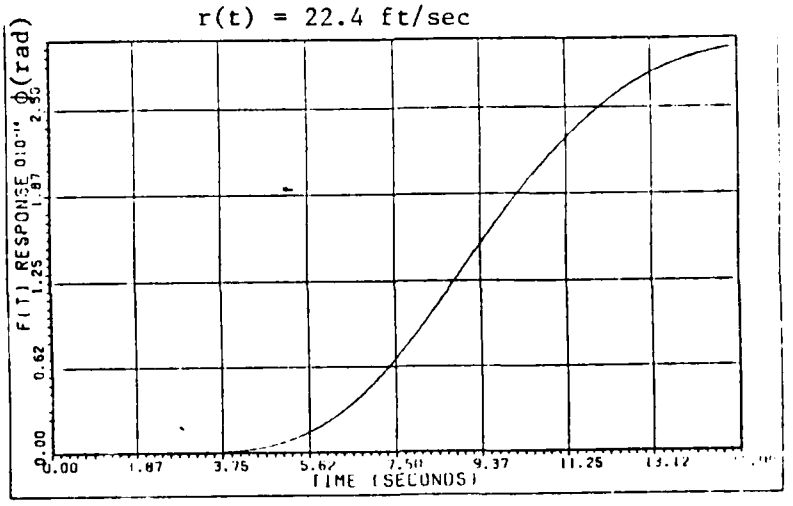

(a)

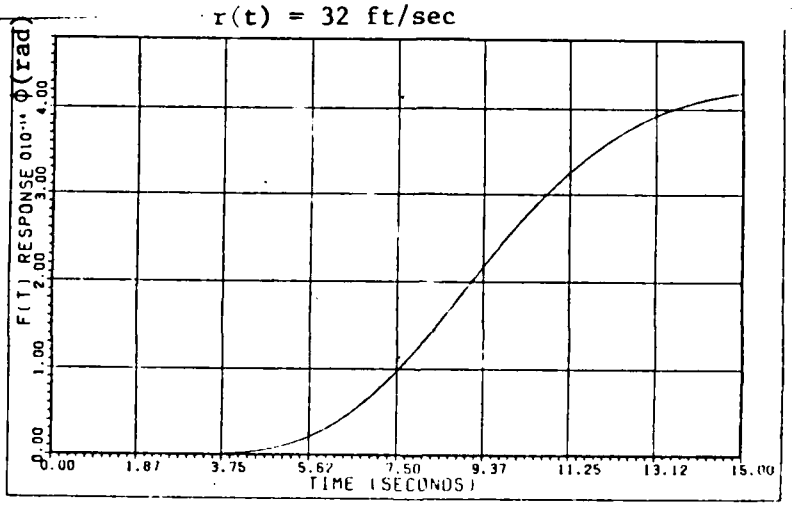

(b)

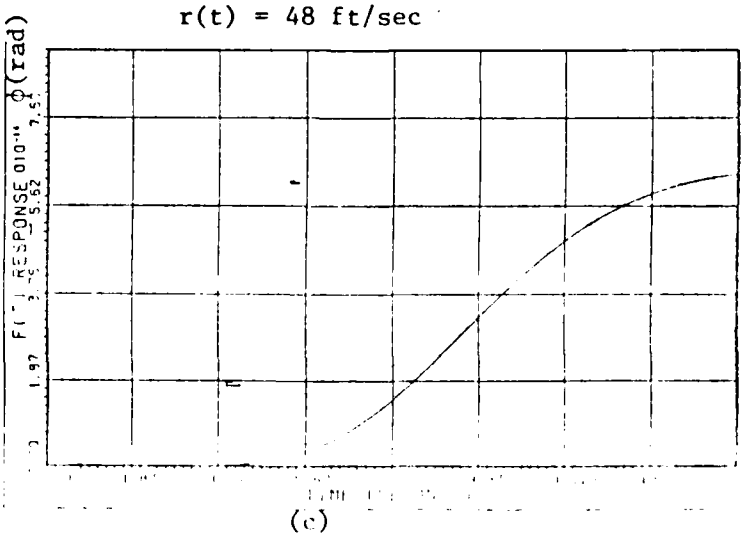

(c)

Fig. 7-7 t_{12} Responses to Different Inputs (FC #2)

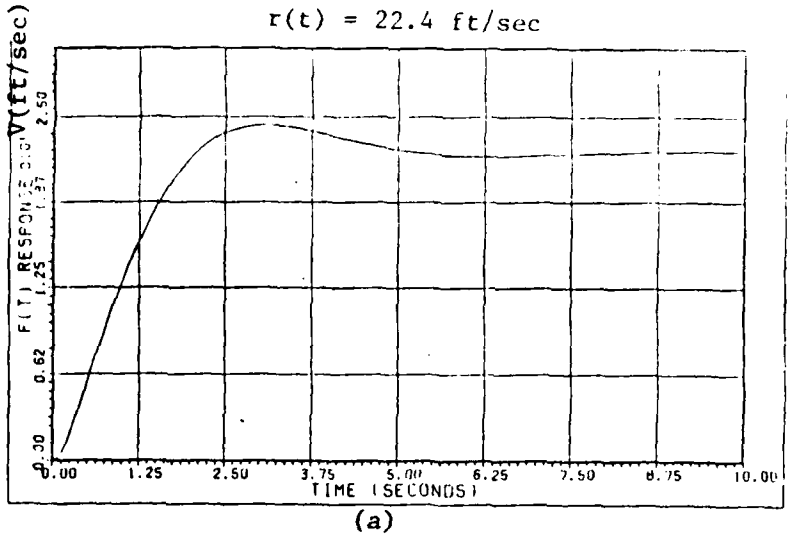

(a)

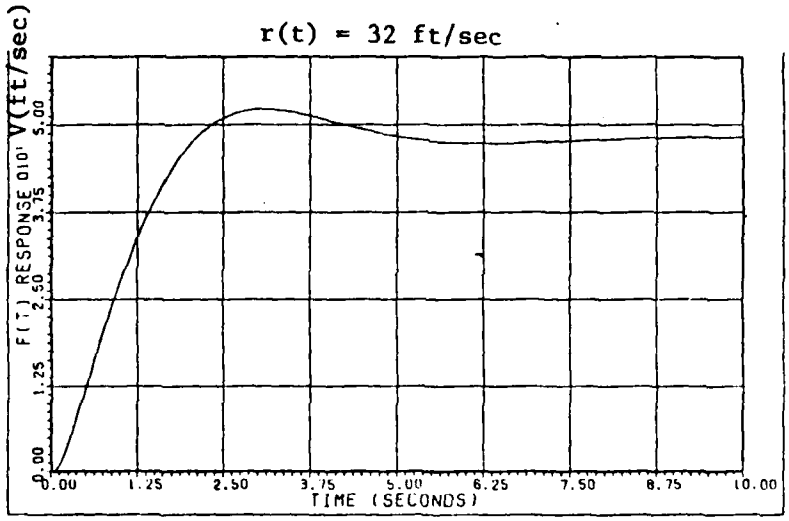

(b)

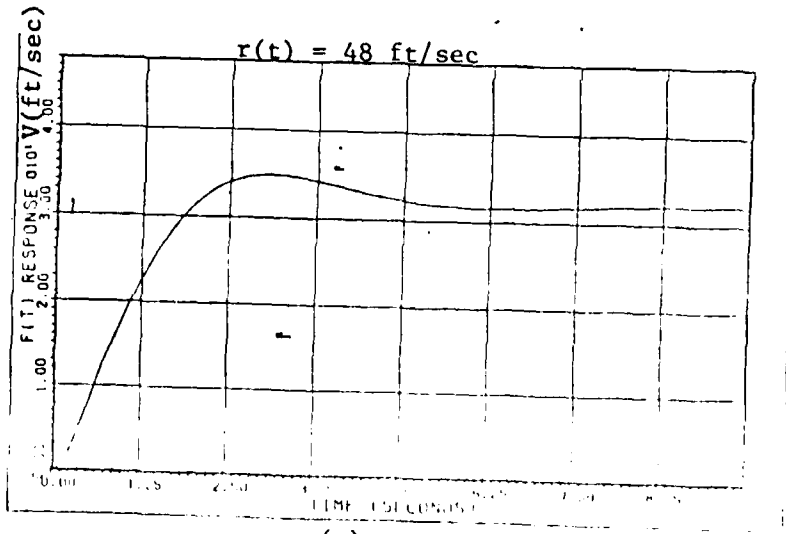

(c)

Fig. 7-8 t_{22} Responses to Different Inputs (FC #2)

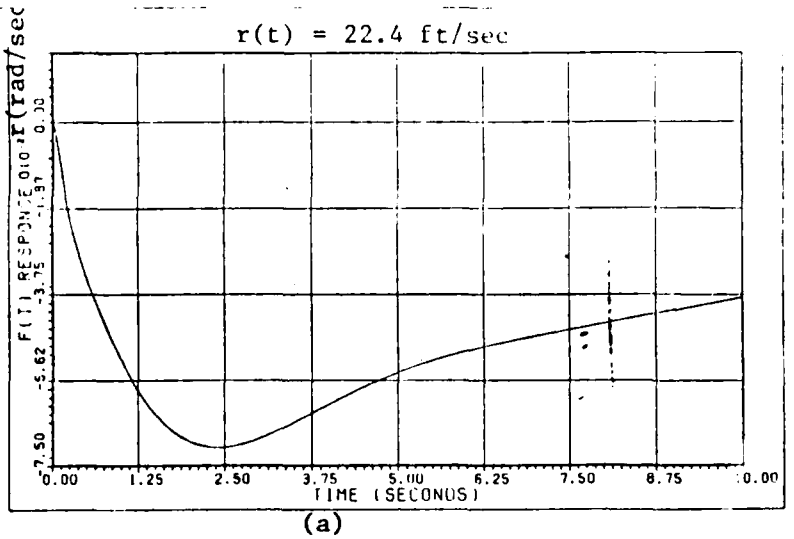

(a)

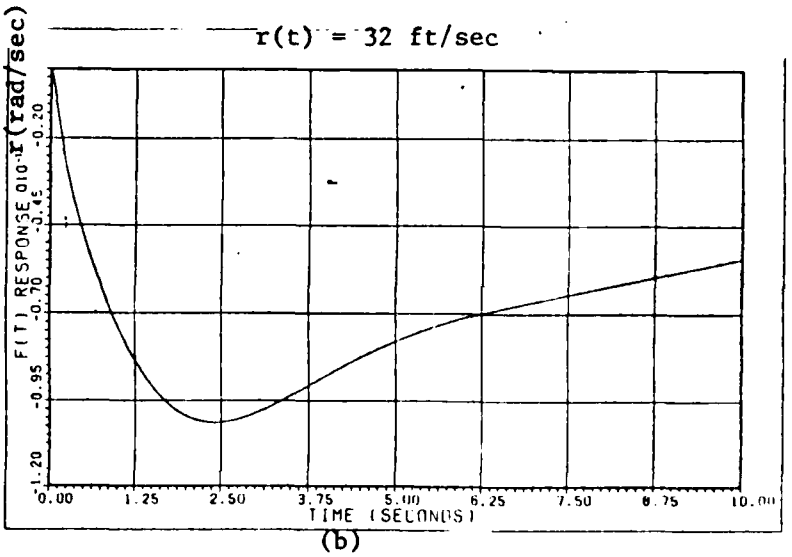

(b)

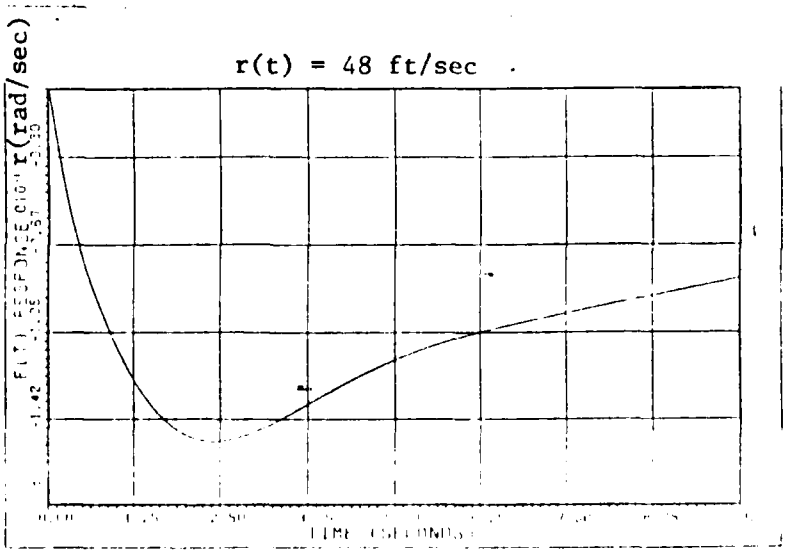

(c)

Fig. 7-9 t_{32} Responses to Different Inputs (FC #2)

48 ft/sec to loop 1 results in M_p = 0.16 rad (48 x 0.0034). These results are compared to their design boundaries in Tables 7-2 through 7-4.

Table 7-2 Loop 1 Responses to Different Inputs

	t_r	t_d	t_p	t_s	M_p	F_v
Step Input of 22.4 ft/sec						
b_{12}			1.60	very large	1.12	0.00
$(t_{12})_1$			6.22	very large	0.075	0.00
$(t_{12})_2$			15.97	very large	0.00	0.00
$(t_{12})_3$			2.93	14.87	0.737	0.00
Step Input of 32.0 ft/sec						
b_{12}			1.60	very large	1.60	0.00
$(t_{12})_1$			6.22	very large	0.108	0.00
$(t_{12})_2$			15.97	very large	0.00	0.00
$(t_{12})_3$			2.39	14.87	1.05	0.00
Step Input of 48 ft/sec						
b_{12}			1.60	very large	2.40	0.00
$(t_{12})_1$			6.22	very large	0.16	0.00
$(t_{12})_2$			15.97	very large	0.00	0.00
$(t_{12})_3$			2.93	14.87	1.58	0.00

The previous thesis contains results for only one flight condition for each different input command. Therefore a comparison is made between the previous thesis and the results from this thesis at the same flight condition and input command. The results from the previous thesis (2:62-63) are in Table 7-5 and Figs. 7-10 through 7-12. The response characteristics are similar. There is a difference in

Table 7-3 Loop 2 Responses to Different Inputs

	t_r	t_d	t_p	t_s	M_p	F_v
			Step Input of 22.4 ft/sec			
b_{22}	0.751	0.950	1.86	5.58	29.4	22.4
$(t_{22})_1$	0.87	11.55	16.17	1.56	22.7	22.4
$(t_{22})_2$	1.46	2.11	3.08	4.61	24.40	22.5
$(t_{22})_3$	0.98	1.37	2.51	very large	27.5	22.4
a_{22}	2.12			3.76	22.4	22.4
			Step Input of 32.0 ft/sec			
b_{22}	0.751	0.950	1.86	5.58	41.99	32.0
$(t_{22})_1$	0.87	11.55	16.17	1.56	32.4	32.0
$(t_{22})_2$	1.45	2.11	3.08	4.61	34.86	32.1
$(t_{22})_3$	0.98	1.37	2.51	very large	39.4	32.1
a_{22}	2.12			3.76	32.0	32.0
			Step Input of 48.0 ft/sec			
b_{22}	0.751	0.950	1.86	5.58	62.98	48.0
$(t_{22})_1$	0.87	11.55	16.17	1.56	48.6	48.0
$(t_{22})_2$	1.46	2.11	3.08	4.61	52.28	48.1
$(t_{22})_3$	0.98	1.37	2.51	very large	59.08	48.1
a_{22}	2.12			3.76	48.0	48.0

Table 7-4 Loop 3 Responses to Different Inputs

	t_r	t_d	t_p	t_s	M_p	F_v
			Step Input of 22.4 ft/sec			
b_{32}			0.237	very large	0.692	0.00
$(t_{32})_1$			0.30	very large	0.12	0.00
$(t_{32})_2$			2.40	very large	0.0710	0.00
$(t_{32})_3$			0.810	very large	0.0209	0.00
			Step Input of 32.0 ft/sec			
b_{32}			0.237	very large	0.988	0.00
$(t_{32})_1$			0.30	very large	0.17	0.00
$(t_{32})_2$			2.40	very large	0.101	0.00
$(t_{32})_3$			0.810	very large	0.0299	0.00
			Step Input of 48.0 ft/sec			
b_{32}			0.237	very large	1.48	0.00
$(t_{32})_1$			0.30	very large	0.25	0.00
$(t_{32})_2$			2.40	very large	0.152	0.00
$(t_{32})_3$			0.810	very large	0.0449	0.00

Table 7-5 Comparison of Responses

Previous Thesis and This Thesis (2:62-63)

	t_r	t_s	M_p
	Previous Thesis		
FC #1 Step input of 48 ft/sec	1.5 sec	7.0 sec	2.1%
FC #2 Step input of 32 ft/sec	0.9 sec	5.8 sec	5%
FC #3 Step input of 22.4 ft/sec	0.8 sec	3.0 sec	4.3%
	This Thesis		
FC #1 Step input of 48 ft/sec	0.87 sec	1.6 sec	1.25%
FC #2 Step input of 32 ft/sec	1.45 sec	4.6 sec	8.6%
FC #3 Step input of 22.4 ft/sec	0.98 sec		22.7%

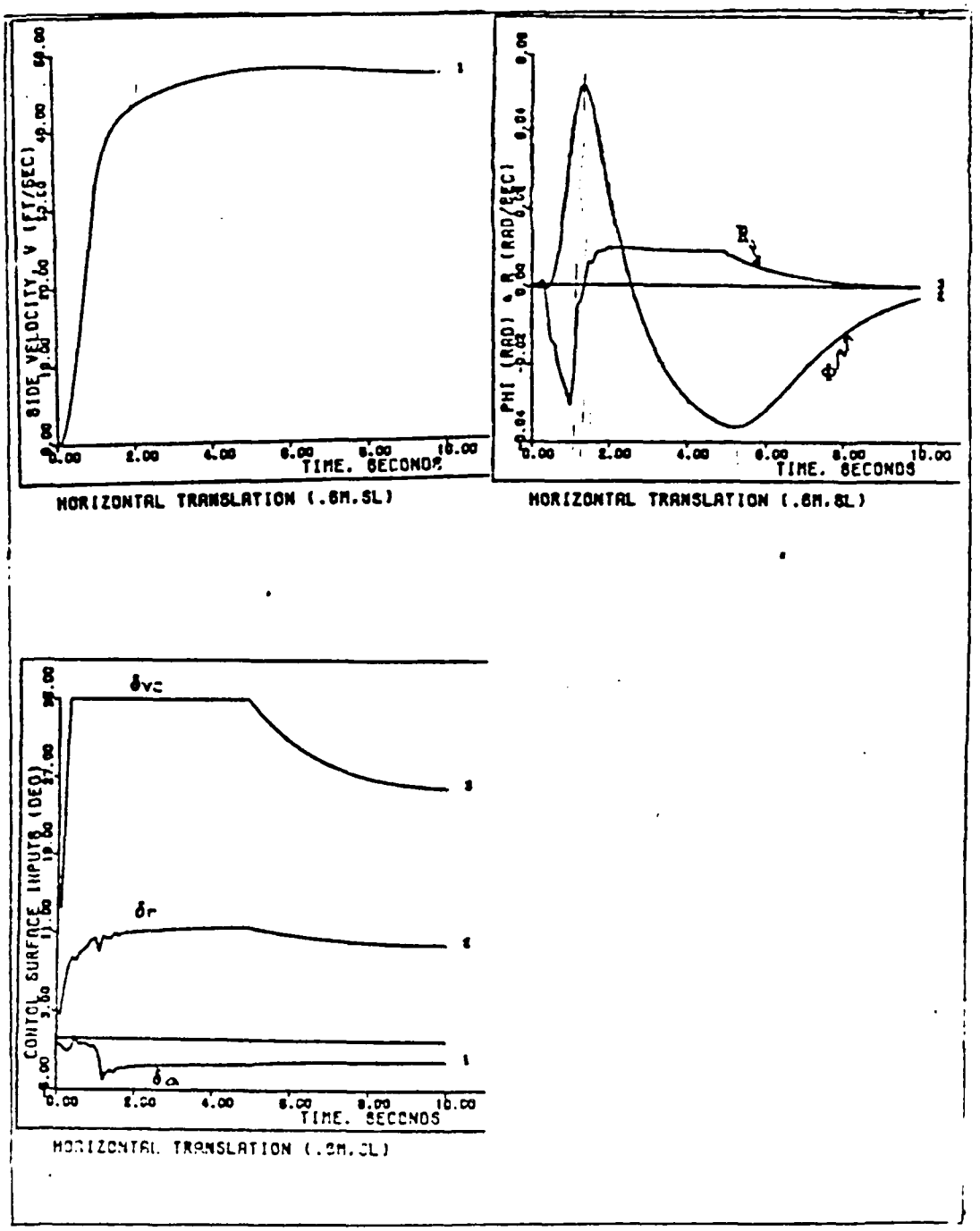

Fig 4. 1.5-g Horizontal Translation (.6M,SL)

Fig. 7-10 Flight Condition #1 Step Input = [illegible] (2:47

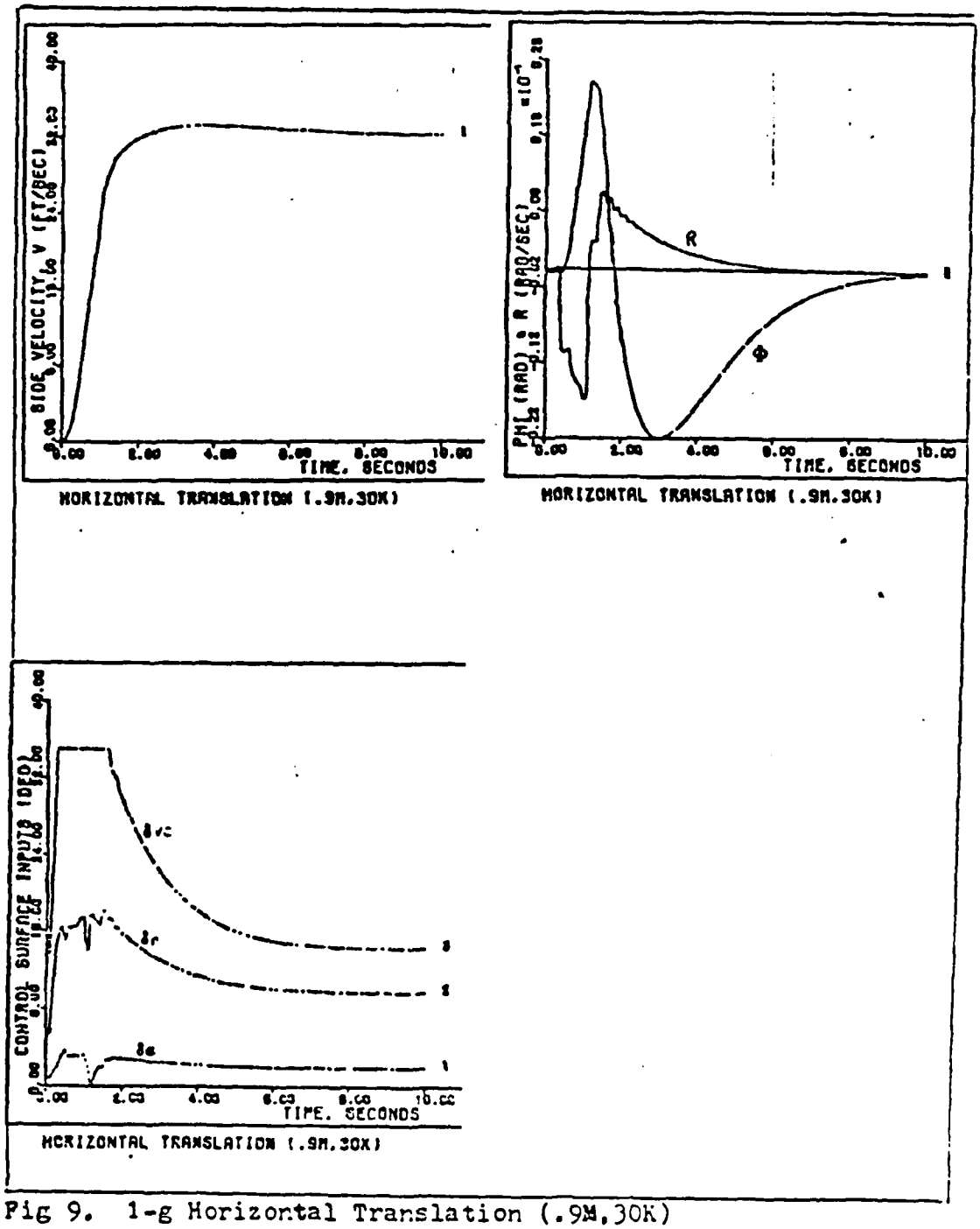

Fig 9. 1-g Horizontal Translation (.9M,30K)

Fig. 7-11 Flight Condition #2 Step Input = 32 ft/sec (2:52)

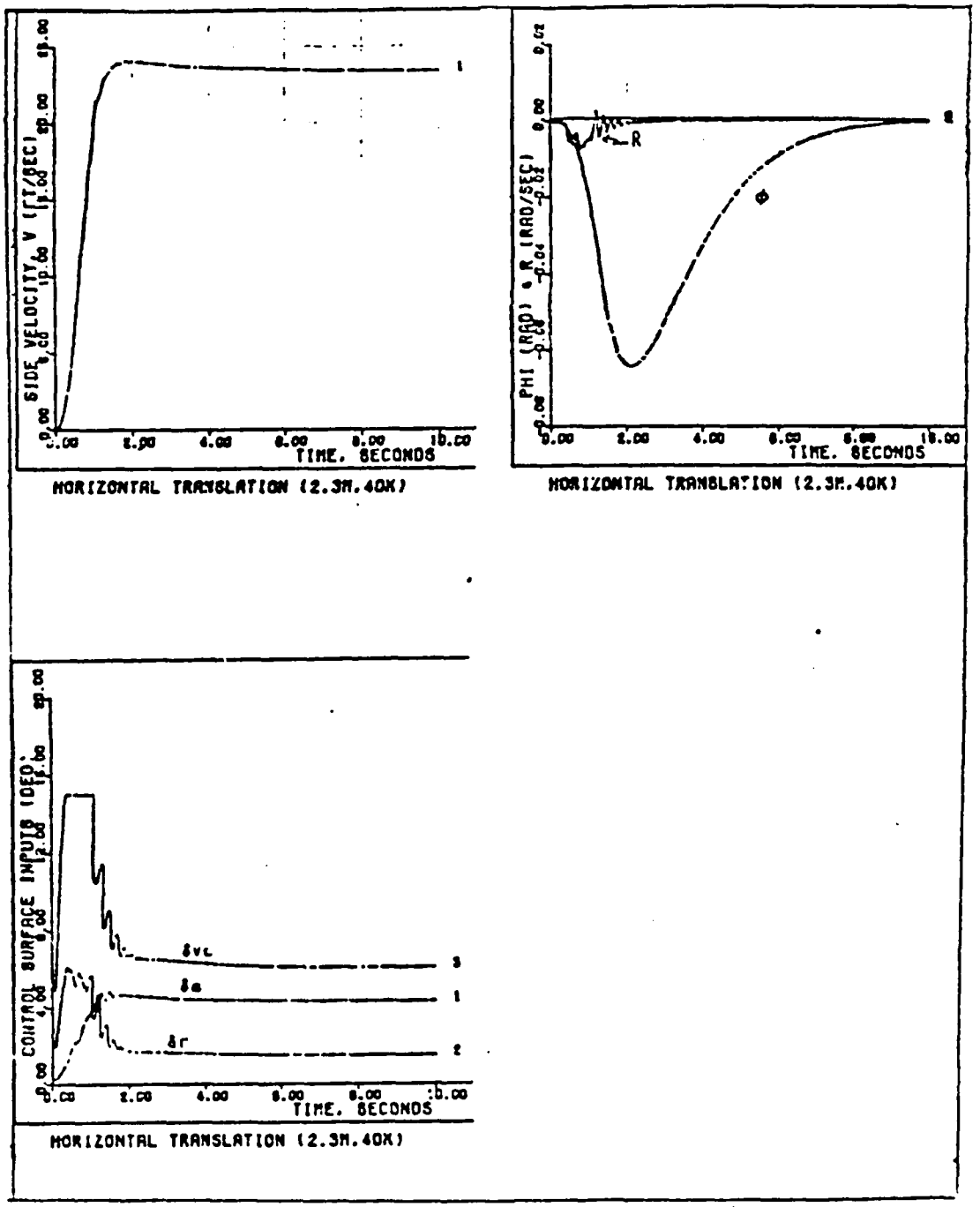

Fig 14. 0.7-g Horizontal Translation (2.3M,40K)

Fig. 7-12 Flight Condition #3 Step Input = 22.4 ft/sec (2:57)

the third flight condition but the specifications are satisfied by the responses.

6. Summary

The compensator responses, G_1, G_{1mod}, G_2 and G_3 are presented. The loop responses are presented with a comparison to their design bounds. Then a comparison is made between the previous thesis's results (2) and the results from the lateral controller designed in this thesis.

VIII. DISCUSSION AND CONCLUSIONS

1. Summary of Thesis

This thesis reviewed the Quantitative Feedback Theory (QFT) technique used to design a lateral controller for a hypothetical fighter type aircraft. Chapter II and Appendix A explains the QFT technique for a single input-single output (SISO) system. Chapter III explains the technique for a multiple input-multiple output (MIMO) system. The three-by-three aircraft model is reviewed in Chapter IV and Appendix B. The design for the first two of the three loops designed are in Chapter V and Appendix C. The final loop design is in Chapter VI and Appendix D. Chapter VII and Appendix E contain the system responses generated from the computer simulation.

2. Discussion of the Results

From the results in Chapter VII and Appendix E, the designed lateral controller satisfies all of the design specifications. The designed system responses are better than the design specification.

Comparing the two methods, the previous thesis results and this one, the responses are similar. This was expected because the response of the previous thesis is used to generate the design specifications for this thesis. The two methods do differ. The Porter technique must test each design for satisfaction of the performance specifications bounds and for robustness. The QFT technique guarantees that any uncertainty designed for is satisfied by the design solution, thereby the performance specifications are satisfied and the robustness (uncertainty range) is satisfied. Remember the uncertainty and performance

specifications are used in the QFT technique to synthesize the controller. Porter's method used straight gains in the feedback loop to achieve a compensator to satisfy the specifications. This generates a compensator bandwidth of unknown size. Since the QFT technique is performed in the frequency domain, the bandwidth can be controlled. Porter's technique might find a solution faster than the QFT technique if a solution is found in the first few iterations. If the specifications are difficult, or impossible though, the Porter method could take much longer. The QFT technique's insight helps here. The difficult or impossible specifications are identified by the designer who then modifies the design bounds and specifications if necessary.

3. Possible Improvements for the Design

There are several ways to improve this design. Do a design trade-off during the generation of the nominal bounds, rearrange the order in which the design is performed, use the improved method or use a non-diagonal G or prediagonalized system.

A trade-off can be made during the generation of the nominal bounds. If one loop has an unacceptable high bandwidth, and the other loops easily meet their specifications, then by requiring the loops which easily meet their specifications to meet more restrictive specifications, it might help reduce the bandwidth of the loop with too high a bandwidth. This is done by decreasing the appropriate design bound during the nominal bound calculation. For example in Eq. 5-1:

$$|1 + L_1|^{-1} = \frac{b_{22} \frac{|q_{11}|}{|q_{12}|} + b_{32} \frac{|q_{11}|}{|q_{13}|}}{b_{12}} \qquad (5\text{-}1)$$

If the L_1 bound is hard to satisfy, but the L_3 bound is not, then by decreasing the b_{32} value (making it more restrictive) decreases the bound on L_1.

If during the design, the designer notices that a loop other than the one suspected hardest to satisfy is hardest, rearrange the order in which the loops are designed. In this paper, looking at the resulting responses, the order of design should change from performing loop 1 and 3 first and then loop 2 to performing loop 3 and 2 first and then loop 1. Loop 1 has a very high bandwidth, therefore by doing this loop last, the bandwidth could be lowered a little because there is less overdesign in the last loop designed (Section V-5).

Another improvement is to use the improved method (Section III-5). This does not change the first loop design. But the second loop designed uses the loop previously designed, thus less uncertainty exists in the terms. This leads to less overdesign throughout the designs.

Another improvement is to use a nondiagonal G matrix. It involves trying to prediagonalize the plant. From the loop transmission synthesized, a $\underline{G}_{eff}$ is derived which effectively includes the diagonalizing matrix, $\underline{H}$, which is used to generate the diagonalized plant matrix, $\underline{P}_{eff}$.

$$H = P_o^{-1} \Lambda$$

$$P_{eff} = PH = PP_o^{-1} \Lambda$$

4. Comments on the QFT Technique

The QFT technique has several advantages. Probably the most important advantage is its transparency. The designer knows during the design phase how well the design is doing. He knows if the design meets its goals or not. If it does not meet its goals, the technique guides the designer to the source of the problem, and thus reveals possible corrective actions.

Another advantage is the algebra is relatively simple. There are no complex integrals or derivatives to manage. This makes the mechanics of the technique easy and the programming (except for the graphical part) of the problem simple.

Probably the biggest disadvantage is the amount of overdesign. There often is overdesign. In other words, though the design is guaranteed to meet the specifications, more bandwidth is used than is necessary. The amount more than necessary cannot be determined without some analysis of the design. Reference B discussed means for reducing the overdesign.

A point of argument is the amount of time and effort needed to design a MIMO system because of the number of loops necessary to design. The QFT technique reduces the n x n MIMO problem into n^2 equivalent SISO problems, with n loops to solve. Consider the alternatives though. Huge matrices with many assumptions to simplify the matrices or fill out the matrices, requiring a computer to solve.

On the other hand, the QFT technique requires the design of many SISO problems. Using a computer program (other techniques require a computer program for almost any real problem), the SISO solutions are found very quickly and remember the solution is guaranteed for minimum phase plants to meet the design criteria (the design could be also performed manually). If the n x n MIMO problem does not have certain inputs or coupling terms, the number of equivalent problems to solve might drop significantly. For example, in this thesis, only loop 2 had a non-zero command input. Thus only three of the possible nine equivalent SISO problems from the 3 x 3 MIMO system needed solving. Many of the other techniques must still solve huge matrices unless the matrices are reconfigured which could take a lot of work, time and approximations.

5. Recommendations and Conclusions

The QFT technique is a method which needs further investigation. The technique's theory says it could work on most any minimum phase problem, linear or non-linear. Only some of these problems have been investigated. This is one of several theses from AFIT investigating the simple linear minimum phase problem. This is the first AFIT thesis to investigate a system higher than a two-by-two. The technique does get more involved with each additional loop, which is expected. Throughout these investigations the QFT technique has been demonstrated for this type of problem. Now non-linear and non-minimum phase systems need investigating more fully (some investigation has been done already). Another area is to complicate the plant by adding bending modes and coupling the lateral and longitudinal axes. A computer program (CAD system) with a screen showing the Bode Plot and Nichols Chart

together, as well as a time response plot would be very helpful and speed up the method significantly.

More research is needed to find the limits of this technique so the designer can put this method in his repertoire and use it to its best advantage.

In conclusion, the technique works as advertised, the design met and exceeded all of the design specifications. The technique uses simple algebra and a graphical technique, which makes it transparent from the solution back to the original specifications.

BIBLIOGRAPHY

1. Ashworth, M. J. Feedback Design of Systems with Significant Uncertainty. Chinchester: Research Studies Press, 1982.

2. Bauschlicher, Jon M. Design of a Complete Multivariable Digital Flight Control System. MS Thesis, School of Engineering, Air Force Institute of Technology, Wright-Patterson Air Force Base, OH, December 1982.

3. Betzold, Robert. Multiple Input-Multiple Output Flight Control Design with Highly Uncertain Parameters; Application to the C-135 Aircraft. MS Thesis, School of Engineering, Air Force Institute of Technology, Wright-Patterson Air Force Base, OH, December 1983.

4. Blakelock, John H. Automatic Control of Aircraft and Missiles. New York: John Wiley and Sons, Inc., 1965.

5. D'Azzo, John J. and Constantine H. Houpis. Linear Control System Analysis and Design, Conventional and Modern (Second Edition). New York: McGraw-Hill, Inc., 1981.

6. Etkin, Bernard. Dynamics of Atmospheric Flight. New York: John Wiley and Sons, Inc., 1972.

7. Heimbold, R. L., et al. Flight Propulsion Control Coupling (FPCC) and Dynamic Interaction Investigation Volume I Phase I. AFFDL TR-75-753, Air Force Flight Dynamics Laboratory, Wright-Patterson Air Force Base, OH, September 1975.

8. Heimbold, R. L., et al. Flight Propulsion Control Coupling (FPCC) and Dynamic Interaction Investigation Volume II Phase II. AFFDL TR-75-753, Air Force Flight Dynamics Laboratory, Wright-Patterson Air Force Base, OH, September 1975.

9. Honeywell, Inc. Systems and Research Department. Users Manual for the Program FPCCSIM. MR 12369, Minneapolis, MN, July 1975.

10. Horowitz, Isaac. "Improved Design Technique for Uncertain Multiple-Input-Multiple Output Feedback Systems," International Journal of Control, 36 (6): 977-988 (1982).

11. Horowitz, Isaac. "Quantitative Feedback Theory," IEE Proceedings; Control Theory and Applications, 129 Part D (6): 215-226 (November 1982).

12. Horowitz, Isaac and T. Kopelman. Multivariable Flight Control Design with Uncertain Parameters. Department of Applied Mathematics, The Weizmann Institute of Science, Rehovot, Israel, Final Report, October 1981.

13. Horowitz, Isaac and Claytin Loecher. "Design of a 3x3 Multivariable Feedback System with Large Plant Uncertainty," International Journal of Control, 33 (4): 677-699 (April 1981).

14. Horowitz, Isaac, et al. Research in Advanced Flight Control Designs. AFFDL-TR-79-3120, Department of Applied Mathematics, The Weizmann Institute of Science, Rehovot, Israel, January 1980.

15. Horowitz, Isaac. "Quantitative Synthesis of Uncertain Multiple Input-Output Feedback System," International Journal of Control, 30 (1): 81-106 (1979).

16. Horowitz, Isaac, and Marcel Sidi. "Synthesis of Feedback Systems with Large Plant Ignorance for Prescribed Time Domain Tolerances," International Journal of Control, 16 (2): 287-309 (1972).

17. Horowitz, Isaac M. Synthesis of Feedback Systems. New York: Academic Press, 1963.

18. Houtz, John E. FPCC Linear Analysis Digital Computer Program. AFFDL/FGL-TM-77-82-FGL, Air Force Flight Dynamics Laboratory, Wright-Patterson Air Force Base, OH, November 1977.

Appendix A

Loop Transmission Shaping Example

This appendix contains an example of shaping a loop transmission. This is a copy of a handout Dr. Horowitz distributed in a class at AFIT. The example, which is complete within itself, is meant to give the reader a better understanding of how to shape a loop transmission.

Example: Shaping of a nominal loop transmission $L_0(j\omega)$ to satisfy boundaries $B(\omega)$ on Nichols Chart.

Previous notes have described how tolerances on the closed-loop system frequency response are readily translated into bounds on a nominal loop transmission function $L_0(j\omega)$. In Fig. 1, for example, $L_0(j2)$ must be on or above the curve labelled B(2), etc. B_h is the "universal high-frequency boundary" applicable, in this example, to $\omega \geq \omega_h = 40$, i.e. $L_0(j\omega)$ (for $\omega \geq 40$) must be contained in the closed curve B_h in Fig. 1. Additional specification is $e_L = 4$, where e_L is excess of poles over zeros of $L_0(s)$. Also, L_0 is to be Type 1 (one pole at the origin). We proceed to describe a reasonable procedure for choosing a rational function $L_0(s)$ which satisfies the above specifications.

In our first step, we try to find the $B(\omega)$ which "dominates" $L_0(j\omega)$. E.g. suppose $L_{01}(j4) = 0db\angle -135°$ (point A in Fig. 1). But at $\omega=1$, $|L_0(j)|$ needed is ≈27db. In order to decrease $|L_0|$ from 27db to about 0db in 2 octaves ($4/1=2^2$), the slope of $|L_0(j\omega)|$ would have to be, on the average, about -14db/octave, involving $\angle L_0 < -180°$. We assume "absolute" stability is required here for $L_0(j\omega)$ with a margin of 40°, not just at crossover ("crossover" is defined as the frequency at which $|L_0(j\omega)| = 1$). Hence B(1) dominates $L_0(j\omega)$, at least more than B(4). In the same way we see that B(1) dominates over all other $B(\omega)$ in Fig. 1.

The $B(\omega)$ for $\omega < 1$ are not shown in Fig. 1. We shall assume that for $\omega < 1$, a slope of -6 db/octave (with 27db at $\omega=1$, i.e. 33 db at $\omega=.5$, 39db at $\omega=.25$ etc.), suffices. We can tolerate ≈-140° for $\omega \geq 1$, so we choose a lag corner frequency (symbol lacf) at $\omega=1$ (i.e. pole at -1), and set $|L_0(j\omega)|$ (asymptotic) at 30 db (to allow for the -3db correction). Thus our L_0 is so far: $L_{01} = 31.6/s(s+1)$, whose phase $\angle L_{01}(j\omega)$ is sketched in Fig. 2.

$\angle L_{01}(j\omega)$ violates the -140° bound at $\omega>1.2$, so a lead corner frequency (symbol lecf) is needed. Where should it be located? At $\omega=5$, $\angle L_{01}(j5)=-169°$ (see Fig. 2), so 29° lead is needed; but we know that later there will be a second lacf, so allow say additional 15° for it giving 15+29~45° lead required at $\omega=5$; which is achieved by a lecf at $\omega=5$ i.e. a zero at -5. The resulting $L_{02}(s)=\frac{31.6(1+\frac{s}{5})}{s(1+s)}$, whose phase $\angle L_{02}(j\omega)$ is sketched in Fig. 2.

In the Nichols Chart (N.C.) we are ($\omega=10$ or so) in the region where the maximum phase lag allowed is 135° (i.e. $\angle L_0(j\omega)$ must be $>-135°$). Consider $\omega=10$, with present $\angle L_{02}(j\omega) = -112°$, so 135°-112°=23° more lag is allowed. But this lacf will be followed by a lecf, so allow say 10° for it, giving 23°+10°=33° more lag allowable. This locates the lacf at 15.4 (tan33°=.65, and 10/.65=15.4), so we set the lacf at $\omega=15$ (i.e. pole at -15), giving $L_{03}(s)=\frac{31.6(1+.2s)}{s(1+s)(1+\frac{s}{15})}$. $\angle L_{03}(j\omega)$ is sketched in Fig. 2.

Looking ahead at $\omega=40$, $|L_{03}(j40)| \approx -20$db, so soon $L_0(j\omega)$ can make its asymptotic left turn under the B_n boundary. Our plan is to add two more lecfs, and finally two complex pole pairs, in order to have an excess e_L of poles over zeros of 4. We try one lecf at $\omega=40$, giving $L_{04}(s)=\frac{31.6(1+.2s)\ (1+\frac{s}{40})}{s(1+s)\ (1+\frac{s}{15})}$. $\angle L_{04}(j\omega)$ is sketched in Fig. 2.

We're ready now for the last lecf, in order to achieve (an asymptotic) horizontal segment for $|L_0(j\omega)|$, before the final -24db/octave slope. (We follow Bode in this respect, a good master to follow.) Where should this horizontal segment be located? The bottom of B_n (see Fig. 1) is at -22.5db. Allow 2db margin, 3db correction due to the last lecf, 1.5db for the effect of the lecf at $\omega=40$, giving a total of -(22.5+2+3+1.5)=-29. We'll use a damping factor of $\zeta=.6$ for the 2 complex pole pairs, so no

correction need be allowed for them. Thus the final break for $|L_0(j\omega)|$ asymptotic is to be at -29db, which $|L_{04}(j\omega)|$ achieves at ω=60. Hence, the last lecf is at ω=60. The resulting phase due to L_{04} and the lecf at ω=60, is -66°. We could have -180° at this point, but we'll allow an additional 15° margin (a matter of taste; it depends on the problem -- presence of higher order modes, etc). This means 100° phase lag is permitted, 50° due to each complex pole pair (180-66-15≈100). For ζ=.6, this locates them at 100. Thus $L_0(s) = \dfrac{31.6(1+.2s)(1+\frac{s}{40})(1+\frac{s}{60})}{s(1+s)(1+\frac{s}{15})[1+\frac{(1.2)}{100}s+\frac{s}{10}4]^2}$.

Discussion

$L_0(j\omega)$ is sketched in Fig. 1. A well-designed, i.e. "economical" $L_0(j\omega)$ is close to its boundary $B(\omega)$ at each ω. The vertical line -140° is the dominating $B(\omega)$ for ω<5 and the right side of B_h (line -135°) is the boundary effectively for 5≤ω≤30; so our $L_0(j\omega)$ is pretty good in this respect since it is pretty close to these boundaries. There is tradeoff between complexity of $L_0(s)$ (number of its poles and zeros) and its final cut-off frequency, now at ω=100. There is some phase to spare between $L_0(j\omega)$ and the boundaries, so use of more poles and zeros in $L_0(s)$ would permit this cut-off frequency to be reduced a bit below 100, but not by much. On the other hand, if we want to reduce the number of poles and zeros of $L_0(s)$, we must pay the price in a larger cut-off frequency. We could economize significantly, of course, by allowing more phase lag in the low frequency range. If -180° was permitted at ω=1, we could decrease $|L_0(j\omega)|$ at a rate of 12db/octave; so with $|L_0|$= 25db at ω=1, it would be 13db at ω=2 (instead of the present 18db). Even with no more saving, this 5db difference, would allow a cut-off frequency at about 70 instead of 100.

Also, Fig. 1 reveals (immediately, without any shaping of L_0 required) that reduction (i.e. easing) of the specifications at ω=1 to about 21db (instead of ≈26db), would have the same effect as the above. One can check how badly the specifications are compromised by such easing. The design technique is thus highly "transparent" in revealing the trade-offs between performance tolerances, complexity of the compensation, stability margins, and the "cost of feedback" in bandwidth.

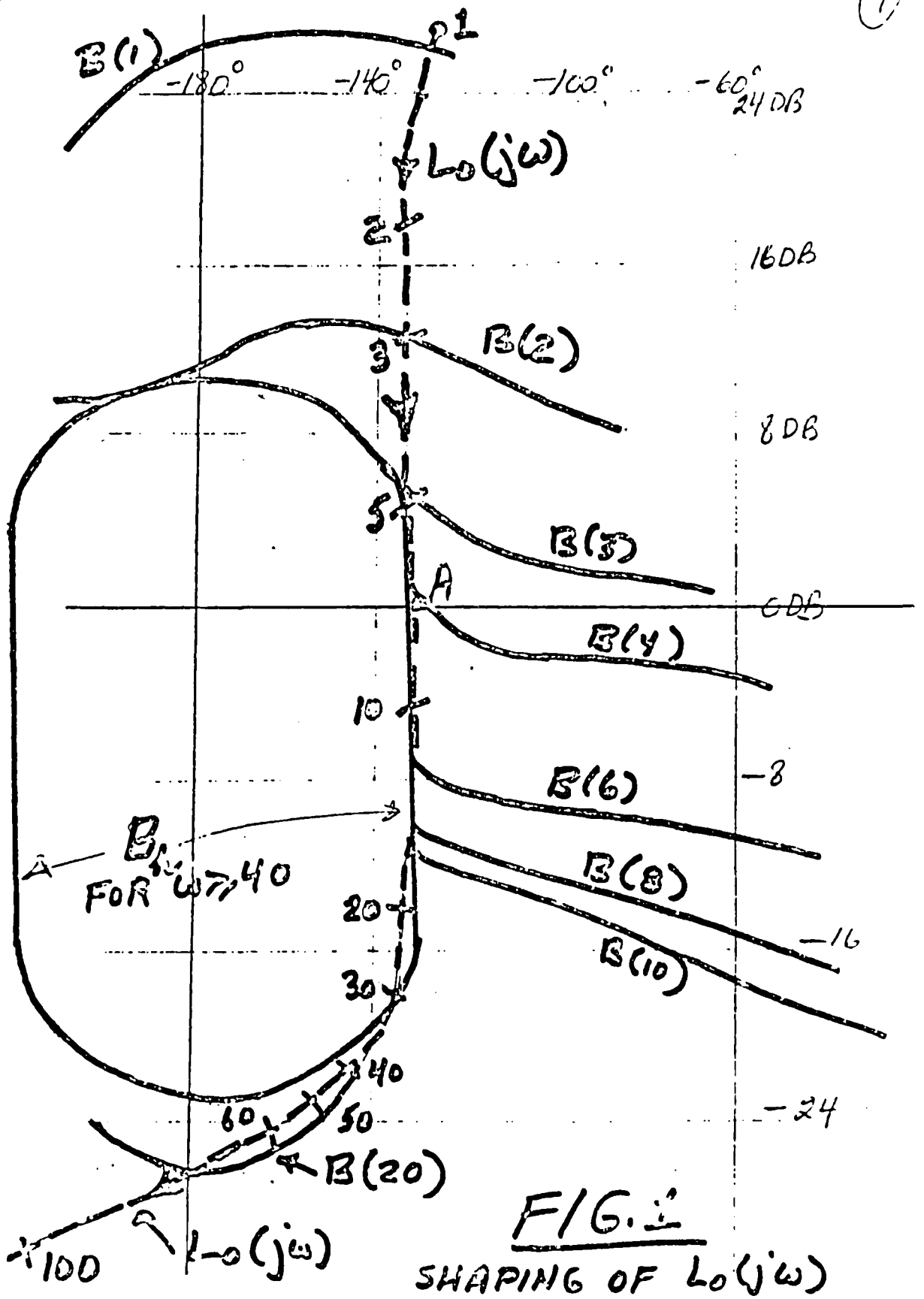

FIG. 1

SHAPING OF $L_o(j\omega)$ ON NICHOLS CHART.

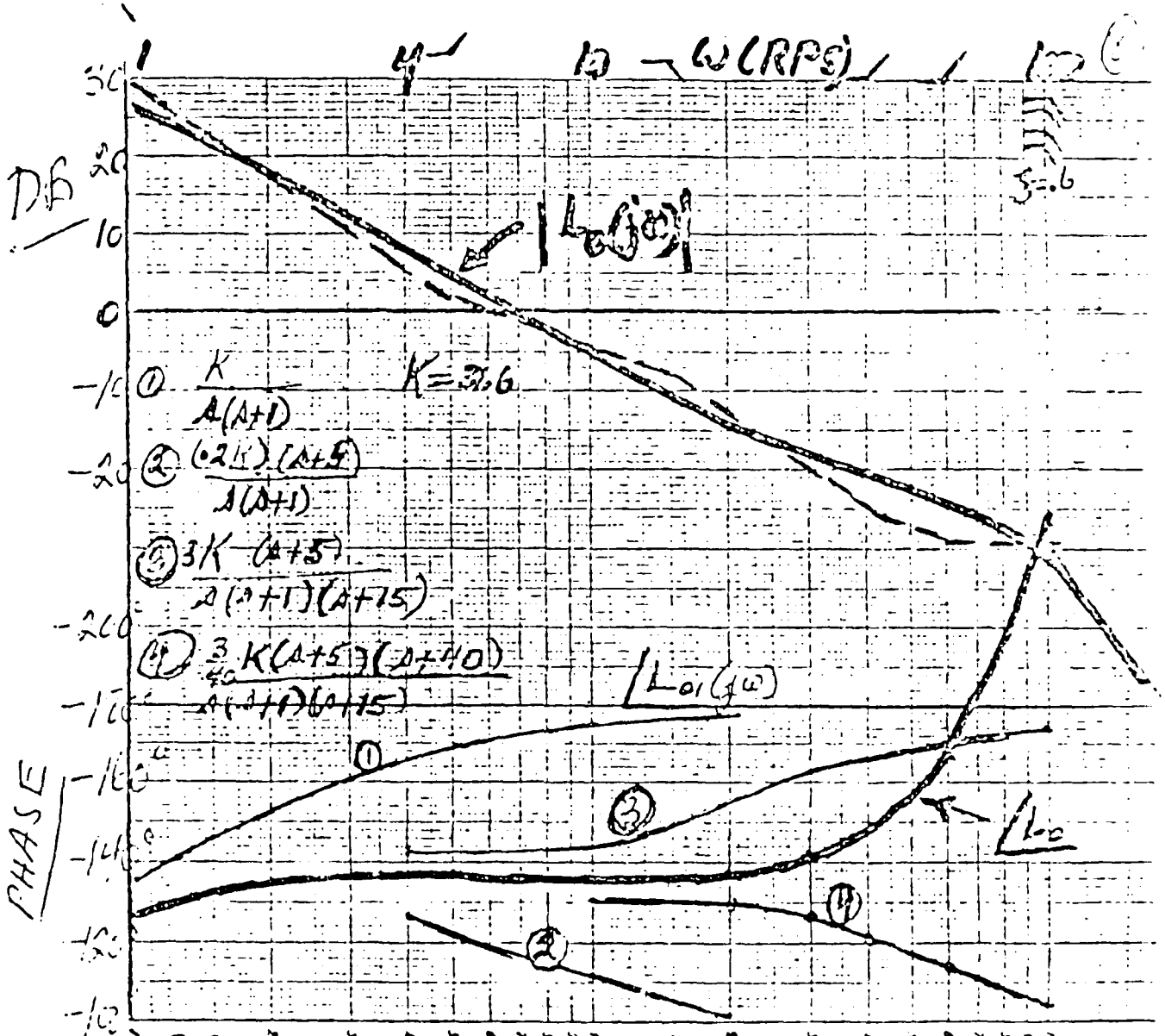

FIG. 2 SHAPING OF $L(j\omega)$ ON BODE PLOT.

DESIGN EXAMPLE: Uncertain Plant $P=\frac{k}{s(s+p)}$

k: [10,80], p: [-2,2].

Note: For part of range of p, plant is unstable.

Note: for w=0, plant template is infinite amplitude

Specifications on $|T(j\omega)|$. (see Fig. A)

ω	0	.5	1	2	5	10
MAX(DB)	0	1.3	1	-6	-17	-33
MIN(DB)	0	-2	-7	-19	-35	-65
(Δ|T|)MAX	0	3.3	8	13	18	32

EXCESS e_L OF POLES OVER ZEROS OF L, IS 3.

ALSO $\left|\frac{L}{1+L}\right| \leq 3DB$, FOR ALL ω&P.

N.B. At high ω, (Δ|T|)MAX MUST BE > |ΔP|MAX. OK.

Step 1 Calculation and Construction of Plant Templates {P(jω)}=

The templates are shown in Fig. B_1. It suffices to calculate (at a fixed ω) several values of $1/j\omega(j\omega+p)$, i.e. at different p values. This gives the bottom curve of the template. Then extend vertically by 18db(80/10=8; 20log8=18).

Step 2 Use the procedure described in the notes (p.17 etc) to find bounds on $L_0(j\omega)$ in order to satisfy the specifications on $|T(j\omega)|$. A nominal plant must be chosen; p=2, k=1 was chosen as nominal and marked heavily in Fig. B_2. (It helps to have the templates on transparent paper or plastic.) Already at ω=1, the bound on $L_0(j)$, denoted by B(1) is determined by $|L/(1+L)| \leq 3DB$, rather than by the constraints on $|T(j\omega)|$. And this is so for ω>1 also, which is not typical for stable plants but more likely for plants which can be open-loop unstable for part of the parameter range.

Shaping of $L_0(j\omega)$

The boundary at $\omega=2$ dominates, i.e. determines the level of $|L_0|$ at $\omega=2$ to be $\approx$10db. The boundary at $\omega=5$ determines the phase there to be $\approx$-85°or so. This necessitates a lead corner frequency at some $\omega<5$. This was chosen to be at 1 and lags introduced thereafter such that at $\omega=5$ the phase > -85°; they were chosen at 5 and 8 (see Figs. B_2,C). A lecf is then needed to be followed by a complex pole pair with $\zeta=0.6$. The corner below the high-frequency bound can be turned when $|L|$ is $\approx$ -25db. If we try a lecf at 40, then phase requirements at $\omega=20$ force the final cut-off frequency to be well beyond the ω value at which $|L_0|$ =-25db. A lecf at $\omega=25$ gives compatibility of phase needs at $\omega=20$ and turning the corner when $|L_0|$ permits it. This gives 100 as the frequency at which the final complex pole pair can be inserted. This gives $L_0(s)=\dfrac{4(1+s)(1+\frac{s}{25})}{s(1+.2s)(1+\frac{s}{8})[1+\frac{1.2s}{100}+(\frac{s}{100})^2]}$

$=GP. = \dfrac{G(s)}{s(s+2)}$, giving G(s), -- see Figs. B_2, C.

Finding F(s)

The proper G guarantees that $\Delta|T|$ does not exceed those allowed. The next step is to find the range of $|L(j\omega)/(1+L(j\omega)|$. Place the template of the plant at $\omega=5$ (for example) on the point $L_0(j5)$ in the Nichols Chart, i.e. on 5db /-82° and it is seen that $|L/(1+L)|$ max$\approx$ 2.4db, min -1.7db. But the specifications require $|T|=|\Gamma L/(1+L)|\in[-35, -17]$ db. Therefore, it is required that: -33.3db$<|F|<$-19.4db. In this way we obtain the bounds on $|F(j\omega)|$ shown in Fig. D. It is easy to find an F(s) which satisfies these bounds, e.g. $F(s)=\dfrac{1}{(s+1)(1+\frac{s}{1.5})(1+\frac{s}{10})}$.

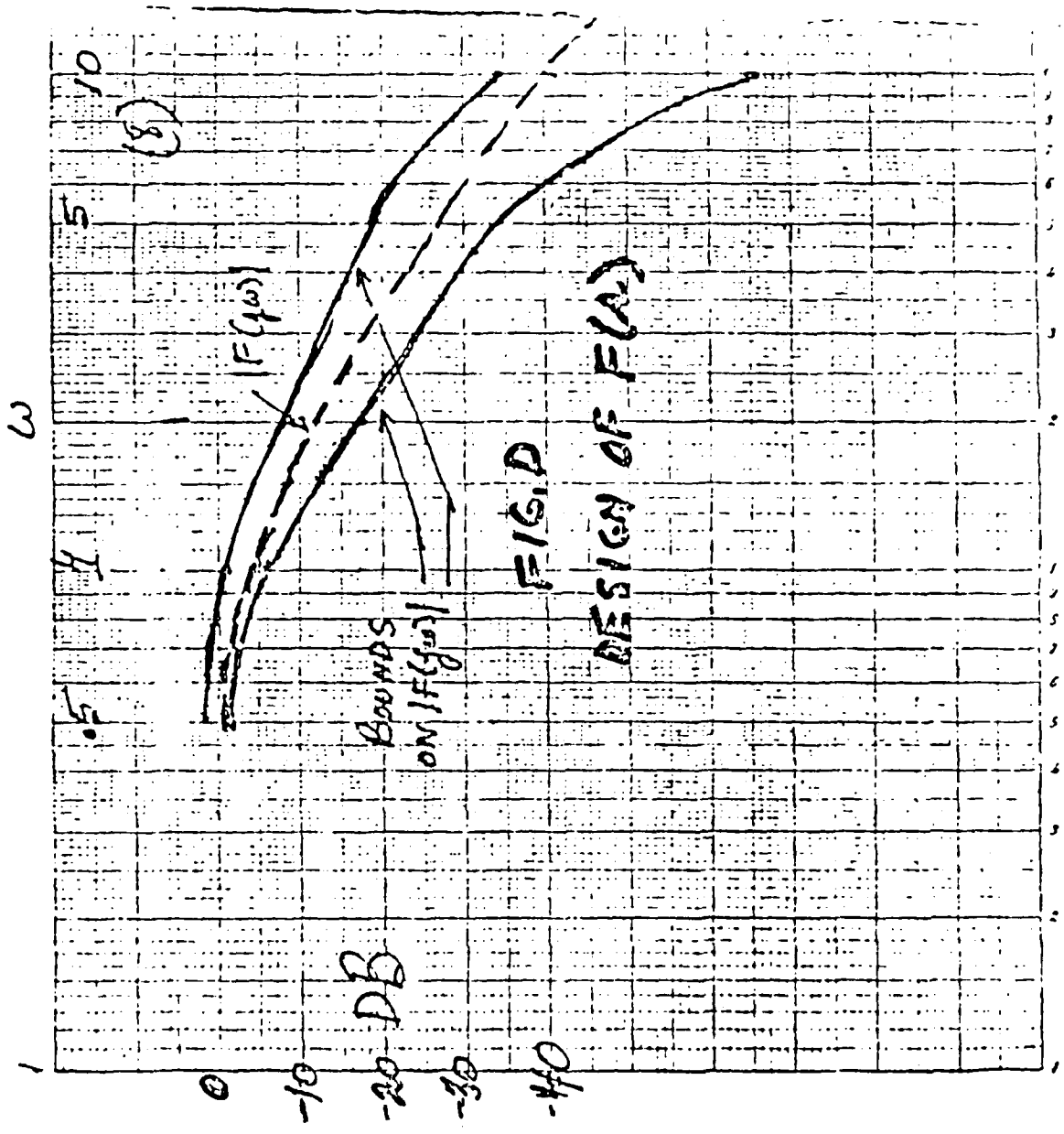

(5)

PLANT TEMPLATES- (NICHOLS CHART)

$P = \frac{k}{s(s+p)}$

FIG. B1

k : 10 to 80

p : −2 to +2

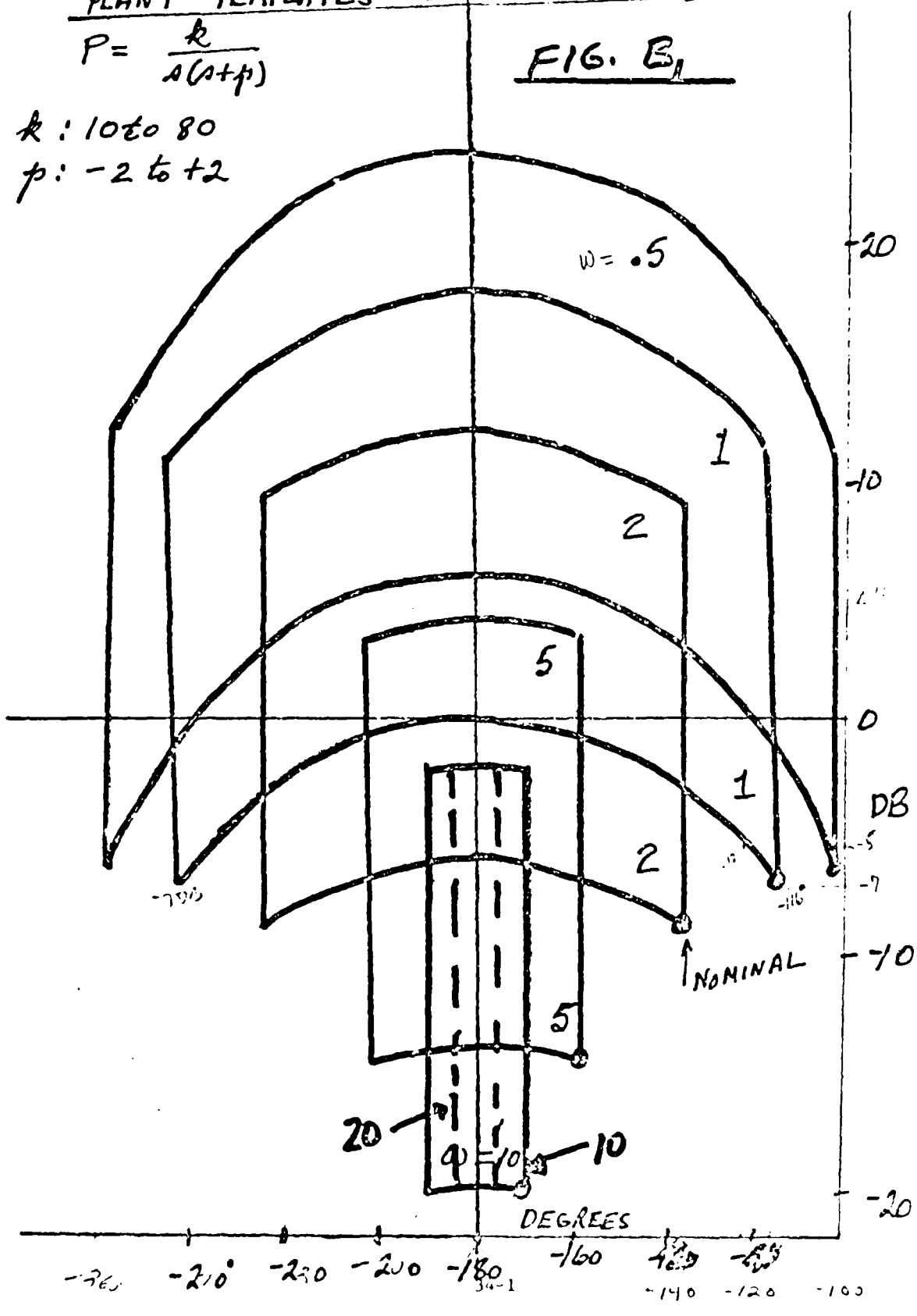

LOCUS OF
$\left|\frac{L}{1+L}\right| = 3DB$
$L_o(j\omega)$
$L_c(j\omega)$
FIG. B.2
SHAPING OF $L_o(j\omega)$
TO SATISFY BOUNDS
ON $L_o(j\omega)$

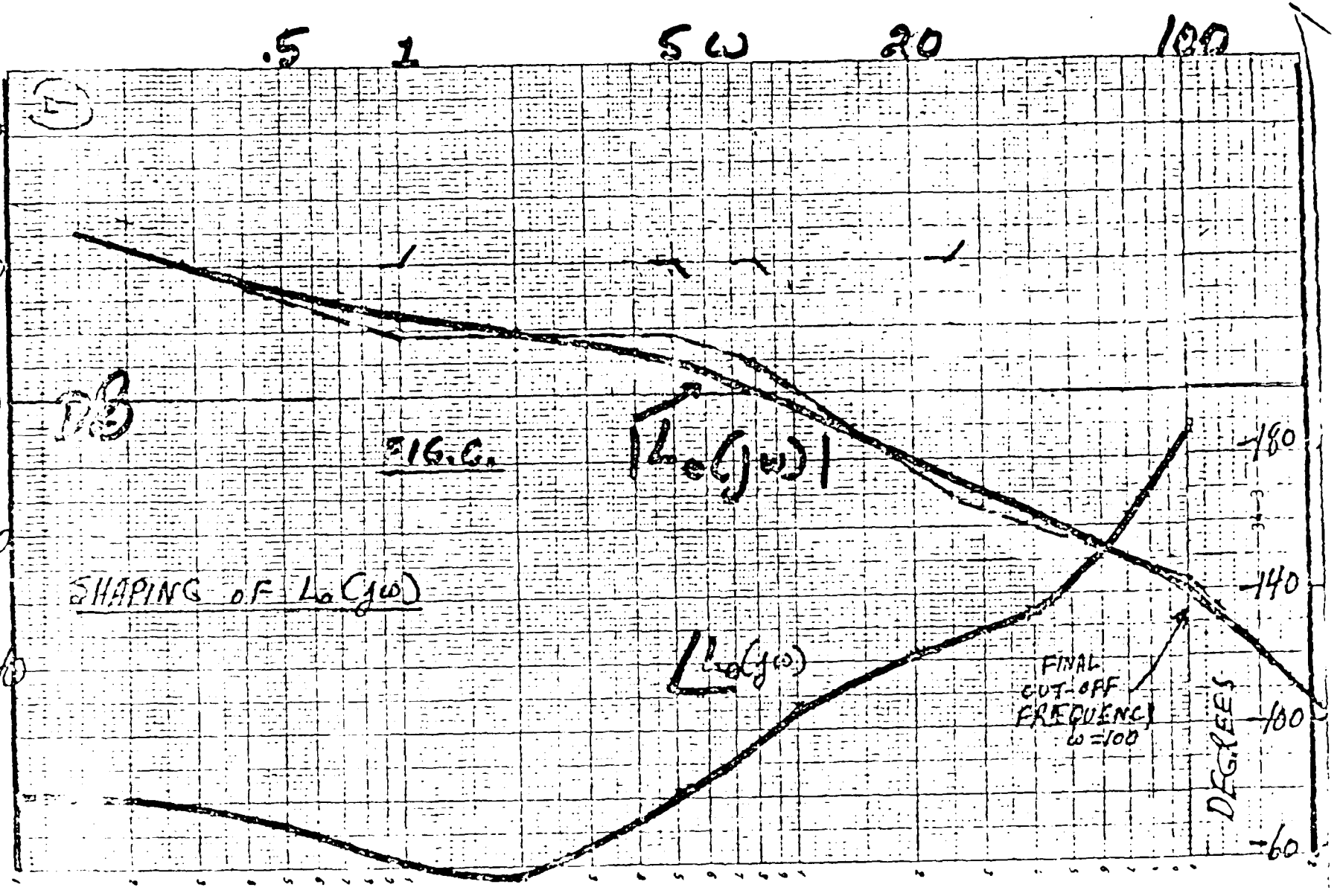

NO. 3115. 30 DIVISIONS PER INCH (180 DIVISIONS) BY 3 3-INCH CYCLES RATIO RULING. CODEX BOOK COMPAN

(4)

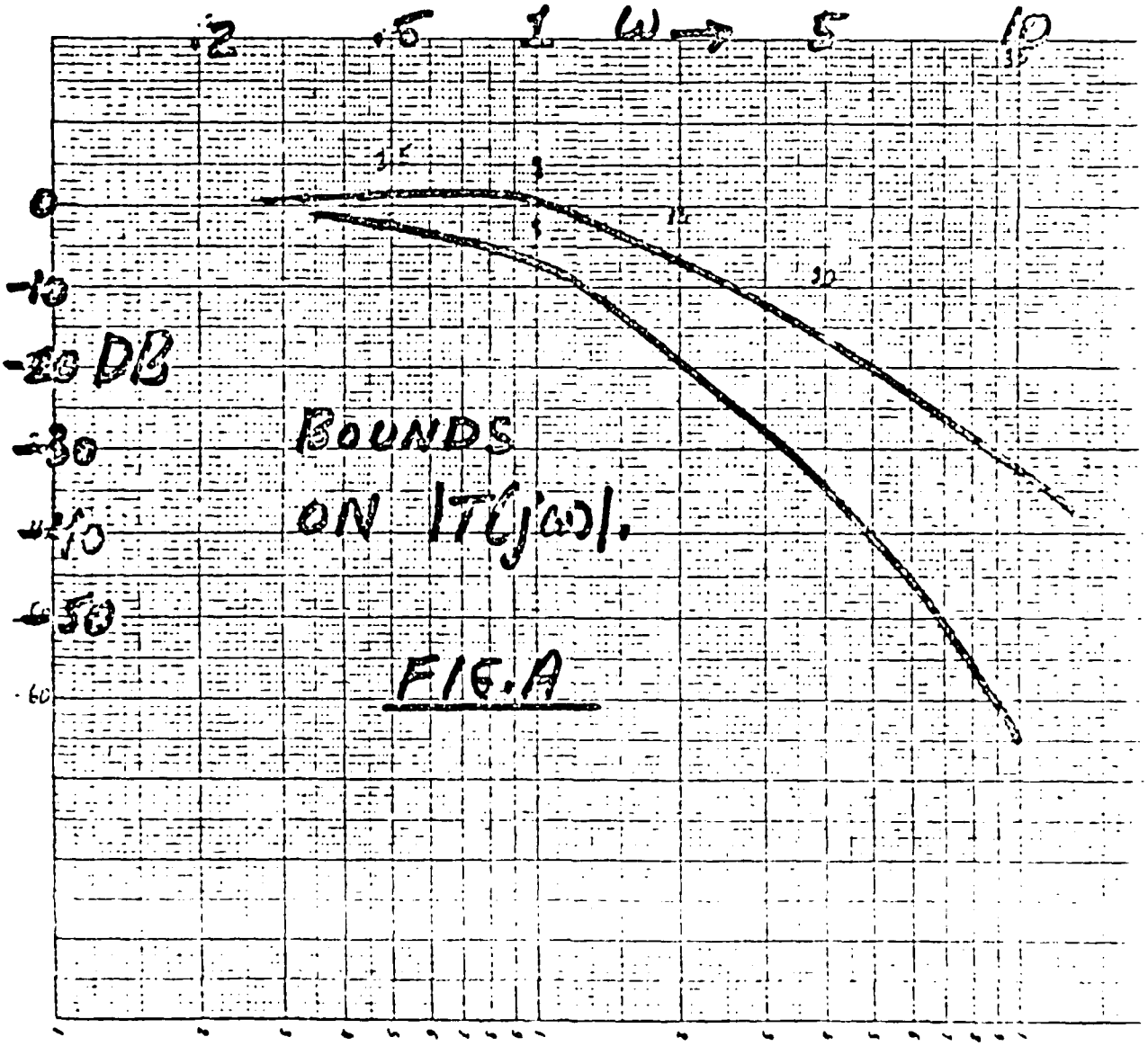

APPENDIX B

Generating the Transfer Function Matrix Models

This appendix contains the full state space matrices from FPCCSIM, the lateral mode matrices derived by simplification of the full state space matrices, the $\underline{P}$ transfer function matrices derived from the lateral mode state space matrices and the $\underline{Q}$ transfer function matrices generated from the $\underline{P}$ matrices using:

$$\underline{P}^{-1} = \underline{Q}' \tag{3-13}$$

$$\underline{Q} = [q_{ij}] = 1/\underline{Q}' \quad \underline{P}^{-1} = [1/q_{ij}] \tag{3-14}$$

The full state space matrices (output of FPCCSIM) are;

1. Flight condition 1 (slow speed condition) at 0.6 mach at sea level (Eq. B-1). The trim conditions are 0.6 mach, the angle of attack is 1.03 degrees, the dynamic pressure is 553.04 lbs/sq in and the forward velocity is 670.5 ft/sec (see Table B-1).

2. Flight condition 2 (cruise condition) at 0.9 mach at 30,000 feet (Eq. B-2). The trim conditions are 0.9 mach, the angle of attack is 1.26 degrees, the dynamic pressure is 356.15 lbs/sq in and the forward velocity is 896.0 ft/sec (see Table B-2).

3. Flight condition 3 (high speed condition) at 2.3 mach at 40,000 feet (Eq. B-3). The trim conditions are mach 2.3, angle of attack is 0.63 degrees, the dynamic pressure is 1449.8 lbs/sq in and the forward velocity is 2229.0 ft/sec (see Table B-3).

Simplify the lateral mode matrix (see Section IV-3 for simplifying assumptions and the matrices become:

$$\underline{A} = \begin{bmatrix}
-2.350 & 1.470 & -0.0106 & 0.0 & 0.0 & 0.0 & 0.0 & 0.0 & 0.0 & 0.0 & 0.0 & 0.0 \\
0.256 & -0.989 & 0.019 & 0.0 & 0.0 & 0.0 & 0.0 & 0.0 & 0.0 & 0.0 & 0.0 & 0.0 \\
13.200 & -666.0 & -0.687 & 32.100 & 0.0 & 0.0 & 0.0 & 0.0 & 0.0 & 0.0 & 0.0 & 0.0 \\
1.000 & 0.018 & 0.0 & 0.0 & 0.0 & 0.0 & 0.0 & 0.0 & 0.0 & 0.0 & 0.0 & 0.0 \\
0.0 & 1.000 & 0.0 & 0.0 & 0.0 & 0.0 & 0.0 & 0.0 & 0.0 & 0.0 & 0.0 & 0.0 \\
0.0 & 0.0 & 1.000 & -12.000 & 669.0 & 0.0 & 0.0 & 0.0 & 0.0 & 0.0 & 0.0 & 0.0 \\
0.0 & 0.0 & 0.0 & 0.0 & 0.0 & 0.0 & -0.463 & 0.0639 & -0.0011 & 0.0 & 0.0 & 0.0 \\
0.0 & 0.0 & 0.0 & 0.0 & 0.0 & 0.0 & 674.0 & -2.820 & -0.0568 & -0.577 & -0.00049 & -0.000461 \\
0.0 & 0.0 & 0.0 & 0.0 & 0.0 & 0.0 & -12.100 & 0.105 & -0.0297 & -32.100 & 0.00067 & -0.000073 \\
0.0 & 0.0 & 0.0 & 0.0 & 0.0 & 0.0 & 1.000 & 0.0 & 0.0 & 0.0 & 0.0 & 0.0 \\
0.0 & 0.0 & 0.0 & 0.0 & 0.0 & 0.0 & 0.0 & -1.000 & 0.018 & 669.0 & 0.0 & 0.0 \\
0.0 & 0.0 & 0.0 & 0.0 & 0.0 & 0.0 & 0.0 & 0.018 & 1.000 & 0.0 & 0.0 & 0.0
\end{bmatrix}$$

(B-1a)

$$\underline{L} = \begin{bmatrix}
0.198 & 0.0 & 0.0 & 0.166 & -0.0275 & 0.0487 & 0.0 & 0.0 & -0.968 & 0.968 \\
0.00727 & 0.0 & 0.0 & -0.188 & 0.0368 & 0.00153 & 0.000029 & -0.000029 & -10.300 & 10.300 \\
0.0 & 0.0 & 0.0 & 1.780 & 0.581 & 0.0 & 0.0 & 0.0 & 0.0 & 0.0 \\
0.0 & 0.0 & 0.0 & 0.0 & 0.0 & 0.0 & 0.0 & 0.0 & 0.0 & 0.0 \\
0.0 & 0.0 & 0.0 & 0.0 & 0.0 & 0.0 & 0.0 & 0.0 & 0.0 & 0.0 \\
0.0 & 0.0 & 0.0 & 0.0 & 0.0 & 0.0 & 0.0 & 0.0 & 0.0 & 0.0 \\
0.0 & 0.640 & -0.0966 & 0.0 & 0.0 & -0.043 & 0.0 & 0.0 & 0.0 & 0.0 \\
0.0 & -1.430 & -4.730 & 0.0 & 0.0 & -0.616 & -0.000035 & -0.000035 & 0.0 & 0.0 \\
0.0 & 0.518 & 0.0198 & 0.0 & 0.0 & 0.00092 & 0.00109 & 0.00109 & 0.0 & 0.0 \\
0.0 & 0.0 & 0.0 & 0.0 & 0.0 & 0.0 & 0.0 & 0.0 & -387.0 & -387.0 \\
0.0 & 0.0 & 0.0 & 0.0 & 0.0 & 0.0 & 0.0 & 0.0 & 0.0 & 0.0 \\
0.0 & 0.0 & 0.0 & 0.0 & 0.0 & 0.0 & 0.0 & 0.0 & 0.0 & 0.0
\end{bmatrix}$$

(B-1b)

$$A = \begin{bmatrix}
-1.19 & 1.16 & -0.0083 & 0.0 & 0.0 & 0.0 & 0.0 & 0.0 & 0.0 & 0.0 & 0.0 & 0.0 \\
0.128 & -0.477 & 0.00774 & 0.0 & 0.0 & 0.0 & 0.0 & 0.0 & 0.0 & 0.0 & 0.0 & 0.0 \\
20.2 & -894.0 & -0.382 & 32.1 & 0.0 & 0.0 & 0.0 & 0.0 & 0.0 & 0.0 & 0.0 & 0.0 \\
1.00 & 0.0219 & 0.0 & 0.0 & 0.0 & 0.0 & 0.0 & 0.0 & 0.0 & 0.0 & 0.0 & 0.0 \\
0.0 & 1.00 & 0.0 & 0.0 & 0.0 & 0.0 & 0.0 & 0.0 & 0.0 & 0.0 & 0.0 & 0.0 \\
0.0 & 0.0 & 1.00 & -19.6 & 895.0 & 0.0 & 0.0 & 0.0 & 0.0 & 0.0 & 0.0 & 0.0 \\
0.0 & 0.0 & 0.0 & 0.0 & 0.0 & 0.0 & -0.253 & 0.0303 & -0.00317 & 0.0 & 0.0 & 0.0 \\
0.0 & 0.0 & 0.0 & 0.0 & 0.0 & 0.0 & 898.0 & -1.68 & -0.0558 & -0.705 & -0.000665 & -0.000581 \\
0.0 & 0.0 & 0.0 & 0.0 & 0.0 & 0.0 & -19.7 & 0.0472 & -0.0822 & -32.1 & -0.000165 & -0.000061 \\
0.0 & 0.0 & 0.0 & 0.0 & 0.0 & 0.0 & 1.00 & 0.0 & 0.0 & 0.0 & 0.0 & 0.0 \\
0.0 & 0.0 & 0.0 & 0.0 & 0.0 & 0.0 & 0.0 & -1.00 & 0.0219 & 895.0 & 0.0 & 0.0 \\
0.0 & 0.0 & 0.0 & 0.0 & 0.0 & 0.0 & 0.0 & 0.0219 & 1.00 & 0.0 & 0.0 & 0.0
\end{bmatrix}$$

(B-2a)

$$B = \begin{bmatrix}
0.141 & 0.0 & 0.0 & 0.0270 & -0.0185 & 0.0367 & 0.0 & 0.0 & -0.647 & 0.647 \\
0.00537 & 0.0 & 0.0 & -0.0639 & 0.0253 & 0.0112 & 0.0 & 0.0 & -6.89 & 6.89 \\
0.0 & 0.0 & 0.0 & 0.595 & 0.0391 & 0.0 & 0.0 & 0.0 & 0.0 & 0.0 \\
0.0 & 0.0 & 0.0 & 0.0 & 0.0 & 0.0 & 0.0 & 0.0 & 0.0 & 0.0 \\
0.0 & 0.0 & 0.0 & 0.0 & 0.0 & 0.0 & 0.0 & 0.0 & 0.0 & 0.0 \\
0.0 & 0.0 & 0.0 & 0.0 & 0.0 & 0.0 & 0.0 & 0.0 & 0.0 & 0.0 \\
0.0 & 0.527 & -0.195 & 0.0 & 0.0 & -0.0325 & 0.0 & 0.0 & 0.0 & 0.0 \\
0.0 & -0.634 & -9.26 & 0.0 & 0.0 & -0.464 & -0.000033 & -0.000037 & 0.0 & 0.0 \\
0.0 & 0.359 & -0.283 & 0.0 & 0.0 & -0.000706 & 0.00109 & 0.00109 & -259.0 & -259.0 \\
0.0 & 0.0 & 0.0 & 0.0 & 0.0 & 0.0 & 0.0 & 0.0 & 0.0 & 0.0 \\
0.0 & 0.0 & 0.0 & 0.0 & 0.0 & 0.0 & 0.0 & 0.0 & 0.0 & 0.0 \\
0.0 & 0.0 & 0.0 & 0.0 & 0.0 & 0.0 & 0.0 & 0.0 & 0.0 & 0.0
\end{bmatrix}$$

(B-2b)

$$A = \begin{bmatrix}
-0.982 & 0.645 & -0.0437 & 0.0 & 0.0 & 0.0 & 0.0 & 0.0 & 0.0 & 0.0 & 0.0 & 0.0 \\
0.0985 & 0.0237 & -0.00678 & 0.0 & 0.0 & 0.0 & 0.0 & 0.0 & 0.0 & 0.0 & 0.0 & 0.0 \\
24.6 & -2230.0 & -0.283 & 32.1 & 0.0 & 0.0 & 0.0 & 0.0 & 0.0 & 0.0 & 0.0 & 0.0 \\
1.00 & 0.0111 & 0.0 & 0.0 & 0.0 & 0.0 & 0.0 & 0.0 & 0.0 & 0.0 & 0.0 & 0.0 \\
0.0 & 1.00 & 0.0 & 0.0 & 0.0 & 0.0 & 0.0 & 0.0 & 0.0 & 0.0 & 0.0 & 0.0 \\
0.0 & 0.0 & 1.00 & -24.6 & 2220.0 & 0.0 & 0.0 & 0.0 & 0.0 & 0.0 & 0.0 & 0.0 \\
0.0 & 0.0 & 0.0 & 0.0 & 0.0 & 0.0 & -0.167 & 0.0123 & -0.000021 & 0.0 & 0.0 & 0.0 \\
0.0 & 0.0 & 0.0 & 0.0 & 0.0 & 0.0 & 2230.0 & -1.42 & -0.0440 & -0.356 & -0.00077 & -0.00077 \\
0.0 & 0.0 & 0.0 & 0.0 & 0.0 & 0.0 & -24.7 & -0.0113 & -0.0297 & -32.1 & -0.00044 & -0.00080 \\
0.0 & 0.0 & 0.0 & 0.0 & 0.0 & 0.0 & 1.00 & 0.0 & 0.0 & 0.0 & 0.0 & 0.0 \\
0.0 & 0.0 & 0.0 & 0.0 & 0.0 & 0.0 & 0.0 & -1.00 & 0.0111 & 2220.0 & 0.0 & 0.0 \\
0.0 & 0.0 & 0.0 & 0.0 & 0.0 & 0.0 & 0.0 & 0.0111 & 1.00 & 0.0 & 0.0 & 0.0
\end{bmatrix}$$

(B-3a)

$$B = \begin{bmatrix}
0.269 & 0.0 & 0.0 & 0.0575 & -0.0361 & 0.0361 & 0.0 & +0.0 & -2.63 & 2.63 \\
0.00928 & 0.0 & 0.0 & -0.130 & 0.0516 & 0.00111 & 0.000029 & -0.000029 & -28.0 & 28.0 \\
0.0 & 0.0 & 0.0 & 1.21 & 0.790 & 0.0 & 0.0 & 0.0 & 0.0 & 0.0 \\
0.0 & 0.0 & 0.0 & 0.0 & 0.0 & 0.0 & 0.0 & 0.0 & 0.0 & 0.0 \\
0.0 & 0.0 & 0.0 & 0.0 & 0.0 & 0.0 & 0.0 & 0.0 & 0.0 & 0.0 \\
0.0 & 0.0 & 0.0 & 0.0 & 0.0 & 0.0 & 0.0 & 0.0 & 0.0 & 0.0 \\
0.0 & 1.05 & -0.832 & 0.0 & 0.0 & -0.0384 & 0.0 & 0.0 & 0.0 & 0.0 \\
0.0 & -9.35 & -26.6 & 0.0 & 0.0 & -0.444 & 0.0 & 0.0 & 0.0 & 0.0 \\
0.0 & 2.96 & -0.513 & 0.0 & 0.0 & 0.0 & 0.00109 & 0.00109 & -1050.0 & -1050.0 \\
0.0 & 0.0 & 0.0 & 0.0 & 0.0 & 0.0 & 0.0 & 0.0 & 0.0 & 0.0 \\
0.0 & 0.0 & 0.0 & 0.0 & 0.0 & 0.0 & 0.0 & 0.0 & 0.0 & 0.0 \\
0.0 & 0.0 & 0.0 & 0.0 & 0.0 & 0.0 & 0.0 & 0.0 & 0.0 & 0.0
\end{bmatrix}$$

(B-3b)

Flight condition 1 (slow speed condition)

0.6 mach at sea level

$$\dot{\underline{x}} = \underline{A}\underline{x} + \underline{B}\underline{u}$$

$$\begin{bmatrix} \dot{\phi} \\ \dot{v} \\ \dot{r} \\ \dot{p} \end{bmatrix} = \begin{bmatrix} 0.0 & 0.0 & 0.018 & 1.000 \\ 32.1 & -0.687 & -666.0 & 13.2 \\ 0.0 & 0.0190 & -0.989 & 0.256 \\ 0.0 & -0.0103 & 1.470 & -2.35 \end{bmatrix} \begin{bmatrix} \phi \\ v \\ r \\ p \end{bmatrix}$$

$$+ \begin{bmatrix} 0.0 & 0.0 & 0.0 \\ 0.0 & 1.78 & 0.581 \\ 0.00727 & -0.188 & 0.0368 \\ 0.198 & 0.166 & -0.0275 \end{bmatrix} \begin{bmatrix} \delta_a \\ \delta_r \\ \delta_{vc} \end{bmatrix}$$

$$\underline{y} = \underline{C}\,\underline{x} + \underline{F}\,\underline{u} \quad (\underline{F} = 0)$$

$$\begin{bmatrix} \phi \\ v \\ r \end{bmatrix} = \begin{bmatrix} 1.0 & 0.0 & 0.0 & 0.0 \\ 0.0 & 1.0 & 0.0 & 0.0 \\ 0.0 & 0.0 & 1.0 & 0.0 \end{bmatrix} \begin{bmatrix} \phi \\ v \\ r \\ p \end{bmatrix}$$

Flight condition 2 (cruise condition)

0.9 mach at 30,000 feet

$$\dot{\underline{x}} = \underline{A}\underline{x} + \underline{B}\underline{u}$$

$$\begin{bmatrix} \dot{\phi} \\ \dot{v} \\ \dot{r} \\ \dot{p} \end{bmatrix} = \begin{bmatrix} 0.0 & 0.0 & 0.0219 & 1.000 \\ 32.1 & -0.352 & -894.0 & 20.2 \\ 0.0 & 0.00774 & -0.477 & 0.128 \\ 0.0 & -0.0083 & 1.160 & -1.19 \end{bmatrix} \begin{bmatrix} \phi \\ v \\ r \\ p \end{bmatrix}$$

$$+ \begin{bmatrix} 0.0 & 0.0 & 0.0 \\ 0.0 & 0.595 & 0.391 \\ 0.00537 & -0.0639 & 0.0253 \\ 0.141 & 0.0270 & -0.0185 \end{bmatrix} \begin{bmatrix} \delta_a \\ \delta_r \\ \delta_{vc} \end{bmatrix}$$

$$\underline{y} = \underline{C}\,\underline{x} + \underline{F}\,\underline{u} \quad (\underline{F} = 0)$$

$$\begin{bmatrix} \phi \\ v \\ r \end{bmatrix} = \begin{bmatrix} 1.0 & 0.0 & 0.0 & 0.0 \\ 0.0 & 1.0 & 0.0 & 0.0 \\ 0.0 & 0.0 & 1.0 & 0.0 \end{bmatrix} \begin{bmatrix} \phi \\ v \\ r \\ p \end{bmatrix}$$

Flight condition 3 (high speed condition)

2.3 mach at 40,000 feet

$$\dot{\underline{x}} = \underline{A}\underline{x} + \underline{B}\underline{u}$$

$$\begin{bmatrix} \dot{\phi} \\ \dot{v} \\ \dot{r} \\ \dot{p} \end{bmatrix} = \begin{bmatrix} 0.0 & 0.0 & 0.0111 & 1.00 \\ 32.1 & -0.283 & -2230.0 & 24.6 \\ 0.0 & -0.00678 & 0.0237 & 0.0985 \\ 0.0 & -0.0437 & 0.645 & -0.982 \end{bmatrix} \begin{bmatrix} \phi \\ v \\ r \\ p \end{bmatrix}$$

$$+ \begin{bmatrix} 0.0 & 0.0 & 0.0 \\ 0.0 & 1.21 & 0.790 \\ 0.00928 & -0.130 & 0.0516 \\ 0.269 & 0.0575 & -0.0361 \end{bmatrix} \begin{bmatrix} \delta_a \\ \delta_r \\ \delta_{vc} \end{bmatrix}$$

$$\underline{y} = \underline{C}\,\underline{x} + \underline{F}\,\underline{u} \quad (\underline{F} = 0)$$

$$\begin{bmatrix} \phi \\ v \\ r \end{bmatrix} = \begin{bmatrix} 1.0 & 0.0 & 0.0 & 0.0 \\ 0.0 & 1.0 & 0.0 & 0.0 \\ 0.0 & 0.0 & 1.0 & 0.0 \end{bmatrix} \begin{bmatrix} \phi \\ v \\ r \\ p \end{bmatrix}$$

Next input the simplified lateral mode state space matrices into a computer program to generate the transfer function matrices, $\underline{P}$. The resulting nine transfer functions are of the form:

$$\frac{1}{\text{characteristics equation (C.E.) of } \underline{P}} \begin{bmatrix} \text{nine numerators; in the form} \\ \text{of a three-by-three matrix} \end{bmatrix}$$

$$\underline{P}_1 = \frac{1}{\begin{matrix} 1.000 & s^{**}4 \\ 4.026 & s^{**}3 \\ 17.032 & s^{**}2 \\ 29.404 & s^{**}1 \\ -0.594 & s^{**}0 \end{matrix}} \begin{bmatrix} -3.126\text{E-}13 & s^{**}3 & -2.842\text{E-}13 & s^{**}3 & -1.137\text{E-}13 & s^{**}3 \\ 0.198 & s^{**}2 & 0.163 & s^{**}2 & -0.0268 & s^{**}2 \\ 0.344 & s^{**}1 & -0.0254 & s^{**}1 & 0.00411 & s^{**}1 \\ 2.699 & s^{**}0 & 0.762 & s^{**}0 & -0.0654 & s^{**}0 \\ -2.228 & s^{**}2 & 1.780 & s^{**}3 & 0.581 & s^{**}3 \\ -36.851 & s^{**}1 & 133.343 & s^{**}2 & -22.932 & s^{**}2 \\ 6.668 & s^{**}0 & 273.145 & s^{**}1 & -52.282 & s^{**}1 \\ & & -3.830 & s^{**}0 & -0.909 & s^{**}0 \\ 0.00727 & s^{**}3 & -0.188 & s^{**}2 & 0.0368 & s^{**}3 \\ 0.0728 & s^{**}2 & -0.183 & s^{**}1 & 0.116 & s^{**}2 \\ 0.0972 & s^{**}1 & 0.0391 & s^{**}0 & 0.7709 & s^{**}1 \\ 0.123 & s^{**}0 & & & -0.00461 & s^{**}0 \end{bmatrix} \quad \text{(B-4a)}$$

$$\underline{P}_1 = \frac{1}{\begin{matrix} \text{Constant} = 1.000 \\ (s+0.866+j3.507) \\ (s+0.866-j3.507) \\ (s-0.0200) \\ (s+2.274) \end{matrix}} \begin{bmatrix} \text{Constant} = -3.126\text{E-}13 \\ (s + 0.8677 + j\ 3.587) \\ (s + 0.8677 - j\ 3.587) \\ (s - 6.337\text{E+}11) \\ \text{Constant} = -2.228 \\ (s - 0.183) \\ (s + 16.362) \\ \text{Constant} = 0.00727 \\ (s + 0.657 + j\ 1.232) \\ (s + 0.657 - j\ 1.232) \\ (s + 8.696) \end{bmatrix} \begin{bmatrix} \text{Constant} = -2.842\text{E-}13 \\ (s - 0.0780 + j\ 2.163) \\ (s - 0.0780 - j\ 2.163) \\ (s - 5.722\text{E+}11) \\ \text{Constant} = 1.780 \\ (s - .0139) \\ (s + 2.122) \\ (s + 72.804) \\ \text{Constant} = -0.188 \\ (s - 0.149) \\ (s + 0.654) \\ (s + 2.127) \end{bmatrix} \begin{bmatrix} \text{Constant} = -1.137\text{E-}13 \\ (s - 0.00765 + j\ 1.559) \\ (s - 0.00765 - j\ 1.559) \\ (s + 2.361\text{E+}11) \\ \text{Constant} = 0.581 \\ (s - 0.0173) \\ (s + 2.178) \\ (s - 41.630) \\ \text{Constant} = 0.0368 \\ (s - 0.0551) \\ (s + 1.062) \\ (s + 2.139) \end{bmatrix} \quad \text{(B-4b)}$$

$$P_2 = \frac{1}{1.000\ s^{**}4 + 2.019\ s^{**}3 + 8.0932\ s^{**}2 + 7.592\ s^{**}1 - 0.1668\ s^{**}0}$$

$$\begin{bmatrix}
2.842E\text{-}13\ s^{**}3 & 8.100E\text{-}13\ s^{**}3 & 6.253E\text{-}13\ s^{**}3 \\
0.141\ s^{**}2 & 0.0256\ s^{**}2 & -0.0179\ s^{**}2 \\
0.124\ s^{**}1 & -0.0587\ s^{**}1 & 0.0116\ s^{**}1 \\
1.042\ s^{**}0 & -0.306\ s^{**}0 & 0.0692\ s^{**}0 \\
-1.953\ s^{**}2 & 0.595\ s^{**}3 & 0.391\ s^{**}3 \\
-15.834\ s^{**}1 & 58.664\ s^{**}2 & -22.340\ s^{**}2 \\
2.376\ s^{**}0 & 64.725\ s^{**}1 & -24.796\ s^{**}1 \\
 & -2.017\ s^{**}0 & 0.678\ s^{**}0 \\
0.00537\ s^{**}3 & -0.0639\ s^{**}3 & 0.0253\ s^{**}3 \\
0.0263\ s^{**}2 & -0.0905\ s^{**}2 & 0.0397\ s^{**}2 \\
0.0315\ s^{**}1 & -0.0272\ s^{**}1 & 0.0143\ s^{**}1 \\
0.0365\ s^{**}0 & -0.0103\ s^{**}0 & 0.00214\ s^{**}0
\end{bmatrix} \quad \text{(B-5a)}$$

$$P_2 = \frac{1}{\text{Constant} = 1.000\ (s+0.473+j2.622)\ (s+0.473-j2.622)\ (s-0.0215)\ (s+1.094)}$$

$$\begin{bmatrix}
\text{Constant} = 2.842E\text{-}13\ (s + 0.438 + j\ 2.682)\ (s + 0.438 - j\ 2.682)\ (s + 4.965E{+}11) & \text{Constant} = 8.100E\text{-}13\ (s + 2.499)\ (s + 6.104E\text{-}5)\ (s + 3.1605E{+}10) & \text{Constant} = 6.253E\text{-}13\ (s + 1.666)\ (s - 2.870E{+}10)\ (s - 6.104E\text{-}5) \\
\text{Constant} = -1.953\ (s + 7.984)\ (s + 0.125) & \text{Constant} = 0.595\ (s - 0.0303)\ (s + 0.0101)\ (s + 98.615) & \text{Constant} = 0.391\ (s - 0.0267)\ (s - 57.092)\ (s - 0.0175) \\
\text{Constant} = 0.00537\ (s + 0.535 + j\ 1.219)\ (s + 0.535 - j\ 1.219)\ (s + 3.832) & \text{Constant} = -0.0639\ (s + 0.123 + j\ 0.351)\ (s + 0.123 - j\ 0.351)\ (s + 1.170) & \text{Constant} = 0.0253\ (s + 0.216 + j\ 0.167)\ (s + 0.216 - j\ 0.167)\ (s + 1.136)
\end{bmatrix} \quad \text{(B-5b)}$$

$$\underline{P}_3 = \frac{1}{\begin{matrix} 1.000 & s^{**}4 \\ 1.241 & s^{**}3 \\ -13.860 & s^{**}2 \\ -22.983 & s^{**}1 \\ 0.111 & s^{**}0 \end{matrix}} \begin{bmatrix} 3.766E\text{-}13 & s^{**}3 & 0.0570 & s^{**}2 & 6.040E\text{-}13 & s^{**}3 \\ 0.269 & s^{**}2 & -0.123 & s^{**}1 & -0.0355 & s^{**}2 \\ 0.0762 & s^{**}1 & -13.568 & s^{**}0 & -0.00995 & s^{**}1 \\ -3.16 & s^{**}0 & & & 5.583 & s^{**}0 \\ \\ -14.876 & s^{**}2 & 1.210 & s^{**}3 & 0.790 & s^{**}3 \\ -76.780 & s^{**}1 & 292.474 & s^{**}2 & -115.199 & s^{**}2 \\ 3.807E\text{-}4 & s^{**}0 & 271.650 & s^{**}1 & -105.436 & s^{**}1 \\ & & -2.779 & s^{**}0 & 1.113 & s^{**}0 \\ \\ 0.00928 & s^{**}3 & -0.130 & s^{**}3 & 0.0516 & s^{**}3 \\ 0.0383 & s^{**}2 & -0.167 & s^{**}2 & 0.0564 & s^{**}2 \\ -0.0248 & s^{**}1 & -0.197 & s^{**}1 & 0.0662 & s^{**}1 \\ -0.0455 & s^{**}0 & -0.195 & s^{**}0 & 0.0802 & s^{**}0 \end{bmatrix} \quad \text{(B-6a)}$$

$$\underline{P}_3 = \frac{1}{\begin{matrix} \text{Constant} = 1.000 \\ (s\text{-}3.871) \\ (s\text{+}3.328) \\ (s\text{+}1.789) \\ (s\text{-}0.00482) \end{matrix}} \begin{bmatrix} \text{Constant} = 3.766E\text{-}13 & \text{Constant} = 0.0570 & \text{Constant} = 6.040E\text{-}13 \\ (s - 3.290) & (s - 1.471) & (s - 12.400) \\ (s + 0.00195) & (s - 0.680) & (s - 5.878E{+}10) \\ (s + 7.147E{+}11) & & (s - 2.441E\text{-}4) \\ \\ \text{Constant} = -14.876 & \text{Constant} = 1.210 & \text{Constant} = 0.790 \\ (s + 4.82) & (s - 0.0101) & (s - 0.0104) \\ (s + 0.207) & (s + 0.00414) & (s - 145.804) \\ & (s + 241.720) & (s - 0.00686) \\ \\ \text{Constant} = 0.00928 & \text{Constant} = -0.130 & \text{Constant} = 0.0516 \\ (s + 0.886) & (s + 1.123) & (s + 1.152) \\ (s + 0.346) & (s + 0.0809 - j\ 0.997) & (s - 0.0294 + j\ 0.999) \\ (s + 2.891) & (s + 0.0809 + j\ 0.997) & (s - 0.0294 - j\ 0.999) \end{bmatrix} \quad \text{(B-6b)}$$

$$
\Sigma_1 = \frac{\begin{matrix}
-0.7483\text{E-}13 & s^{**}9 \\
0.03565 & s^{**}8 \\
0.2871 & s^{**}7 \\
1.7924 & s^{**}6 \\
6.9865 & s^{**}5 \\
18.7422 & s^{**}4 \\
35.5422 & s^{**}3 \\
30.1073 & s^{**}2 \\
-1.2444 & s^{**}1 \\
0.01256 & s^{**}0
\end{matrix}}{\begin{matrix}
4.026 & s^{**}4 \\
17.032 & s^{**}3 \\
29.404 & s^{**}2 \\
-0.594 & s^{**}1 \\
 & s^{**}0
\end{matrix}}
\begin{bmatrix}
\begin{matrix}
0.1747 & s^{**}6 \\
1.0893 & s^{**}5 \\
4.5594 & s^{**}4 \\
11.8302 & s^{**}3 \\
11.7539 & s^{**}2 \\
0.6572 & s^{**}1 \\
-0.01790 & s^{**}0
\end{matrix} &
\begin{matrix}
0.2858\text{E-}13 & s^{**}6 \\
-0.0009388 & s^{**}5 \\
-0.005387 & s^{**}4 \\
-0.02246 & s^{**}3 \\
-0.05499 & s^{**}2 \\
-0.04672 & s^{**}1 \\
0.0009545 & s^{**}0
\end{matrix} &
\begin{matrix}
-0.4638\text{E-}13 & s^{**}6 \\
0.1423 & s^{**}5 \\
-0.1724 & s^{**}4 \\
-0.5770 & s^{**}3 \\
-8.5086 & s^{**}2 \\
-21.9966 & s^{**}1 \\
0.4426 & s^{**}0
\end{matrix} \\
\begin{matrix}
0.004224 & s^{**}6 \\
-0.04244 & s^{**}5 \\
-0.4077 & s^{**}4 \\
-1.8557 & s^{**}3 \\
-5.8433 & s^{**}2 \\
-7.0309 & s^{**}1 \\
0.1427 & s^{**}0
\end{matrix} &
\begin{matrix}
-0.1507\text{E-}13 & s^{**}6 \\
0.007486 & s^{**}5 \\
0.03751 & s^{**}4 \\
0.1572 & s^{**}3 \\
0.3457 & s^{**}2 \\
0.2123 & s^{**}1 \\
-0.004377 & s^{**}0
\end{matrix} &
\begin{matrix}
0.2477\text{E-}12 & s^{**}6 \\
-0.1151 & s^{**}5 \\
4.4035 & s^{**}4 \\
17.6339 & s^{**}3 \\
79.5079 & s^{**}2 \\
143.1791 & s^{**}1 \\
-2.8895 & s^{**}0
\end{matrix} \\
\begin{matrix}
-0.01294 & s^{**}6 \\
-0.6800 & s^{**}5 \\
-3.9821 & s^{**}4 \\
-16.0419 & s^{**}3 \\
-39.4672 & s^{**}2 \\
-35.9018 & s^{**}1 \\
0.7322 & s^{**}0
\end{matrix} &
\begin{matrix}
-0.8263 & s^{**}6 \\
0.03843 & s^{**}5 \\
0.1743 & s^{**}4 \\
0.7333 & s^{**}3 \\
1.4634 & s^{**}2 \\
0.5527 & s^{**}1 \\
-0.01162 & s^{**}0
\end{matrix} &
\begin{matrix}
-0.7589\text{E-}12 & s^{**}6 \\
0.3527 & s^{**}5 \\
27.3937 & s^{**}4 \\
110.5774 & s^{**}3 \\
452.7489 & s^{**}2 \\
763.5401 & s^{**}1 \\
-15.4153 & s^{**}0
\end{matrix}
\end{bmatrix}
\qquad \text{(B-7a)}
$$

$$
\underline{Q}_{-1} = \frac{\text{Const.} = -0.7483\text{E-}13\ (s-0.01994)(s-0.01996)(s+2.2716)(s+2.2757)(s+0.8875+j3.5059)(s+0.8875-j3.5059)(s+0.8849+j3.5078)(s+0.8849-j3.5078)(s-4.7647\text{E+}11)}{\text{Constant} = 1.000\ (s+0.886+j3.507)(s+0.886-j3.507)(s-0.0200)(s+2.274)}
$$

$$
\begin{bmatrix}
\frac{1}{\text{Constant} = 0.1747\ (s+0.08111)(s-0.01996)(s+2.1268)(s+2.2737)(s+0.8862+j3.5068)(s+0.8862-j3.5068)} & \frac{1}{\text{Constant} = 0.2858\text{E-}13\ (s-3.2847\text{E+}10)(s+1.7125)(s-0.01996)(s+2.2737)(s+0.8861+j3.5068)(s+0.8861-j3.5068)} & \frac{1}{\text{Constant} = -0.4638\text{E-}13\ (s-3.0672\text{E+}12)(s-5\ 2379)(s-0.01996)(s+2.2737)(s+0.8862+j3.5068)(s+0.8862-j3.5068)} \\
\frac{1}{\text{Constant} = 0.004224\ (s+3.2788)(s-17.3521)(s-0.01996)(s+2.2737)(s+0.8861+j3.5068)(s+0.8861-j3.5068)} & \frac{1}{\text{Constant} = -0.1507\text{E-}13\ (s+0.9848)(s-4.9681\text{E+}11)(s-0.01996)(s+2.2737)(s+0.8861+j3.5068)(s+0.8861-j3.5068)} & \frac{1}{\text{Constant} = 0.2477\text{E-}12\ (s-42.2798)(s-4.6474\text{E+}11)(s-0.01996)(s+2.2737)(s+0.8861+j3.5068)(s+0.8861-j3.5068)} \\
\frac{1}{\text{Constant} = -0.01294\ (s+2.0513)(s+46.4722)(s-0.01995)(s+2.2737)(s+0.8862+j3.5068)(s+0.8862-j3.5068)} & \frac{1}{\text{Constant} = -0.8263\ (s+0.5093)(s-4.6510\text{E+}11)(s-0.01996)(s+2.2737)(s+0.8861+j3.5068)(s+0.8861-j3.5068)} & \frac{1}{\text{Constant} = -0.7589\text{E-}12\ (s+73.6488)(s-4.6474\text{E+}11)(s-0.01995)(s+2.2737)(s+0.8861+j3.5068)(s+0.8861-j3.5068)}
\end{bmatrix}
\tag{B-7b}
$$

$$
\begin{array}{ll}
0.1108E-13 & s^{**}9 \\
0.005761 & s^{**}8 \\
0.02326 & s^{**}7 \\
0.1167 & s^{**}6 \\
0.2758 & s^{**}5 \\
0.5520 & s^{**}4 \\
0.7041 & s^{**}3 \\
0.3165 & s^{**}2 \\
-0.0146 & s^{**}1 \\
0.0001604 & s^{**}0
\end{array}
=
\frac{\begin{array}{ll}
1.000 & s^{**}4 \\
2.019 & s^{**}3 \\
8.0932 & s^{**}2 \\
7.592 & s^{**}1 \\
-0.1668 & s^{**}0
\end{array}}{
\begin{array}{ll}
0.04003 & s^{**}6 \\
0.1156 & s^{**}5 \\
0.3783 & s^{**}4 \\
0.5533 & s^{**}3 \\
0.1279 & s^{**}2 \\
-0.1274 & s^{**}1 \\
0.002673 & s^{**}0
\end{array}
\quad
\begin{array}{ll}
-0.6045E-13 & s^{**}6 \\
0.0004990 & s^{**}5 \\
0.001349 & s^{**}4 \\
0.004728 & s^{**}3 \\
0.006549 & s^{**}2 \\
0.002506 & s^{**}1 \\
-0.00005691 & s^{**}0
\end{array}
\quad
\begin{array}{ll}
-0.5532E-13 & s^{**}6 \\
0.02069 & s^{**}5 \\
0.4510 & s^{**}4 \\
0.9937 & s^{**}3 \\
3.4690 & s^{**}2 \\
3.1033 & s^{**}1 \\
-0.06828 & s^{**}0
\end{array}
}
$$

$$
\frac{\begin{array}{ll}
0.002100 & s^{**}6 \\
-0.06027 & s^{**}5 \\
-0.2310 & s^{**}4 \\
-0.7438 & s^{**}3 \\
-1.4427 & s^{**}2 \\
-0.8828 & s^{**}1 \\
0.01964 & s^{**}0
\end{array}}{
\begin{array}{ll}
-0.003195 & s^{**}6 \\
-0.2059 & s^{**}5 \\
-0.7225 & s^{**}4 \\
-2.2319 & s^{**}3 \\
-3.8921 & s^{**}2 \\
-2.1977 & s^{**}1 \\
0.04903 & s^{**}0
\end{array}
\quad
\begin{array}{ll}
0.3833E-14 & s^{**}6 \\
0.003667 & s^{**}5 \\
0.009138 & s^{**}4 \\
0.03318 & s^{**}3 \\
0.04188 & s^{**}2 \\
0.01256 & s^{**}1 \\
-0.0002894 & s^{**}0
\end{array}
\quad
\begin{array}{ll}
-0.1111E-12 & s^{**}6 \\
-0.05518 & s^{**}5 \\
3.1393 & s^{**}4 \\
6.1165 & s^{**}3 \\
25.8892 & s^{**}2 \\
24.6870 & s^{**}1 \\
-0.5424 & s^{**}0
\end{array}
}
$$

$$
\frac{\begin{array}{ll}
0.2251E-13 & s^{**}6 \\
0.009155 & s^{**}5 \\
0.02103 & s^{**}4 \\
0.07923 & s^{**}3 \\
0.09011 & s^{**}2 \\
0.01781 & s^{**}1 \\
-0.0004249 & s^{**}0
\end{array}}{
\begin{array}{ll}
0.1691E-12 & s^{**}6 \\
0.08396 & s^{**}5 \\
8.4021 & s^{**}4 \\
17.3011 & s^{**}3 \\
67.2649 & s^{**}2 \\
62.4847 & s^{**}1 \\
-1.3735 & s^{**}0
\end{array}
}
$$

(B-8a)

$$
\underline{D}_2 = \frac{\begin{array}{l}\text{Const.} = 0.1108\text{E-}13 \\ (s-0.02147) \\ (s-0.02150) \\ (s+1.0936+j0.004506) \\ (s+1.0936-j0.004506) \\ (s+0.4731+j2.6231) \\ (s+0.4731-j2.6231) \\ (s+0.4738+j2.6218) \\ (s+0.4738-j2.6218) \\ (s+5.1985\text{E+}11)\end{array}}{\begin{array}{l}\text{Constant} = 1.000 \\ (s+0.473+j2.622) \\ (s+0.473-j2.622) \\ (s-0.0215) \\ (s+1.094)\end{array}}
\begin{bmatrix}
\frac{1}{\begin{array}{l}\text{Constant} = 0.04003 \\ (s - 0.3329) \\ (s + 1.2021) \\ (s - 0.02148) \\ (s + 1.0936) \\ (s + 0.4734 + j\ 2.6225) \\ (s + 0.4734 - j\ 2.6225)\end{array}} &
\frac{1}{\begin{array}{l}\text{Constant} = -0.6045\text{E-}13 \\ (s - 8.2558\text{E+}9) \\ (s + 0.6834) \\ (s - 0.02148) \\ (s + 1.0936) \\ (s + 0.4734 + j\ 2.6225) \\ (s + 0.4734 - j\ 2.6225)\end{array}} &
\frac{1}{\begin{array}{l}\text{Constant} = -0.5532\text{E-}13 \\ (s - 3.7394\text{E+}11) \\ (s + 19.7814) \\ (s - 0.02148) \\ (s + 1.0936) \\ (s + 0.4734 + j\ 2.6225) \\ (s + 0.4734 - j\ 2.6225)\end{array}} \\
\frac{1}{\begin{array}{l}\text{Constant} = 0.002100 \\ (s + 1.7274) \\ (s - 32.4517) \\ (s - 0.02148) \\ (s + 1.0936) \\ (s + 0.4734 + j\ 2.6225) \\ (s + 0.4734 - j\ 2.6225)\end{array}} &
\frac{1}{\begin{array}{l}\text{Constant} = 0.03833\text{E-}14 \\ (s + 9.5661\text{E+}11) \\ (s + 0.4731) \\ (s - 0.02148) \\ (s + 1.0936) \\ (s + 0.4734 + j\ 2.6225) \\ (s + 0.4734 - j\ 2.6225)\end{array}} &
\frac{1}{\begin{array}{l}\text{Constant} = -0.1111\text{E-}12 \\ (s + 4.9651\text{E+}11) \\ (s - 58.9133) \\ (s - 0.02148) \\ (s + 1.0936) \\ (s + 0.4734 + j\ 2.6225) \\ (s + 0.4734 - j\ 2.6225)\end{array}} \\
\frac{1}{\begin{array}{l}\text{Constant} = -0.003195 \\ (s + 60.9191) \\ (s + 1.5098) \\ (s - 0.02148) \\ (s + 1.0936) \\ (s + 0.4734 + j\ 2.6224) \\ (s + 0.4734 - j\ 2.6224)\end{array}} &
\frac{1}{\begin{array}{l}\text{Constant} = 0.2251\text{E-}13 \\ (s + 4.0668\text{E+}11) \\ (s + 0.2782) \\ (s - 0.02148) \\ (s + 1.0936) \\ (s + 0.4734 + j\ 2.6225) \\ (s + 0.4734 - j\ 2.6225)\end{array}} &
\frac{1}{\begin{array}{l}\text{Constant} = 0.1691\text{E-}12 \\ (s + 4.9651\text{E+}11) \\ (s + 98.0477) \\ (s - 0.02148) \\ (s + 1.0936) \\ (s + 0.4734 + j\ 2.6225) \\ (s + 0.4734 - j\ 2.6225)\end{array}}
\end{bmatrix}
\tag{B-8b}
$$

$$
\begin{bmatrix}
\begin{array}{|l|l|}\hline 1 & \\ \hline
0.1651 & s**6 \\
0.3160 & s**5 \\
-2.2017 & s**4 \\
-5.3925 & s**3 \\
-1.7583 & s**2 \\
1.2862 & s**1 \\
-0.006157 & s**0 \\ \hline
\end{array} &
\begin{array}{|l|l|}\hline 1 & \\ \hline
-0.1289E-12 & s**6 \\
0.001675 & s**5 \\
0.01033 & s**4 \\
-0.01375 & s**3 \\
-0.1548 & s**2 \\
-0.1907 & s**1 \\
0.0009303 & s**0 \\ \hline
\end{array} &
\begin{array}{|l|l|}\hline 1 & \\ \hline
0.2701E-13 & s**6 \\
0.08797 & s**5 \\
3.7342 & s**4 \\
3.1922 & s**3 \\
-53.9809 & s**2 \\
-85.9527 & s**1 \\
0.4154 & s**0 \\ \hline
\end{array} \\
\begin{array}{|l|l|}\hline 1 & \\ \hline
0.007331 & s**6 \\
-0.3124 & s**5 \\
-0.9598 & s**4 \\
3.7184 & s**3 \\
13.7151 & s**2 \\
10.4520 & s**1 \\
-0.05068 & s**0 \\ \hline
\end{array} &
\begin{array}{|l|l|}\hline 1 & \\ \hline
0.1383E-13 & s**6 \\
0.01422 & s**5 \\
0.02056 & s**4 \\
-0.1934 & s**3 \\
-0.3672 & s**2 \\
-0.06536 & s**1 \\
0.0003175 & s**0 \\ \hline
\end{array} &
\begin{array}{|l|l|}\hline 1 & \\ \hline
-0.2975E-12 & s**6 \\
-0.2126 & s**5 \\
31.4449 & s**4 \\
42.3084 & s**3 \\
-434.5330 & s**2 \\
-728.6971 & s**1 \\
3.5215 & s**0 \\ \hline
\end{array} \\
\begin{array}{|l|l|}\hline 1 & \\ \hline
-0.01123 & s**6 \\
-0.9304 & s**5 \\
-2.1291 & s**4 \\
11.5330 & s**3 \\
36.8528 & s**2 \\
26.0914 & s**1 \\
-0.1266 & s**0 \\ \hline
\end{array} &
\begin{array}{|l|l|}\hline 1 & \\ \hline
0.5786E-13 & s**6 \\
0.03552 & s**5 \\
0.05590 & s**4 \\
-0.4774 & s**3 \\
-0.9795 & s**2 \\
-0.2669 & s**1 \\
0.001299 & s**0 \\ \hline
\end{array} &
\begin{array}{|l|l|}\hline 1 & \\ \hline
0.4557E-12 & s**6 \\
0.3257 & s**5 \\
79.6125 & s**4 \\
93.8820 & s**3 \\
-1104.866 & s**2 \\
-1819.842 & s**1 \\
8.7950 & s**0 \\ \hline
\end{array}
\end{bmatrix}
\qquad \text{(B-9a)}
$$

$$
Q_3 = \frac{\begin{array}{|l|l|}\hline 0.6244E-13 & s**9 \\
0.04526 & s**8 \\
0.1121 & s**7 \\
-1.1846 & s**6 \\
-3.6319 & s**5 \\
6.1204 & s**4 \\
28.8176 & s**3 \\
23.7450 & s**2 \\
-0.2320 & s**1 \\
0.0005632 & s**0 \\ \hline\end{array}}{\begin{array}{|l|l|}\hline 1.000 & s**4 \\
1.241 & s**3 \\
-13.860 & s**2 \\
-22.983 & s**1 \\
0.111 & s**0 \\ \hline\end{array}}
$$

$$
Q_3 = \frac{\begin{array}{l}\text{Const.} = 0.6244\text{E-}13 \\ (s+1.7890) \\ (s+7.2490\text{E+}11) \\ (s-0.004819) \\ (s-0.004865) \\ (s+1.7928) \\ (s+3.3299) \\ (s-3.8748) \\ (s+3.3164) \\ (s-3.8676)\end{array}}{\begin{array}{l}\text{Constant} = 1.000 \\ (s-3.871) \\ (s+3.328) \\ (s+1.789) \\ (s-0.00482)\end{array}}
\left[
\begin{array}{lll}
\dfrac{1}{\begin{array}{l}\text{Constant} = 0.1651 \\ (s - 0.3342) \\ (s + 1.0054) \\ (s - 0.004820) \\ (s + 1.7918) \\ (s + 3.3225) \\ (s - 3.8672)\end{array}} &
\dfrac{1}{\begin{array}{l}\text{Constant} = -0.1280\text{E-}12 \\ (s - 1.3084\text{E+}10) \\ (s + 5.0656) \\ (s - 0.004860) \\ (s + 1.7957) \\ (s + 3.2179) \\ (s - 3.9046)\end{array}} &
\dfrac{1}{\begin{array}{l}\text{Constant} = 0.2701\text{E-}13 \\ (s + 3.2580\text{E+}12) \\ (s + 41.2222) \\ (s - 0.004819) \\ (s + 1.7851) \\ (s + 3.3834) \\ (s - 3.9363)\end{array}} \\
\dfrac{1}{\begin{array}{l}\text{Constant} = 0.007331 \\ (s + 1.3769) \\ (s - 45.2440) \\ (s - 0.004819) \\ (s + 1.7849) \\ (s + 3.3360) \\ (s - 3.8678)\end{array}} &
\dfrac{1}{\begin{array}{l}\text{Constant} = 0.1383\text{E-}13 \\ (s + 1.0282\text{E+}12) \\ (s + 0.2047) \\ (s - 0.004732) \\ (s + 1.7902) \\ (s + 3.3268) \\ (s - 3.8709)\end{array}} &
\dfrac{1}{\begin{array}{l}\text{Constant} = -0.2975\text{E-}12 \\ (s + 7.1467\text{E+}11) \\ (s - 149.1300) \\ (s - 0.004819) \\ (s + 1.7894) \\ (s + 3.3275) \\ (s - 3.8707)\end{array}} \\
\dfrac{1}{\begin{array}{l}\text{Constant} = -0.01123 \\ (s + 80.3502) \\ (s + 1.2633) \\ (s - 0.004819) \\ (s + 1.7867) \\ (s + 3.3351) \\ (s - 3.8677)\end{array}} &
\dfrac{1}{\begin{array}{l}\text{Constant} = 0.5786\text{E-}13 \\ (s + 6.1388\text{E+}11) \\ (s + 0.3318) \\ (s - 0.004782) \\ (s + 1.7900) \\ (s + 3.3271) \\ (s - 3.8701)\end{array}} &
\dfrac{1}{\begin{array}{l}\text{Constant} = 0.4557\text{E-}12 \\ (s + 7.1470\text{E+}11) \\ (s + 243.2179) \\ (s - 0.004819) \\ (s + 1.7893) \\ (s + 3.3277) \\ (s - 3.8700)\end{array}}
\end{array}
\right]
\tag{B-9b}
$$

Eq. B-4, B-5 and B-6 are the resulting matrices for FC #1 (slow speed condition), FC #2 (cruise condition) and FC #3 (high speed condition), respectively.

Using Eq. 3-13 and 3-14, the $\underline{Q}$ transfer functions matrices are generated. With $\underline{P}$ in the form described above, the inverse of $\underline{P}$, is in the form:

$$\underline{P}^{-1} = \frac{\text{C.E. of } \underline{P}[3 \times 3]}{\text{determinant of } \underline{P} \text{ (det } \underline{P})} = \underline{Q}'$$

From Eq. 3-14, $\underline{Q}$ is equal to the inverse elements of $\underline{Q}'$. All nine transfer functions have a set of common numerators (zeros), the det $\underline{P}$. Also, all nine transfer functions have a common set of denominators (poles), the C.E. of $\underline{P}$. Therefore all nine transfer functions have these common poles and other poles. The common poles are removed from the nine terms and listed separately. Therefore the $\underline{Q}$ matrices are in the form:

$$\frac{\text{common numerator (poles generated from det P)}}{\text{C.E. of } \underline{P}} \left[\begin{array}{c} 3 \times 3 \ q_{ij} \\ \text{matrix} \end{array} \right]$$

The $\underline{Q}$ transfer function matrices are Eq. B-7 (FC #1), B-8 (FC #2) and B-9 (FC #3).

Notice that many of the terms have a singular root which is quite large in magnitude, i.e. $> 10^{10}$ larger than any other roots. This very far off root has very little effect on the system performance until long

$$\Omega_{-1} = \text{Const} = -0.7483\text{E-}13 \text{ Gain} = -4.7647\text{E+}11 \begin{bmatrix} \frac{1}{\text{Constant} = 0.1747 \\ (s + 0.008111) \\ (s + 2.1268)} & \frac{1}{\text{Constant} = 0.2858\text{E-}13 \\ \text{Gain} = -3.2847\text{E+}10 \\ (s + 1.7125)} & \frac{1}{\text{Constant} = -0.4638\text{E-}13 \\ \text{Gain} = -3.0672\text{E+}12 \\ (s - 5.2379)} \\ \\ \frac{1}{\text{Constant} = 0.004224 \\ (s + 3.2788) \\ (s - 17.3521)} & \frac{1}{\text{Constant} = -0.1507\text{E-}13 \\ \text{Gain} = -4.9681\text{E+}11 \\ (s + .9848)} & \frac{1}{\text{Constant} = 0.2477\text{E-}12 \\ \text{gain} = -4.6474\text{E+}11 \\ (s - 42.2798)} \\ \\ \frac{1}{\text{Constant} = -0.01294 \\ (s + 2.0513) \\ (s + 46.4722)} & \frac{1}{\text{Constant} = -0.8263\text{E-}13 \\ \text{Gain} = -4.6510\text{E+}11 \\ (s + 0.5093)} & \frac{1}{\text{Constant} = -0.7588\text{E-}12 \\ \text{Gain} = -4.6474\text{E+}11 \\ (s + 73.6488)} \end{bmatrix} \quad \text{(B-10)}$$

$$
\begin{bmatrix} \\ \\ \\ \\ \\ \\ \\ \\ \\ \end{bmatrix}_2 = \text{Const.} = 0.1108\text{E-}13 \\ \text{Gain} = 5.1985\text{E+}11
\begin{bmatrix}
\dfrac{1}{\begin{array}{l}\text{Constant} = 0.04003\\ (s - 0.3328)\\ (s + 1.2021)\end{array}} & \dfrac{1}{\begin{array}{l}\text{Constant} = -0.6045\text{E-}13\\ \text{Gain} = -8.2558\text{E+}9\\ (s + 0.6834)\end{array}} & \dfrac{1}{\begin{array}{l}\text{Constant} = -0.5532\text{E-}13\\ \text{Gain} = -3.7394\text{E+}11\\ (s + 19.7814)\end{array}} \\ \\
\dfrac{1}{\begin{array}{l}\text{Constant} = 0.002100\\ (s + 1.7274)\\ (s - 32.4517)\end{array}} & \dfrac{1}{\begin{array}{l}\text{Constant} = 0.3833\text{E-}14\\ \text{Gain} = 9.5661\text{E+}11\\ (s + 0.4731)\end{array}} & \dfrac{1}{\begin{array}{l}\text{Constant} = -0.1111\text{E-}12\\ \text{Gain} = 4.9651\text{E+}11\\ (s - 58.9133)\end{array}} \\ \\
\dfrac{1}{\begin{array}{l}\text{Constant} = -0.003195\\ (s + 60.9191)\\ (s + 1.5098)\end{array}} & \dfrac{1}{\begin{array}{l}\text{Constant} = 0.2251\text{E-}13\\ \text{Gain} = 4.0668\text{E+}11\\ (s + 0.2782)\end{array}} & \dfrac{1}{\begin{array}{l}\text{Constant} = 0.1691\text{E-}12\\ \text{Gain} = 4.9651\text{E+}11\\ (s + 98.0477)\end{array}}
\end{bmatrix}_2 \qquad \text{(B-11)}
$$

$$
C_{23} = \begin{matrix}\text{Const.} = 0.6244\text{E-}13 \\ \text{Gain} = -7.2490\text{E+}11\end{matrix}
\begin{bmatrix}
\dfrac{1}{\begin{matrix}\text{Constant} = 0.1651 \\ (s - 0.3342) \\ (s + 1.0054)\end{matrix}} & \dfrac{1}{\begin{matrix}\text{Constant} = -0.1280\text{E-}12 \\ \text{Gain} = -1.3084\text{E+}10 \\ (s + 5.0656)\end{matrix}} & \dfrac{1}{\begin{matrix}\text{Constant} = 0.2701\text{E-}13 \\ \text{Gain} = 3.2580\text{E+}12 \\ (s + 41.2222)\end{matrix}} \\
\dfrac{1}{\begin{matrix}\text{Constant} = 0.007331 \\ \text{Gain} = 1.3769 \\ (s - 45.2440)\end{matrix}} & \dfrac{1}{\begin{matrix}\text{Constant} = 0.1383\text{E-}13 \\ \text{Gain} = 1.0282\text{E+}12 \\ (s + 0.2047)\end{matrix}} & \dfrac{1}{\begin{matrix}\text{Constant} = -0.2975\text{E-}12 \\ \text{Gain} = 7.1467\text{E+}11 \\ (s - 149.1300)\end{matrix}} \\
\dfrac{1}{\begin{matrix}\text{Constant} = -0.01123 \\ (s + 80.3502) \\ (s + 1.2633)\end{matrix}} & \dfrac{1}{\begin{matrix}\text{Constant} = 0.5786\text{E-}13 \\ \text{Gain} = 6.1388\text{E+}11 \\ (s + 0.3318)\end{matrix}} & \dfrac{1}{\begin{matrix}\text{Constant} = 0.4557\text{E-}12 \\ \text{Gain} = 7.1470\text{E+}11 \\ (s + 243.2179)\end{matrix}}
\end{bmatrix}
\qquad \text{(B-12)}
$$

after the range of frequencies of interest, thus it effectively has no effect on the design except as a gain. Therefore this root is treated as a gain. Also, delete the common roots in the numerators and the denominators (these common roots are listed last for each term above and the simplified matrices are in Eq. B-10 (FC #1), B-11 (FC #2) and B-12 (FC #3).

Simplify and rewrite into a more useful form. Thus the final Q matrices are:

Flight Condition 1 (slow speed condition) 0.6 mach at sea level

$$\underline{Q}_1 = 0.03565 \begin{bmatrix} \frac{1}{0.1747(s+0.08111)(s+2.1268)} & \frac{1}{-0.00094(s+1.7127)} & \frac{1}{0.1423(s-5.2379)} \\ \frac{1}{0.004224(s+3.2787)(s-17.352)} & \frac{1}{0.00749(s+0.9848)} & \frac{1}{-0.1151(s-42.2798)} \\ \frac{1}{-0.01294(s+2.0513)(s+46.4722)} & \frac{1}{0.03843(s+0.5093)} & \frac{1}{0.3526(s+73.6488)} \end{bmatrix}$$

Flight Condition 2 (cruise condition) 0.9 mach at 30,000 feet

$$\underline{Q}_2 = 0.005761 \begin{bmatrix} \frac{1}{0.04003(s-0.3329)(s+1.2021)} & \frac{1}{0.000499(s+0.6835)} & \frac{1}{0.02069(s+19.7814)} \\ \frac{1}{0.002100(s-32.4517)(s+1.7274)} & \frac{1}{0.003667(s+0.4731)} & \frac{1}{-0.05518(s-58.9133)} \\ \frac{1}{-0.003195(s+60.919)(s+1.5098)} & \frac{1}{0.009155(s+0.2782)} & \frac{1}{0.08397(s+98.0476)} \end{bmatrix}$$

Flight condition 3 (high speed condition) 2.3 mach at 40,000 feet

$$\underline{Q}_3 = 0.04526 \begin{bmatrix} \frac{1}{0.1651(s+1.0054)(s-0.3343)} & \frac{1}{0.001675(s+5.0656)} & \frac{1}{0.08797(s+41.2222)} \\ \frac{1}{0.007331(s-45.244)(s+1.3769)} & \frac{1}{0.01422(s+0.2047)} & \frac{1}{-0.2126(s-149.13)} \\ \frac{1}{-0.01123(s+80.350)(s+1.2633)} & \frac{1}{0.03552(s+0.3318)} & \frac{1}{0.3257(s+243.218)} \end{bmatrix}$$

Appendix C

Calculations and Tables for the L_1 and L_3

This appendix contains the calculations necessary to design L_1 and L_3. Use q_{33} (Table C-2) to generate the plant templates for L_3 (Fig. C-3). Using:

$$|1 + L_3|^{-1} \leq \frac{b_{22}\frac{|q_{33}|}{|q_{32}|} + b_{12}\frac{|q_{33}|}{|q_{31}|}}{b_{32}} \qquad (5\text{-}2)$$

the bounds for each flight condition for $(1 + L_3)$ are generated (Tables C-2, C-3, C-4 and C-7). The bounds for the nominal design bounds are listed in Table C-8.

Using the plant templates, transfer the nominal bounds to the Nichols Chart to generate the nominal design bounds (Fig. C-5). With the nominal design bounds drawn, shape the L_{30} (Fig. C-6). The L_{30} synthesized is in Table C-10. The compensator for the third loop, G_3, derived from L_{30} is in Table C-11. L_3 for the three FC are listed in Tables C-10 (since $(L_3)_1$ was the nominal case, $L_{30} = (L_3)_1$, C-12 and C-13.

$$(L)_2 = \frac{6.7879}{s\,(s + 98.048)(s + 0.700 + j0.714)(s + 0.700 - j0.714)}$$

$$(L)_3 = \frac{13.748}{s\,(s + 243.218)(s + 0.700 + j0.714)(s + 0.700 - j0.714)}$$

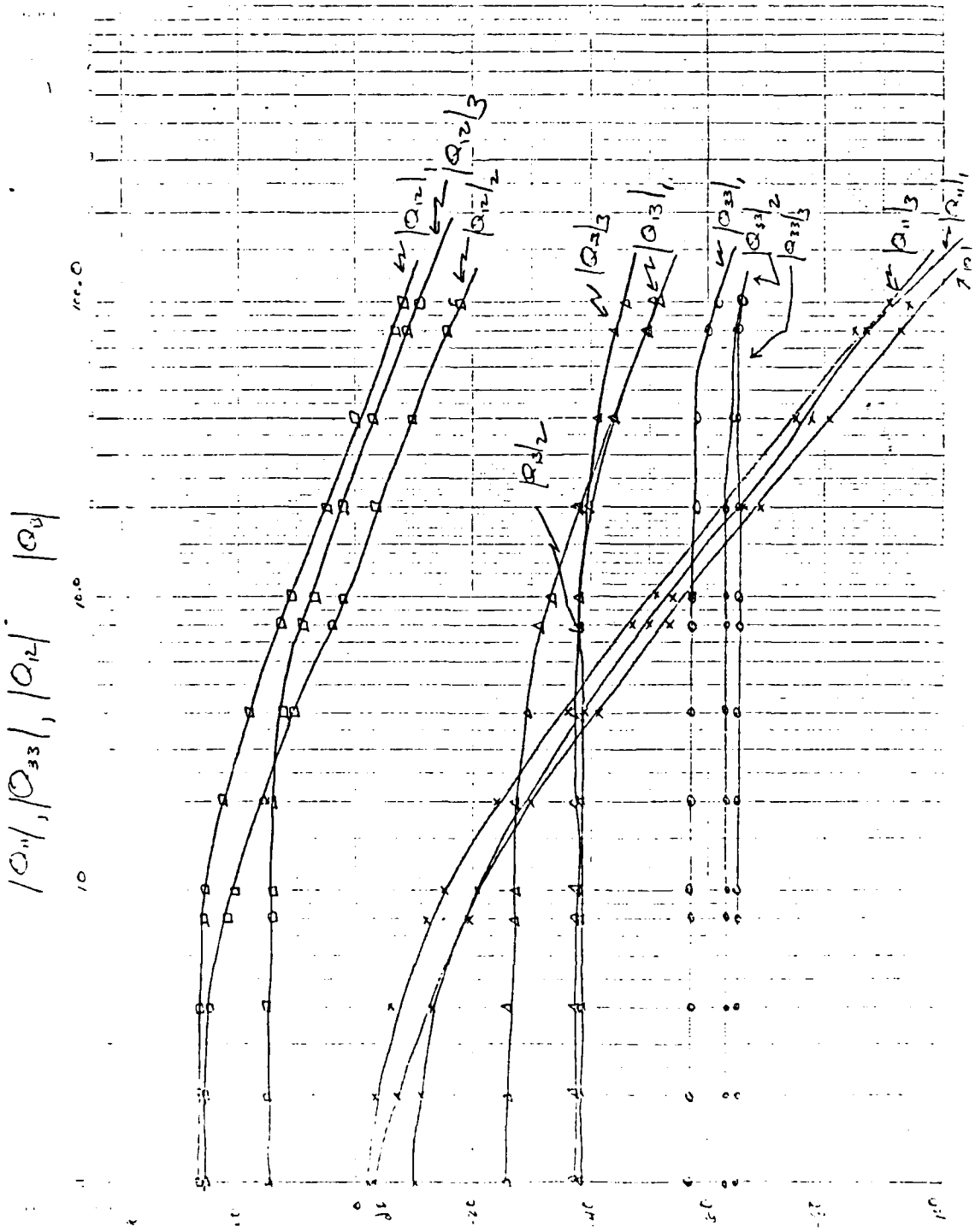

Fig. C-1 Bode Plot of $|q_{11}|$ and $|q_{33}|$

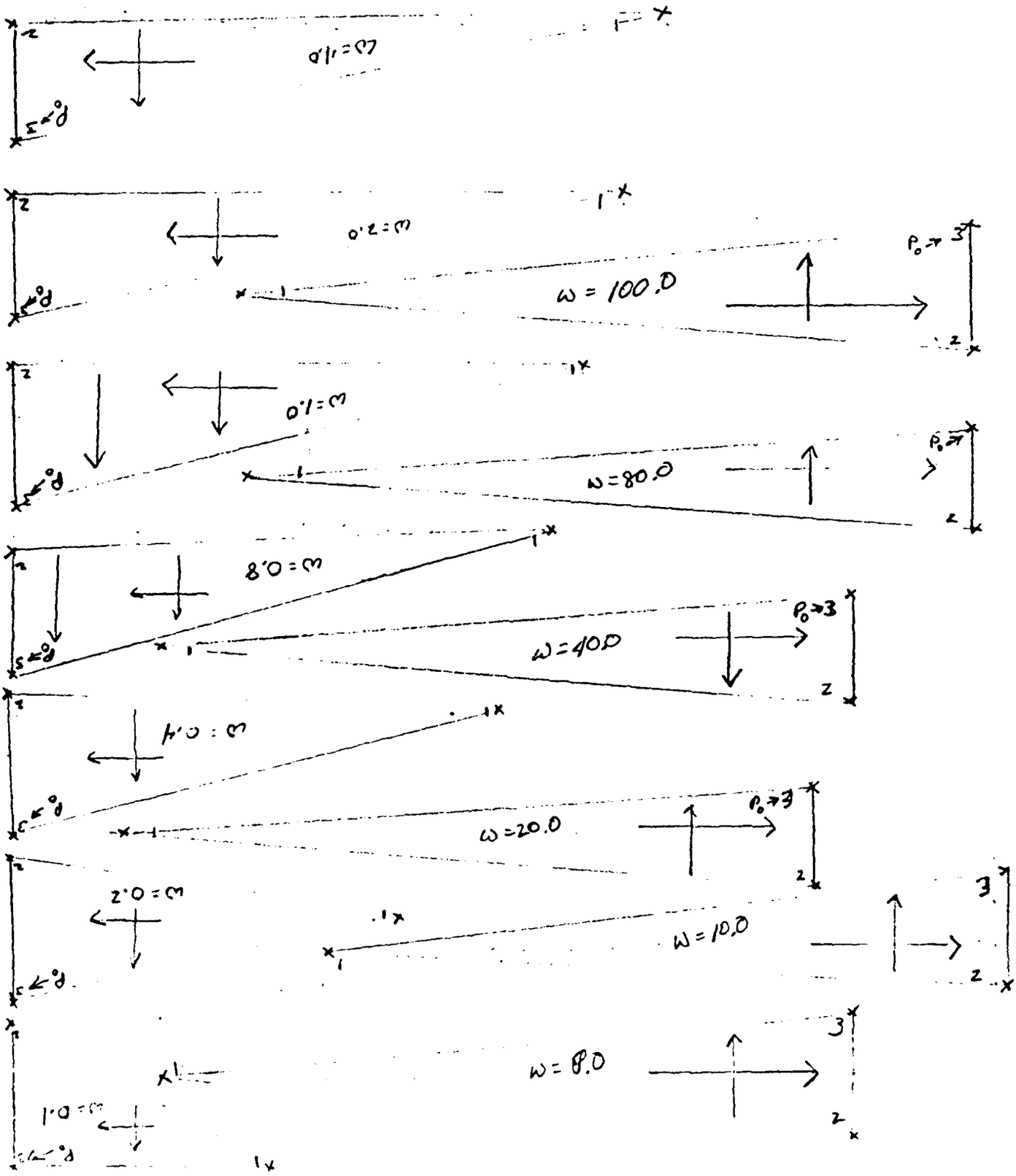

Fig. C-2 Plant (q_{11}) Templates for Loop 1

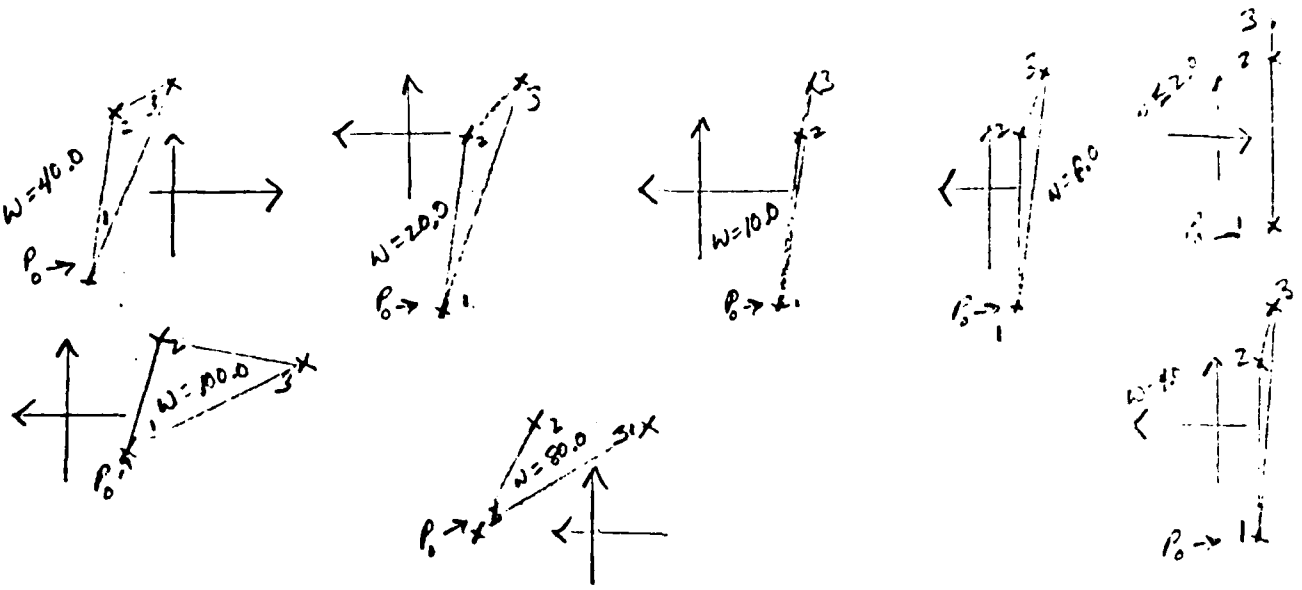

Fig. C-3 Plant (q_{33}) Templates for Loop 3

Table C-1 q_{11} Values (magnitudes in decibels)

Freq.	FC #1		FC #2		FC #3	
(rad/sec)	(db)	(degrees)	(db)	(degrees)	(db)	(degrees)
0.1	-2.5761	-53.6500	-9.2205	11.9692	-2.1774	10.9735
0.2	-7.0914	-73.2996	-10.2728	21.5582	-3.2598	19.6399
0.4	-12.7385	-89.1902	-13.1533	31.8346	-6.2597	28.4176
0.8	-19.0523	-104.8253	-18.7188	33.7688	-12.1708	28.8118
1.0	-21.2673	-110.5459	-21.1117	31.8363	-14.7268	26.6695
2.0	-29.1507	-130.9180	-30.2719	21.5605	-24.3723	17.1994
4.0	-38.9823	-150.8389	-41.2605	11.9708	-35.6117	9.3316
8.0	-50.2375	-164.5315	-53.0007	6.1633	-47.4322	4.7702
10.0	-54.0093	-167.5286	-56.8398	4.9485	-51.2815	3.8265
20.0	-65.9070	-173.6976	-68.8307	2.4863	-63.2864	1.9202
40.0	-77.9115	-176.8403	-80.8593	1.2447	-75.3184	0.9610
80.0	-89.9435	-178.4191	-92.8973	0.6225	-87.3523	0.4806
100.0	-93.8188	-178.9352	-96.7733	0.4980	-91.2335	0.3845

Table C-2 q_{33} Values (magnitudes in decibels)

Freq.	FC #1		FC #2		FC #3	
(rad/sec)	(db)	(degrees)	(db)	(degrees)	(db)	(degrees)
0.1	-57.2600	-0.0778	-63.0458	-0.0584	-64.8543	-0.0236
0.2	-57.2600	-0.1556	-63.0458	-0.1169	-64.8543	-0.0471
0.4	-57.2601	-0.3112	-63.0458	-0.2337	-64.8543	-0.0942
0.8	-57.2605	-0.6223	-63.0461	-0.4675	-64.8544	-0.1885
1.0	-57.2608	-0.7779	-63.0462	-0.5843	-64.8544	-0.2356
2.0	-57.2632	-1.5555	-63.0476	-1.1686	-64.8546	-0.4711
4.0	-57.2728	-3.1088	-63.0530	-2.3362	-64.8555	-0.9422
8.0	-57.3109	-6.1994	-63.0746	-4.6646	-64.8590	-1.8839
10.0	-57.3393	-7.7323	-63.0907	-5.8235	-64.8616	-2.3544
20.0	-57.5690	-15.1928	-63.2228	-11.5292	-64.8836	-4.7009
40.0	-58.3826	-28.5072	-63.7144	-22.1937	-64.9702	-9.3393
80.0	-60.6443	-47.3670	-65.2618	-39.2120	-65.3005	-18.2072
100.0	-61.7987	-53.6288	-66.1425	-45.5648	-65.5326	-22.3502

Table C-3 q_{32} Values (magnitudes in decibels)

Freq. (rad/sec)	FC #1 (db)	FC #2 (db)	FC #3 (db)
0.1	5.04	6.56	11.31
0.2	4.59	5.28	10.34
0.4	3.12	2.22	7.79
0.8	-0.19	-2.58	3.35
1.0	-1.65	-4.35	1.65
2.0	-6.95	-10.13	-4.03
4.0	-12.76	-16.09	-9.97
8.0	-18.73	-22.09	-15.96
10.0	-20.66	-24.03	-17.90
20.0	-26.68	-30.05	-23.92
40.0	-32.69	-36.06	-29.94
80.0	-38.71	-42.09	-35.96
100.0	-40.65	-44.02	-37.89

Table C-4 q_{31} Values (magnitudes in decibels)

Freq. (rad/sec)	FC #1 (db)	FC #2 (db)	FC #3 (db)
0.1	-30.79	-34.17	-28.05
0.2	-30.82	-34.23	-28.13
0.4	-30.95	-34.45	-28.44
0.8	-31.40	-35.23	-29.49
1.0	-31.71	-35.73	-30.14
2.0	-33.69	-38.56	-33.47
4.0	-37.63	-43.21	-38.46
8.0	-43.01	-48.86	-44.20
10.0	-44.92	-50.79	-46.13
20.0	-51.35	-57.06	-52.29
40.0	-59.00	-64.18	-59.00
80.0	-68.59	-72.99	-67.05
100.0	-72.05	-76.25	-70.06

Table C-5 q_{12} Values (magnitudes in decibels)

Freq. (rad/sec)	FC #1 (db)	FC #2 (db)	FC #3 (db)
0.1	26.89	25.38	14.54
0.2	26.85	25.11	14.54
0.4	26.68	24.19	14.51
0.8	26.05	21.72	14.43
1.0	25.65	20.50	14.38
2.0	23.17	15.66	13.91
4.0	18.81	10.00	12.44
8.0	13.32	4.07	9.11
10.0	11.45	2.14	7.64
20.0	5.53	-3.86	2.34
40.0	-0.47	-9.88	-3.48
80.0	-6.49	-15.90	-9.44
100.0	-8.42	-17.84	-11.38

Table C-6 q_{13} Values (magnitudes in decibels)

Freq. (rad/sec)	FC #1 (db)	FC #2 (db)	FC #3 (db)
0.1	-26.41	-37.03	-38.07
0.2	-26.41	-37.03	-38.07
0.4	-26.43	-37.03	-38.07
0.8	-26.50	-37.04	-38.08
1.0	-26.56	-37.04	-38.08
2.0	-27.00	-37.07	-38.08
4.0	-28.40	-37.20	-38.12
8.0	-31.63	-37.69	-38.24
10.0	-33.07	-38.02	-38.32
20.0	-38.33	-40.09	-38.99
40.0	-44.14	-44.10	-40.96
80.0	-50.10	-49.42	-44.86
100.0	-52.03	-51.27	-46.45

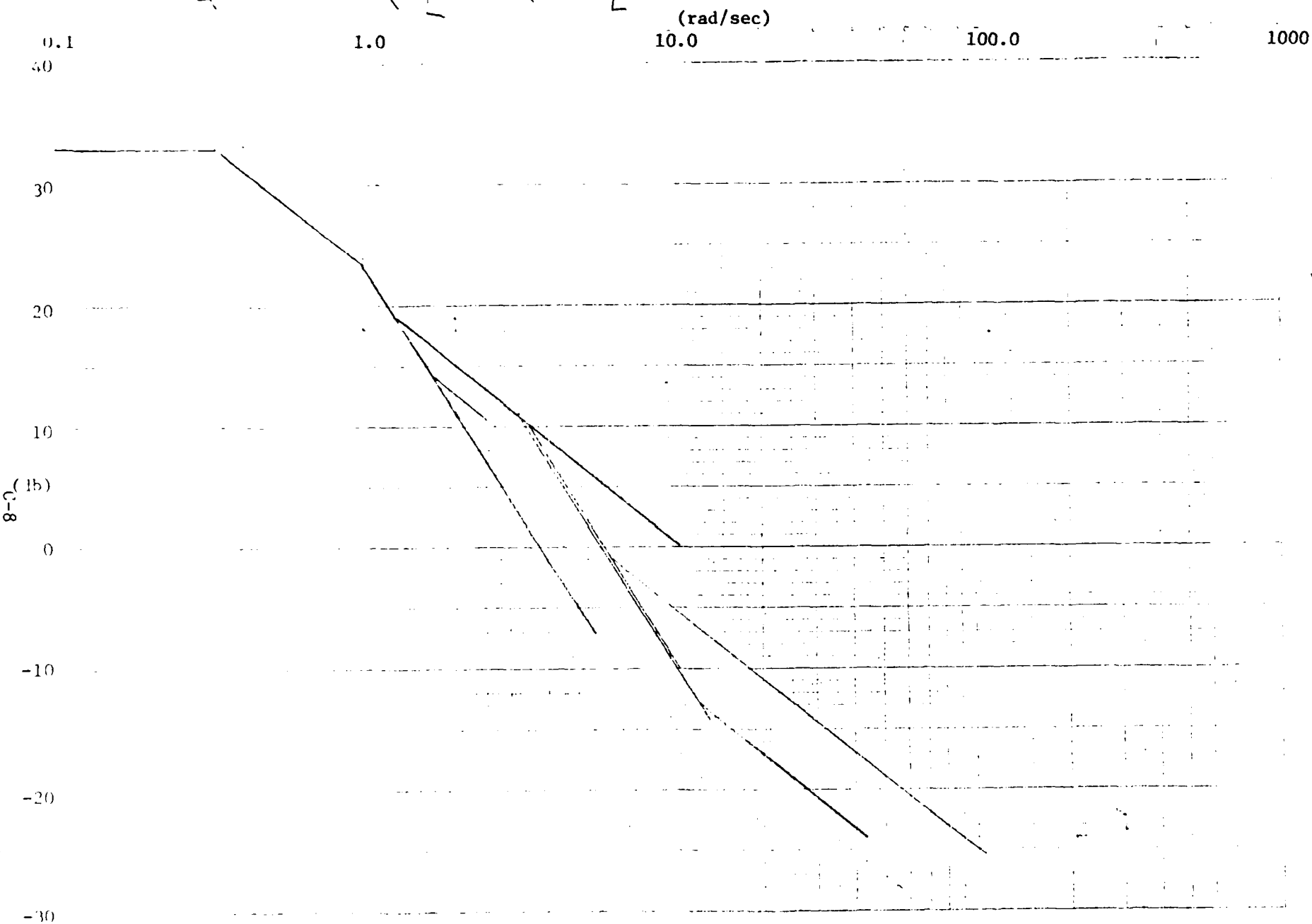

Fig. C-4 Using the Bode Plot to Shape L_{10} Magnitude

Table C-7 Boundary magnitudes (decibels) for frequencies of interest

Freq. (rad/sec)	b_{22} (db)	a_{22} (db)	b_{32} (db)	b_{12} (db)
0.1	0.04	0.04	-38.26	-33.52
0.2	0.13	-0.14	-33.28	-29.32
0.4	0.62	-0.55	-29.76	-26.11
0.8	2.4	-2.0	-27.39	-24.14
1.0	3.3	-2.9	-26.69	-23.83
2.0	-1.1	-8.2	-24.98	-23.72
4.0	-9.8	-17.1	-25.48	-25.06
8.0	-15.7	-28.7	-28.88	-28.38
10.0	-17.3	-32.8	-30.42	-29.85
20.0	-22.8	-46.9	-35.86	-35.16
40.0	-28.6	-63.0	-41.72	-40.98
80.0	-34.5	-80.4	-47.70	-46.95
100.0	-36.5	-86.2	-49.64	-48.88

Table C-8 L_3 Loop bounds

Freq. (rad/sec)	FC #1 (db)	FC #2 (db)	FC #3 (db)	Composite Bound (db)
0.1	-23.12	-24.91	-32.17	-23.12
0.2	-22.96	-24.73	-31.98	-22.96
0.4	-21.76	-23.38	-30.37	-21.76
0.8	-17.80	-19.00	-25.22	-17.80
1.0	-15.97	-16.95	-22.83	-15.97
2.0	-24.51	-25.40	-32.38	-24.51
4.0	-36.39	-37.55	-47.03	-36.39
8.0	-34.96	-36.89	-46.82	-34.96
10.0	-33.09	-34.42	-45.18	-33.09
20.0	-25.70	-27.19	-38.36	-25.70
40.0	-16.97	-19.39	-29.86	-16.97
80.0	-8.04	-9.25	-19.82	-8.04
100.0	-5.42	-6.33	-15.85	-5.42

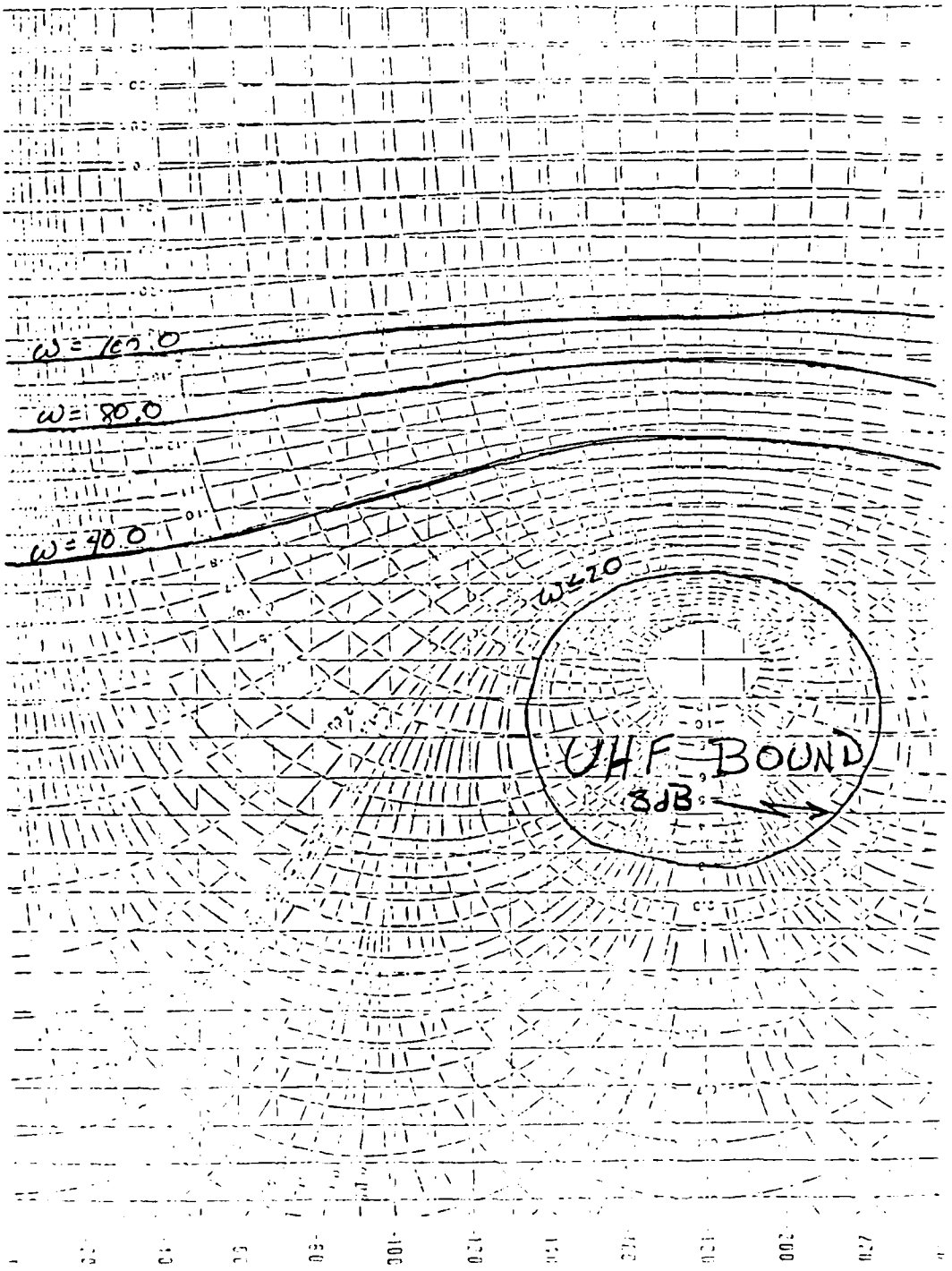

Fig. C-5 Loop 3 (L_3) Design Bounds

Table C-9 L_{10} Design Iterations (Phase Angle)

Poles	Zeros	Frequency (rad/sec) 0.1	0.2	0.4	0.8	1.0	2.0	4.0	8.0	10.0	20.0	40.0	80.0	100.0
.3343														
1.0054		-169	-160	-182	-151	-153	-163	-170	-175	-176	-178	-179	-180	-180
	1.3	+4	+9	+17	+32	+38	+57	+72	+81	+83	+86	+88	+89	+90
3.2		-2	-4	-7	-14	-17	-32	-51	-68	-72	-81	-85	-88	-88
	12.5	+0	+1	+2	+4	+5	+9	+18	+33	+39	+58	+73	+81	+83
		-167	-157	-144	-137	-136	-139	-142	-140	-138	-125	-110	-100	-99
3.5		-2	-3	-7	-13	-16	-30	-49	-66	-71	-80	-85	-85	-88
		-167	-150	-144	-136	-135	-137	-140	-138	-137	-124	-110	-97	-99
	6.5	+1	+2	+4	+7	+9	+17	+32	+51	+57	+72	+81	+85	+86
		-166	-155	-142	-133	-131	-129	-126	-120	-119	-110	-100	-93	-96

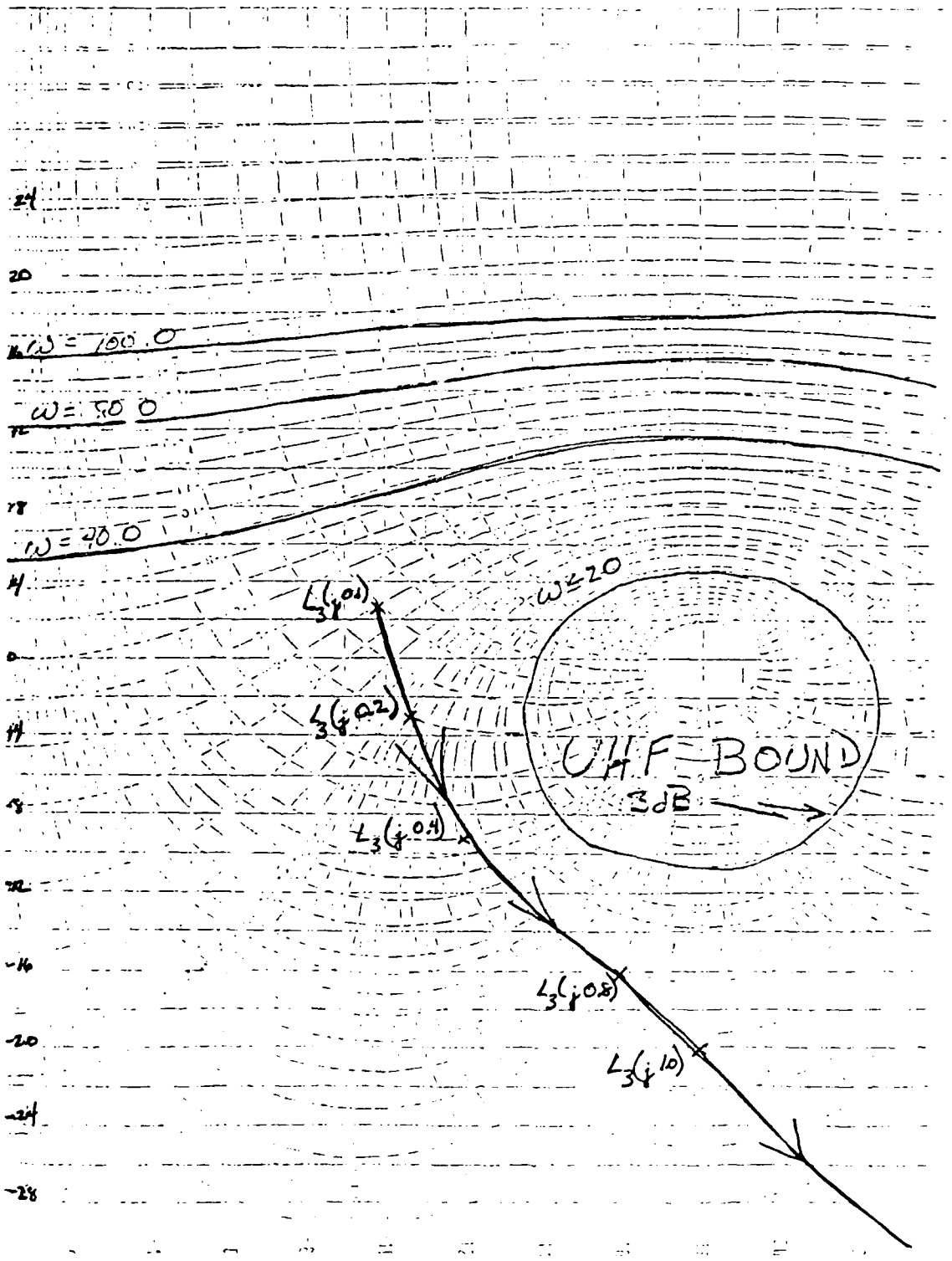

Fig. C-6 Nominal Loop 3 (L_{30}) Design

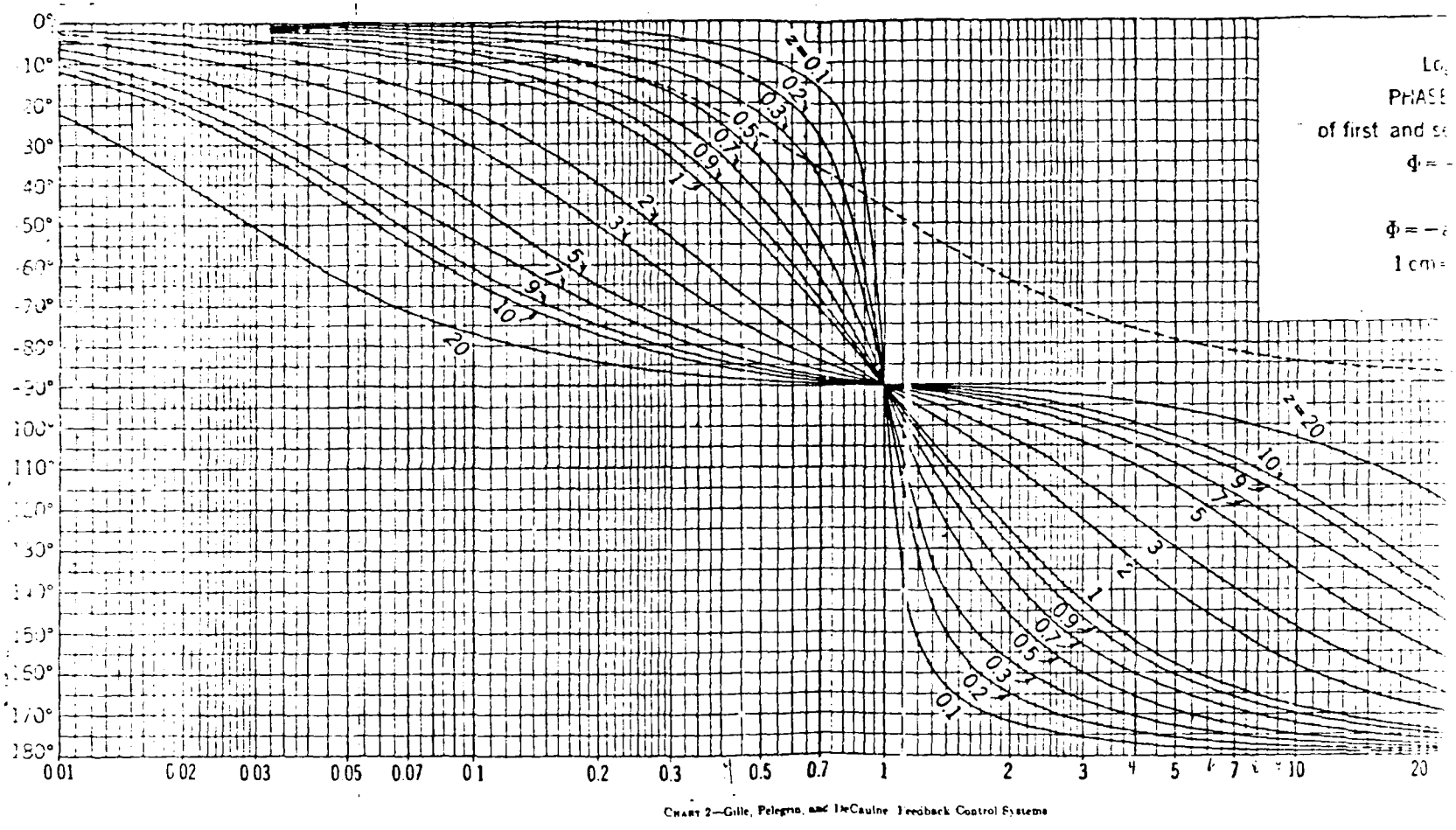

CHART 2—Gille, Pelegrin, and DeCaulne Feedback Control Systems

Fig. C-7 Logarithmic Phase Response

Table C-10 L_{30} Values

$$L_{30} = \frac{10}{s(s + 73.65)(s + 0.70 + j\ .714)(s + 0.70 - j\ .714)}$$

Freq. (rad/sec)	(db)	(degrees)
0.1000	2.6596	-98.1285
0.2000	-3.3624	-106.4191
0.4000	-9.4659	-124.0077
0.8000	-16.8167	-162.8129
1.0000	-20.2668	-180.7863
2.0000	-35.6310	-228.5324
4.0000	-53.4861	-252.6367
8.0000	-71.5782	-266.1187
10.0000	-77.4215	-269.6832
20.0000	-95.7139	-281.1784
40.0000	-114.5895	-296.5010
80.0000	-134.9131	-316.3638
100.0000	-141.8820	-322.8262

Table C-11 G_1 Values

$$G_3 = \frac{98.9173}{s(s + 0.70 + j\ .714)(s + 0.7 - j\ .714)}$$

Freq. (rad/sec)	(db)	(degrees)
0.1000	59.9085	-98.0507
0.2000	53.8865	-106.2635
0.4000	47.7831	-123.6965
0.8000	40.4327	-162.1906
1.0000	36.9829	-180.0084
2.0000	21.6211	-226.9769
4.0000	3.7756	-249.5280
8.0000	-14.2783	-259.9194
10.0000	-20.0933	-261.9510
20.0000	-38.1560	-265.9658
40.0000	-56.2181	-267.9942
80.0000	-74.2799	-268.9973
100.0000	-80.0946	-269.1978

Appendix D

Calculations for Q_{22e}

This section contains the calculations for Q_{22e} (Chapter VI). For loop 2, the exact loop equation is used to synthesize L_{20}. The terms enclosed are used to generate the plant template, Q_{22e}. The exact equation is:

$$Q_{22e} = \frac{q_{22}[(1 + L_1)(1 + L_3) - \gamma_{13}]}{[(1 + L_1)(1 + L_3) - \gamma_{13}] - [\gamma_{12}(1 + L_3) + \gamma_{23}(1 + L_1) - \Gamma]} \quad (6\text{-}3)$$

The Q_{22e} values are listed in Table 6-1.

Table 6-1 Q_{22e} Values

Freq.	FC #1		FC #2		FC #3	
(rad/sec)	(db)	(degrees)	(db)	(degrees)	(db)	(degrees)
0.1	14.65	11.98	12.72	21.36	24.48	87.27
0.2	15.90	17.09	14.62	19.95	26.77	118.18
0.4	17.73	18.48	16.02	17.45	27.32	-220.24
0.8	20.49	12.92	18.58	15.97	25.96	-203.39
1.0	21.37	5.94	19.99	11.33	25.51	-196.86
2.0	22.93	-17.96	25.61	-23.91	24.33	-183.65
4.0	24.93	-110.00	15.63	-157.93	19.94	-180.43
8.0	7.72	-158.38	0.076	-168.43	11.39	-178.00
10.0	3.27	-160.53	-4.13	-168.00	8.08	-177.15
20.0	-9.27	-159.08	-16.48	-165.83	-3.05	-174.62
40.0	-20.64	-148.40	-28.13	-156.39	-14.75	-170.14
80.0	-30.42	-130.91	-38.63	-139.97	-26.38	-161.38
100.0	-33.14	-124.94	-41.62	-133.75	-30.02	-157.26

For example, at FC #1 for ω = 1 rad/sec; q_{33} = 10.61 db and -45.44 degrees, $(1 + L_1)_1$ = 15.88 db and -72.46 degrees, $(1 + L_3)_1$ = -0.89 db and 0.073 degrees, γ_{12} = -19.40 db and -112.04 degrees, γ_{13} = -20.23 db

and -94.91 degrees, γ_{23} = -2.28 db and 15.44 degrees and Γ = -14.74 db and 263.3 degrees. Using Eq. 6-3, solve for Q_{22e}:

$$Q_{22e} = \frac{10.61\angle -45.44[(15.88\angle -72.46)(-0.89\angle 0.073)-(-20.23\angle -94.91)]}{[(15.88\angle -72.46)(-0.89\angle 0.073)-(-20.23\angle -94.91)]}$$

$$- [(-19.40\angle -112.04)(-0.89\angle 0.073)+(-2.28\angle 15.44)(15.88\angle -72.16)$$

$$- (-14.74\angle 263.3)]$$

$$= \frac{10.61\angle -45.44[(14.99\angle -72.39)-(-20.23\angle -94.91)]}{(14.99\angle -72.39) - (-20.23\angle -94.91)}$$

$$- [(-20.29\angle -111.97) + (13.60\angle -57.02) - (-14.74\angle 263.3)]$$

$$= \frac{(10.61\angle -45.44)\ (15.13\angle -72.77)}{(15.13\angle -72.77) - (4.86\angle -57.78)}$$

$$= \frac{25.74\angle -118.21}{4.16\angle -123.89}$$

$$Q_{22e}\ (\omega = 1\ \text{rad/sec at FC \#1}) = 21.58\angle 5.68$$

Thus the nominal bound for $L_{20}(j_1)$ = 21.58 db and 5.68 degrees. After all of these bounds are calculated, then they are transferred to the Nichols Chart to generate a nominal design bound.

Table D-1 q_{22} Values

$$(q_{22})_1 = \frac{4.7597}{(3 + 0.9848)}$$

$$(q_{22})_2 = \frac{1.5676}{(s + 0.4731)}$$

$$(q_{22})_3 = \frac{0.3190}{(s + 0.2047)}$$

Freq. (rad/sec)	$(q_{22})_1$ (db)	$(q_{22})_1$ (degrees)	$(q_{22})_2$ (db)	$(q_{22})_2$ (degrees)	$(q_{22})_3$ (db)	$(q_{22})_3$ (degrees)
0.1	13.64	-5.80	1 22	-11.94	22.92	-26.04
0.2	13.51	-11.48	9.69	-22.92	20.94	-44.33
0.4	13.02	-22.11	8.06	-40.21	17.02	-62.90
0.8	11.48	-39.09	4.54	-59.40	11.74	-75.65
1.0	10.61	-45.44	3.03	-64.68	9.90	-78.43
2.0	6.59	-63.78	-2.35	-76.69	4.01	-84.16
4.0	1.25	-76.17	-8.20	-83.25	-1.98	-87.07
8.0	-4.58	-82.98	-14.17	-86.62	-7.99	-88.53
10.0	-6.49	-84.38	-16.11	-87.29	-9.93	-88.83
20.0	-12.48	-87.18	-22.12	-88.64	-15.94	-89.41
40.0	-18.49	-88.59	-28.14	-89.32	-21.97	-89.71
80.0	-24.51	-89.29	-34.16	-89.66	-27.99	-89.85
100.0	-26.45	-89.44	-36.10	-89.73	-29.92	-89.88

Table D-2 $(1 + L_1)$ Values

$$(1+L_1)_1 = \frac{(s+4.809+j3.936)(s+4.809-j3.936)(s+1.209)(s+36.440+j.37.508)(s+36.440-j57.508)}{(s+0.0811)(s+2.127)(s+3.500)(s+39+j40)(s+39-j40)}$$

$$(1+L_1)_2 = \frac{(s+1.325)(s+3.189+j3.480)(s+3.189-j3.480)(s+37.334+j38.273)(s+37.334-j38.273)}{(s-0.333)(s+1.202)(s+3.500)(s+39+j40)(s+39-j40)}$$

$$(1+L_1)_3 = \frac{(s+4.870+j4.890)(s+4.870-j4.890)(s+1.335)(s+35.54+j36.560)(s+35.548-j36.560)}{(s-0.334)(s+1.005)(s+3.500)(s+39+j40)(s+39-j40)}$$

Freq. (rad/sec)	$(1+L_1)_1$ (db)	$(1+L_1)_1$ (degrees)	$(1+L_1)_2$ (db)	$(1+L_1)_2$ (degrees)	$(1+L_1)_3$ (db)	$(1+L_1)_3$ (degrees)
0.1	32.62	-49.12	25.33	-163.70	32.68	-165.19
0.2	28.19	-64.30	24.34	-149.83	31.66	-152.74
0.4	22.84	-71.65	21.70	-131.28	28.89	-136.67
0.8	17.51	-72.69	16.92	-114.66	23.77	-123.60
1.0	15.88	-72.46	15.01	-110.32	21.70	-120.50
2.0	10.74	-72.57	8.19	-96.67	14.37	-111.94
4.0	4.59	-66.54	1.12	-68.74	6.04	-96.47
8.0	-0.06	-40.46	-1.25	-29.81	-0.41	-58.11
10.0	-0.63	-31.60	-1.21	-22.01	-1.19	-44.83
20.0	-1.10	-13.11	-0.91	-8.59	-1.63	-17.86
40.0	-0.90	-2.69	-0.64	-1.70	-1.25	-3.43
80.0	-0.20	0.76	-0.14	0.55	-0.27	1.06
100.0	-0.09	0.56	-0.06	0.40	-0.12	0.77

Table D-3 $(1+L_3)$ Values

$$(1+L_3)_1 = \frac{(s+0.173)(s+0.614+j0.640)(s+73.649)}{(s+73.649)\ s\ (s+0.700+j0.714)(s+0.700-j0.714)}$$

$$(1+L_3)_2 = \frac{(s+0.0772)(s+0.661+j0.678)(s+0.661-j0.678)(s+98.048)}{(s+98.048)\ s\ (s+0.700+j0.714)(s+0.700-j0.714)}$$

$$(1+L_3)_3 = \frac{(s+0.0616)(s+0.667+j0.687)(s+0.667-j0.687)(s+243.22)}{(s+243.218)\ s\ (s+0.700+j0.714)(s+0.700-j0.714)}$$

Freq. (rad/sec)	$(1+L_3)_1$ (db)	$(1+L_3)_1$ (degrees)	$(1+L_3)_2$ (db)	$(1+L_3)_2$ (degrees)	$(1+L_3)_3$ (db)	$(1+L_3)_3$ (degrees)
0.1	3.91	-58.99	1.09	-37.24	0.65	-31.32
0.2	0.32	-38.86	-0.34	-20.21	-0.36	-16.47
0.4	-1.32	-18.95	-0.77	-8.94	-0.64	-7.28
0.8	-1.28	-2.84	-0.63	-1.35	-0.54	-1.16
1.0	-0.89	0.07	-0.44	0.03	-0.39	0.01
2.0	-0.10	0.71	-0.05	0.36	-0.05	0.38
4.0	-0.01	0.11	0.00	0.06	-0.01	0.10
8.0	0.00	0.01	0.00	0.01	0.00	0.04
10.0	0.00	0.01	0.00	0.00	0.00	0.03
20.0	0.00	0.00	0.00	0.00	0.00	0.01
40.0	0.00	0.00	0.00	0.00	0.00	0.01
80.0	0.00	0.00	0.00	0.00	0.00	0.00
100.0	0.00	0.00	0.00	0.00	0.00	0.00

Table D-4 γ_{12} Values

$$(\gamma_{12})_1 = \frac{-0.00300(s-17.352)(s+3.279)(s+1.713)}{(s+0.0811)(s+2.126)(s+0.985)}$$

$$(\gamma_{12})_2 = \frac{0.0071(s+0.683)(s+1.727)}{(s-0.333)(s+1.202)(s+0.473)}$$

$$(\gamma_{12})_3 = \frac{0.0052(s+5.066)(s+1.377)(s-45.244)}{(s-0.334)(s+1.005)(s+0.205)}$$

Freq. (rad/sec)	$(\gamma_{12})_1$ (db)	$(\gamma_{12})_1$ (degrees)	$(\gamma_{12})_2$ (db)	$(\gamma_{12})_2$ (degrees)	$(\gamma_{12})_3$ (db)	$(\gamma_{12})_3$ (degrees)
0.1	0.66	-54.69	2.66	11.50	26.23	-9.90
0.2	-3.92	-75.29	1.39	21.21	23.24	-14.42
0.4	-9.84	-92.51	-2.02	34.29	16.60	-14.27
0.8	-16.87	-107.80	-8.02	47.30	6.40	-8.72
1.0	-19.40	-112.04	-10.29	51.11	2.64	-5.87
2.0	-27.81	-120.47	-17.55	61.66	-9.34	7.51
4.0	-35.86	-122.51	-24.32	68.64	-20.24	26.51
8.0	-42.39	-126.63	-30.45	68.63	-28.98	44.10
10.0	-44.09	-129.73	-32.29	66.82	-31.34	47.83
20.0	-47.93	-144.14	-37.35	55.30	-37.54	50.51
40.0	-49.69	-159.12	-40.77	37.52	-42.03	40.59
80.0	-50.25	-169.05	-42.31	21.31	-44.46	25.51
100.0	-50.33	-171.19	-42.54	17.37	-44.86	21.16

Table D-5 γ_{13} Values

$$(\gamma_{13})_1 = \frac{-0.0299\ (s-5.238)(s+2.051)(s+46.472)}{(s+0.0811)(s+2.127)(s+73.649)}$$

$$(\gamma_{13})_2 = \frac{-0.0197\ (s+1.510)(s+19.781)(s+60.919)}{(s-0.333)(s+1.202)(s+98.048)}$$

$$(\gamma_{13})_3 = \frac{-0.0184\ (s+41.222)(s+1.263)(s+80.350)}{(s-0.334)(s+1.005)(s+243.218)}$$

Freq. (rad/sec)	$(\gamma_{13})_1$ (db)	$(\gamma_{13})_1$ (degrees)	$(\gamma_{13})_2$ (db)	$(\gamma_{13})_2$ (degrees)	$(\gamma_{13})_3$ (db)	$(\gamma_{13})_3$ (degrees)
0.1	-2.61	-51.91	-1.17	-343.92	-0.91	-344.31
0.2	-7.09	-69.83	-2.16	-330.25	-1.91	-330.99
0.4	-12.60	-82.34	-4.83	-312.03	-4.60	-313.27
0.8	-18.38	-91.84	-9.60	-295.71	-9.46	-297.35
1.0	-20.23	-94.91	-11.49	-291.40	-11.37	-293.10
2.0	-25.70	-106.63	-17.79	-279.00	-17.67	-281.35
4.0	-30.20	-123.55	-24.00	-265.86	-23.90	-270.75
8.0	-32.88	-142.13	-29.63	-249.69	-29.85	-259.42
10.0	-33.33	-147.06	-31.23	-243.32	-31.69	-255.00
20.0	-33.77	-156.79	-35.07	-219.87	-36.89	-236.54
40.0	-33.13	-160.10	-36.40	-196.14	-40.33	-209.58
80.0	-31.87	-163.66	-35.85	-180.85	-40.76	-181.02
100.0	-31.51	-165.47	-35.50	-178.47	-40.26	-173.87

Table D-6 γ_{23} Values

$$(\gamma_{23})_1 = \frac{-1.675\ (s-42.280)(s+0.509)}{(s+0.985)(s+73.649)}$$

$$(\gamma_{23})_2 = \frac{-1.641\ (s-58.913)(s+0.278)}{(s+0.473)(s+98.048)}$$

$$(\gamma_{23})_3 = \frac{-1.631\ (s-149.130)(s+0.332)}{(s+0.205)(s+248.218)}$$

Freq. (rad/sec)	$(\gamma_{23})_1$ (db)	$(\gamma_{23})_1$ (degrees)	$(\gamma_{23})_2$ (db)	$(\gamma_{23})_2$ (degrees)	$(\gamma_{23})_3$ (db)	$(\gamma_{23})_3$ (degrees)
0.1	-5.94	5.10	-4.45	7.68	3.64	-9.33
0.2	-5.62	9.53	-3.64	12.49	2.63	-13.38
0.4	-4.64	15.19	-2.21	14.34	1.26	-12.82
0.8	-2.87	16.72	-0.93	10.18	0.41	-8.67
1.0	-2.28	15.44	-0.67	8.22	0.28	-7.41
2.0	-1.00	7.67	-0.27	2.28	0.07	-4.82
4.0	-0.50	-1.94	-0.15	-3.45	0.02	-4.29
8.0	-0.29	-13.54	-0.08	-11.00	0.01	-5.86
10.0	-0.21	-18.33	-0.05	-14.34	0.02	-6.92
20.0	0.22	-39.15	0.17	-29.72	0.05	-12.70
40.0	1.31	-71.24	0.86	-56.09	0.19	-24.54
80.0	2.88	-109.17	2.20	-92.70	0.65	-46.51
100.0	3.31	-120.44	2.67	-104.95	0.93	-56.27

Table D-7 Γ Values

$$(\Gamma)_1 = \frac{0.0470\ (s+0.916)(s+2.951)(s-12.198+j8.710)(s-12.198-j8.710)}{(s+0.0811)(s+2.127)(s+0.985)(s+73.649)}$$

$$(\Gamma)_2 = \frac{0.0394\ (s+0.484)(s+1.625)(s+29.603)(s-39.683)}{(s-0.333)(s+1.202)(s+0.473)(s+98.048)}$$

$$(\Gamma)_3 = \frac{0.0352\ (s+1.233)(s+2.911)(s+50.931)(s-66.320)}{(s-0.334)(s+1.000)(s+0.205)(s+243.218)}$$

Freq. (rad/sec)	$(\Gamma)_1$ (db)	$(\Gamma)_1$ (degrees)	$(\Gamma)_2$ (db)	$(\Gamma)_2$ (degrees)	$(\Gamma)_3$ (db)	$(\Gamma)_3$ (degrees)
0.1	3.15	308.03	5.45	15.22	26.82	-8.46
0.2	-1.33	290.02	4.43	28.10	23.86	-11.55
0.4	-6.85	277.22	1.69	44.99	17.32	-8.67
0.8	-12.76	266.79	-3.25	59.34	7.45	1.53
1.0	-14.74	263.25	-5.21	62.86	3.89	6.27
2.0	-21.23	250.80	-11.76	71.99	-7.03	25.93
4.0	-27.94	235.51	-18.19	79.32	-16.28	49.18
8.0	-33.71	208.97	-24.06	83.67	-23.55	67.64
10.0	-35.06	195.75	-25.78	83.36	-25.59	71.92
20.0	-35.89	143.15	-30.09	83.58	-31.17	80.65
40.0	-32.52	95.89	-31.67	74.98	-34.91	83.04
80.0	-29.12	59.69	-30.56	56.32	-35.42	76.63
100.0	-28.37	50.00	-30.02	49.15	-34.88	72.34

AD-A174 518 DESIGN OF A MULTIPLE INPUT-MULTIPLE OUTPUT FLIGHT CONTROL SYSTEM CONTAINI..(U) AIR FORCE WRIGHT AERONAUTICAL LABS WRIGHT-PATTERSON AFB OH D L SEGNER 3/3

UNCLASSIFIED NOV 84 AFWAL-TR-84-3093 F/G 1/3 NL

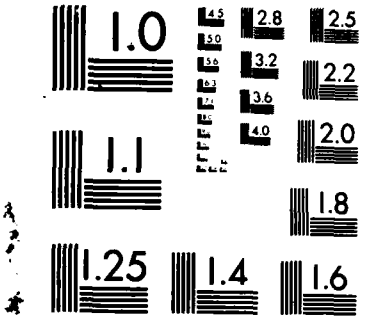

Appendix E

Designed Controller Responses

This appendix contains the results of the computer simulation. Note the magnitude scales are different for each plot.

The exact equation was used to generate these plots (Eq. 7-2). Using simple algebra, Eq. 7-2(a) and 7-2(c) are solved in terms of Eq. 7-2(b). The results are;

$$t_{12} = \frac{\frac{q_{11}q_{33}}{q_{13}q_{32}} t_{22} - \frac{q_{11}}{q_{12}} t_{22} (1 + L_3)}{(1 + L_1)(1 + L_3) - \frac{q_{11}q_{33}}{q_{13}q_{31}}} \qquad \text{(E-1)}$$

$$t_{32} = \frac{\frac{q_{11}q_{33}}{q_{12}q_{31}} t_{22} - \frac{q_{33}}{q_{32}} (1 + L_1)}{(1 + L_1)(1 + L_3) - \frac{q_{11}q_{33}}{q_{13}q_{31}}} \qquad \text{(E-2)}$$

FC #1

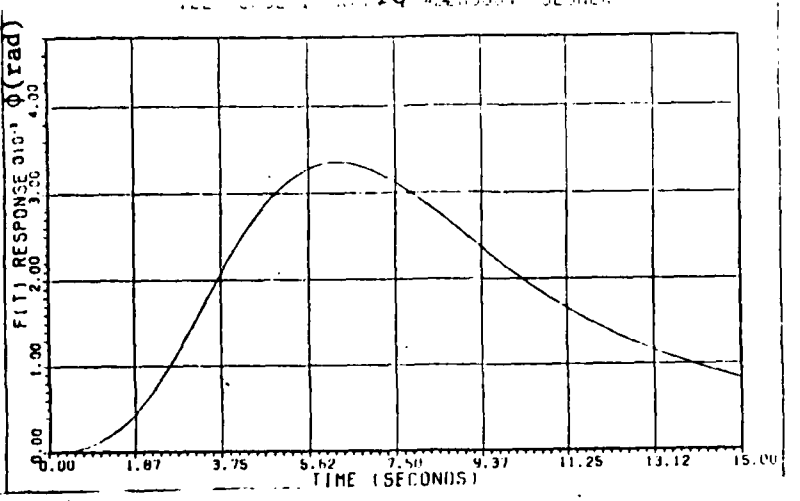

FC #2

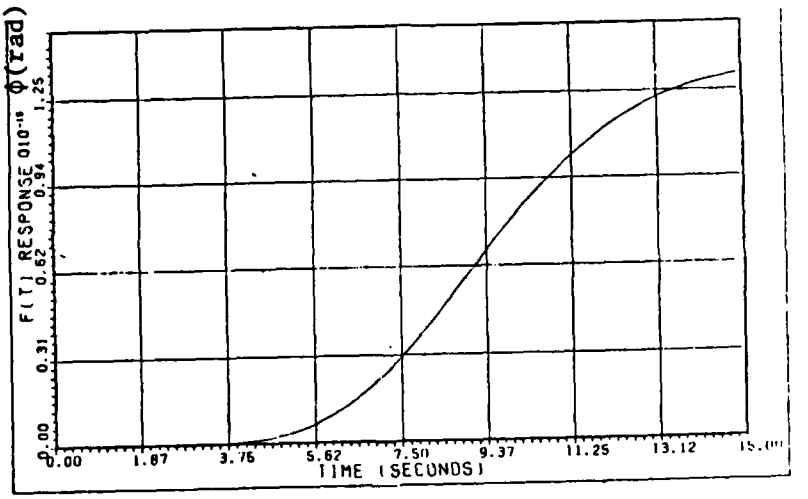

FC #3

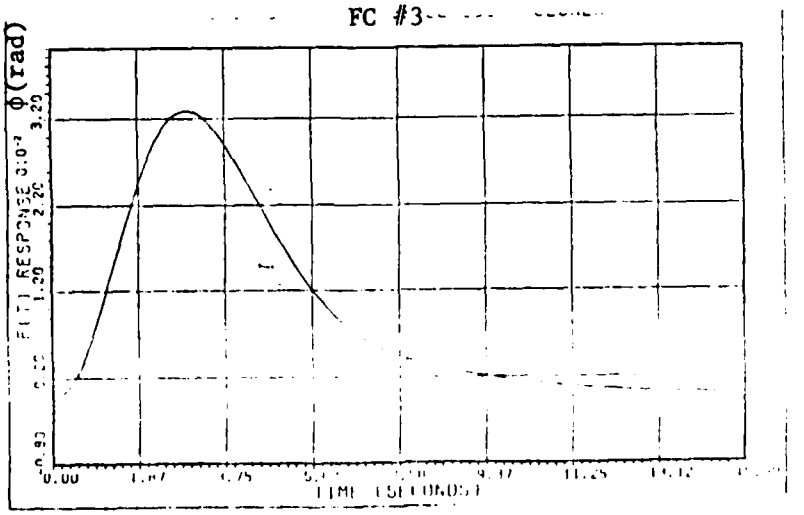

Fig. E-1 t_{12} Responses r(t) = 1 ft/sec

FC #1

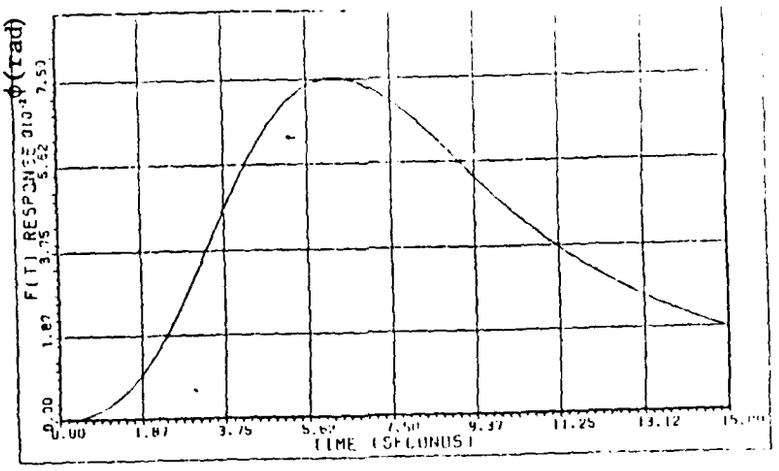

FC #2

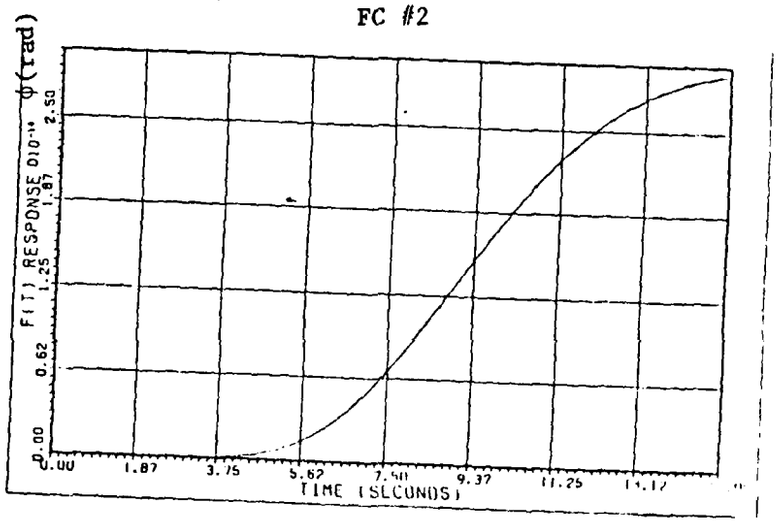

FC #3

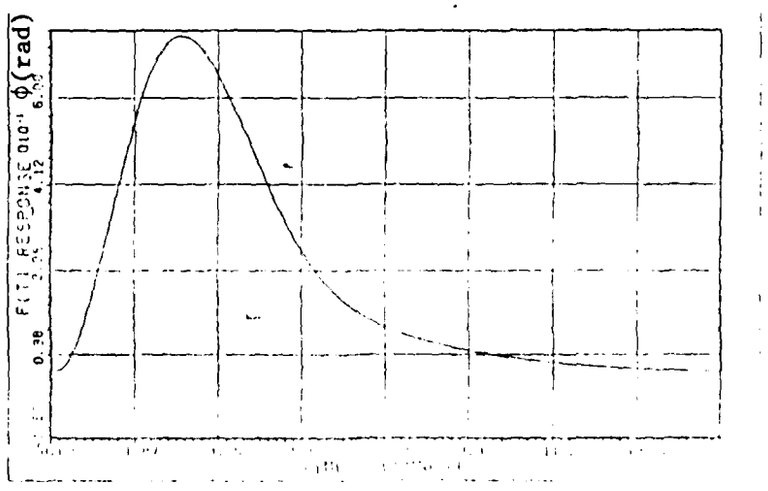

Fig. E-2 t_{12} Responses r(t) = 22.4 ft/sec

FC #1

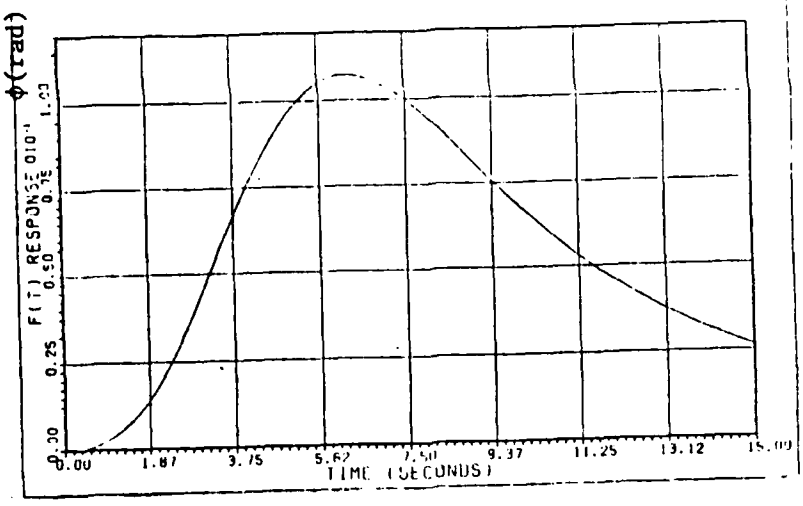

FC #2

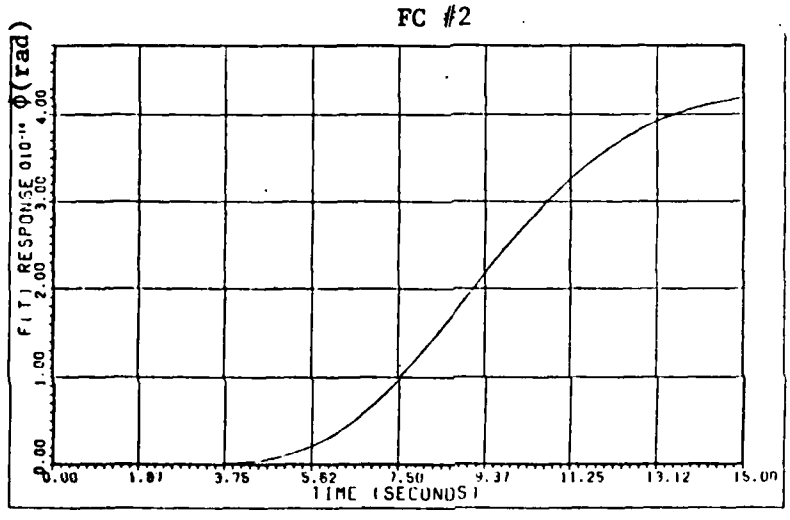

FC #3

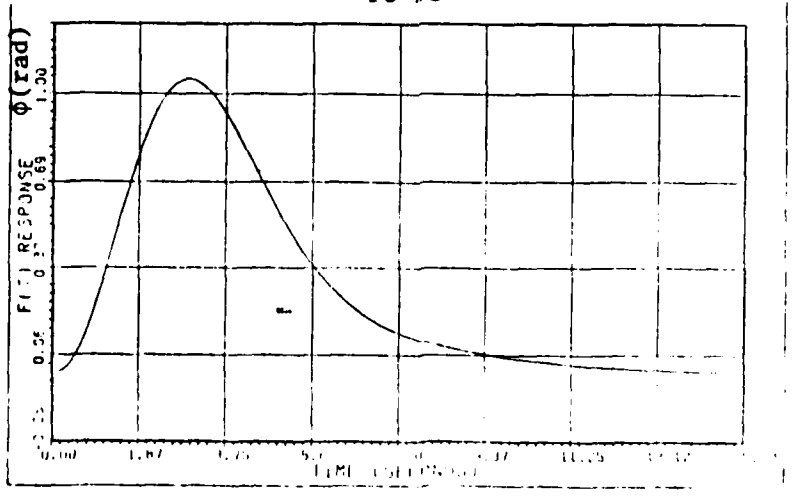

Fig. E-3 t_{12} Responses r(t) = 32 ft/sec

FC #1

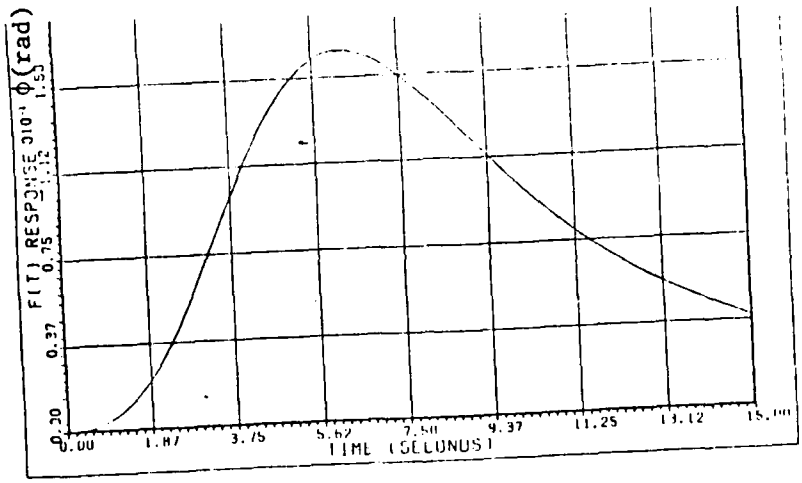

FC #2

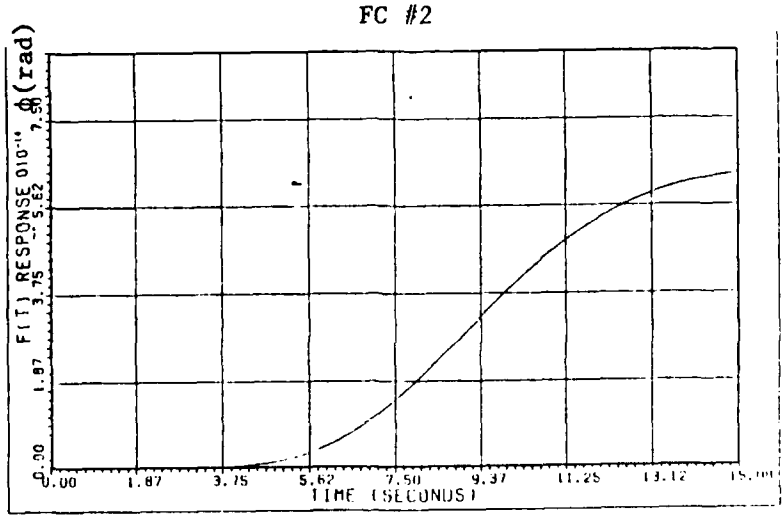

FC #3

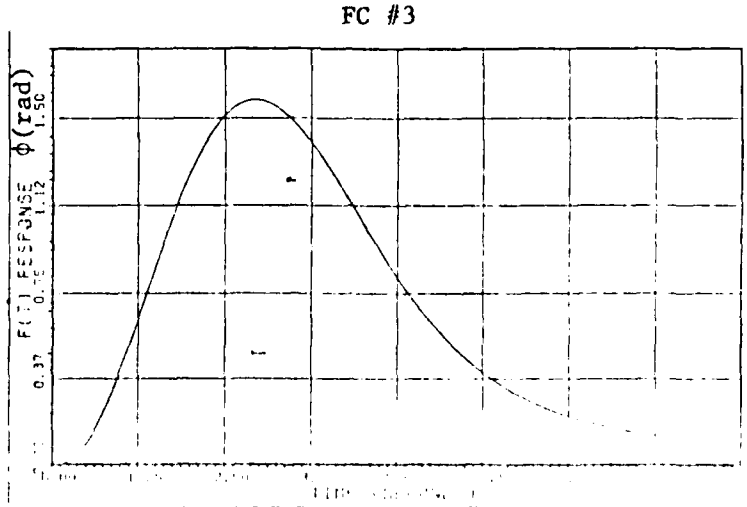

Fig. E-4 t_{12} Responses r(t) = 48 ft/sec

FC #1

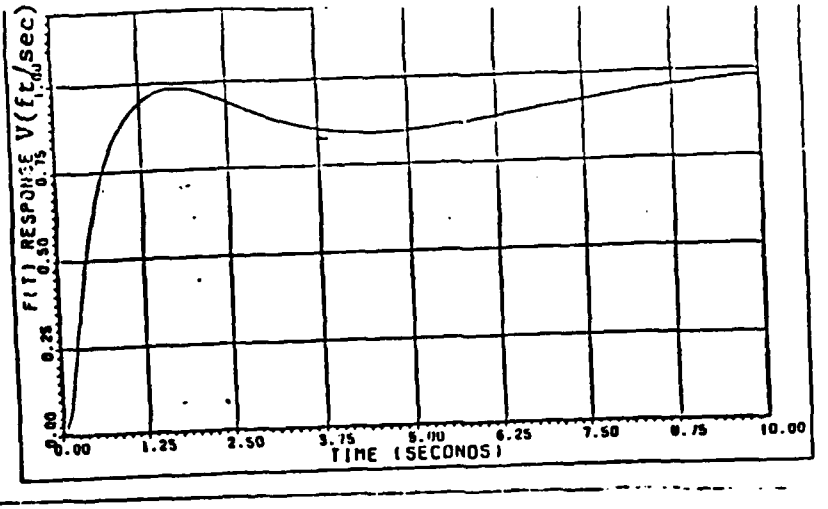

FC #2

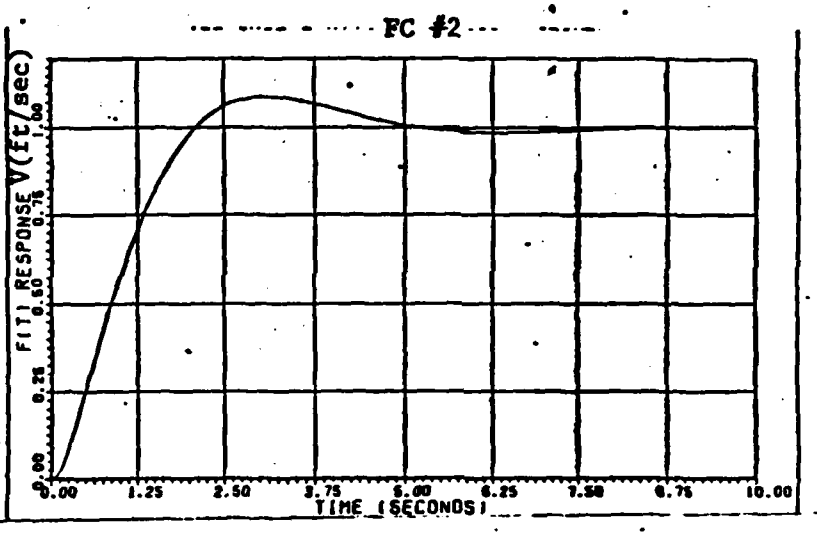

FC #3

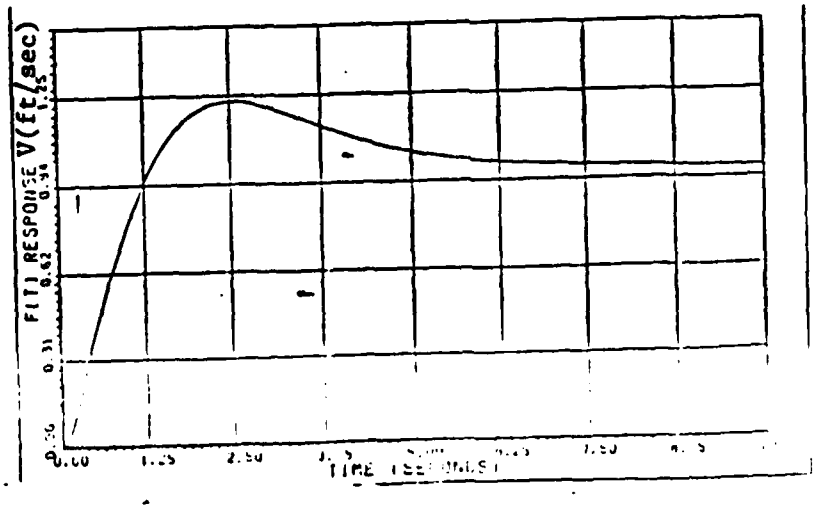

Fig. E-5 t_{22} Responses r(t) = 1 ft/sec

FC #1

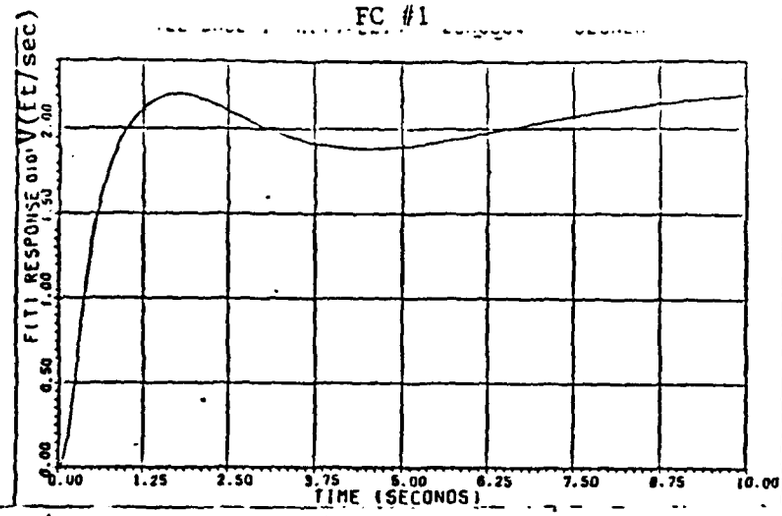

FC #2

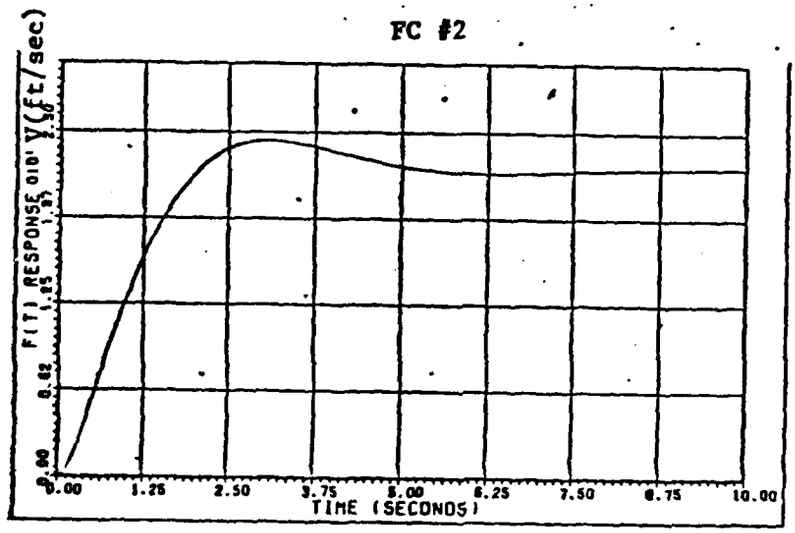

FC #3

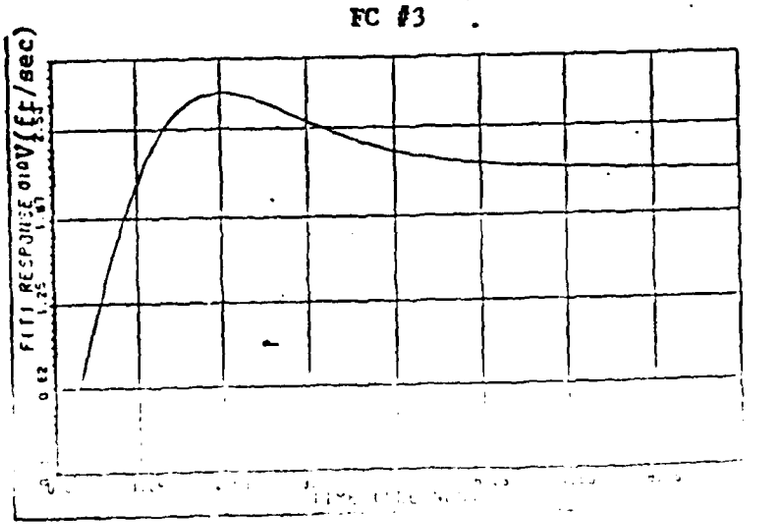

Fig. E-6 t_{22} Responses r(t) = 22.4 ft/sec

FC #1

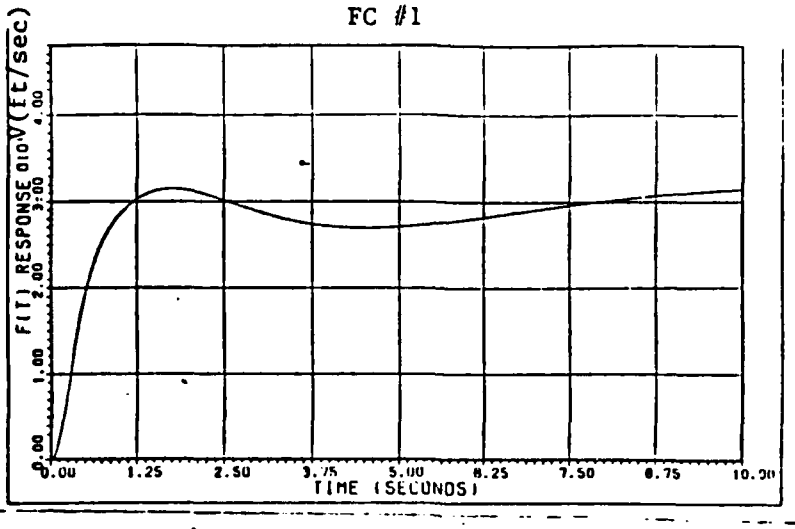

FC #2

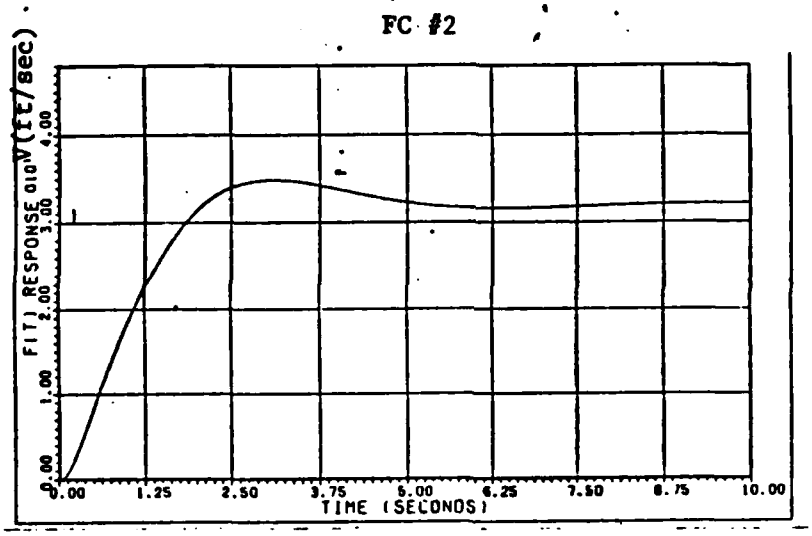

FC #3

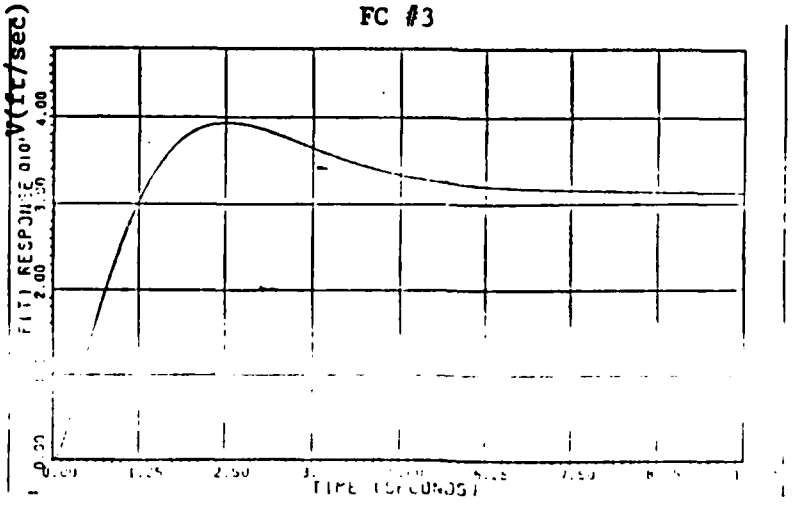

Fig. E-7 t_{22} Responses r(t) = 32 ft/sec

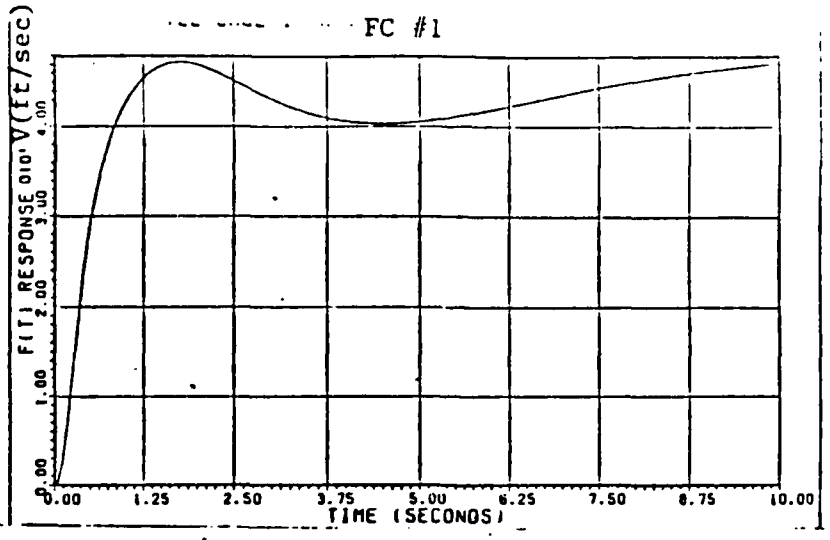

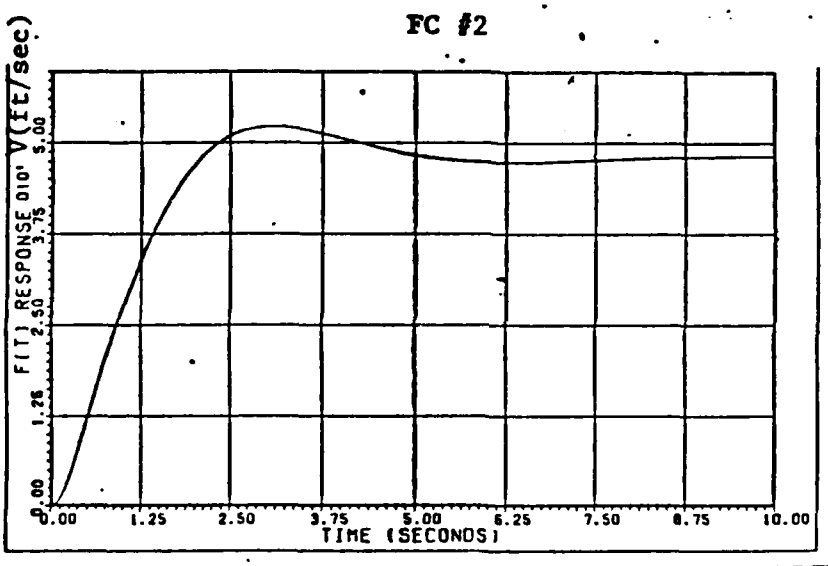

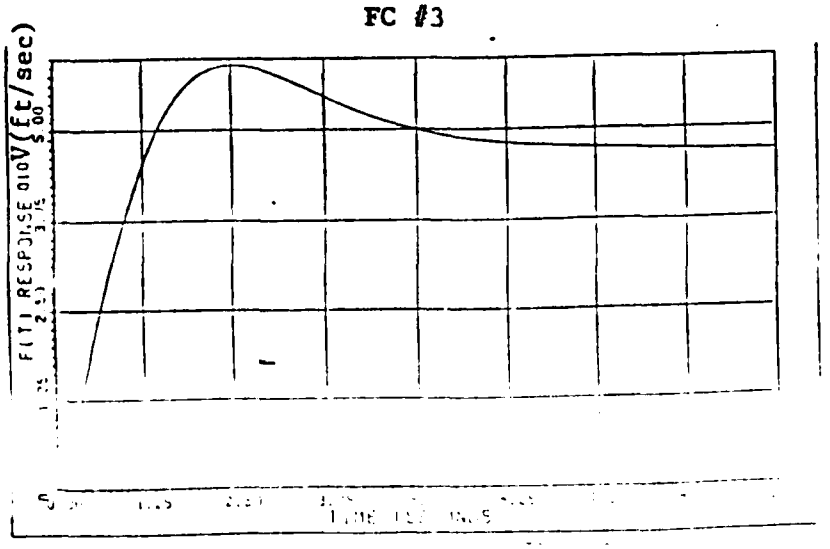

Fig. E-8 t_{22} Responses r(t) = 48 ft/sec

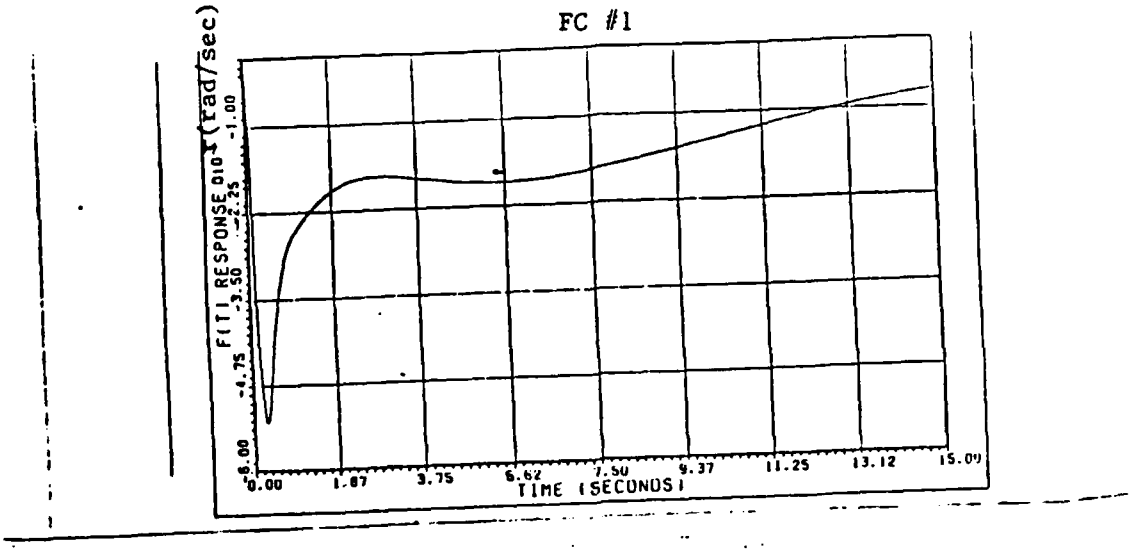

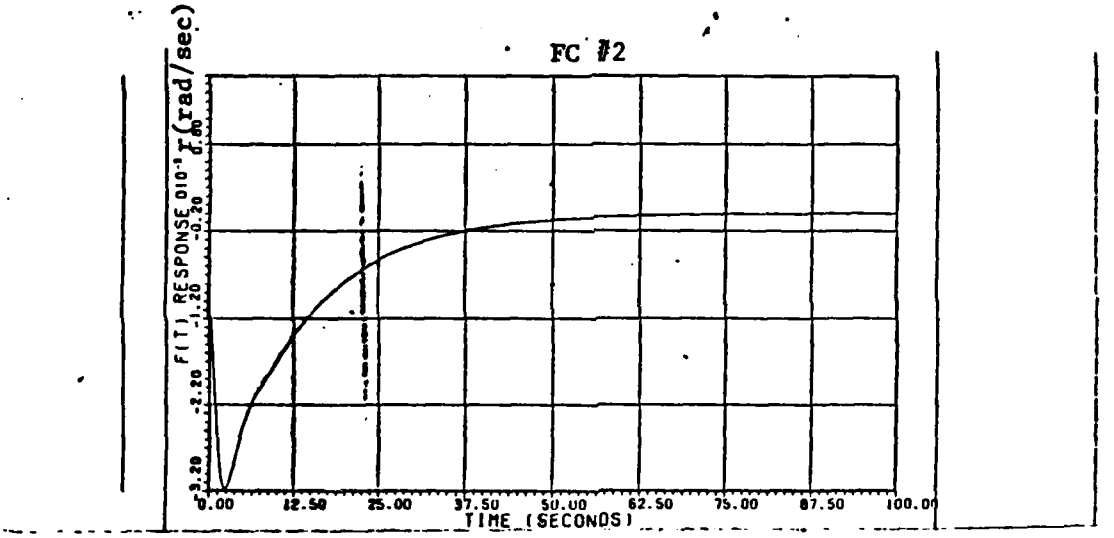

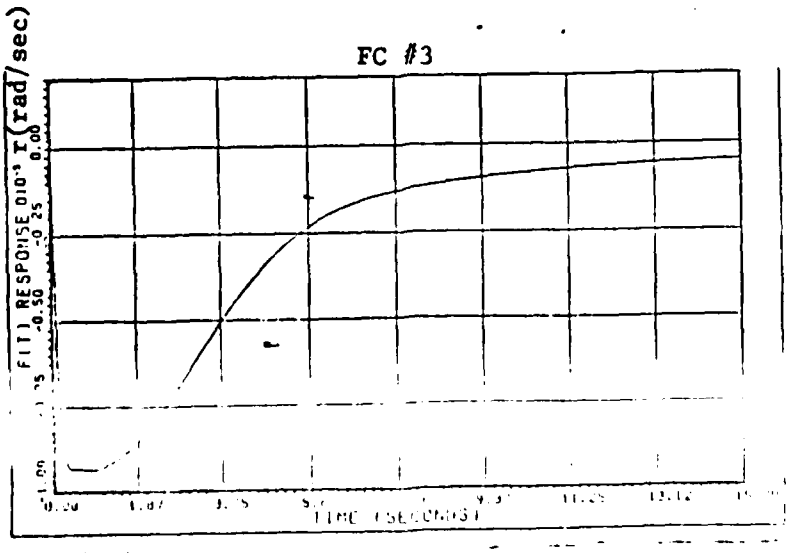

Fig. E-9 t_{32} Responses r(t) = 1 ft/sec

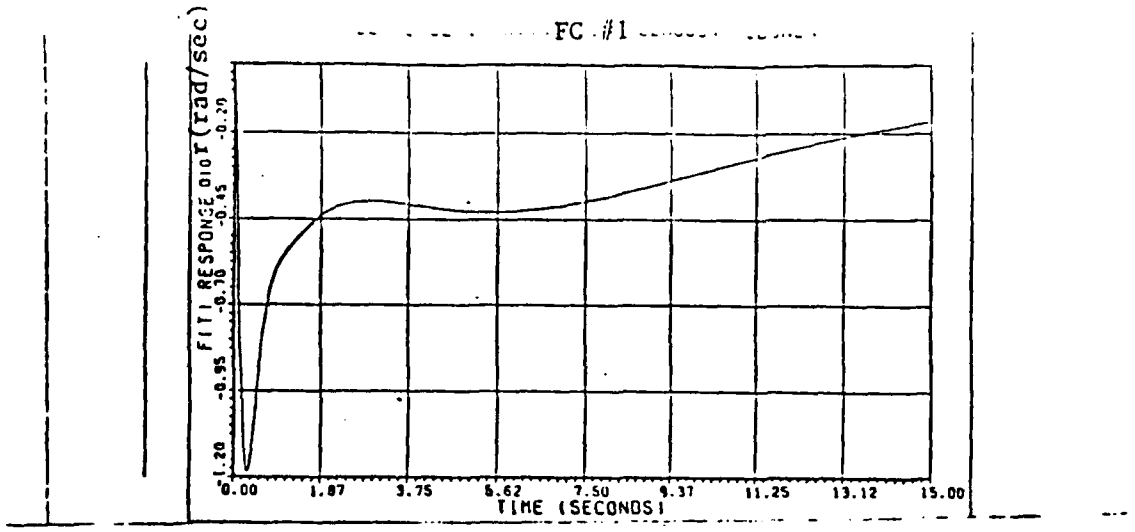

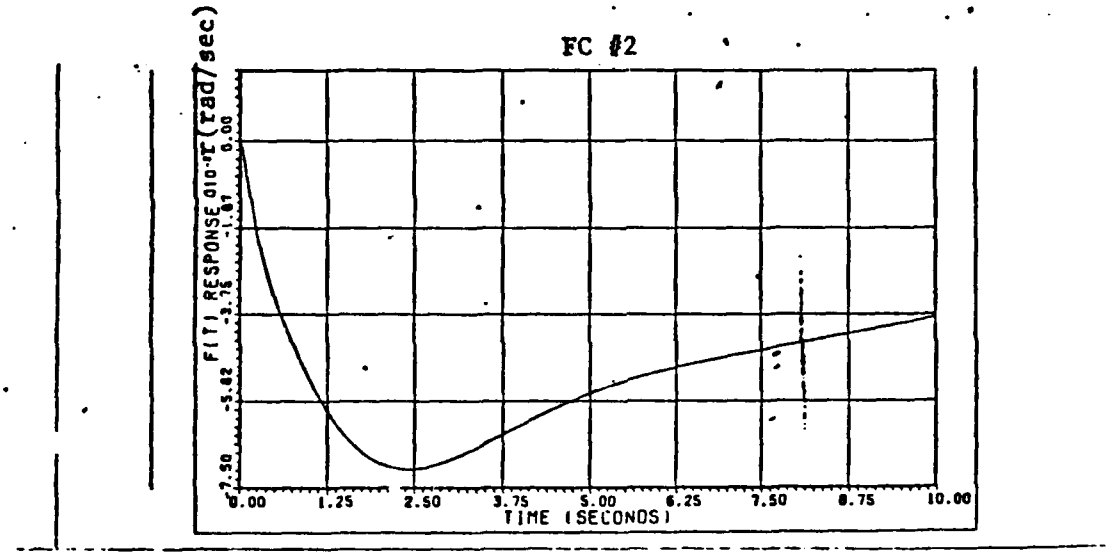

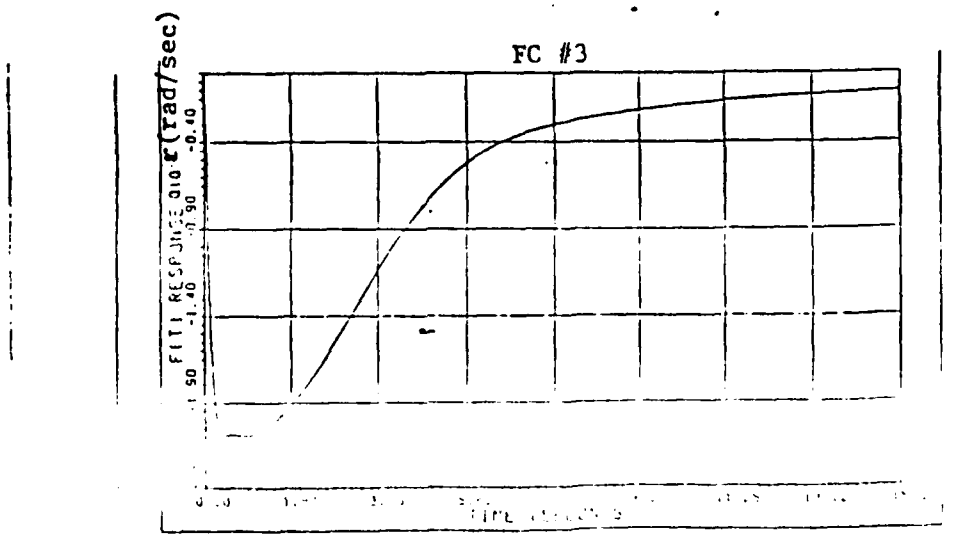

Fig. E-10 t_{32} Responses r(t) = 22.4 ft/sec

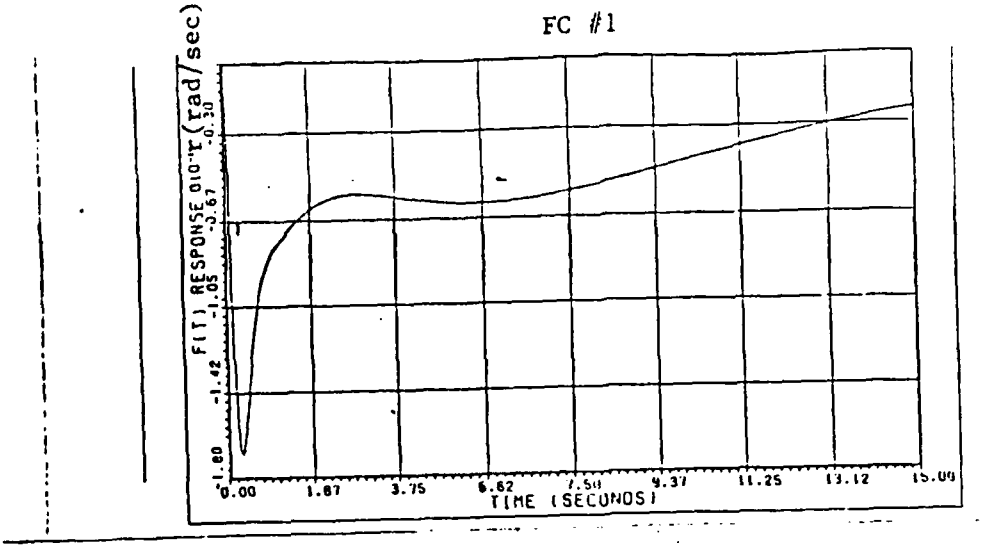

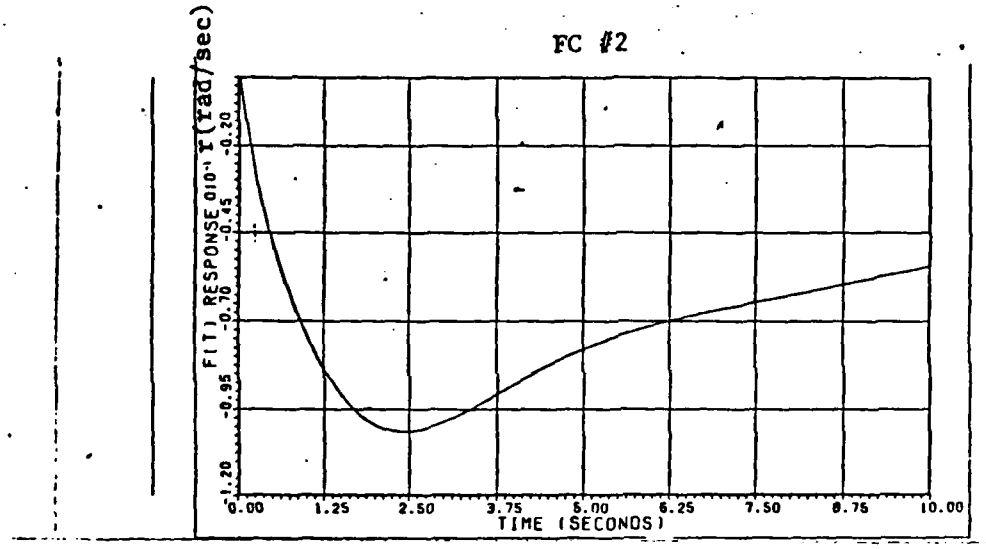

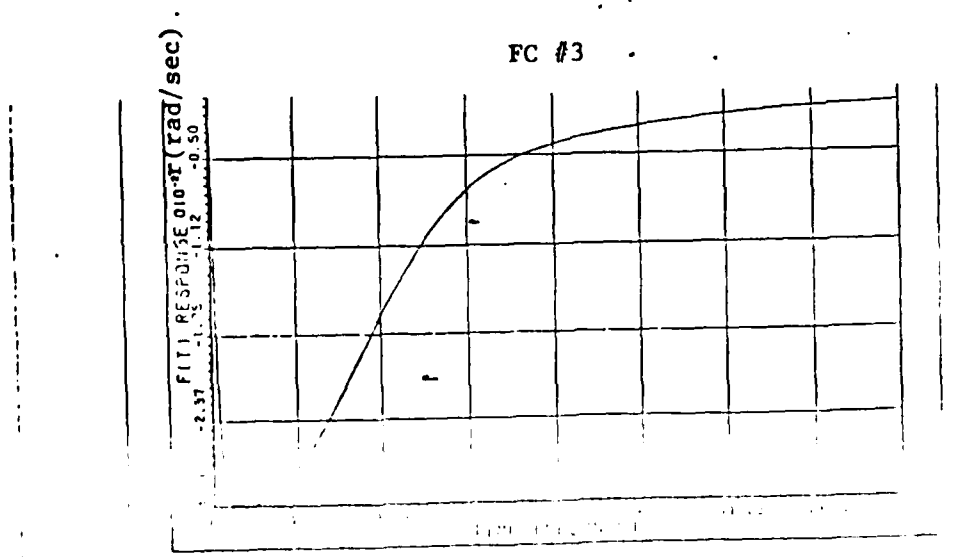

Fig. E-11 t_{32} Responses r(t) = 32 ft/sec

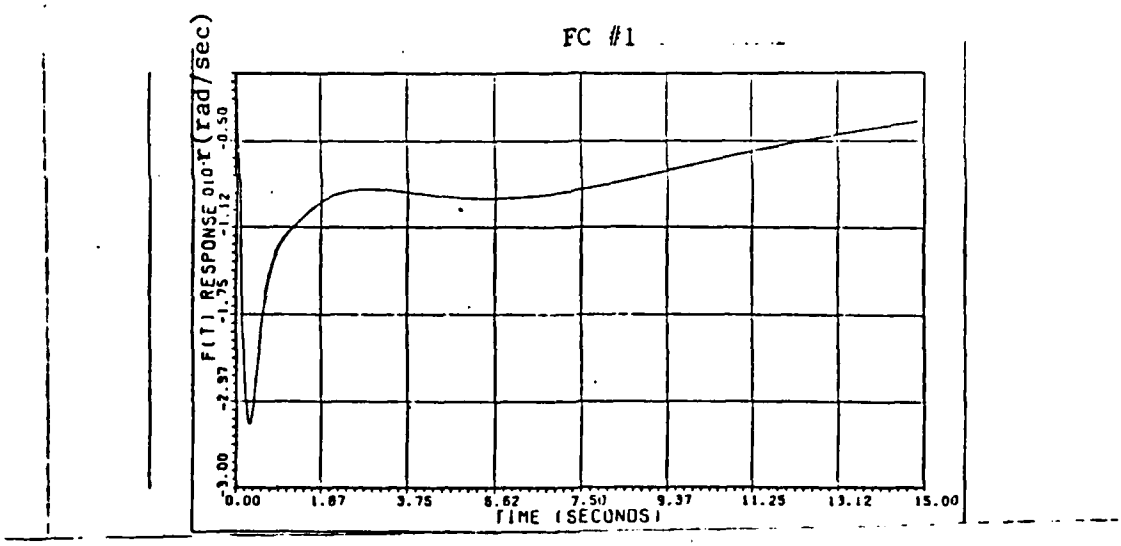

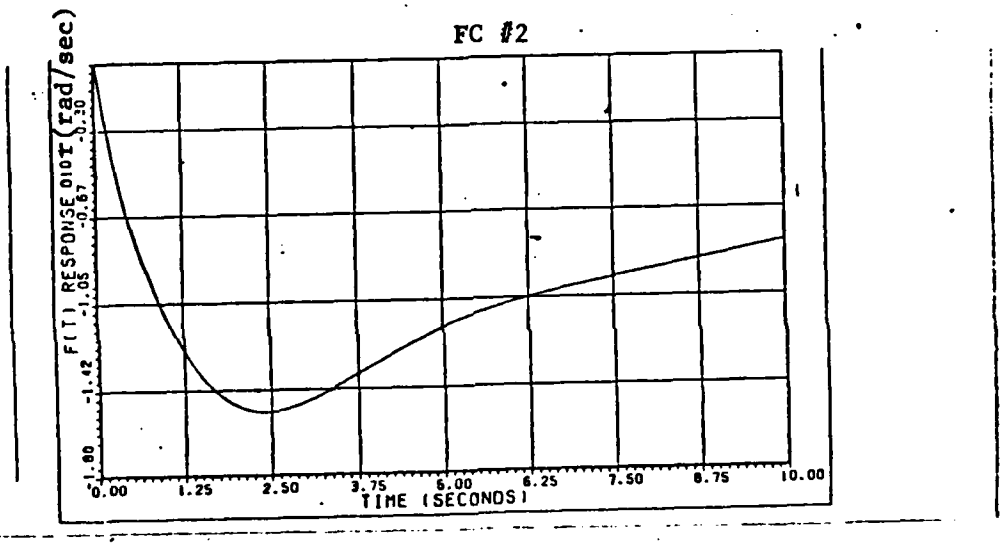

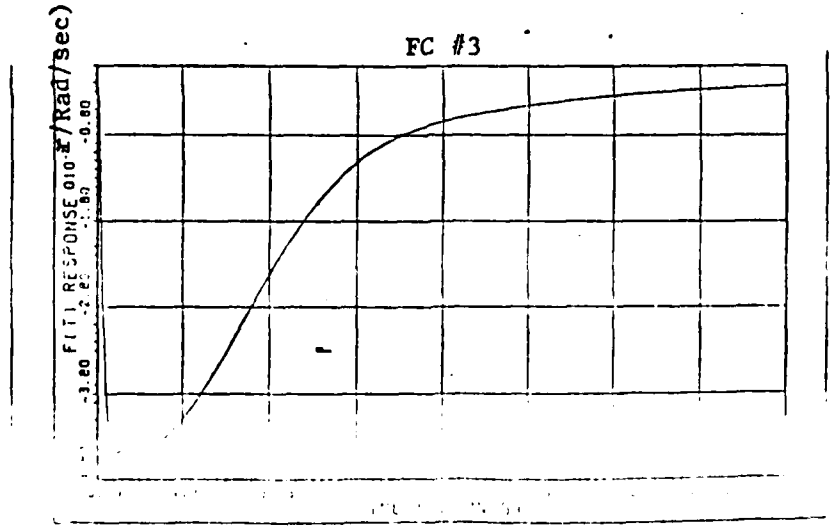

Fig E-12 t_{32} Responses r(t) = 48 ft/sec

*U.S. GPO 646-06

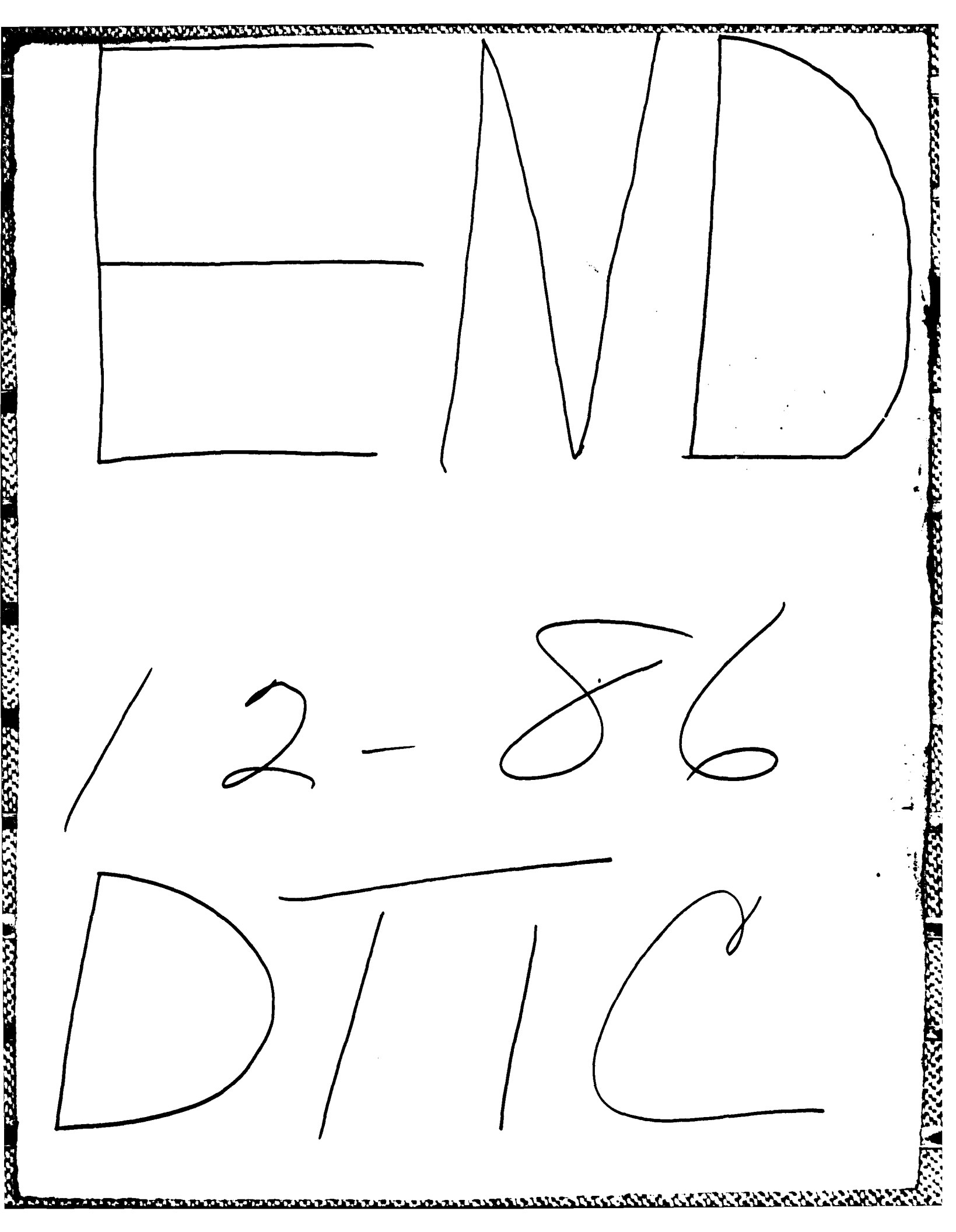
END
12-86
DTIC